



— BUREAU OF —
RECLAMATION

Field Validation of Impedance Spectroscopy Coating Assessments

Science and Technology Program
Research and Development Office
Final Report No. ST-2020-1884-01
8540-2020-43



REPORT DOCUMENTATION PAGE				Form Approved OMB No. 0704-0188	
The public reporting burden for this collection of information is estimated to average 1 hour per response, including the time for reviewing instructions, searching existing data sources, gathering and maintaining the data needed, and completing and reviewing the collection of information. Send comments regarding this burden estimate or any other aspect of this collection of information, including suggestions for reducing the burden, to Department of Defense, Washington Headquarters Services, Directorate for Information Operations and Reports (0704-0188), 1215 Jefferson Davis Highway, Suite 1204, Arlington, VA 22202-4302. Respondents should be aware that notwithstanding any other provision of law, no person shall be subject to any penalty for failing to comply with a collection of information if it does not display a currently valid OMB control number. PLEASE DO NOT RETURN YOUR FORM TO THE ABOVE ADDRESS.					
1. REPORT DATE (DD-MM-YYYY) 09-30-20		2. REPORT TYPE Research		3. DATES COVERED From FY18 to FY20	
4. TITLE AND SUBTITLE Field Validation of Impedance Spectroscopy Coating Assessments				5a. CONTRACT NUMBER XXXR4524KS-RR4888FARD1800201/FA691	
				5b. GRANT NUMBER	
				5c. PROGRAM ELEMENT NUMBER 1541 (S&T)	
6. AUTHOR(S) Bobbi Jo Merten, Coatings Specialist Stephanie Prochaska, Materials Engineer Matt Jermyn, Materials Engineer Elizabeth Monblatt, Engineering Intern Jessica Elder, Engineering Intern				5d. PROJECT NUMBER Final Report ST-2020-1884-01 8540-2020-43	
				5e. TASK NUMBER	
				5f. WORK UNIT NUMBER 86-68540	
7. PERFORMING ORGANIZATION NAME(S) AND ADDRESS(ES) Materials and Corrosion Laboratory Technical Service Center Bureau of Reclamation U.S. Department of the Interior Denver Federal Center PO Box 25007, Denver, CO 80225-0007				8. PERFORMING ORGANIZATION REPORT NUMBER 8540-2020-43	
9. SPONSORING/MONITORING AGENCY NAME(S) AND ADDRESS(ES) Science and Technology Program Research and Development Office Bureau of Reclamation U.S. Department of the Interior Denver Federal Center PO Box 25007, Denver, CO 80225-0007				10. SPONSOR/MONITOR'S ACRONYM(S) Reclamation	
				11. SPONSOR/MONITOR'S REPORT NUMBER(S) Final Report ST-2020-1884-01	
12. DISTRIBUTION/AVAILABILITY STATEMENT Final Report may be downloaded from https://www.usbr.gov/research/projects/index.html					
13. SUPPLEMENTARY NOTES					
14. ABSTRACT Determining the remaining service life of coatings on Reclamation structures improves maintenance timing and lowers overall costs. Traditional visual condition assessments quantify coating areas with visible damage but do not evaluate the coating performance. Electrochemical impedance spectroscopy (EIS) measures the coating performance where there is no visible coating damage. This research applied field demonstrations and laboratory experiments to expand on previous work and advance the validity and usefulness of field EIS testing. The research concluded that the distance between test cells has no effect on the results, reported accuracy and impedance upper limits for field potentiostats, drafted an approach for extrapolating long-term laboratory EIS data to aid estimate remaining service life for EIS data from coated structures, and contributed to a draft ASTM International test method.					
15. SUBJECT TERMS Electrochemical impedance spectroscopy (EIS), field EIS testing, impedance testing, maintenance planning, coating service life					
16. SECURITY CLASSIFICATION OF:			17. LIMITATION OF ABSTRACT	18. NUMBER OF PAGES 268	19a. NAME OF RESPONSIBLE PERSON Bobbi Jo Merten
a. REPORT U	b. ABSTRACT U	THIS PAGE U			19b. TELEPHONE NUMBER 303-445-2380

Mission Statements

The Department of the Interior (DOI) conserves and manages the Nation's natural resources and cultural heritage for the benefit and enjoyment of the American people, provides scientific and other information about natural resources and natural hazards to address societal challenges and create opportunities for the American people, and honors the Nation's trust responsibilities or special commitments to American Indians, Alaska Natives, and affiliated island communities to help them prosper.

The mission of the Bureau of Reclamation is to manage, develop, and protect water and related resources in an environmentally and economically sound manner in the interest of the American public.

Disclaimer

Information in this report may not be used for advertising or promotional purposes. The data and findings should not be construed as an endorsement of any product or firm by the Bureau of Reclamation, Department of Interior, or Federal Government. The products evaluated in the report were evaluated for purposes specific to the Bureau of Reclamation mission. Reclamation gives no warranties or guarantees, expressed or implied, for the products evaluated in this report, including merchantability or fitness for a particular purpose.

Acknowledgements

The Science and Technology Program, Bureau of Reclamation, sponsored this research. Jim Geisbush, the Central Arizona Project (CAP), contributed to the development and demonstration of the test method during condition assessments of CAP structures.

Validation of Coating Assessment for Field Impedance Spectroscopy

**Final Report No. ST-2020-1884-01
8540-2020-43**

prepared by

**Technical Service Center
Bobbi Jo Merten, Coatings Specialist
Stephanie Prochaska, Materials Engineer
Matt Jermyn, Materials Engineer
Elizabeth Monblatt, Engineering Intern
Jessica Elder, Engineering Intern**

Cover photo: Electrochemical impedance spectroscopy test cell set-up for coating evaluation near pipe crown at Salt River Siphon. Photo courtesy of Jim Geisbush, Central Arizona Project.

Peer Review

Bureau of Reclamation
Research and Development Office
Science and Technology Program

Final Report ST-2020-1884-01
8540-2020-43

Validation of Coating Assessment for Field Impedance Spectroscopy

Prepared by: Bobbi Jo Merten, Ph.D., PCS
Coatings Specialist, Materials and Corrosion Lab, 86-68540

Checked by: Stephanie Prochaska, M.S.
Materials Engineer, Materials and Corrosion Lab, 86-68540

Technical Approval by: Matt Jermyn
Materials Engineer, Materials and Corrosion Lab, 86-68540

Peer Review by: Allen Skaja, Ph.D., PCS
Coatings Specialist, Materials and Corrosion Lab, 86-68540

“This information is distributed solely for the purpose of pre-dissemination peer review under applicable information quality guidelines. It has not been formally disseminated by the Bureau of Reclamation. It does not represent and should not be construed to represent Reclamation’s determination or policy.”

Acronyms and Abbreviations

CAP	Central Arizona Project
CE	counter electrode
CompactStat	CompactStat.h10800
CPE _{coat}	coating constant phase element
DFT	dry film thickness
EIS	electrochemical impedance spectroscopy
NaCl	sodium chloride
(NH ₄) ₂ SO ₄	ammonium sulfate
OCP	open circuit potential
RE	reference electrode
Reclamation	Bureau of Reclamation
R _{pore}	coating pore resistance
TSC	Technical Service Center
UT	ultrasonic thickness
WE	working electrode

Measurements

\$	dollars
%	percent
Z	impedance magnitude
Z _{0.01 Hz}	impedance magnitude at 0.01 Hz
°F	degree Fahrenheit
cm	centimeter
ft	feet
Hz	hertz
in	inch
mil	milli-inches
mV	millivolts

Contents

	Page
Mission Statements	iii
Disclaimer	iii
Acknowledgements	iii
Peer Review	v
Acronyms and Abbreviations	vi
Measurements	vi
Executive Summary	1
Introduction	2
Motivation	2
Field Impedance Spectroscopy Testing	2
Methods	4
Comparison of Field and Laboratory EIS Data	4
Development of Field Experiment Testing Method	4
Approaches for Large Structures	5
Agua Fria River Siphon (2018)	5
Salt River Siphon (2018)	5
Approaches for Non-Horizontal Surfaces	5
Fontana Dam (2019)	6
Salt River Siphon (2019)	7
Laboratory Experiments of Field Testing Parameters	7
Distance Between Test Cells	7
Evaluation of Equidistant Test Cells	7
Evaluation of Test Cell Separation Distance	8
Coupled Counter and Reference Electrodes	9
Field Potentiostat Accuracy Measurements	10
Long-Term Laboratory EIS Data and Field Template	10
Results and Discussion	11
Comparison of Field and Laboratory EIS Data	11
Development of Field Experiment Testing Method	12
Approaches for Large Structures	12
Agua Fria River Siphon (2018)	14
Salt River Siphon (2018)	14
Approaches for Non-Horizontal Surfaces	15
Fontana Dam (2019)	15
Salt River Siphon (2019)	17
Standardization of Testing Method	19
Laboratory Experiments of Field Testing Parameters	20
Distance Between Test Cells	20
Equidistant Test Cells with Derived Impedance Values	20
Varied Test Cell Distance with Measured Impedance Values	21
Coupled Counter and Reference Electrodes	22
Field Potentiostat Accuracy Measurements	23

Long-Term Laboratory EIS Data and Field Template	25
Conclusions.....	29
References	30
Data Supporting the Final Report	33
Appendix A – SSPC 2019 Manuscript	A-1
Appendix B – Agua Fria River Siphon Report (2018).....	B-1
Appendix C – Salt River Siphon Report (2018).....	C-1
Appendix D – Agua Fria River Siphon Report (2019)	D-1

Executive Summary

Determining the remaining service life of a coating on infrastructure susceptible to corrosion is an important planning tool for scheduling timely maintenance. Traditional condition assessments are qualitative, which limits their ability to confirm the corrosion protection being provided by the coating. Qualitative or visual inspections provide reliable information for areas of the coating with visible damage. This is an important contribution to condition assessments, but it does not provide information about the undamaged coating areas, which generally cover most of a structure. Quantitative analysis is needed to assess areas of the structure with no visible coating damage. This would provide a more accurate estimation of a coating's effectiveness and remaining service life—ultimately providing Reclamation with better assessment tools for making project planning decisions.

Previous research showed that electrochemical impedance spectroscopy (EIS) is an effective quantitative technique for evaluating protective coatings on Reclamation structures [1, 2]. The current work advanced the validity and usefulness of the field EIS method through a series of demonstrations and experiments. Field EIS data from several coating systems were compared to laboratory data from the same coatings. Field demonstrations to advance the test method occurred at the Salt River Siphon, the Agua Fria River Siphon, and Fontana Dam. Laboratory experiments investigated the impact of modified test set ups for field EIS, the accuracy of the available field potentiostats, and an approach for extrapolating long-term laboratory EIS data to aid estimation of remaining service life for field EIS data.

The research found the following:

- Good agreement between the field EIS data and the corresponding laboratory data.
- Improvements to the recommendations for the field EIS test method, including a testing plan for large structures and approaches for testing non-horizontal surfaces, that is in the process of standardization for international applications via ASTM International work group WK67789.
- No effect of the distance between test cells on the accuracy of field EIS data.
- No effect on results of the coupling of the reference and counter electrode compared to the traditional set-up having unique electrodes for each.
- Recommendations for usage of the Ivium CompactStat for field EIS testing and limited usage of the Ivium PocketSTAT, pending further investigation of its accuracy with resistors less than 10^9 ohms.
- A first approximation for an approach to determining the remaining service life of a coating in the field based on laboratory data for the same coating system.

The recommended next steps are to continue the refinement of the field EIS testing method and the understanding of EIS data in its relationship to the coating's remaining service life. The standardization of the method, if successful, would allow for inclusion of the test method in coating specifications to ensure a good product is received. Further investigation into the use of the

PocketSTAT for investigating lower impedance coatings and coatings nearing the end of their service life is recommended.

Introduction

Motivation

Protective coatings are the primary defense against corrosion of Bureau of Reclamation (Reclamation) steel structures, and they are the most cost-effective method of protection available. However, coatings degrade while in service and must undergo a complete removal and replacement, i.e., recoating, once adequate protection is lost. Determining the most cost-effective timing for recoating has historically been nebulous and is often complicated by the logistics of scheduling the recoating work.

This research matures a field technique used to improve the timing of coating maintenance, which is important because the cost implications of poor coating replacement timing can be high [3]. Replacing coating systems too soon greatly increases the annualized cost of the coating system and results in unnecessary facility outages, resources, and non-contract costs. Waiting too long to repair or replace a coating system may result in costly corrosion repairs or impaired structure function.

Facility personnel and coatings specialists routinely perform coating condition assessments of protective coatings on Reclamation structures, which are particularly valuable for steel structures that are critical to the reliable delivery of water and power. Traditional condition assessments of these structures are predominantly visual. To determine where coating repair is needed, the inspector looks for corroding or bare areas, documenting their size and location. The industry guidance is to calculate the percent area requiring repair and to perform total removal and replacement when the area in need of repair approaches a given percentage of the total surface area. The approach is subjective, and the accuracy of this assessment in determining the end of a coating's service life is low because it does not assess the physical degradation of the undamaged coating occurring on the molecular level, i.e., that is not visible to the human eye.

Field electrochemical impedance spectroscopy (EIS), or impedance spectroscopy, testing offers a method to quantify condition assessments and better-time coating maintenance by physically testing the corrosion protection properties of undamaged coating [4-8]. Specifically, the technique measures an electrical property—the impedance—to investigate the coating [9]. Therefore, implementation of field EIS incorporates measurement of the actual corrosion protection performance of the undamaged coating into these assessments to estimate the remaining service life.

Field Impedance Spectroscopy Testing

Reclamation began demonstrations of a field EIS technique in 2013, in partnership with the U.S. Army Corps of Engineers to adapt a common coating laboratory technique into a field-ready coating

evaluation tool. The initial demonstrations showed promise for the technique to quantify coating performance but also revealed challenges related to ease of use. The demonstrations also raised questions about data reliability and how to best apply the data to improve coating maintenance decisions [10]. The ensuing work sought to make progress on these items. The ease of use was improved by developing a field test method that specifically addressed the guidance for commonly encountered field challenges [1, 11]. The method also adopted the two test cell method so that direct connection to the steel structure is not needed—an approach introduced and investigated by other researchers for laboratory studies [12-14]. Figure 1 provides a schematic of the test cell set up for the field EIS test method. The method requires only the field instrument, i.e., the potentiostat, its corresponding electrical lead wires, several common laboratory electrodes, test cells made from plastic beakers, and water as the electrolyte solution. Tap water is generally suitable as the electrolyte solution; adding a few percent by weight of sodium chloride (NaCl), or table salt, to the water ensures the solution resistance is much lower than the coating being analyzed.

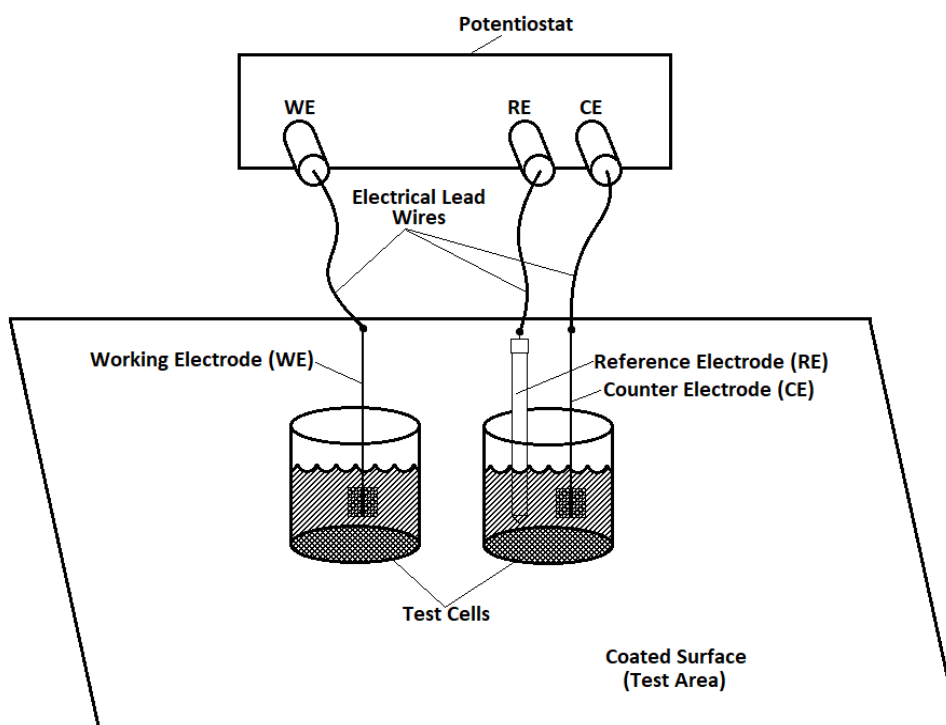


Figure 1. Schematic of field electrochemical impedances spectroscopy set-up using two test cells.

Continued previous research of the field EIS technique lead to experiments to statistically and comprehensively evaluate the accuracy and precision of the measurements [2]. The results confirmed that field EIS data is reliable when applied correctly. The revised test method incorporates simple checks to help the user confirm data reliability at the outset of each field investigation.

The present research objective was two-fold: 1) to conduct experiments to answer technical questions that remain in the method's implementation and 2) to determine how to best apply the data to improve coating maintenance recommendations in order to minimize the cost of corrosion protection and repairs for Reclamation's assets. The first objective utilized several laboratory and field experiments to investigate specific questions. The field experiments refined the method by

advancing current testing procedures. The laboratory experiments evaluated the effects of method variables to confirm the approach and identify sensitivities of the field experiment. The variables explored were the distance between test cells, the accuracy of several potentiostats, and pseudo-electrode performance. The second objective compared existing field EIS data to laboratory data and subsequently analyzed a library of existing laboratory EIS data to extract useful degradation behaviors and performance thresholds for coating systems commonly used on Reclamation structures.

Methods

The research applied a variety of laboratory and field experiments as well as desktop analysis to further the implementation of field EIS testing for coating evaluation and remaining service life estimation. The method applied in each experiment is outlined below.

Comparison of Field and Laboratory EIS Data

EIS testing occurred on coated structures in the field and on laboratory coupons containing the same coating system. The resulting EIS data from these field and laboratory tests were compared. The field experiments evaluated structures containing coal tar enamel, polyurethane, and coal tar epoxy. The approximate coating age and exposure conditions were noted. The laboratory test coupons underwent the typical 25-week accelerated weathering and received EIS testing periodically throughout the exposure period. Appendix A provides the full paper [15].

Development of Field Experiment Testing Method

Field testing occurred at three facilities to advance the test method from the test planning perspective as well as to evaluate an approach for non-horizontal surfaces. The facilities supporting these investigations are as follows:

- Salt River Siphon near Phoenix, Arizona, Central Arizona Project (CAP)
- Agua Fria River Siphon near Phoenix, Arizona, CAP
- Fontana Dam Radial Gates in western North Carolina, Tennessee Valley Authority

The field experiments used a CompactStat.h10800 (CompactStat) from Ivium Technologies (Eindhoven, The Netherlands) potentiostat with dedicated software. The potentiostatic EIS measurement used a frequency range of 10^5 Hz to 10^{-1} Hz, applied a voltage perturbation of 50 mV at the open circuit potential (OCP), and measured 5 points per decade. An OCP scan prior to each EIS measurement allowed the user to confirm that the set up was correct, the signal stable, and the coating adequately hydrated to determine its properties.

Approaches for Large Structures

Field EIS method testing plan development occurred during inspection planning for the Salt River and Agua Fria River Siphons. The condition assessments included the traditional visual qualitative inspection as well as quantitative inspection that included EIS. Both structures carry critical water supplies for Arizona communities and exceed 500,000 square feet in coated steel surface area. The testing plan needed to conduct the testing in a short outage window and be able to inform upcoming maintenance decisions on these critical structures. Details of the experiment are given below. The results section includes extensive commentary on the approaches taken to develop the testing plans for these large structures.

Agua Fria River Siphon (2018)

The interior coating of Agua Fria River Siphon was evaluated by TSC researchers. The condition of the coating and underlying steel required inspection to evaluate their condition and determine if repair or replacement was needed during an upcoming maintenance opportunity. Originally constructed from prestressed concrete cylinder pipe by Reclamation, the siphon was replaced with a steel pipeline in 1997 and the interior lined with Amercoat 78HB coal tar epoxy. The more than 20-ft. diameter and approximately 10,000-ft. long siphon is now operated and maintained by the CAP.

Visual inspection of each pipe segment was performed before the quantitative measurements were taken. The dry film thickness (DFT) was measured on the pipe segments that did not have visual damage. This data was collected with a PosiTector 6000 coating thickness gauge. Ultrasonic thickness (UT) measurements were then taken with a Cygnus Instruments M5-C4 + UT gauge. In order to perform EIS data collection, two test cells were mounted at each location; occasionally, a third was added to ensure that at least two had sufficient data intake. A two cell test method, as illustrated in Figure 1, was used for the analysis. The test sites alternated between the left and right walls of the pipe, when facing downstream. UT and DFT measurements were taken in accordance with internationally recognized testing standards.

Monsoon-rains reduced the ability to evaluate the lining throughout some portions due to mud accumulation at the lowest points of the siphon. The mud also prevented DFT, UT, and EIS testing on the same inaccessible regions of the pipeline. A more detailed account of the inspection can be found in Appendix B.

Salt River Siphon (2018)

The more than 20-foot diameter and approximately 10,000-ft long Salt River Siphon has a similar history to the Agua Fria River Siphon. Investigators from Reclamation's TSC evaluated the condition of the interior Amercoat 78HB coal tar epoxy lining. Visual inspection, UT testing, DFT, and EIS analysis were performed on the pipe.

The testing utilized similar parameters and set up to the Agua Fria River Siphon evaluation. For a more detailed account of the inspection, see Appendix C.

Approaches for Non-Horizontal Surfaces

EIS testing had previously been limited to horizontal surfaces which in turn limited the type of structure and locations that could be tested. For example, testing structures such as gates and the interior crown position of pipes were not possible due to the need for saturation with electrolyte. In previous open cell test designs, such as Figure 1, liquid electrolyte would either not completely cover

a test cell surface or flow out of the test cells beyond a given level of inclination. This drove the need to develop a testing method that was independent of orientation of the test cells. The test method described below provides an example approach for handling non-horizontal surfaces that is also applicable to fully upside-down surfaces. Other approaches include suction cups, magnetic test cells, pipe elbows, or other commercially available options.

The test method utilizes a closed cell approach that prevents electrolyte from escaping in any orientation. For saturation of the coating, the top side of the test cells are sealed using paraffin wax and zip ties, as shown in Figure 2. Electrolyte is then injected through a port in the side of the test cell. Because the cell is an air-tight enclosure, it is also necessary to vent the test cell air during the filling process via a second port. Both ports are quarter-inch drilled holes in the side of the test cells, prepared prior to field use, and filled with silicon adhesive. The electrolyte is injected and air is exhausted through the respective ports using hypodermic needles.

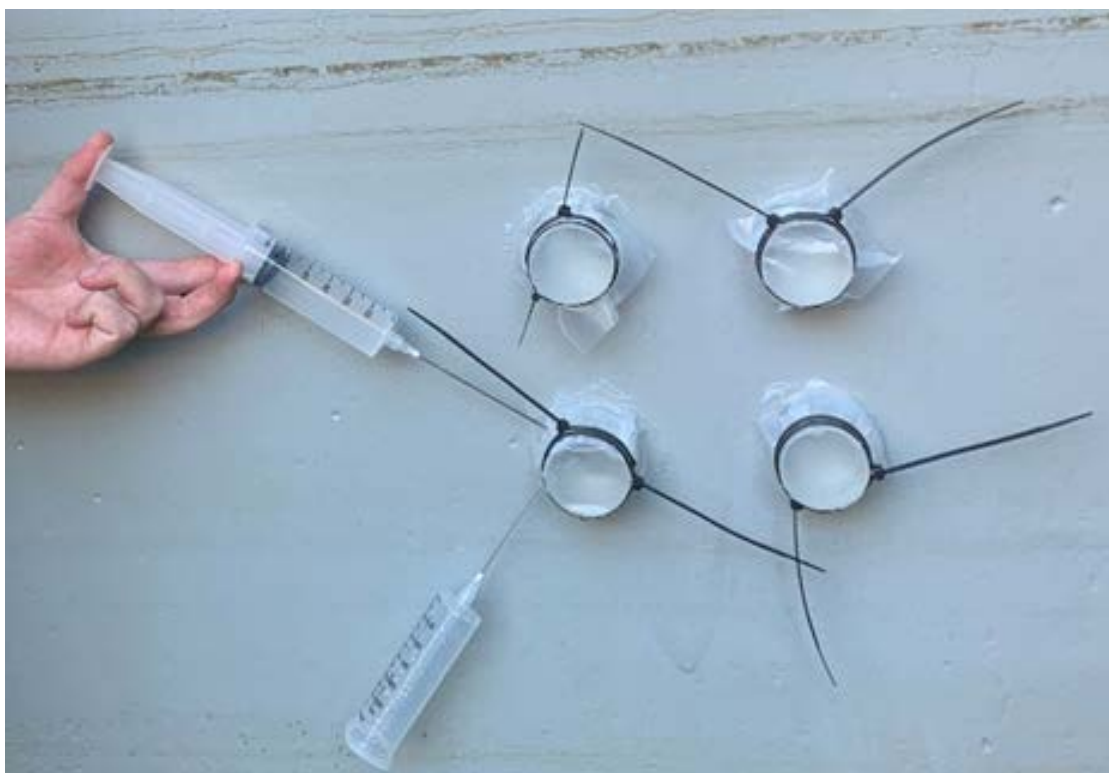


Figure 2. Four EIS test cells affixed to a vertical surface and filled via electrolyte-inlet and air-outlet ports using syringes.

To perform the EIS test, the electrolyte, paraffin wax, and zip ties are removed. A rubber gasket containing the measurement electrodes is placed in the top side of the cell to regain an air-tight seal. The electrolyte is again injected and air exhausted as previously discussed.

Fontana Dam (2019)

This experiment evaluated methods for preparing EIS test cells for non-horizontal surfaces. The test surface was a radial gate at Fontana Dam, which was coated with Amerlock 2 primer and intermediate coats and PSX 700 polysiloxane topcoat. The water level of the dam had dropped, exposing the coating to atmosphere for approximately one week prior to testing. The surface was

shaded and the weather much cooler than other testing reported here, with a temperature at the time of testing of approximately 30 °F to 40 °F. Researchers accessed the gate crest area by boat, and all attendees placed electronics and phone in airplane mode during testing.

The coating surface was wiped clean and test cells adhered with a silicone adhesive. The cell opening was covered with parafilm, held in place by zip ties. An electrolyte solution comprised of tap water and approximately 5 percent (%) sodium chloride by weight was added following a 1-hr cure time using a syringe via electrolyte inlet and air outlet ports in the test cell, which comprised of a hole filled with silicone. The solution was left overnight to soak into the coating until testing.

Salt River Siphon (2019)

Following the Fontana Dam experiment outlined above, this experiment sought to confirm previous results and evaluate overhead surfaces inside the 21-foot diameter Salt River Siphon. The siphon had been dewatered for coating remediation work prior to arrival of TSC staff. The interior of the siphon utilizes a coal tar epoxy system that was originally placed in service in 1997.

Each test location was prepared by wiping or scraping mud from the surface and using a rag to dry the area. The test cells were adhered in a similar manner to those at Fontana Dam and placed at the 10:30 and 1:30 clock positions facing downstream in the siphon. Four test cells were placed at each location, two more than required to provide insurance in case adhesion issues were encountered. The cells were filled with water and left overnight to ensure the coating was re-hydrated.

Laboratory Experiments of Field Testing Parameters

The laboratory experiments used an Ivium CompactStat potentiostat with dedicated software unless otherwise noted. The potentiostatic measurement used a frequency range of 10^5 Hz to 10^{-1} Hz, a voltage perturbation of 50 mV at the OCP, and 5 points per decade. An OCP scan prior to each EIS measurement allowed the user to confirm that the set up was correct and the coating adequately hydrated to determine its properties.

Distance Between Test Cells

The purpose of this experiment was to assess the effect of distance between test cells on the accuracy of impedance values. This work aimed to determine if the distance needed to be defined (standardized) when performing field EIS. Two experiments were performed for this investigation. Both experiments evaluated test cells at varying distances.

Evaluation of Equidistant Test Cells

Nine test cells were glued to an 11-inch diameter disk coated direct-to-metal with a Sherwin Williams polysiloxane XLE-80 coating system according to the scheme shown in Figure 3. This arrangement allows for three test cells in each of three sets to be equidistant from each other. Test cells were grouped based on their distance from the center of the disk—the three cells closest to the center (and to each other) were denoted as set “R,” the three cells at mid-distance from the center (approximately one test -cell diameter separation) were denoted as set “G,” and the three cells farthest away from the center were denoted as set “B.” Within each set, test cells replicates were designated as “1,” “2,” and “3.”

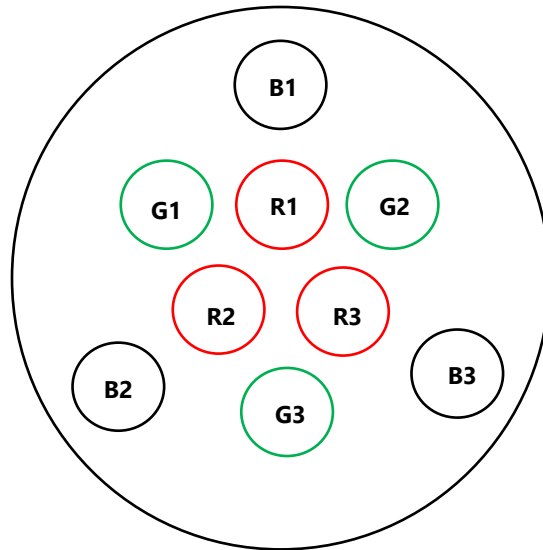


Figure 3. Schematic of the test cell sets and arrangement for the equidistant test cell set-up.

Test cells were filled with dilute Harrison's solution (0.05% NaCl and 0.35% ammonium sulfate ((NH₄)₂SO₄)) as the electrolyte, and the coating was left to hydrate overnight. When running the impedance analysis, only the two test cells being measured contained electrolyte. The coating within all other test cells was thoroughly dried between each measurement to prevent unintended current pathways through any solution in these cells.

Three replicates of each combination were measured per set of equidistant test cells to calculate the impedance of the individual test cells in that set. Then, additional measurements were performed using test cell combinations across different test sets. The analysis calculated the theoretical impedance of the test cell combinations and compared it to the measured impedance values at various test cell distances.

Evaluation of Test Cell Separation Distance

Eleven test cells were glued to the side of the laboratory's test gate, which is coated with U.S. Army Corps of Engineers System 5-E-Z vinyl zinc-rich coating system. The test expanded on the previous evaluation—testing across a wider range of tests cell distances—and utilized individual EIS measurements for each test cell via the traditional setup with an electrical connection to the steel substrate. Each test cell had an average coating film thickness of 12 mils with a standard deviation of 1 mil. Figure 4 provides the test cell # for the experiment (top schematic) as well as the separation distance between test cells during the measurement (bottom schematic), measured as the shortest edge-to-edge distance. Test cell #1 served as the origin in the experiment; the distance to all other cells is measured from this cell.

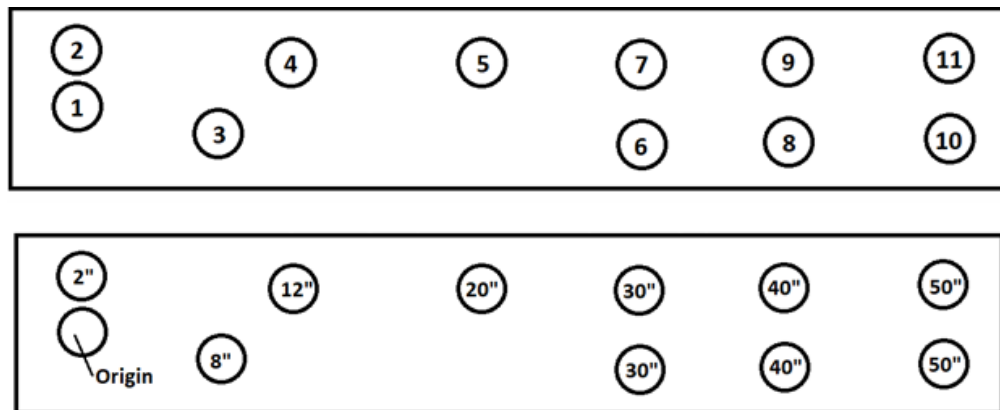


Figure 4. Schematic of the test cell # (top) and edge-to-edge separation distance (bottom) to evaluate the effect of test cell separation distance.

EIS measurements were completed for each test cell using the traditional test set-up connected to the substrate. The two test cell method was then used to measure EIS for different combinations of cells. The solution remained in all test cells during each measurement. The geometry of this experimental setup ensures no significant unintended current pathways through in-path test cells during the two test cell method because it could not reduce the test cell separation distance by more than a few percent.

Coupled Counter and Reference Electrodes

To evaluate the need for a reference electrode in the two test cell EIS set-up, measurements were taken using two experimental set-ups. The first approach, which is the common technique, separated the reference and counter electrodes, as shown in Figure 1. The measurement used a copper/copper sulfate reference electrode and a platinum mesh counter electrode. The second approach used a modified set-up that coupled the reference and counter electrodes. Here, the measurement connected the platinum mesh electrode to both the reference and counter electrode leads, as shown in Figure 5. The test applied EIS measurements via each set-up and compared the resulting data.

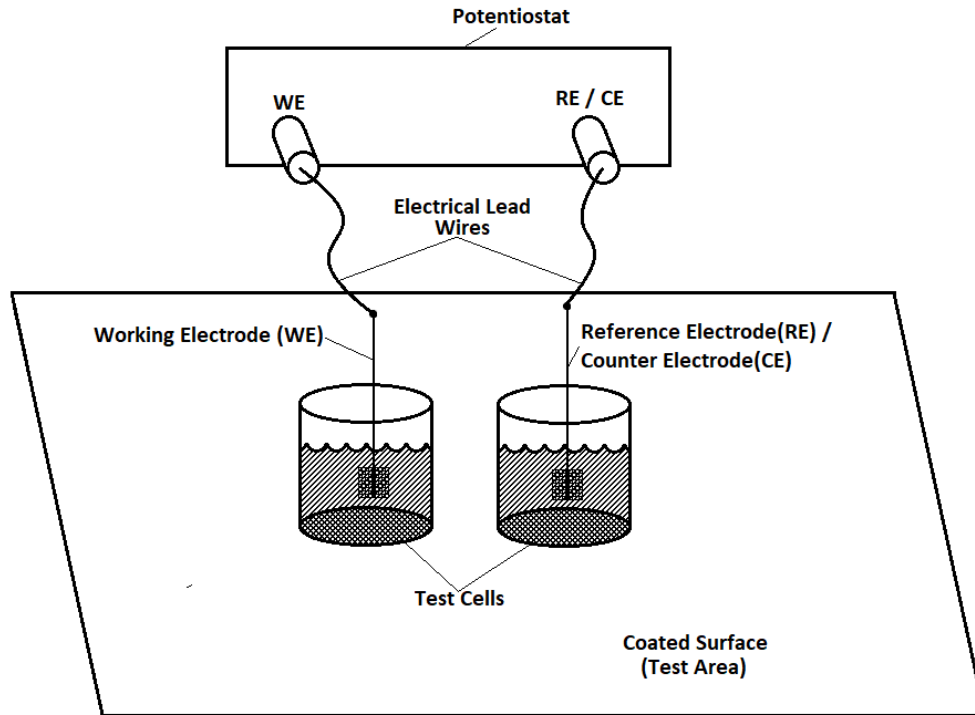


Figure 5. EIS set-up with coupled reference and counter electrodes.

Field Potentiostat Accuracy Measurements

The accuracy of two field-ready potentiostats, the CompactStat and pocketSTAT, also from Ivium, were evaluated by performing EIS measurements on calibrated resistors. Subsequent measurements were performed on a traditional laboratory potentiostat, the Femtostat FAS2 from Gamry Instruments Inc. (Warminster, PA), for comparison. The experiment used calibrated resistors, alone or in series, to produce EIS data with resistor values ranging from 10^9 ohms to 10^{12} ohms.

The resulting data was plotted via Bode plot. A line of best fit was generated for the range of low frequency impedance magnitude, $|Z|$, data containing a phase angle of approximately zero, which is representative of a resistor. For several experimental set-ups, the EIS measurement was re-run to include a lower frequency range, generally 0.01 Hz, or until at least several frequencies recorded phase angle values of approximately zero.

The y-intercept of the linear trendline was used to represent the measured resistance of the resistor, i.e., the experimental value. The data measured with the PocketStat did not sustain a phase angle of zero, and instead, the four lowest frequency $|Z|$ data points were used to create the linear trend line. Then, each of these experimental resistor values for were compared to the known, or theoretical, value using a percent error calculation to determine accuracy of each device at different resistor values.

Long-Term Laboratory EIS Data and Field Template

In order to study long-term trends in EIS data collected, a compilation analysis with data extrapolation was completed. The coating systems evaluated are shown in Table 1. The coatings

analyzed are common on Reclamation structures: epoxy, polyurethane, coal tar epoxy, coal tar enamel, and vinyl. Each coating received at least one year of laboratory exposure.

Table 1. Coatings evaluated for long-term laboratory EIS data.

Coating ID	Coating type	Total years of exposure analyzed (years)
Ep-01	Epoxy	7.50
Ep-02	Epoxy	9.81
Ep-03	Epoxy	3.82
Ep-04	Epoxy	6.96
Ep-05	Epoxy	9.98
Ep-06	Epoxy	9.97
Ep-07	Epoxy	9.90
Pu-01	Polyurethane	9.05
CTEn-01	Coal tar enamel	4.38
CTEp-01	Coal tar epoxy	4.38
CTEp-02	Coal tar epoxy	10.04
VZn-01	Zinc-rich vinyl	13.27

The EIS data was evaluated to draw conclusions on the impedance and phase angle properties and degradation trends. The final analysis included a subset of these coating systems, and a template was developed for the purpose advancing the interpretation of field EIS testing data.

Results and Discussion

Comparison of Field and Laboratory EIS Data

Equivalent circuit modeling was used to analyze data generated from laboratory and field EIS testing. The pore resistance, R_{pore} , and the constant phase element, CPE_{coat} , used in the modeling are compared for each dataset. R_{pore} is the resistance of the ion path that traverses from the electrolyte solution to the substrate through interconnected pores in the coating. The CPE_{coat} relates to the capacitive nature of the coating itself. In real world analyses, coatings do not perform as ideal capacitors and so the concept of a constant phase element is introduced to account for the differences.

The analysis compared the R_{pore} and CPE_{coat} results for the laboratory data as 25-week average to the field data. There is good agreement in the overall ranking of R_{pore} and CPE_{coat} for the three systems evaluated, but the values are not similar. The laboratory coating results exhibited a higher pore resistance by approximately one order of magnitude compared to the field coating results. Physically, this could be interpreted that the field coatings were showing a higher degree of degradation than their laboratory counterparts. This result is expected as the field coatings had been in service for a longer period than the laboratory coupons. Comparing the CPE_{coat} of both coating

sets, the laboratory coatings had a lower capacitance, by approximately half an order of magnitude, than the field coating results. Physically, a larger capacitance can be related to a higher degree of water uptake by the coating. The higher capacitance of the field coating again correlates to lower performance. As previously mentioned, the field coatings had been in service for a longer duration and the result is expected; the field coatings are showing a higher degree of saturation. Consistent results between the coating systems analyzed helps to verify that laboratory coupons can be used to approximate the condition of field applied coatings. A full discussion of this research can be found in Appendix A [15].

Development of Field Experiment Testing Method

Approaches for Large Structures

Planning a field condition assessment and collecting a statistically significant number of data points on a large structure is no easy feat, especially when subject to extremely short outage periods. The 2018 inspections of the Agua Fria River and Salt River siphons were planned down to the minute to accomplish evaluation of a large diameter pipeline that was nearly two miles in length. In preparation for this work, researchers performed a series of small studies to ensure the optimization of testing logistics and execution.

To plan test locations, pipe segment drawings were combined to form one scale drawing of the siphon profile. Initially, the goal was to perform EIS testing at approximately 30 locations along the siphon in order to get a statistically significant number of datapoints. The outage period time allocated for EIS setup and testing was divided by 30 to calculate the maximum time allowed per test. The siphon length was also divided by 30 to calculate the distances between each test location. Time needed to clean the siphon wall, apply adhesive to and affix the test cell to the wall, and fill the test cell with water was calculated by timing those activities in the lab. The total time to perform each EIS test including test set-up, testing time, test disassembly, and equipment repacking was similarly calculated. Finally, researchers timed themselves walking the distance calculated by dividing the siphon length by 30 and added that time to the total test set-up, execution, disassembly, and repacking time. A buffer of approximately one minute was added to the total to account for any unforeseen circumstances.

The test timing analysis showed that there would be enough time to increase the number of test locations to 50, or one test per approximately every four pipe segments. Exact test locations were then marked on the compiled siphon profile drawing. Based on pipe entry and exit points and timings provided by the CAP team lead, testing sites were numbered on the drawing to reflect the order that they would be visited initially for cell setup and then later for performing the test. Arrows indicating walking direction between each location were also added. Test location numbering and directional arrows were exceedingly helpful during the data evaluation phase post-inspection.

One major process bottleneck observed during prior field EIS evaluations was the hand kneading/mixing of the two-part epoxy adhesive that had been used to affix the test cells to pipe walls. In addition to being cumbersome to work with, the epoxy required long curing times and often failed to create a tight seal, resulting in cell leakage. Prior to the Agua Fria inspection, researchers tested a variety of commercially available adhesives on test coupons coated with coal tar epoxy. To replicate potential pipe wall conditions inside of the siphons, test coupons were cooled in

a freezer and then taken outside on a high temperature day to form condensation on the surfaces. Test cells were glued to the coupons and the adhesive was left to cure before the cells were filled with water. Adhesives were evaluated for ease of application, cure time needed before water could be poured into the cell, and long-term leak resistance.

An aquarium-grade silicone adhesive outperformed all other adhesive in each evaluation category. The silicone could be easily applied to the cell right out of the tube, the test cells could hold water almost immediately after being affixed to the substrate (even when wet), and none of the test cells leaked. In field conditions, the adhesive performed even better than anticipated. While efforts were made to allow the silicone to cure for a time before filling the cells with water, some unforeseen timing restrictions in certain segments of the pipe made it necessary to glue the test cells, add water, and perform the test within just a few minutes; despite these conditions the adhesive held up very well. Confidence in the adhesive also enabled inspectors to affix just the two necessary test cells to the surface, whereas in previous field work, time was taken to affix a third cell as insurance in case one of the cells leaked. Finally, as a bonus, the silicone could be removed cleanly from the pipe wall at the conclusion of the test, usually in one piece, with no visible residue remaining on the coating.

Other minor modifications to the field-testing procedure included modifying the test parameters in the testing software to shorten the duration of the testing run time. Although the result accuracy was slightly reduced, testing run time was cut in half from approximately five minutes to just over two minutes. In addition, testing the siphon very short times after dewatering also aided in decreasing the time needed to prep each test location. Because the coating was still hydrated, inspectors did not need to wait the typical overnight-to-24-hour period to re-hydrate the coating before performing the test. In some cases, as noted above, water was added to the test cells and the test could be performed within minutes.

Additional process optimizations and small tweaks to the testing plan were made during the Agua Fria inspection and applied to the Salt River trip. For example, inspectors developed efficient methods to carrying and transporting equipment, such as stringing the test cells in a stack across their bodies with an easy way to unhook one end to access the cells when needed and keeping EIS test electrodes connected and stored in a plastic bag while transporting them to the next site. Additionally, the amount of equipment carried was whittled down to the bare minimum, with carrying cases for the potentiostat and other equipment left in a safe location at the facility and not taken from site to site.

The optimum number of inspectors needed to efficiently perform the work was found to be two. After setting up the test cells and performing tests at the first few locations, inspectors fell into a consistent setup and testing procedure. During setup, one individual would thoroughly clean and dry the test area. As the second individual prepared the test cells and affixed them to the pipe wall, the first individual had already moved on to prepare the next test location. Typically, test cells were filled with water as the inspectors walked in the reverse direction, toward their pipe entry point. During testing, there was a similar staggered approach. One inspector, carrying the field laptop and all EIS supplies, would set up and perform the test. During the test disassembly and while the first inspector was moving on to the next location, the second inspector would collect DFT and UT measurements at the testing location. Due to concerns of signal interference, the DFT and UT measurements were never performed at the same time and location as the EIS testing.

Agua Fria River Siphon (2018)

Figure 6 shows the results of the EIS testing as $|Z|$ versus pipe segment tested in the Agua Fria River Siphon along with a 5-pt moving average line. The siphon profile is also shown in the inset to show the relative elevation changes from the water entry to exit points. The first 80 segments of the pipeline had much lower $|Z|$ values than at other locations throughout the pipe, likely because the steep slope at the inlet accelerated coating degradation. The direction of the waterflow, sediment in the water, pinholes, cracks, and debris could all be contributing to these decreased values. Due to the advanced coating degradation in these segments, the inspectors suggested that coating maintenance, removal, and replacement be performed on the siphon invert, around the joints, and around the full circumference in the most damaged areas. Data collected from pipe segment 120 to the outlet (excluding pipe segment 200) showed very high $|Z|$ values that suggest the coating in those areas has a life expectancy of another 10 to 20 years.

The investigation showed that coating degradation may not be uniform across a large structure. Changes to hydrologic conditions along this pipeline, i.e., slope, sediment, and turbulence, likely contributed to unique coating degradation based on these conditions. The full inspection report and specific recommendations given based on the data in Figure 6 can be found in Appendix B.

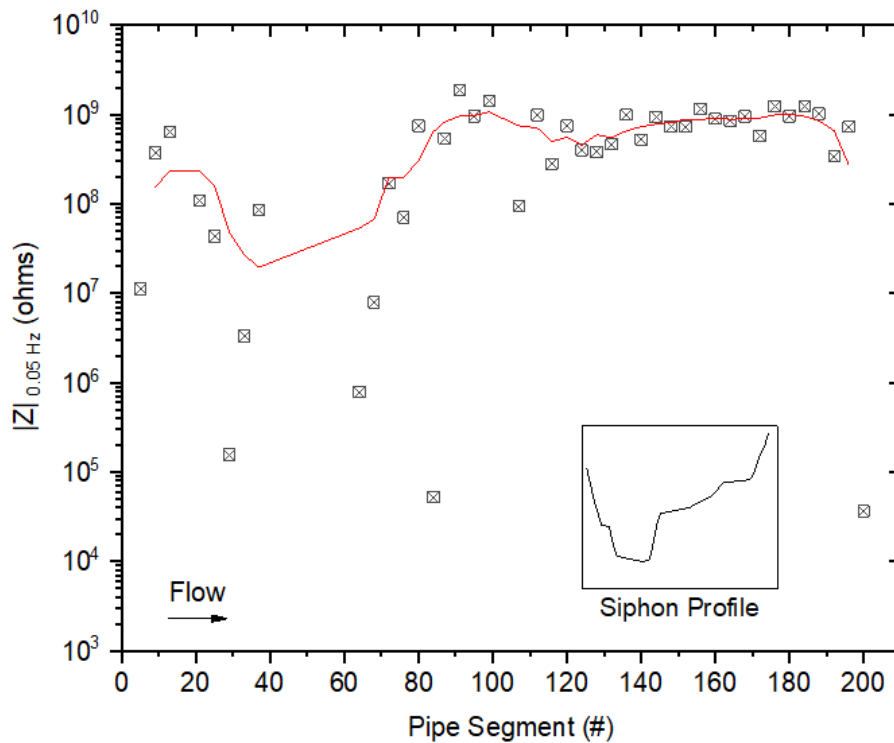


Figure 6. Low frequency $|Z|$, adjacent-averaging trendline, and siphon profile versus pipe segment at the Agua Fria Siphon.

Salt River Siphon (2018)

Figure 7 shows the results of the EIS testing performed in the Salt River Siphon, a 5-pt moving average line, and an inset graph of the siphon profile. The EIS data showed that the coating was performing well on the pipe segments nearest to the inlet as well as segments 90 to 160, where the pipe's slope was relatively gradual. At the middle and end stretches of the siphon, the slope trends

drastically downward and then up again. These locations correspond to an approximately one order of magnitude reduction in the average $|Z|$ from pipe segments 50 to 90 signifying a reduction in corrosion protection. Visual inspection of the pipe segments approaching the end of the siphon revealed severely degraded coating which was corroborated by the very low $|Z|$ measured by EIS.

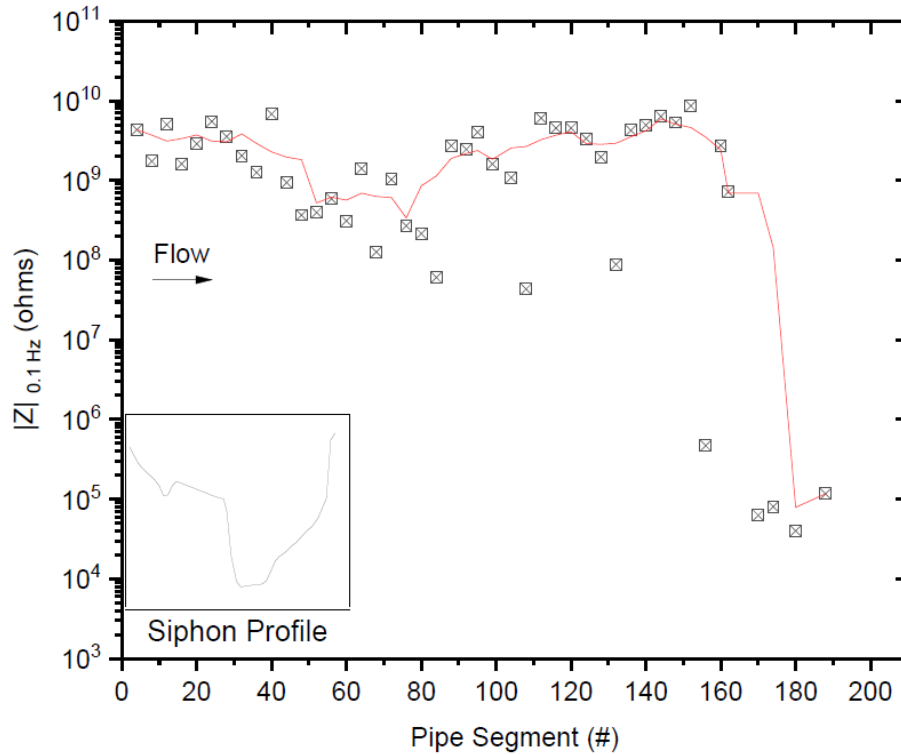


Figure 7. Low frequency $|Z|$, adjacent-averaging trendline, and siphon profile versus pipe segment at the Salt River Siphon.

The maintenance recommendations and supporting visual coating defects, DFT, and UT data can be seen with the full inspection report in Appendix C. Visual inspection aided in the evaluation by identifying locations with obvious coating damage. In general, the coal tar epoxy showed the most corrosion and coating degradation where there was a steep incline in the pipe, supporting the earlier claim that the local hydrologic conditions can have a significant impact the rate of coating degradation.

Approaches for Non-Horizontal Surfaces

Fontana Dam (2019)

Figure 8 shows the test location for the EIS evaluation of a polysiloxane coating on a non-horizontal surface. The water surface elevation allowed the researchers to access the concrete sill of the radial gates, but it limited the physical distance between the researchers and the test cells during measurement to approximately ten feet, maximum, which may have increased the amount of noise in the data.



Figure 8. Fontana Dam radial gates accessed by boat to evaluate polysiloxane coating.

The test cell locations were cleaned to improve test cell adhesion and ensure no visible defects within the test cell. Four test cells were adhered to the coating surface, as shown in Figure 2. The researcher is injecting electrolyte via the inlet port, and the needle of the second syringe is positioned at the upper-most section of the test cell to force the air bubble to evacuate. This approach reliably covered more than 95% of the coating surface area defined by the test cell with electrolyte. If left for several days, more electrolyte may be needed to replace that which hydrated the coating.

Two of the four radial gates shown in Figure 8 were selected for the inspection and three locations on each gate were identified for analysis. Although four test cells were attached at each location, the silicone sealant used did not cure properly which caused leaks that prevented analysis in all but three locations.

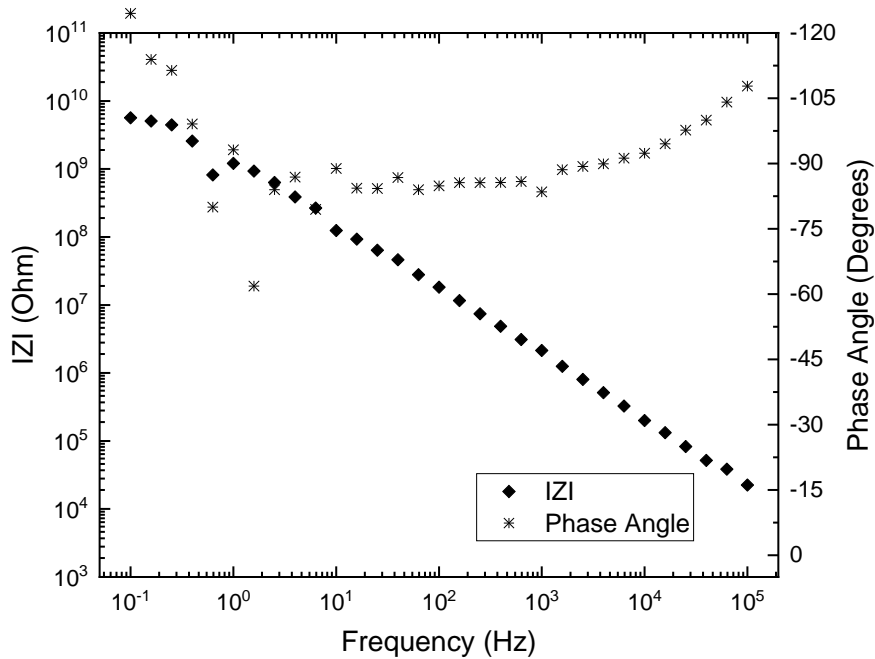


Figure 9. EIS Bode plot results for vertical test cell set-up at Fontana Dam Gate 3, Location 2.

An example of the EIS results obtained can be seen in Figure 9. The results suggest the coating was performing adequately; however, the phase angle displayed noise at frequencies below 10 Hz, likely from electromagnetic interference, which reduces confidence in the accuracy of the $|Z|$ values. In laboratory EIS testing, a Faraday cage is used to limit such interference; however, this is not feasible if field testing, resulting in ambient background electromagnetic radiation and stray capacitance in these results. Nevertheless, the testing demonstrated that EIS testing could be performed horizontally with the above described method.

Salt River Siphon (2019)

Figure 10 displays $|Z|$ values, taken at 0.1 Hz, plotted for the overhead position of every pipe segment tested. The $|Z|$ results were generally between 10^9 and 10^{10} ohms, indicating the coating was still providing protection to the structure. The $|Z|$ results at pipe segment 19 however, were significantly lower, indicating poor performance. The coating in the part of the pipe segment tested was observed to have blisters, as shown in Figure 11, which both accounted for the low values and confirmed the test method was accurately detecting impedance changes. The phase angle was approximately 50 degrees for most pipe segments, suggesting that some capacitive properties remained, and corrosion protection is being provided by the coating. The exception is for pipe segment 19, where the phase angle is 0, and the pipe is likely corroding beneath the observed blisters.

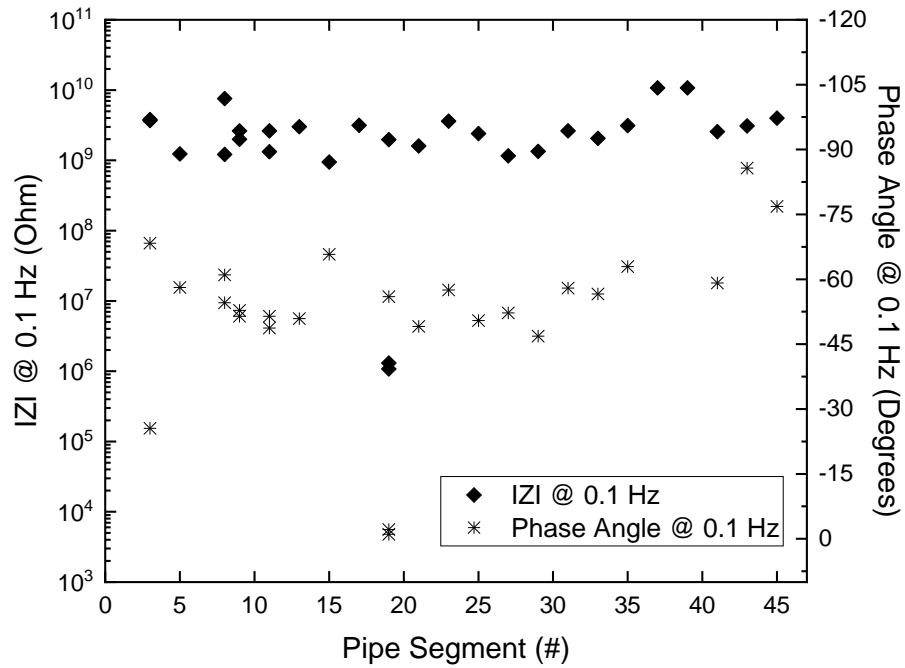


Figure 10. Low frequency $|Z|$ and phase angle versus pipe segment for overhead testing of the pipe crown at the Salt River Siphon.



Figure 11. Blistering observed at the 10:30 pipe position in pipe segment 19 of the Salt River Siphon and non-horizontal EIS test set-up.

Figure 11 also shows the test set-up during the EIS measurement with the electrodes secured by a rubber stopper. The approach is consistent with the set-up in Figure 1. All measurements were made possible by scaffolding that provided safe access to the pipe crown by the inspectors. A typical example of the Bode plots obtained at each section is shown in Figure 12; see Appendix D for the full report. Compared with the results obtained at Fontana Dam, minimal apparent noise was observed inside the siphon. The difference was attributed to electromagnetic shielding provided by the siphon structure itself, effectively acting as a large Faraday cage. At locations nearer to the opening of the siphon, scatter in the phase angle again became apparent, further evidencing the hypothesis. The smooth phase angle data greatly increases the confidence in the accuracy of the $|Z|$ values obtained, allowing for conclusions to be drawn about the coating performance.

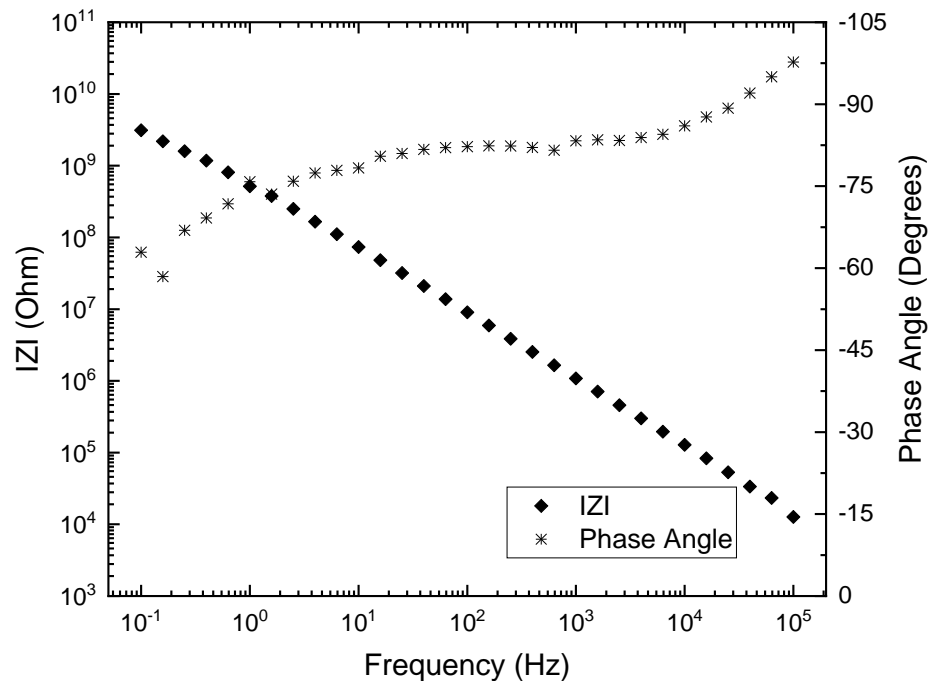


Figure 12. Representative EIS Bode plot from the 10:30 pipe position in pipe segment 35 of the Salt River Siphon.

The practice of affixing more tests cells than required at a given location proved useful as leaks were observed in several test cells. In such instances, there were enough test cells remaining to proceed with testing. Future testing of non-horizontal surfaces should apply aquarium-grade silicone. Overall, the results obtained at Salt River Siphon EIS provided a second verification that EIS testing can successfully be performed on non-horizontal surfaces.

Standardization of Testing Method

Researchers combined the advancements gained during field testing experiments to develop a draft test method under ASTM International subcommittee D01.48 with contribution from G01.11 subcommittee members. ASTM work group WK67789 drafted the test method in 2019, sending it for ballot in August 2019. The second ballot was submitted in August 2020. If accepted, the test method will be available internationally. It is anticipated that the test method will be used by coating manufacturers, quality assurance personnel, coating inspectors conducting condition assessments, etc.

Laboratory Experiments of Field Testing Parameters

Distance Between Test Cells

The objective of the test cell separation distance experiments was to determine if the measured impedance of two test cells deviated from the calculated value, based on derived impedance values for the individual test cells as a function of the test cell separation distance. The experiment also investigated the correlation of other possible experimental factors.

Equidistant Test Cells with Derived Impedance Values

The equidistant test cell arrangement on an 11-inch disk applied the two-test cell method with no electrical connection to the substrate for all measurements. The method required derivation of the individual test cells by sequentially measuring all combinations of a set of three equidistant test cells and then solving for the three unknowns.

The experiment contained three sets of three equidistant test cells, and each set provided a different distance between the respective test cells, see Figure 13 below.

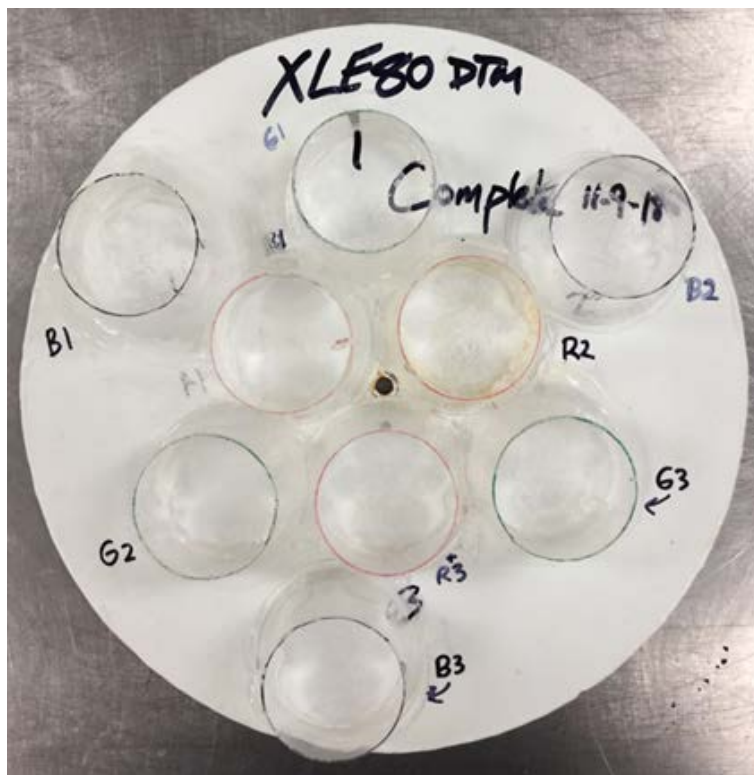


Figure 13. Image of the three equidistant test cells.

The impedance of each individual cell was obtained by evaluating the $|Z|$ of each combination of test cells within each set (e.g. R1 and R2, R2 and R3, and R3 and R1) and the average $|Z|$ for each combination was calculated. The impedance of each individual cell was then calculated by solving a system of three equations and three unknowns. Therefore, the values of X, Y, and Z are known (the average $|Z|$ for each combination), and the equations below are used to solve for R1, R2, and R3.

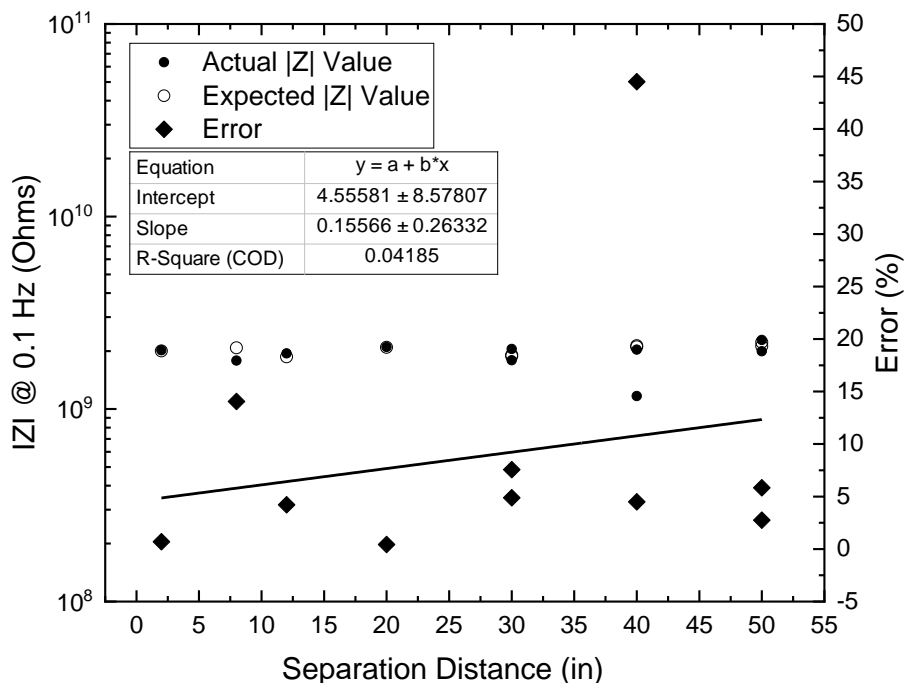


Figure 15. Effect of test cell separation distance on the accuracy of EIS measurements.

The test cell separation distance results showed no correlation between the percent error and the separation distance of the test cells, as indicated by the near-zero R^2 . The largest error observed was 45% at 40-in, which is not shown, and the $|Z|$ values were consistent—approximately 2×10^9 ohms at each of distances measured.

Coupled Counter and Reference Electrodes

Figure 16 shows the results of the uncoupled and coupled measurements, in which the RE and CE were connected to a unique, separate, electrode or connected to the same electrode, respectively. The closed symbols are $|Z|$, and the open symbols are phase angle. The data shows no significant differences in the impedance or phase angle. Therefore, the uncoupled and coupled measurement provide the same result, and either a three-electrode or two-electrode set-up can be performed for a field EIS evaluation. The experiment used several replicates with the same result; a more robust and statistical evaluation could be undertaken if necessary.

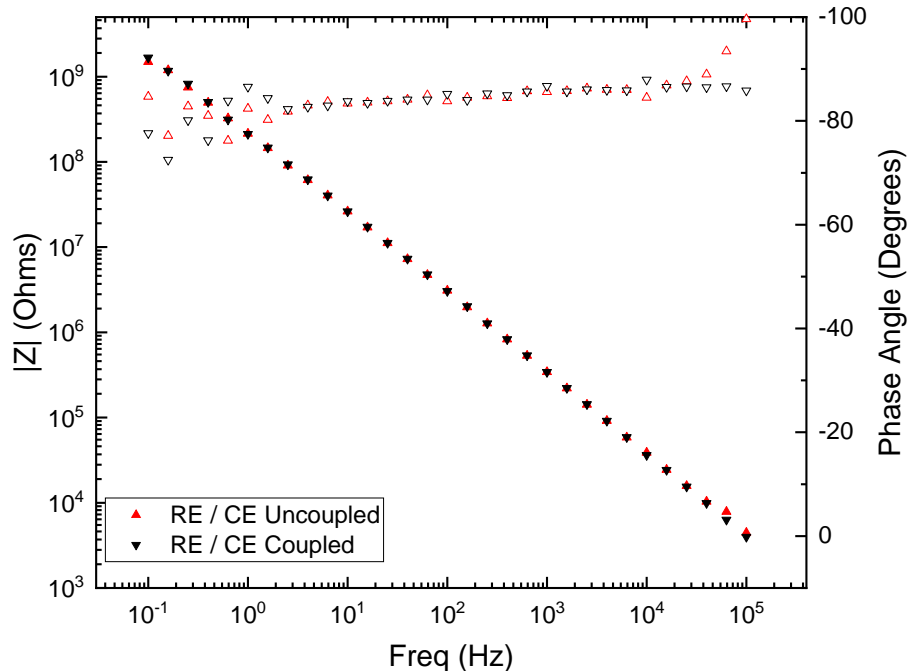


Figure 16. Bode plot of coupled and uncoupled EIS set-ups for the RE and CE.

Field Potentiostat Accuracy Measurements

The anticipated potentiostat performance is sometimes expressed by an accuracy contour plot, which shows the measurement accuracy over a range of frequencies. In these plots, limit lines are shown to represent the “contours” where a given measurement accuracy can be expected [16]. This experiment used a modified approach to evaluate the potentiostat accuracy at known resistance values, by measuring EIS on high precision resistors. The purpose of the experiment is to identify the maximum value, or the range of values, at which impedances are accurately measured.

An example of the raw data measured is shown in Figure 17. Above 10^2 Hz, the high frequency data is relatively stable. Below 10^2 Hz the data becomes unstable with the phase angle reaching up to -150 degrees. A typical coating phase angle is not more negative than -90 degrees, and the reason this occurred during the measurement of the resistor is unknown. However, the data was relatively free from noise and accuracy contour plots require only the data at frequencies less than 10^1 Hz.

Figure 18 shows the percent error for each of the combinations of resistors measured and for each of the three instruments evaluated. The lab instrument, the Femtostat, provided the highest accuracy across the broadest range of frequencies. The percent error is less than 5%, with one outlier of 20% at 3×10^{11} ohms. An example of a 20% error is a measured value of 1.2×10^9 ohms for a 1.0×10^9 ohm resistor. Whereas, a 50% error misses the expected value by half an order of magnitude, a 90% error is one order of magnitude, and a 99% error is two orders of magnitude. For the purposes of field evaluations, a percent error of less than 20% is preferred.

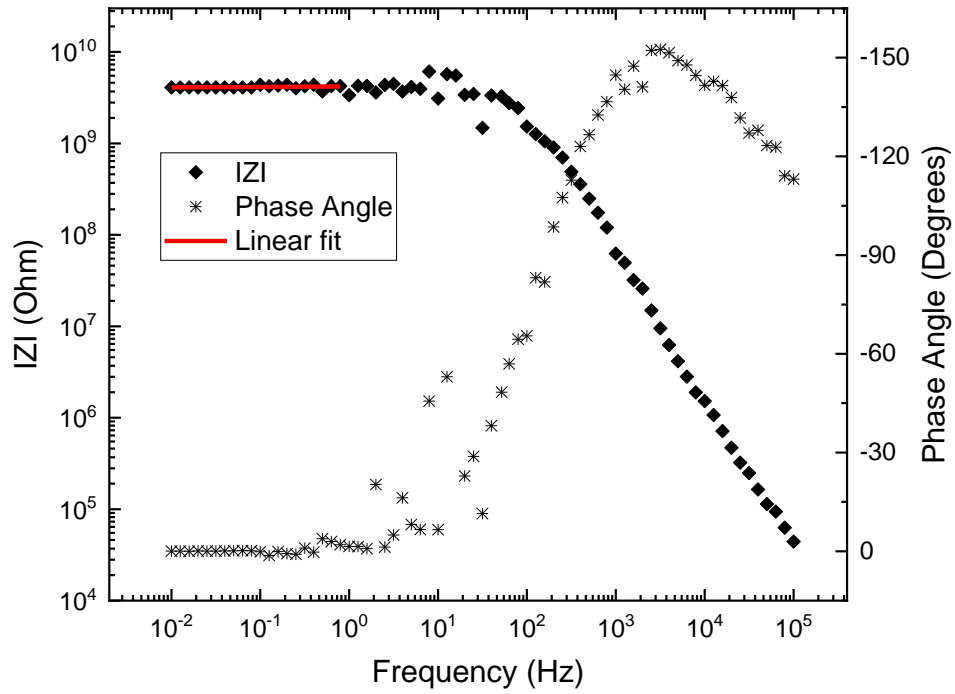


Figure 17. Bode plot of a 4×10^9 ohm resistor measured with a CompactStat.

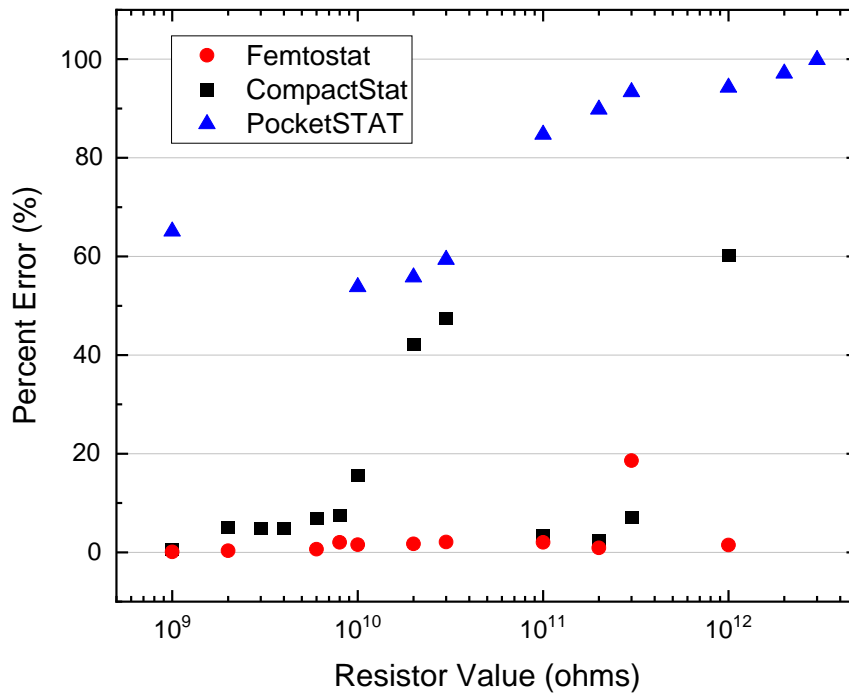


Figure 18. Percent error versus resistor value for three instruments.

The CompactStat maintained an error of less than 20% between 1×10^9 ohms and 1×10^{10} ohms. The error rose to 50% for 2×10^{10} -ohm and 3×10^{10} -ohm resistors before dropping back to less than 10% for resistors near 10^{11} ohms. The value rose again to 60% for the 1×10^{12} -ohm resistor. The reason for the increase in error around the 1×10^{10} -ohm resistors is unknown but may have been related to a poor connection of the experiment's resistor components and leads. The results suggest that the instrument provides reliable data up to approximately 1×10^{10} ohms that is sufficiently accurate for field evaluations. Additional investigations could help to better determine the accuracy between 10^{10} and 10^{11} ohms.

The PocketSTAT measured the resistors at approximately 50% error in the range of 10^9 to 10^{10} ohms. At 10^{11} ohms and higher, the error increased from 90% to 99%. This means that the instrument is missing the expected value by more than one order of magnitude at 10^{11} ohms. Some error is allowable during field measurements because a value with some known potential error is better than no data at all; however, more than one order of magnitude is too high to safely draw any conclusions. Use of the PocketSTAT for field measurements of approximately 10^{10} ohms or less should proceed with caution and account for an expected error of approximately 50%. Further investigation of the PocketSTAT using resistors less than 10^9 ohms should be completed to ensure the data is accurate in this range.

The evaluation highlights the increase in measurement error that occurs when using a potentiostat designed for field use as opposed to lab use. The CompactStat provides low error for EIS measurements at resistances that are common for typical coatings, especially when evaluating an aged for coating maintenance decisions. Caution is needed for the quality control or quality assurance evaluation of coating with initial impedance values above 10^{11} ohms (see Compilation of Long-Term Laboratory EIS Data). The PocketSTAT requires further evaluation, and in the meantime, is appropriate only for cursory coating maintenance evaluation of coatings with impedance values expected to be 10^9 ohms or less.

Long-Term Laboratory EIS Data and Field Template

For the coatings listed in Table 1, $|Z|$ at 0.01 Hz ($|Z|_{0.01 \text{ Hz}}$) and phase angle data were collected for exposure durations ranging from approximately 5 to 13 years, with most coatings containing about 10 years of data. The data was plotted by coating type, with the epoxies on one set of graphs in Figure 19, and the coal tar enamel, coal tar epoxy, polyurethane, and vinyl coatings on another set in Figure 20.

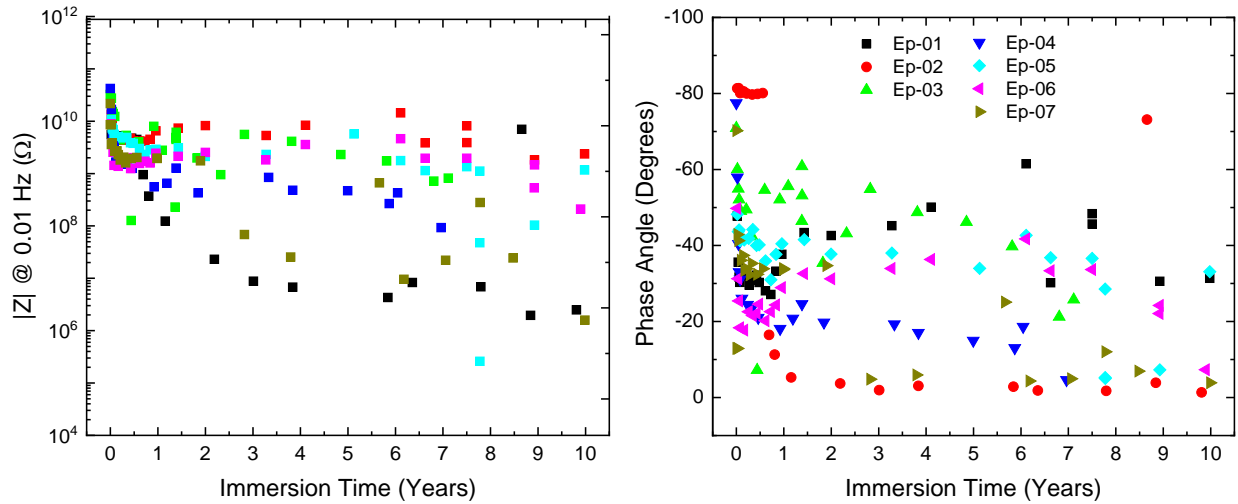


Figure 19. Epoxy coating EIS data for $|Z|$ at 0.01 Hz (left) and phase angle (right) versus immersion time in years—legend provided in right plot.

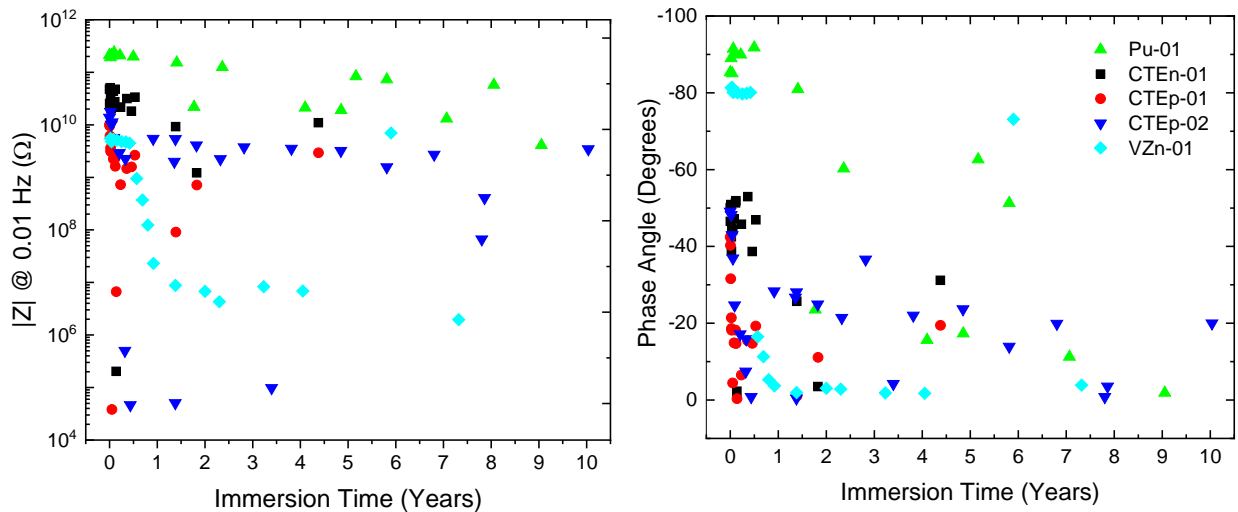


Figure 20. Coal tar, polyurethane, and vinyl coating EIS data for $|Z|$ at 0.01 Hz (left) and phase angle (right) versus immersion time in years—legend provided in right plot.

The epoxy coatings in Figure 19 have a $|Z|_{0.01 \text{ Hz}}$ of approximately 10^{10} ohms at the initial exposure, i.e., year zero. They all follow a similar trend of $|Z|$ reduction near one order of magnitude during the initial months. The ingress of water into the coating is likely contribution to this initial reduction in the $|Z|_{0.01 \text{ Hz}}$ value. After this initial coating hydration period, the continued reduction rate varied. Several coatings quickly reduced to 10^8 ohms within the first couple of years. Other coatings stabilized and remained around 10^8 or 10^9 ohms after ten years, while still a few others showed intermediate behaviors.

The epoxy coatings phase angle data in Figure 19 also varied for the different systems evaluated. However, the general trend is that the data begins in the range between -80 and -40 degrees and is quickly reduced in the first year to a value between -60 and 0 degrees. Most systems continue a gradual decline in the phase angle data to a range of -30 to 0 by year ten. A phase angle of zero indicates resistive behavior, which may be a result of corrosion at the steel interface. Based on these results, a generalization could be made for epoxy systems that a $|Z|_{0.01 \text{ Hz}}$ greater than 10^8 ohms and a phase angle more negative than -20 degrees may indicate good corrosion protection and that coating maintenance is not yet needed. Additional research is needed to verify this guideline and to validate the reduction in corrosion protection via analytical means.

The coal tar, polyurethane, and vinyl coatings in Figure 20 have a wider variation of behaviors than observed for the epoxy systems. This demonstrates that EIS can ascertain the unique material properties associate with different coating types. For each of the materials shown, data for only one or two coatings were used in the analysis. For example, the polyurethane, Coating H, recorded initial $|Z|_{0.01 \text{ Hz}}$ values above 10^{11} ohms that decreased by approximately one order of magnitude during the 9 years evaluated while the phase angle decreased from -90 to 0 degrees over the same time period. Although the $|Z|_{0.01 \text{ Hz}}$ is higher for this coating, the phase angle of 0 degrees may suggest corrosion at the interface.

The coal tar enamel, Coating I, had a $|Z|_{0.01 \text{ Hz}}$ about half an order of magnitude lower than the polyurethane with an initial phase angle of -50 degrees. There is one data point near 10^5 ohms that is likely due to an instrument artifact or short circuit as the properties are retained in future measurements. The $|Z|_{0.01 \text{ Hz}}$ decreases by about half an order of magnitude, with 5 years of testing data available, with the phase angle reducing to about -20 degrees.

The vinyl, Coating L, had a $|Z|_{0.01 \text{ Hz}}$ less than 10^{10} ohms that reduced to 10^7 ohms within 2 years and then retained this value through the remainder of the evaluation. The phase angle begins at -80 degrees then reduces to 0 degrees along the same timeline. The vinyl coating has a high volume percent of zinc pigments, and the contribution of these conductive pigments to the EIS data for interpreting its corrosion protection requires further research.

The two coal tar epoxies, Coatings J and K, have similar trends to each other with the $|Z|_{0.01 \text{ Hz}}$ near 10^{10} ohms and reduces quickly, much like the epoxy systems discussed previously. Both systems have several low-value data points, both $|Z|_{0.01 \text{ Hz}}$ and phase angle, in the first four years that appear to be instrument artifacts or short circuits in which the properties are retained in future measurements. The $|Z|_{0.01 \text{ Hz}}$ decreased to approximately 10^9 ohms during the 10 years of exposure from -50 to near 0 degrees.

A template was created to initiate the consolidation of the laboratory EIS data for the various coating evaluated. The purpose of the template is to serve as a model for future guidance toward field EIS data interpretation, as it contains information for coatings typically used on Reclamation structures.

The template in Table 2 provides the data for seven epoxy coatings, one polyurethane, one coal tar enamel, two coal tar epoxies, and a vinyl coating, each shown respectively. The data point at time year 0 represents EIS test data at one week of exposure, whereas year 5 and 10 are the nearest data points to those milestones. There is a double line to the right of the year 10 data, to the right of which are extrapolated results for years 15, 20, 25, and 30. The extrapolation utilized an arithmetic

trendlines for all available data up to year 10. The initial years are excluded due to account for hydration and stabilization of the coating. Once the data points leveled out to a linear trend, which occurred around the three-year mark for most coatings, the trend was then calculated. The trend excluded outliers that did not follow between 10-15% of the trend line. Further, the data in the table denoted with an asterisk, *, is an extrapolated value due to the test data not being available. This data is considered an estimation of the $|Z|_{0.01 \text{ Hz}}$ and phase angle that may be realized at these future exposure times.

Table 2. Long term EIS data template for $|Z|$ at 0.01 Hz and phase angle using lab data (left of break) and extrapolated information (right of break).

Coating	Year →	Lab data			Extrapolated			
		0	5	10	15	20	25	30
Ep-01	$ Z _{0.01 \text{ Hz}} (\Omega)$	1×10^{10}	4×10^9	3×10^9	3×10^9	3×10^9	2×10^9	2×10^9
Ep-01	Phase Angle (°)	-48	-31	-30	-29	-28	-27	-26
Ep-02	$ Z _{0.01 \text{ Hz}} (\Omega)$	6×10^9	5×10^9	2×10^6	5×10^5	2×10^5	9×10^4	4×10^4
Ep-02	Phase Angle (°)	-81	-6	0	0	0	0	0
Ep-03	$ Z _{0.01 \text{ Hz}} (\Omega)$	3×10^{10}	1×10^9	$4 \times 10^{8*}$	8×10^7	2×10^7	5×10^6	1×10^6
Ep-03	Phase Angle (°)	-71	-46	-17*	0	0	0	0
Ep-04	$ Z _{0.01 \text{ Hz}} (\Omega)$	4×10^{10}	5×10^8	$1 \times 10^{8*}$	4×10^7	1×10^7	5×10^6	2×10^6
Ep-04	Phase Angle (°)	-77	-15	-3*	0	0	0	0
Ep-05	$ Z _{0.01 \text{ Hz}} (\Omega)$	1×10^{10}	6×10^8	8×10^7	1×10^7	1×10^6	2×10^5	2×10^4
Ep-05	Phase Angle (°)	-48	-37	-32	-28	-24	-19	-15
Ep-06	$ Z _{0.01 \text{ Hz}} (\Omega)$	5×10^{10}	1×10^8	8×10^7	3×10^7	9×10^6	3×10^6	1×10^6
Ep-06	Phase Angle (°)	-81	-14	-6	0	0	0	0
Ep-07	$ Z _{0.01 \text{ Hz}} (\Omega)$	9×10^9	1×10^9	6×10^8	3×10^8	2×10^8	1×10^8	5×10^7
Ep-07	Phase Angle (°)	-50	-35	-13	0	0	0	0
Pu-01	$ Z _{0.01 \text{ Hz}} (\Omega)$	2×10^{11}	4×10^{10}	7×10^9	1×10^9	3×10^8	5×10^7	9×10^6
Pu-01	Phase Angle (°)	-88	-31	-8	0	0	0	0
CTEn-01	$ Z _{0.01 \text{ Hz}} (\Omega)$	5×10^{10}	$4 \times 10^{9*}$	$8 \times 10^{8*}$	2×10^8	3×10^7	6×10^6	1×10^6
CTEn-01	Phase Angle (°)	-50	-24*	-2*	0	0	0	0
CTEp-01	$ Z _{0.01 \text{ Hz}} (\Omega)$	1×10^{10}	$5 \times 10^{8*}$	$1 \times 10^{8*}$	4×10^7	9×10^6	2×10^6	6×10^5
CTEp-01	Phase Angle (°)	-42	-14*	-2*	0	0	0	0
CTEp-02	$ Z _{0.01 \text{ Hz}} (\Omega)$	1×10^{10}	3×10^9	3×10^9	2×10^9	2×10^9	1×10^9	1×10^9
CTEp-02	Phase Angle (°)	-49	-24	-20	-17	-15	-13	-10
VZn-01	$ Z _{0.01 \text{ Hz}} (\Omega)$	6×10^9	2×10^7	3×10^6	2×10^6	9×10^5	5×10^5	3×10^5
VZn-01	Phase Angle (°)	-81	-7	-4	-1	0	0	0

* Extrapolated value due to the lab test data not being available.

The data format provided in Table 2 is a first approximation for evaluating remaining service life of interest to this discussion, and the extrapolated values do not necessarily correlate to observed field performance. For example, coal tar enamel provides a service life near 50 years, which may not be well reflected by the short exposure of this laboratory analysis. Further analysis of these coatings at additional years of exposure and with additional replicates is needed to increase accuracy and

validate the table. A verified version of this template can be used in conjunction with field EIS analysis to estimate a coating's remaining service life. In the field, for example, the $|Z|_{0.01 \text{ Hz}}$ and phase angle values are measured for a known coating and then compared to the table. When the values are found, the estimated service life remaining can be directly read by moving up the column to the year row. This evaluation advances the practice of estimating remaining service life of the coating.

To further this advancement, a possible next step is to perform laboratory exposure and EIS measurement on additional replicates of the coatings shown in Table 2. The additional replicates will help to confirm the degradation curve for each coating. Once the degradation curve is reliable in terms of repeatability and statistical significance, the end of the coating's usable service life should be determined. The full degradation curve, which identifies the final year of service, could then be converted to a percent-based curve that shows $|Z|_{0.01 \text{ Hz}}$ and phase angle versus percent service life remaining.

Conclusions

Field and laboratory experiments were undertaken to further develop and validate the EIS testing method for coating analysis. The following conclusions were made as a result those experiments:

- Agreement between field and laboratory data indicates the method is suitable for quantitative analysis of coatings on Reclamation infrastructure.
- Robust testing plans can and should be utilized to analyze coatings on large structures.
- EIS testing can successfully be performed on non-horizontal surfaces.
- Test cell separation distance is not a factor in the accuracy of results, increasing ease of use in field applications.
- A single electrode can serve as both counter and reference electrode, further simplifying set up.
- The accuracy of EIS results varies with instruments, and of the portable instruments assessed, the Ivium CompactStat was recommended for field use for coatings anticipated to have impedance values less than 10^{10} ohms. The PocketSTAT is not recommended for coatings anticipated to have impedance values greater than 10^9 ohms.
- A suggested template format that could serve as a guide for determining the remaining service life of a coating based on extrapolated EIS laboratory data for the same systems was proposed.

In conjunction with traditional coating analysis techniques, EIS testing can be used to determine the effectiveness of a coating at preventing corrosion. The method provides a quantitative means to approximate remaining service life which is essential for scheduling maintenance at appropriate intervals. The field EIS testing method, if standardized through ASTM, should be considered for maintenance inspections and quality control during coating contracts. Future research should continue to improve the applicability and accuracy of the information within the long-term EIS data template.

References

- [1] Merten, B. J., "Coating Evaluation by Electrochemical Impedance Spectroscopy (EIS)," Report No. ST-2016-7673-1, U.S. Department of the Interior, Bureau of Reclamation, Research and Development Office, 2015.
- [2] Merten, B. J. E., Walsh, M. T., and Torrey, J. D., "Validation of Coated Infrastructure Examination by Electrochemical Impedance Spectroscopy," *Advances in Electrochemical Techniques for Corrosion Monitoring and Laboratory Corrosion Measurements, ASTM STP1609*, S. Papavinasam, R. B. Rebak, L. Yang, and N. S. Berke Eds. ASTM International, West Conshohocken, PA, 2019.
- [3] Merten, B. J., Gaston, T., Torrey, J., and Skaja, A., "Developing a Life-Cycle Cost Analysis Framework to Evaluate the Cost- Effectiveness of Hydroelectric Penstock Corrosion Control Strategies," presented at *CORROSION 2017*, New Orleans, LA, March 2017, NACE, Houston, TX.
- [4] Sonke, J., "Scientific Coating Inspection," *Protective Coatings Europe*, 2012.
- [5] Bordziłowski, J., Królikowska, A., Bonora, P. L., Maconi, I., and Sollichc, A., "Underwater EIS Measurements," *Progress in Organic Coatings*, Vol. 67, 2010.
- [6] Gray, L. G. S., Drader, B., O'Donoghue, M., Garrett, R., Graham, R., Datta., V.J., "Using EIS to Better Understand Tank Lining Performance in Laboratory and Field Evaluation," presented at *CORROSION 2003*, NACE International.
- [7] Gray, L. G. S., and Appleman, B. R., "EIS: Electrochemical Impedance Spectroscopy, A Tool to Predict Remaining Coating Life?," *Journal of Protective Coatings & Linings*, Vol. 20, No. 2, 2003.
- [8] Bordziłowski, J., Darowicki, K., Krakowiak, S., and Królikowska, A., "Impedance Measurements of Coating Properties on Bridge Structures," *Progress in Organic Coatings*, Vol. 46, 2003.
- [9] Tsai, C. H., and Mansfeld, F., "Determination of Coating Deterioration with EIS: Part II. Development of a Method for Field Testing of Protective Coatings," *CORROSION*, Vol. 49, No. 9, 1993.
- [10] Merten, B. J., Skaja, A., Tordonato, D., and Little, D., "Re-evaluating Electrochemical Impedance Spectroscopy (EIS) for the Field Inspector's Toolbox: A First Approach," SSPC 2014, SSPC: The Society for Protective Coatings.
- [11] Merten, B. E., "Electrochemical Impedance Methods to Assess Coatings for Corrosion Protection " Technical Publication No. 8540-2019-03, U.S. Department of Interior, Bureau of Reclamation, Denver Technical Service Center, Materials and Corrosion Laboratory, 2019.
- [12] Allahar, K., Su, Q., and Bierwagen, G., "Non-substrate EIS Monitoring of Organic Coatings with Embedded Electrodes," *Progress in Organic Coatings*, Vol. 67, No. 2, 2010.

[13] Qi, X., Hinderliter, B., and Gelling, V. J., "A New Two Electrode Surface Impedance Sensor: Responses to the Accelerated Weathering Induced Coating Inhomogeneity," NACE, Houston, TX, 2007.

[14] Qi, X., Hinderliter, B., and Gelling, V. J., "Two-Electrode Electrochemical Impedance Sensor: Part 1—Response to Coating Degradation on Conductive Substrates," presented at *CORROSION 2009*.

[15] Merten, B. J. E., Prochaska, S. O., and Tordonato, D. S., Pittsburgh, PA, "Comparison of Field Impedance Measurements to Laboratory Data," Orlando, FL, 2019.

[16] "Accuracy Contour Plots-Measurement and Discussion," Gamry Instruments, accessed September 28, 2020 from <https://www.gamry.com/application-notes/EIS/accuracy-contour-plots-measurement-and-discussion/>, 2012.

Data Supporting the Final Report

Data from this project is stored within the folders at the following file path:

- Share Drive folder name and path where data are stored:
T:\Jobs\DO_NonFeature\Science and Technology\2013-PRG-Field Validation of Impedance Spectroscopy Coating Assessments
- Point of Contact: Bobbi Jo Merten, bmerten@usbr.gov, 303-445-2386
- Data saved for this project includes raw data files for field and laboratory electrochemical impedance spectroscopy (EIS) measurements, compiled plots of EIS data, supporting figures or images. Data was collected using software from Gamry Instruments and Ivium and the resulting file types are .idf, .dta, .xlsx, .opj, and .jpeg.
- Keywords: field impedance spectroscopy, electrochemical impedance spectroscopy (EIS), field EIS testing, impedance testing, maintenance planning, coating service life
- Approximate total size of all files: 600 MB

Appendix A – SSPC 2019 Manuscript

COMPARISON OF FIELD IMPEDANCE MEASUREMENTS TO LABORATORY DATA

Bobbi Jo E. Merten, Ph.D. Coatings Specialist, Bureau of Reclamation
Stephanie O. Prochaska, M.S. Materials Engineer, Bureau of Reclamation
David S. Tordonato, Ph.D., PE Materials Engineer, Bureau of Reclamation

Abstract

Ongoing validation of field electrochemical impedance spectroscopy (EIS) testing has shown that the method can provide valuable information for evaluating coated structures, particularly hydraulic steel structures. EIS data gives a quantitative value for a barrier coating's resistance to water and ions. Therefore, it is a good indicator of the overall corrosion protection. Possible uses of EIS data include determining the correct timing of coating maintenance and quality assurance testing during coating contracts.

This research evaluates EIS data obtained from coated structures in the field and laboratory coupons of the same coatings. The coupons undergo accelerated weathering and immersion exposures, whereas the coated structures have a defined, but variable, in-service exposure. Both test approaches are non-destructive, and the testing apparatus is temporary and is removed after testing is complete. Data collection requires specialized potentiostats to perform the respective lab and field evaluations.

EIS data from polyurethane, coal tar epoxy, and coal tar enamel linings are analyzed. The degradation modes of the field and lab exposures are compared and contrasted. Discussion includes the use of laboratory data as a benchmark for evaluating the same coating products in the field while considering possible variations as a result of different batches, film formation conditions, or service conditions. Quantitative criterion for failing or underperforming coating systems is suggested.

INTRODUCTION

Electrochemical impedance spectroscopy (EIS) is a quantitative test used to evaluate protective coatings on metal substrates (1-6). It provides a sophisticated, non-destructive analysis of the coated substrate as if it were an electrical circuit composed of resistors and capacitors. Determining this circuit and its properties is important to assess the level of corrosion protection provided by barrier-style protective coatings. These coatings prevent corrosion by impeding the ionic current transfer between anodic and cathodic locations on the metal substrates. This requires good adhesion and a high coating resistance (3,7).

The coating pore resistance, R_{pore} , is responsible for limiting ionic diffusion and is attributable to the physical arrangement and chemical properties of the coating's polymer chains. As the polymer chains shift or degrade, pores and channels develop in the coating, which increases the mobility of water or electrolyte. A low or reduced R_{pore} correlates to a decrease in corrosion protection.

The coating capacitance, C_{coat} , is also attributable to the properties of the polymer chains in the coating. Equation 1 provides the relationship between C_{coat} and the dielectric constant, ϵ_y , for a coated substrate immersed in an electrolyte, where ϵ_o is the electrical permittivity, A is the surface area exposed to electrolyte, and d is the distance between the metal and the electrolyte, i.e., the coating thickness.

$$C_{coat} = \frac{\epsilon_o \epsilon_y A}{d} \quad \text{Equation 1}$$

Coatings have a ϵ_y ranging from 2-7, whereas water is 78.4 at 25 °C (1,8). This large difference between the two materials allows the derived C_{coat} value to be approximated to the water uptake of a coating (9). An increased water concentration in the coating may correlate to a reduction in corrosion protection.

Data Interpretation and Analysis

EIS has several options for processing the data. The extraction of R_{pore} and C_{coat} via an equivalent circuit model (ECM) is one approach, which provides a theoretical model of a coated substrate as some combination of resistors and capacitors. Computer software is commonly used to perform an ECM analysis.

The simplest approach to EIS analysis is through interpretation of the raw impedance data using a Bode plot and Nyquist plot. The Bode plot shows the impedance magnitude, $|Z|$, versus the measurement frequency, typically 10^{-2} Hz to 10^5 Hz. This allows the user to evaluate the results at each frequency. The ECM describing coated substrates arranges a resistor and capacitor in parallel for each component of the circuit, and the capacitors are frequency dependent. Therefore, high frequency data corresponds to the electrolyte solution resistance, mid-range frequencies reveal coating properties, and the lowest frequencies include long timescale activities such as the corrosion reactions occurring at the coating-substrate interface (8,10). The resistive elements are in series, therefore additive, which means that the low frequency data is the sum of all resistances in the circuit. Assuming that the electrolyte solution, cables, and instrument components contribute negligible resistance, the low frequency EIS data is equivalent to the total corrosion resistance of the coating itself.

The Bode plot also shows the phase angle versus frequency. The phase angle is the difference, in degrees, by which the current response lags the applied voltage signal of the electrical circuit established in the EIS test. Pure resistors are in phase, i.e., 0 degrees, whereas pure capacitors are -90 degrees out of phase.

The Nyquist plot is a complex plane presentation of the EIS data. It shows the imaginary impedance versus the real impedance, where $|Z|$ is the radius of a data point, positioned at the phase angle, in degrees, to the x-axis. Frequency-dependent information is not easily determined in this plot type. However, the shape of the curve in the Nyquist plot helps to identify the number of time constants, or resistor-capacitor ECM elements in the coated substrate. Other features of the circuit, such as the Warburg element for diffusion limited corrosion reactions, may also be apparent.

Field EIS Testing

EIS is an assessment tool which can be used to complement traditional non-destructive examinations techniques such as visual inspection and dry film thickness (DFT) testing in the field. EIS allows for consistent, data-based decision making by providing data to quantitatively determine the level of corrosion protection provided by the coating. All coatings degrade while in service, and the field EIS data allows facility owners to establish a pre-determined threshold for removing and replacing a coating. Similarly, including field EIS quality control testing as a component of coating specifications could lead to more successful coating projects.

A thorough assessment of an aged, coated structure includes field EIS testing. Field EIS focuses on the undamaged coating, allowing the inspector to quantify coating performance in these areas. Traditional inspection enhances field EIS testing and results in the qualification and quantification of visible coating defects and damage. Both sets of information are valuable in order to provide a comprehensive analysis of the protective coating on critical structures.

Field EIS testing evaluates distinct locations rather than the entire coating surface. A probability plot of the data can help to determine whether a specified threshold value was exceeded (11,12). This approach requires at least thirty data points for the result to be statistically significant. The research presented here gives examples of this approach.

Laboratory EIS Testing

Laboratory EIS data provides a baseline for interpreting field EIS data. This research compares field EIS data to analogous materials in laboratory immersion exposure. Laboratory data is important because it allows for controlled experiments. The investigations often span long time scales with occasional EIS test measurements. These controlled experiments provide insight to the typical process of coating degradation. Understanding this process for a specific product, or even for a generic coating type, allows for the information to be applied during interpretation of field results.

EXPERIMENT

Materials and Exposure

Water resource structures provided the coating materials evaluated in their field exposure. The structures are mild steel with a protective lining in raw water immersion service. Facility staff supplied information on the coating type, age, and service conditions, which was verified by observations during the field experiments. Table 1 provides the service data for each lining.

Table 1. Service data for raw water linings evaluated.

Coating	Structure	Thickness (mils)	Time in Service (Years)	Service Notes
Coal tar enamel	Hydroelectric Penstock	30-40	85	American Water Works Association (AWWA) C203 material in service at an elevation of 7,800 feet
Polyurethane	Conduit Pipe	20	20	Municipal pipe in service at an elevation of 5,500 feet
Coal tar epoxy	Siphon	30	21	In service at an elevation of 1,500 feet

Laboratory testing proceeded by application of nominally identical products to those evaluated in the field experiments. The coupons received immersion exposure using an aerated water bath of dilute Harrison solution (DHS). The DHS is 0.35 weight percent (wt. %) ammonium sulfate and 0.05 wt. % sodium chloride at $25\text{ }^{\circ}\text{C} \pm 2\text{ }^{\circ}\text{C}$. The coupons were removed from the water bath exposure for periodic EIS evaluation.

Sample Preparation

The field structure steel surface preparation likely involved abrasive blasting, but exact details are unknown. The linings were factory-applied with field application occurring at joints and post-installation repair areas.

Laboratory evaluation utilized steel coupons measuring 3-inch x 6-inch x 1/8-inch. The surface was solvent cleaned in accordance with Society for Protective Coatings (SSPC)-SP1 and abrasive blasted to SSPC-SP10 near-white metal. Coating application proceeded in accordance with manufacturer data sheets.

Test Cell Set-Up

Preparation for field test cells required cleaning with a wet rag, followed by a dry rag. Each selected test cell surface contained no visible defects and was accessible for the testing equipment. The horizontal surface or lower side wall of the pipe provided the most practical site for the test location. A 2.25-inch diameter disposable plastic test cell served as the electrolyte reservoir for EIS testing. The test cell was adhered to the prepared surface using an aquarium-grade silicone or two-part marine epoxy adhesive (Figure 1). Following at least one hour of cure time, approximately 50 mL of electrolyte was added to each test cell. The coal tar enamel and polyurethane experiments used DHS, while the coal tar epoxy used tap water. The solution was allowed to saturate the coating overnight, which also begets an electrochemical steady-state at the coating-steel interface.



Figure 1. Surface preparation and application of three temporary EIS test cells along lower pipe wall.

The laboratory test set-up affixed a 2.25-inch diameter glass cylinder to the coated coupon surface via an *o*-ring and a clamp. Approximately 50 mL of DHS solution is added to the test cell. The EIS test did not require a wait time provided the test cell assembly occurs at the time the coupon is removed from immersion.

Instruments and Equipment

Field EIS testing employed an Ivium Compactstat potentiostat. The instrument received power from a ruggedized laptop and was operated using dedicated software on the same laptop. Each measurement required two test cells in lieu of connection to the substrate (12-15). The instrument cables completed the electrical circuit via attachment to a copper-copper sulfate (CSE) pencil-style reference electrode (RE) and platinum mesh counter electrode (CE) suspended in Cell 1 and a second platinum mesh suspended in Cell 2 as the working/working sense electrode (WE). The third cell provides an alternative cell that can be used if the Cell 1 or Cell 2 adhesive does not seal properly or if additional testing is desired at that location. Figure 2 shows this set-up.



Figure 2. EIS test set-up with three test cells (behind the laptop) at a test location within pipe; two of the test cells contain the suspended electrodes for the EIS test measurement.

Laboratory testing employed a Gamry Femtostat with dedicated software. The set-up used the traditional three cell method. The RE and CE were a saturated calomel electrode (SCE) and platinum mesh, respectively. A corner of coupon was ground to bare substrate for direct instrument cable connection as the WE.

Test Method

The field EIS test applied a 50 mV sinusoidal perturbation to the coated substrate. The measurement frequency range was 10^5 Hz to 0.05 Hz, recording five points per decade.

Measurements were performed at the open circuit potential. Occasional variation in the applied experimental parameters occurred in an effort to reduce measurement time, acquire lower frequency data, etc.

The laboratory test applied a 15 mV sinusoidal perturbation to the coated substrate. The applied frequency range was 10^5 Hz to 10^{-2} Hz at ten points per decade. Measurements were performed at the open circuit potential.

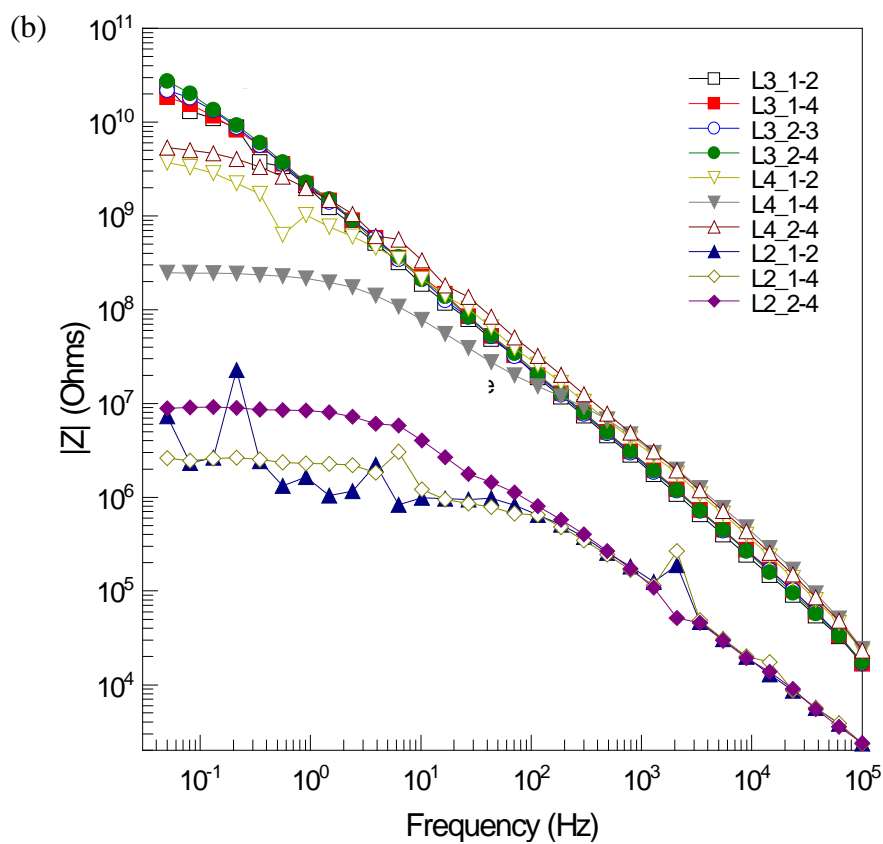
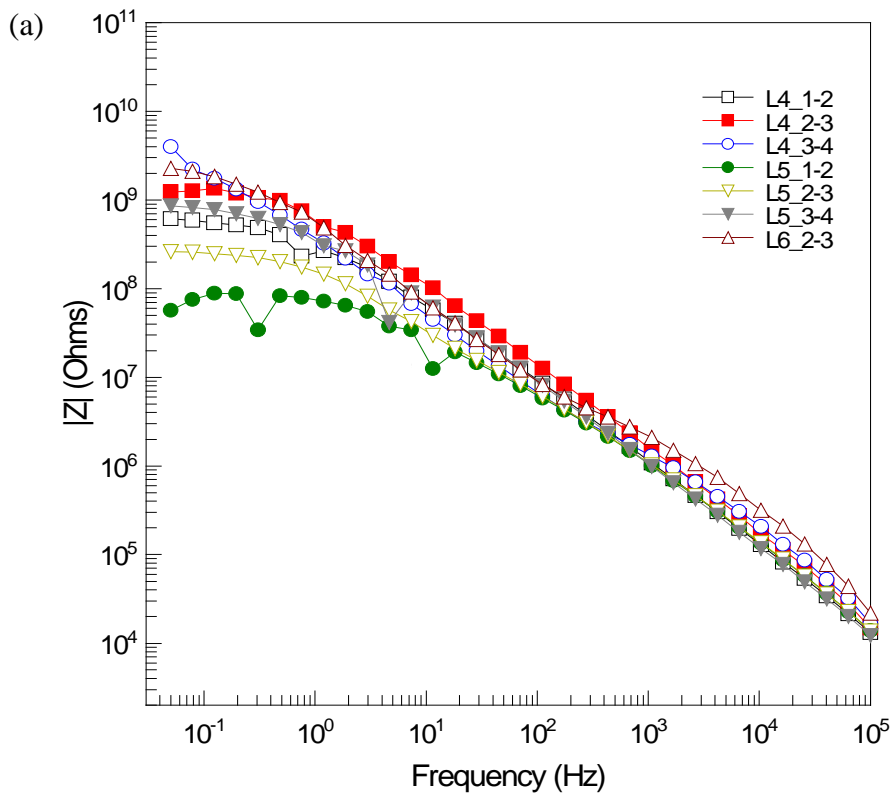
RESULTS AND DISCUSSION

The conditions of the substrate surface preparation and coating application are unknown for most in-service coated structures. In some cases, the question of whether it was field-applied or factory-applied is also not known or easily determined. The application of field EIS testing method and analysis must provide a robustness that overcomes these unknown conditions.

Field EIS Data

Plotting the raw field EIS data using Bode plots provides the inspector information on the degree to which the coating prevents water and ions from migrating through the coating. Most equipment displays this data as the measurement is being performed. A high $|Z|$ value at the lower frequencies of the Bode plot indicates a strong barrier to water and ions, which generally indicates a good corrosion resistance. An approximate value for good corrosion resistance is $|Z| > 10^8$ ohms at 0.1 Hz, whereas $|Z| < 10^6$ ohms indicates low corrosion resistance (3,16). These values can be established as thresholds for corrosion protection of a structure and may be most applicable to structures that are critical, in immersion service, or infrequently accessible for inspection or maintenance. A selected corrosion resistance threshold value should trigger a maintenance activity, typically a full recoating. The threshold for an atmospheric coating on a non-critical structure may be lower, such as a $|Z|$ of 10^6 ohms, at 0.1 Hz.

Figure 3 provides field EIS Bode plots of coal tar enamel, polyurethane, and coal tar epoxy linings, respectively, showing $|Z|$ versus frequency only. The low frequency is 0.05 Hz, which extends slightly beyond the 0.1 Hz threshold value discussed above. Each dataset represents an EIS test measurement. Figure 3(a) and 3(b) include data for three test locations within the pipe, defined as $L\#$, whereas Figure 3(c) shows a unique test location for each dataset. The test location characterizes a distinct area of the coated structure, often several hundred feet from the next location, while the test cells evaluated are separated by several inches. Similarly, as shown in Figure 3(a) legend, L4_1-2 and L4_2-3 both evaluated test cell #2. The former did so in combination with test cell #1, while the latter used test cell #3.



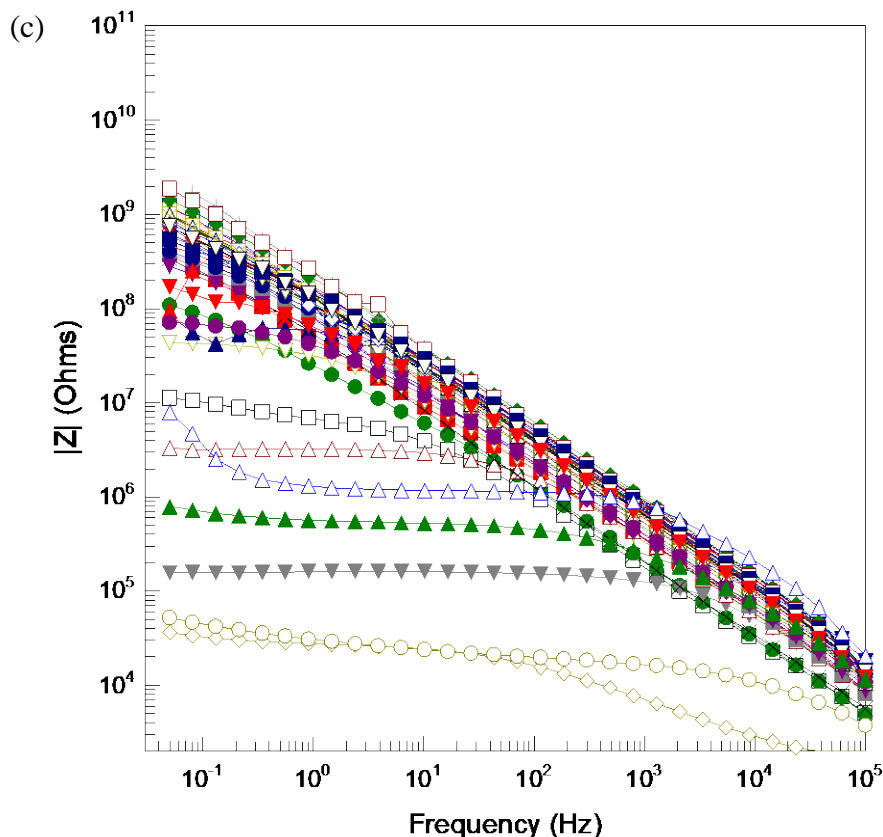


Figure 3. Field EIS data showing impedance magnitude, $|Z|$, versus measurement frequency for (a) coal tar enamel, (b) polyurethane, and (c) coal tar epoxy linings.

The data in Figure 3(a) show good agreement between the three locations evaluated, with an overall rating of good corrosion resistance, i.e., $> 10^8$ ohms. One or two of the test cells at L5 likely has a lower corrosion resistance. This could be caused by a small crack or pinhole that is not visible. All of the datasets in Figure 3(a) deviate from a 45-degree slope at frequencies less than 10^1 Hz, suggesting that resistive behavior is present (see phase angle discussion below).

Figure 3(b) has poor agreement between the three test locations; L3 has very good corrosion resistance, L4 has good corrosion resistance, and L2 has a corrosion resistance sufficiently low to trigger a maintenance activity. The test cells for L4 likely have a few small cracks or pinholes and L2 has more extensive degradation. The data in Figure 3(b) suggests that areas of the lining are experiencing degradation at different rates. Another explanation could be that certain locations received underperforming lining at the time of application. Either way, the results indicate that more data is needed to determine meaningful or statistically significant conclusions for decision making purposes.

Figure 3(c) presents forty-two datasets, each taken at a unique test location on the pipe lining, occurring approximately every fourth pipe stick within the 10,000-foot-long coated structure. All but seven of these measurements show consistent $|Z|$ results of approximately 10^8 to 10^9 ohms at 0.05 Hz, suggesting that the lining is providing good corrosion resistance. The seven measurements with lower $|Z|$ values may be caused by a small crack or pinhole that is not visible.

Figure 4 provides the Bode plot for phase angle versus measurement frequency for the polyurethane lining as an example; the coal tar enamel and coal tar epoxy linings are similar. The objective of a barrier coating is to behave as a pure capacitor, which has a phase angle of -90 degrees. The onset of resistive behavior indicates the movement of charge, either as ions through the coating or electrons across the interface. Charge transfer across the interface is the result of corrosion reactions.

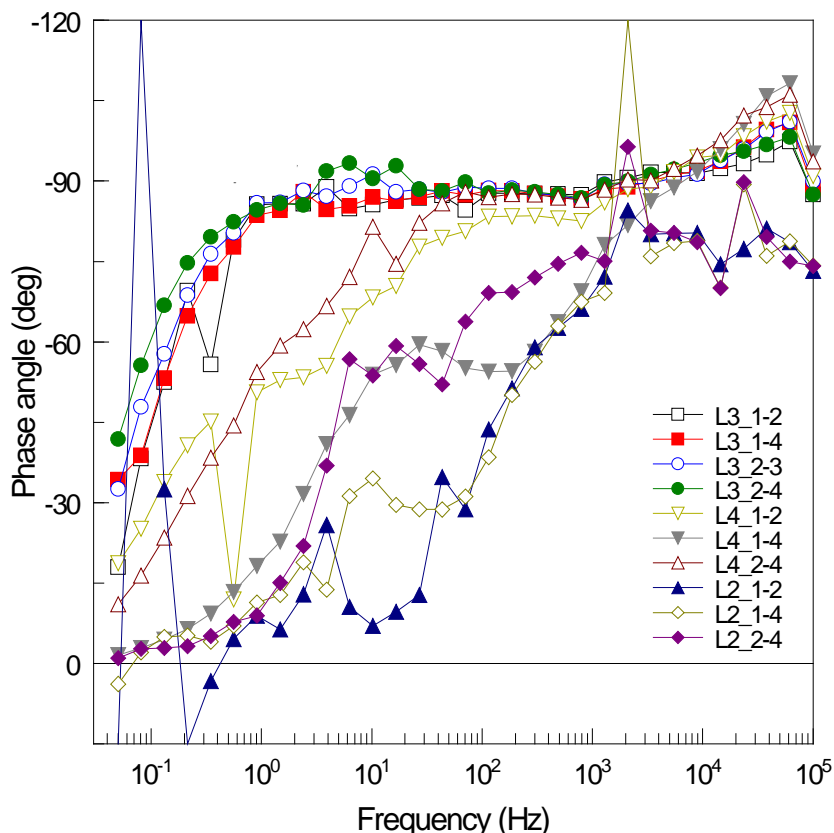


Figure 4. Field EIS data showing phase angle versus measurement frequency for the polyurethane lining.

All data in Figure 4 shows the onset of resistive behavior at some frequency less than approximately 10^3 Hz as the phase angle approaches 0 degrees. The data for L2 has the most resistive behavior, which is consistent with the $|Z|$ data previously discussed. Likewise, the polyurethane L3 data is the least resistive and is likely providing the best corrosion protection. However, for each of these results, the data suggests that corrosion activity beneath the lining is possibly occurring.

Probability plots provide a simple technique for organizing the raw field EIS data into a useful approach for decision making. Application of a 10% probability method allows an end-user to make a decision based on quantitative data and statistical analysis. In this proposed approach, if there is greater than a 10% probability that the mean impedance ($|Z|$) fails to meet a defined threshold, coating maintenance is recommended. The method involves plotting the $|Z|$ values (of a pre-determined low frequency) versus the calculated percentiles on a lognormal-

probability plot. The result should be an approximately linear distribution of data points. If the 10% point on the linear trendline for the $|Z|$ data is lower than the selected maintenance threshold value for $|Z|$, coating maintenance is recommended. Note that this method assumes the data fits a lognormal distribution.

Figure 5 provides a 10% probability plot with linear trendlines for the three linings for interpreting results based on a maintenance threshold of 10^7 ohms. The coal tar enamel and polyurethane datasets contain too few data points for the resulting trendline to be significant. However, for illustration purposes, the trendline for polyurethane fails to meet the threshold for $|Z|_{0.05\text{ Hz}} > 10^7$ ohms at 10% probability, triggering a coating maintenance activity, whereas the coal tar enamel trendline surpasses 10^7 ohms and would not require maintenance. The coal tar epoxy data is statistically significant and gives a $|Z|_{0.05\text{ Hz}}$ value of approximately 8×10^6 ohms at 10% probability, indicating that maintenance or replacement of the lining should be considered.

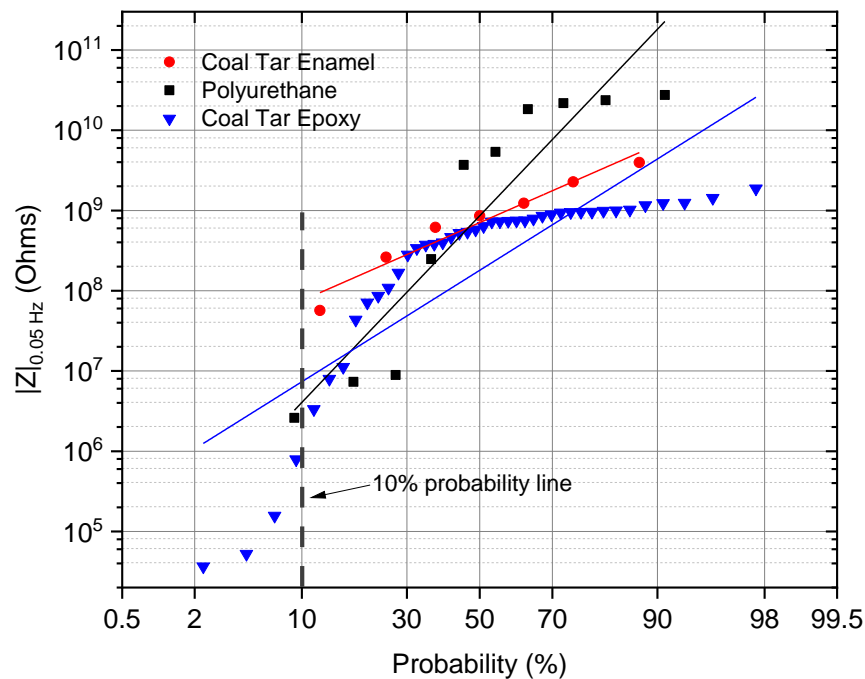


Figure 5. Probability plot of $|Z|_{0.05\text{ Hz}}$ for field EIS data.

The linear fit for coal tar epoxy has a value of $R^2 = 0.69$, which is apparent by the poor correlation of the fit line to the data points. The poor fit indicates a deviation from the assumed lognormal-probability distribution and requires further investigation. The seven measurements identified as possibly containing a crack or pinhole, shown in Figure 3(c), may be contributing to the non-linear outcome. A crack or pinhole allows current to easily pass through the linings and results in an artificially low plotted value. Put another way, the corresponding data does not represent the condition of a defect-free lining at that test location.

The change from a defect-free lining to one with non-visible defects likely occurs below the 30% probability line in Figure 5. This is supported by a distinguishable change in the slope of the data. A linear analysis of the two perceived trends provides an R^2 of 0.97 for the 13 lowest

data points and an R^2 of 0.91 for the remaining range; both results suggest a good fit. A subsequent review of the residuals versus fits reveals a non-random pattern, confirming that additional bias is present in the data.

Figure 6 further investigates the randomness of the distribution by plotting the $|Z|_{0.05 \text{ Hz}}$ versus the test location, by pipe segment, within the 10,000-foot-long, coal tar epoxy-coated structure. A 5-point adjacent-averaging trendline is also included in the plot. The results show anomalous data points from pipe segment 0 to 90, while the subsequent data has excellent corrosion resistance, with $|Z|_{0.05 \text{ Hz}}$ consistently near 10^9 ohms. Pipe segment 0 is the inlet, which possibly experiences more severe conditions. The visual inspection notes and photographs indicate that sediment and turbulent water due to pipe slope changes contributed to the low $|Z|$ data in pipe segments 0 to 90. Therefore, traditional inspection techniques must be used in conjunction with EIS data analysis to identify and explain causes for variations in data as a result of dependence on other parameters, such as location within the pipe. In this case, the outcome for data-based decision making is location-specific and supports a recommendation to reline underperforming stretches of the coated structure, i.e., pipe segment 0 to 90.

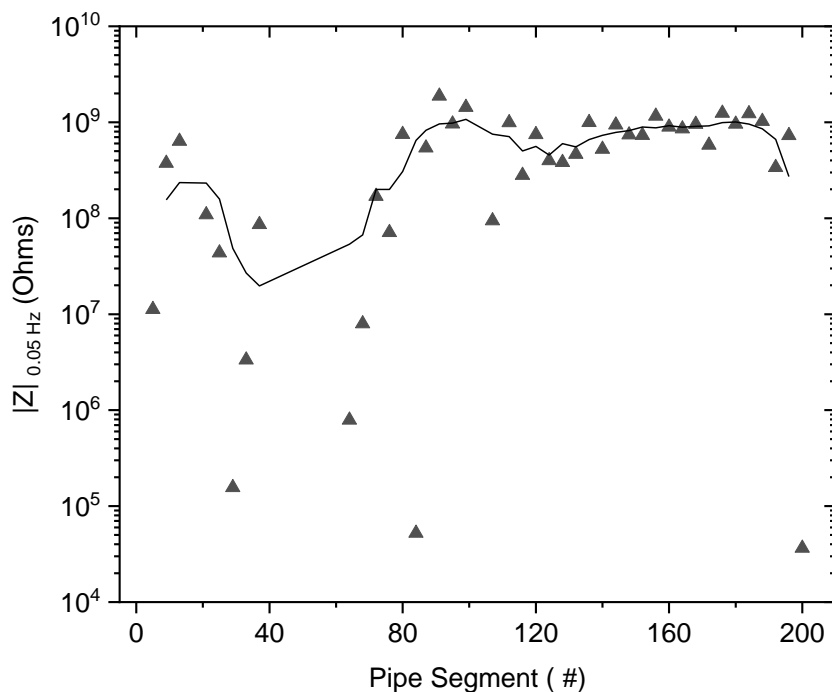


Figure 6. Field EIS $|Z|_{0.05 \text{ Hz}}$ results versus test location for coal tar epoxy along 10,000 foot long coated structure.

ECM enhances the EIS analysis by deriving the data into theoretical, physical circuits. Although it adds another layer of complexity, the approach can help determine if corrosion is occurring at the coating-substrate interface. If no significant corrosion is occurring, a basic ECM is sufficient, as shown in Figure 7. This ECM includes solution resistance, R_s , R_{pore} , and C_{coat} as a constant phase element, i.e., CPE_{coat} .

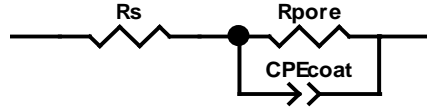


Figure 7. Basic ECM for a non-corroding coated substrate.

Figure 8 provides an example of the field EIS data ECM results for R_{pore} and CPE_{coat} using raw data, i.e., no adjustments for surface area. The linings do not behave as an ideal capacitor, so a CPE offers a versatile circuit element for this approach. The R_{pore} data in Figure 8(a) closely resembles the $|Z|_{0.05 Hz}$ data in Figure 5. This demonstrates the close relationship between $|Z|$ at low frequencies and the selection of a single resistor during ECM analysis, and it reinforces the use of the low frequency data as a proxy for total coating resistance. Further, it supports the correctness of the ECM chosen. An ECM that incorporates two resistor-capacitor elements in series could be investigated in a future study to determine any effect of the two-cell test setup with no connection to the substrate.

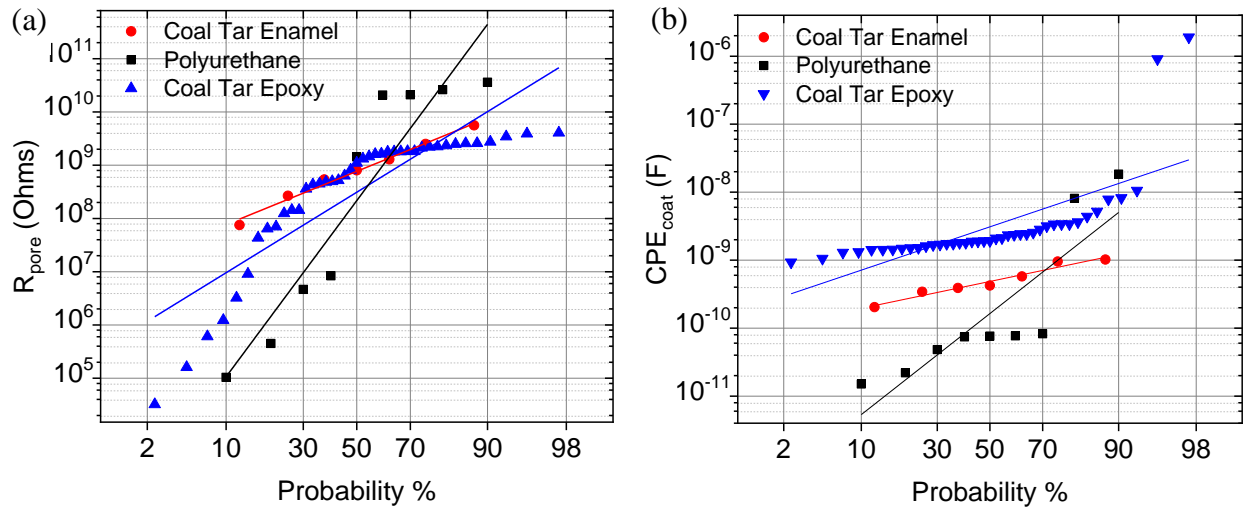


Figure 8. Probability plot of (a) R_{pore} and (b) CPE_{coat} for field EIS data.

The CPE_{coat} data in Figure 8(b) reveals greater consistency in test results than observed for $|Z|$ and the derived R_{pore} . This suggests that the capacitive behavior of the coating system is not influenced by lining defects, or that the influence is reduced. Confirming this result would allow for a more direct comparison of the ECM capacitor data to actual coating degradation and would support incorporating ECM capacitor results for data-based decision making.

Mathematical analysis of the Figure 8(b) coal tar epoxy data paralleled the corresponding data in Figure 5; the residuals show a non-random pattern. The bias may again be a result of location-specific contributions to coating degradation and requires further investigation.

Comparison to Laboratory Coupons

Laboratory EIS data provides an opportunity to evaluate coating degradation as it proceeds through time. The typical approach includes more frequent EIS testing at the initiation of coating exposure and then a relaxation of the testing schedule after approximately six months.

The early exposure data provides insight to coating water uptake and any resulting irreversible degradation of properties that occurs. The analysis provided here averages the first 25 weeks of data which should extend substantially beyond the initial changes that take place.

Figure 9 compares the ECM results of the laboratory 25-week average to the average field data result, which is the 50% probability value from Figure 5 for each lining. The results for $|Z|_{0.05\text{ Hz}}$ are assumed to be similar to R_{pore} Figure 9(a). Again, the ECM uses raw data and does not include adjustment for surface area or for minor DFT differences between the lab and field data. The surface area of the field test is similar when comparing the test cells; however, there are two in series. To correct for the field set-up effect, the R_{pore} values were halved and the CPE_{coat} values were doubled in accordance with electrical circuit theory.

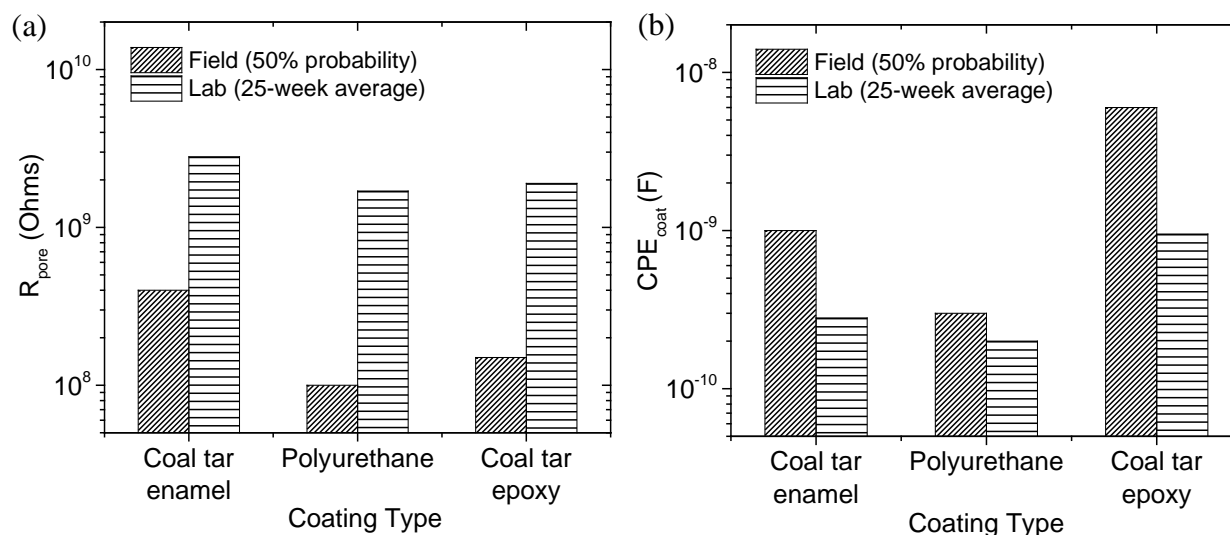


Figure 9. Comparison of field EIS data to laboratory coupons for (a) R_{pore} and (b) CPE_{coat} .

Field data for R_{pore} trends lower than the laboratory coupons by approximately one order of magnitude. Whereas the CPE_{coat} field data is greater than the laboratory coupons by approximately half that amount. One interpretation is that the field data represents a coating that is significantly more degraded, which could be expected based on the ages of each structure. Further, the laboratory data may be skewed by the results of the earliest exposure dates, assuming each coating experienced degradation during this period. Further research should explore a broader range of laboratory exposure periods as well as types of exposures that may provide better correlation to field results.

The laboratory EIS data presented in Figure 9 may be better suited for aiding contractors in their quality control testing at the time of coating application. Comparing the properties of a newly applied lining to a laboratory coupon can quickly provide insight into the quality of the application and may be a tool for early identification and rectification of areas susceptible to premature failure. This area necessitates future research as well.

CONCLUSIONS

- The field EIS results for a coal tar enamel, polyurethane, and coal tar epoxy lining provide unique, quantitative insight to the degradation of these materials in their service environment. The results indicate that a coated structure requires a statistically significant number of EIS datasets across many locations for the most appropriate use of this tool during decision making. For example, the structure with a polyurethane lining had a wide range of test results for the three distinct locations evaluated. If only one location had been tested, the results would not have provided the full story.
- A Bode Plot provides the most practical organization of the data for interpretation purposes. The probability plot, with an evaluation for location-specific trends, should be applied as an analysis tool for decision making; however, at least 30 data points are needed for the results to be significant. ECM of the EIS data provides a more complex approach with additional insight.
- The R_{pore} and $|Z|_{0.05 Hz}$ field EIS results are strongly influenced by invisible lining defects such as cracks and pinholes. However, the CPE_{coat} results may not be affected by these features. The outcome supports the incorporation of ECM capacitor or constant phase element values for data-based decision making, which should be confirmed and further evaluated through additional experiments.
- The 50% probability for R_{pore} and CPE_{coat} field EIS data showed coating degradation approximately one order of magnitude more advanced than the 25-week average for the respective laboratory coupons. The outcome may be a combined result of the initial exposure results of the pristine coating within the 25-week average as well as the long time in service for each of the coated structure's lining. Further research should explore a broader range of laboratory exposure dates and lining types to continue to investigate correlations between laboratory and field data.
- The 25-week average laboratory EIS data should be further examined for relevance to quality control testing of newly applied coatings on structures.

ACKNOWLEDGEMENTS

The authors acknowledge the field testing support provided the Bureau of Reclamation's Green Mountain Powerplant, Denver Water's Marston Water Treatment Plant, and the Central Arizona Project and Agua Fria River Siphon personnel. The authors are grateful for funding support by the Bureau of Reclamation Science and Technology Program, Project ID 1884.

REFERENCES

- (1) V. F. Lvovich, *Impedance Spectroscopy: Applications to Electrochemical and Dielectric Phenomena*, Wiley, Hoboken, N.J., 2012.
- (2) G.S. Frankel, "Electrochemical Techniques in Corrosion: Status, Limitations, and Needs," *Journal of ASTM International*, Vol. 5, No. 2, p. 1 (2008).

- (3) R.C. Bacon, J.J. Smith, and F.M. Rugg, "Electrolytic Resistance in Evaluating Protective Merit of Coatings on Metals," *Industrial & Engineering Chemistry*, Vol. 40, No. 1, p. 161 (1948).
- (4) M. Kendig, F. Mansfeld, and S. Tsai, "Determination of the long term corrosion behavior of coated steel with A.C. impedance measurements," *Corrosion Science*, Vol. 23, No. 4, p. 317 (1983).
- (5) J.R. Scully, "Electrochemical Impedance of Organic-Coated Steel: Correlation of Impedance Parameters with Long-Term Coating Deterioration," *Journal of the Electrochemical Society*, Vol. 136, No. 4, p. 979 (1989).
- (6) ASTM G106-89(2015), *Standard Practice for Verification of Algorithm and Equipment for Electrochemical Impedance Measurements*, ASTM International, West Conshohocken, PA, 2015, www.astm.org.
- (7) O. Negele and W. Funke, "Internal stress and wet adhesion of organic coatings," *Progress in Organic Coatings*, Vol. 28, No. 4, p. 285 (1996).
- (8) D. Loveday, P. Peterson, and B. Rodgers, "Evaluation of organic coatings with electrochemical impedance spectroscopy Part 2: Application of EIS to coatings," *JCT Coatings Tech*, Vol. 1, No. 10, p. 88 (2004).
- (9) D.M. Brasher and A.H. Kingsbury, "Electrical measurements in the study of immersed paint coatings on metal. I. Comparison between capacitance and gravimetric methods of estimating water-uptake," *Journal of Applied Chemistry*, Vol. 4, p. 62 (1954).
- (10) R. Hirayama and S. Haruyama, "Electrochemical Impedance for Degraded Coated Steel Having Pores," *CORROSION*, Vol. 47, No. 12, 1991, p. 952.
- (11) Bureau of Reclamation, "The 10% Soil Resistivity Method," MERL-05-19, U.S. Department of the Interior, Bureau of Reclamation, Denver, CO, 2005.
- (12) B.J.E. Merten, M.T. Walsh, J.D. Torrey, "Validation of Coated Infrastructure Examination by Electrochemical Impedance Spectroscopy" ASTM G01.11 Committee, Symposium on Recent Advances in Electrochemical Techniques for Field Corrosion Monitoring and Laboratory Corrosion Measurements, Atlanta, GA, November 13, 2017.
- (13) D. Mills, M. Broster and I. Razaq, "Continuing work to enable electrochemical methods to be used to monitor the performance of organic coatings in the field," *Progress in Organic Coatings*, Vol. 63, p. 267 (2008).
- (14) K. Allahar, Q. Su, and G. Bierwagen, "Non-substrate EIS monitoring of organic coatings with embedded electrodes," *Progress in Organic Coatings*, Vol. 67, No. 2, p. 180 (2010).
- (15) D. Mills, P. Picton, and L. Mularczyk, "Developments in the electrochemical noise method (ENM) to make it more practical for assessment of anti-corrosive coatings," *Electrochimica Acta*, Vol. 124, p. 199 (2014).
- (16) D.J. Mills and S.S. Jamali, "The best tests for anti-corrosive paints. And why: A personal viewpoint," *Progress in Organic Coatings*, Vol. 102, Part A, p. 8 (2017).

Appendix B – Agua Fria River Siphon Report (2018)

RECLAMATION

Managing Water in the West

Agua Fria Siphon Coating Inspection and Impedance Analysis

Materials and Corrosion Laboratory, 8540-2018-58

Agua Fria River Siphon, Hayden-Rhodes Division—Arizona



Mission Statements

The U.S. Department of the Interior protects America’s natural resources and heritage, honors our cultures and tribal communities, and supplies the energy to power our future.

The mission of the Bureau of Reclamation is to manage, develop, and protect water and related resources in an environmentally and economically sound manner in the interest of the American public.

Disclaimer:

Information in this report may not be used for advertising or promotional purposes. The data and findings should not be construed as an endorsement of any product or firm by the Bureau of Reclamation, Department of Interior, or Federal Government. The products evaluated in the report were evaluated for purposes specific to the Bureau of Reclamation mission. Reclamation gives no warranties or guarantees, expressed or implied, for the products evaluated in this report, including merchantability or fitness for a particular purpose.

Agua Fria Siphon Coating Inspection and Impedance Analysis

REPORT DOCUMENTATION PAGE			Form Approved OMB No. 0704-0188		
T1. REPORT DATE October 2018		T2. REPORT TYPE Technical Memorandum		T3. DATES COVERED	
T4. TITLE AND SUBTITLE Agua Fria Siphon Coating Inspection and Impedance Analysis			5a. CONTRACT NUMBER XXXR4079V4-RX122553011000000		
			5b. GRANT NUMBER		
			5c. PROGRAM ELEMENT NUMBER		
6. AUTHOR(S) Stephanie Prochaska, M.S., sprochaska@usbr.gov, 303-445-2323 Jessica Torrey, Ph.D., jtorrey@usbr.gov, 303-445-2376 Bobbi Jo Merten, Ph.D., bmerten@usbr.gov, 303-445-2380			5d. PROJECT NUMBER		
			5e. TASK NUMBER		
			5f. WORK UNIT NUMBER 86-68540		
7. PERFORMING ORGANIZATION NAME(S) AND ADDRESS(ES) Bureau of Reclamation Technical Service Center, Materials and Corrosion Lab 6 th and Kipling St, Denver, CO 80225-0007			8. PERFORMING ORGANIZATION REPORT NUMBER 8540-2018-58		
9. SPONSORING / MONITORING AGENCY NAME(S) AND ADDRESS(ES) Bureau of Reclamation Technical Service Center, Materials and Corrosion Lab 6 th and Kipling St, Denver, CO 80225-0007 Central Arizona Project P.O. Box 43020 Phoenix, AZ 85080-3020			10. SPONSOR/MONITOR'S ACRONYM(S) BOR/USBR: Bureau of Reclamation DOI: Department of the Interior		
			11. SPONSOR/MONITOR'S REPORT NUMBER(S)		
12. DISTRIBUTION / AVAILABILITY STATEMENT Final report can be downloaded from Reclamation's website: https://www.usbr.gov/research/					
13. SUPPLEMENTARY NOTES					
14. ABSTRACT The Agua Fria River Siphon is a [REDACTED] steel pipe near Phoenix, AZ, that is operated and maintained by the Central Arizona Project (CAP). Investigators from the Bureau of Reclamation's Technical Service Center travelled to the CAP's Agua Fria River Siphon to evaluate the condition of the interior coating by traditional visual inspection techniques as well as quantitative film thickness, steel thickness, and electrochemical impedance spectroscopy analysis (EIS). The visual inspection showed that the coal tar epoxy was in poor condition along the invert. The quantitative inspection by EIS showed that the coal tar epoxy provides poor corrosion protection near the siphon inlet and outlet as well as in the pipe segments approaching the lowest elevations, as indicated by low frequency impedance magnitude ($ Z _{0.05 \text{ Hz}}$) values less than 10^8 ohms. DFT results showed that the coating is severely degraded along the invert. UT testing showed that the steel thickness closely matches or exceeds the values provided on the pipe manufacturer's erection drawings. A full coating replacement is recommended because the repairs needed exceed 15 percent of the total surface. Performing spot repairs to all damaged areas now may result in satisfactory corrosion protection for the entire pipe for at least another 10 years.					
15. SUBJECT TERMS Coatings, coal tar enamel, coatings survey, electrochemical impedance spectroscopy, film thickness, ultrasonic thickness					
16. SECURITY CLASSIFICATION OF:			17. LIMITATION OF ABSTRACT U	18. NUMBER OF PAGES 81	19a. NAME OF RESPONSIBLE PERSON Stephanie Prochaska
a. REPORT U	b. ABSTRACT U	c. THIS PAGE U			19b. TELEPHONE NUMBER 303-445-2323

BUREAU OF RECLAMATION

Materials and Corrosion Laboratory

Report Number 8540-2018-58

Agua Fria Siphon Coating Inspection and Impedance Analysis

STEPHANIE PROCHASKA  Digitally signed by STEPHANIE PROCHASKA
Date: 2018.12.03 14:49:02 -07'00'

Prepared by: Stephanie Prochaska, M.S.
Materials Engineer, Materials and Corrosion Lab

JESSICA TORREY  Digitally signed by JESSICA TORREY
Date: 2018.12.03 15:11:54 -07'00'

Checked by: Jessica Torrey, Ph.D.
Materials Engineer, Materials and Corrosion Lab

BOBBI JO MERTEN  Digitally signed by BOBBI JO MERTEN
Date: 2018.12.03 15:03:27 -07'00'

Technical Approval: Bobbi Jo Merten, Ph.D.
Coatings Specialist, Materials and Corrosion Lab

ALLEN SKAJA  Digitally signed by ALLEN SKAJA
Date: 2018.12.03 14:57:55 -07'00'

Peer Review: Allen Skaja, Ph.D.
Protective Coatings Specialist, Materials and Corrosion Lab

WILLIAM KEPLER  Digitally signed by WILLIAM KEPLER
Date: 2018.12.03 14:54:04 -07'00'

Peer Review: William Kepler, Ph.D., P.E.
Manager, Materials and Corrosion Lab

Acronyms and Abbreviations

CAP	Central Arizona Project
CE	Counter electrode
DFT	Dry film thickness
EIS	Electrochemical impedance spectroscopy
PCCP	Prestressed concrete cylinder pipe
RE	Reference electrode
Reclamation	Bureau of Reclamation
TSC	Technical Service Center
UT	Ultrasonic thickness
WE	Working electrode

Symbols

ft	Foot
Hz	Hertz
kHz	Kilohertz
mV	Millivolt
$ Z $	Impedance magnitude
$ Z _{0.05 \text{ Hz}}$	Impedance magnitude at 0.05 hertz applied frequency

Executive Summary

The Agua Fria River Siphon is a [REDACTED] long steel pipe near Phoenix, AZ, operated and maintained by the Central Arizona Project (CAP). The structure was originally constructed as prestressed concrete cylinder pipe (PCCP). In 1997, Reclamation replaced the PCCP with a steel pipeline with an Amercoat 78HB coal tar epoxy interior coating. The condition of the coating and underlying steel require occasional inspection to evaluate their condition and plan for maintenance or replacement in a timely manner.

Investigators from the Bureau of Reclamation's Technical Service Center (TSC) travelled to the CAP's Agua Fria River Siphon to evaluate the condition of the interior coating by traditional visual inspection techniques as well as dry film thickness (DFT), ultrasonic/steel thickness (UT), and electrochemical impedance spectroscopy analysis (EIS).

The visual inspection showed that the coal tar epoxy was in poor condition along the invert. In addition, there was more extensive coating degradation and corrosion near the siphon inlet and at the pipe field joints, which were coated after installation. The higher rate of coating degradation in these areas is likely caused by the combination of sediment and turbulence along the pipe's directional changes. EIS testing revealed that much of the undamaged interior coating is providing excellent corrosion protection. Mud accumulation in the lowest elevations of the siphon impeded a thorough inspection of those pipe segments. The upper half of the pipe walls and crown also received limited inspection because close-up access was not possible, and the surfaces were covered by a significant amount of mud and dirt.

Reclamation coatings inspectors recommend a full coating replacement because the repairs needed exceed 15 percent of the total surface. However, less expensive spot repairs to all damaged areas throughout the pipe may result in satisfactory corrosion protection for another 10 years.

Reclamation coatings inspectors recommend that, at a minimum, removal and replacement of the coating in the following areas should be performed:

- Full length of the siphon invert.
- Around all field joints.
- Full circumference of pipe segments 1 through approximately 80.
- Additional spot repairs may be needed throughout the portion of the pipe that was inaccessible to the inspection team.

Recommended coating materials include coal tar epoxy, 100% solids epoxy, solution vinyl coating, or a coating with enhanced abrasion resistance. Spot repairs, if performed, should use an array of these materials to determine the optimum material for a future full recoating of the Agua Fria River Siphon. TSC can provide assistance with the specification paragraphs.

Agua Fria Siphon Coating Inspection and Impedance Analysis

Contents

Agua Fria Siphon Coating Inspection and Impedance Analysis	iii
Acronyms and Abbreviations	iv
Symbols	iv
Executive Summary	v
Background.....	1
Conclusions and Recommendations	1
Inspection Methods	2
General Observations	2
Electrochemical Impedance Spectroscopy	3
Dry Film Thickness.....	4
Ultrasonic Thickness	4
Results, Analyses, and Discussion.....	5
General Observations	5
Electrochemical Impedance Spectroscopy	12
Dry Film Thickness.....	13
Ultrasonic Thickness	14

Background

The Agua Fria Siphon, a [REDACTED] long Central Arizona Project (CAP) pipeline near Phoenix, AZ, was installed from 1975-78. Originally constructed out of prestressed concrete cylinder pipe (PCCP), the siphon was replaced with steel and returned to service in 1997. The steel pipeline is composed of 200 individual pipe pieces, joined in the field. The interior of the siphon is lined with Amercoat 78HB coal tar epoxy. Warranty work was performed on the lining in 1999, and CAP made lining repairs, predominantly to the siphon's invert, in 2003 using grey and red coats of International Paint Devgrip 238.

CAP invited corrosion mitigation specialists from the Bureau of Reclamation's (Reclamation's) Technical Service Center (TSC) to assess the condition of the coal tar epoxy lining and perform quantitative field inspection techniques within the pipe. The TSC's Stephanie Prochaska and Jessica Torrey conducted the inspection from August 13-15, 2018, along with several CAP engineers and inspectors.

Conclusions and Recommendations

Visual inspection revealed a severely degraded and often absent coating at the invert for most pipe sections, primarily where previous coating repairs had been performed. The coating is not serviceable in these areas, and coating removal and replacement should be performed along the pipe invert. Visual inspection also indicated rust-through at many pipe section joints; these should also be repaired by coating removal and replacement of the pipe field joint coatings.

Several sections near the low elevations of the siphon had severe rust speckling around the entire pipe circumference and will likely need a full recoat. It should be noted that 27 sections at the lowest elevations were inaccessible for quantitative inspection but would be expected to have similar or more severe coating degradation than neighboring sections due to their location. Additionally, while CAP staff cleaned pipe walls in the majority of the siphon, much of the pipe wall remained covered with a hard mud layer, obscuring visual inspection of the coating without vigorous scraping. It should, therefore, be anticipated that some coating defects and corroded areas were missed that may ultimately need spot repair once the pipe is fully cleaned. CAP staff recorded detailed visual inspection data for each pipe segment which is presented in Appendix E.

Investigators conducted three quantitative inspection techniques for a more thorough condition assessment. Electrochemical impedance spectroscopy (EIS) data indicated the lining is in poor condition near the inlet, the lowest portion (approximately between pipe segments 35 and 85), and the outlet of the siphon. In addition, dry film thickness (DFT) follows a similar trend, with thinned lining found near the inlet; DFT throughout the entire length invert was significantly lower than on the siphon walls. Ultrasonic thickness (UT) measurements were found to closely match or exceed metal thickness values indicated on the pipe manufacturer's erection drawings. Some pitting was noted at the invert where the coating was damaged, and this would need to be further examined for possible repair before recoating.

Agua Fria Siphon Coating Inspection and Impedance Analysis

The results of the inspection indicated that a full coating removal and replacement should be considered because the repairs needed exceed 15 percent of the total surface. A full coating removal and replacement of the entire pipe interior should be performed by abrasive blasting and applying new coating. Recommendations for a new coating include coal tar epoxy, 100% solids epoxy, solution vinyl coating, or a coating with enhanced abrasion resistance. It should be noted that the existing coal tar epoxy performed adequately with the exception of the pipe invert; the 2003 repair material applied to the pipe invert provided marginal performance.

However, the quantitative testing showed that the much of the intact coating is providing excellent corrosion protection. Therefore, an alternative approach of spot repairing the missing and degraded coating areas, i.e. the pipe invert, joints, and pipe segments 1 through approximately 80, should be considered if advantageous from a time or budget perspective. This approach could delay the recoating of the entire pipe interior by as much as 10 to 20 years.

Spot repairs can be performed by abrasive blast or power tool surface preparation to remove the existing coating. The surface preparation should impart an angular profile on the steel surface and lightly abrade the adjacent 2- to 3-inches of intact coating. Apply new coating to the freshly prepared surfaces. Recommendations for a spot repair coating include coal tar epoxy, 100% solids epoxy, or a coating with enhanced abrasion resistance.

Performing a round of spot repairs using several different candidate materials for the next full recoating could result in a systematic, in-service evaluation. Specifically, this may result in identifying a material that is better suited for protection of the pipe invert. The goal would be to obtain a much longer service life than the coal tar epoxy or the Devgrip 238 provided in the invert, which was 10 years or less in many areas. A number of coating materials are marketed to provide enhanced abrasion resistance. Further, a solution vinyl coating provides superior performance in impacted immersion service. Evaluation of the vinyl coating would determine if that material is resistant to the sediment or debris experienced along the Agua Fria siphon invert. There are also products with higher costs, such as composites of epoxy and reinforcing ceramics or other materials, which may be cost effective in the harshest abrasion areas if the service life is proportionally lengthened.

Inspection Methods

General Observations

The visual inspection documents all defects that are visible, such as missing and damaged coating, i.e., cracks, blisters, rust-through, etc. TSC investigators worked alongside CAP staff to collect visual inspection data. The pipe entrants passed through each pipe segment at least twice while conducting quantitative analysis.

The CAP staff dewatered the pipe, low-pressure washed pipe walls, and removed debris and fish prior to inspection. However, untimely monsoon rains re-filled lower elevations of the siphon with water, mud, and other storm debris; CAP staff continued to pump mud and water from these sections to increase the accessibility of these areas. Despite these efforts, much of the pipe wall in the lower elevation of the siphon remained covered with a layer of mud, either dried or wet,

and several sections persisted with mud and water in the invert, hampering visual inspection of the coating.

Electrochemical Impedance Spectroscopy

As described above, mud and water accumulation in the invert and on pipe walls prevented EIS testing between segments 37 and 64. The remainder of the pipe was examined using quantitative testing techniques approximately every four pipe segments. Any persisting mud, dried or wet, was removed with a flat-edge stiff painter's tool and rinsed and wiped with a rag to reveal a clean coating surface prior to testing.

Disposable, 2.25-inch diameter test cells were affixed to the coal tar epoxy for EIS testing. A fast-curing aquarium-grade silicone adhesive provided a seal for attachment of each test cell to the lining. Tap water was added to the test cells as an electrolyte. To ensure that the coating in the dry sections of the pipe was re-saturated before EIS testing, the filled test cells were left overnight. In the lower siphon elevations where water or wet mud remained on the coating until just prior to testing, the test cells were filled and tested immediately after application to the pipe wall.

Each prepared test location comprised three test cells; two test cells are required for the measurement and an extra test cell was attached for insurance against leakage (Figure 1). The test cell positions were along the lower side wall, approximately four feet up the pipe wall adjacent to the upstream pipe joint. In most cases, the test sites alternated between the left-hand (north) and right-hand (south) pipe wall, referenced to facing downstream.

EIS measurements were performed using an Ivium Compactstat portable potentiostat that was powered by a ruggedized laptop (Figure 1). The laptop also provided the necessary software to run the measurements. Each measurement utilized two test cells: one containing a copper/copper sulfate reference electrode (RE) and a platinum mesh counter electrode (CE) and the other containing a platinum mesh working electrode (WE). This arrangement allows for a 4-electrode measurement of current and voltage through a circuit consisting of the four test leads and cables, the instrument, the test cell electrolyte, the coating beneath each test cell, and the pipe wall between the two test cells. The current and voltage leads are separate in the RE/CE test cell and together in the WE test cell. These two parameters allow for interrogation of the complex resistance, i.e., impedance, of the coating; all other resistances in the circuit are assumed to be negligible by comparison.

Agua Fria Siphon Coating Inspection and Impedance Analysis



Figure 1. Left: Typical EIS set-up during measurement at pipe segment 164 with ruggedized laptop (bottom left) connected to portable potentiostat (bottom right). Right: Close up of test cell set-up.

During the test, a 50 millivolt (mV) amplitude (root mean squared) sinusoidal voltage perturbation is applied, and the current required to achieve the desired voltage is measured. The evaluated perturbation frequencies were 100 kilohertz (kHz) to 0.05 hertz (Hz) at five points per decade, resulting in an array of points during a test time of approximately two to three minutes.

Dry Film Thickness

DFT measurements were taken on the coal tar epoxy using a PosiTector 6000 coating thickness gage. Fifteen measurements were recorded for each pipe segment where EIS testing occurred: five measurements each on the right-hand side of the pipe wall, the pipe invert, and the left-hand side of the pipe wall. DFT was measured in the clean area adjacent to the EIS test cells as applicable; any obstructing mud was removed with a flat-edge stiff painter's tool in all other locations before measurement. Aside from the 42 pipe segments where EIS was performed, DFT was also recorded within the following pipe segments: 7, 17, 48, 52, 56, 103, 149, and 150.

Repaired areas in the invert were not measured for DFT. In addition, areas with missing coating or visible coating damage were also not measured. Rather, measurements were taken at the most proximate area of visually sound coal tar epoxy coating.

Ultrasonic Thickness

UT measurements were taken using a Cygnus Instruments M5-C4+ UT gage and coupling fluid. Fifteen total measurements were recorded for each pipe segment where EIS was performed: five measurements each on the right-hand side of the pipe wall, the pipe invert, and the left-hand side of the pipe wall. UT was measured in the clean area adjacent to the EIS test cells where applicable; the coupling fluid from the measurement locations is seen above the test cells in Figure 1. Any obstructing mud was removed with a flat-edge stiff painter's tool in all other locations before measurement. Aside from the 42 pipe segments where EIS was performed, UT was also taken at the following pipe segments: 52, 56, 103, 149, and 150.

Results, Analyses, and Discussion

General Observations

The cursory visual inspection performed by TSC investigators resulted in photo-documentation of approximately every fourth pipe segment and evaluation of visible coating damage. CAP staff produced systematic visual inspection data at every pipe segment which can be found in Appendix E.

A sequential evaluation of the visual inspection data follows, beginning at the upstream end of the pipe. The actual inspection required a deviation in the order of data acquired due to impassible sections in the middle, lowest elevations of the siphon preventing a continuous walk-through of the siphon. Instead, inspectors progressed by entering and exiting from the upstream end of the siphon, followed by entering and exiting from the downstream end of the siphon and through manholes, to circumvent the impassible section. The siphon elevation profile is shown in Figure 2.

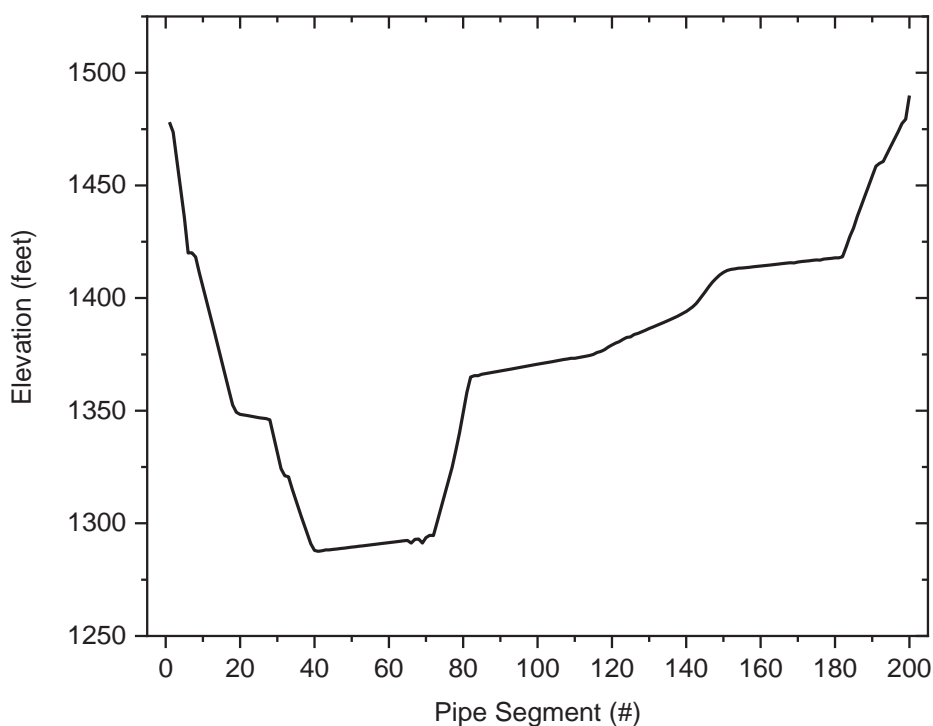


Figure 2. Siphon elevation profile.

Several decreases in pipe elevation occur near the upstream entrance, which represent the steepest slope of the siphon. The coating condition near the upstream entrance is varied, with some segments appearing to be in excellent condition and other segments are severely degraded. Figure 3 provides an example of the condition within pipe segment 9. The center of the

Agua Fria Siphon Coating Inspection and Impedance Analysis

photograph has no visible damage and provided a location for quantitative testing. The left and right edge of the photograph have significant coating damage and rust-through.



Figure 3. Test cell set-up and coating condition at pipe segment 9.

The pipe invert had extensive coating repairs areas from the 2003 maintenance activities. Figure 4 provides an example of the condition of a failing repair area within pipe segment 21. Surface preparation was reportedly conducted by water jetting which is a method to clean the surface but does not provide the necessary anchor profile; it can uncover the existing profile from the original surface preparation. Similar areas were found in other locations throughout the siphon, several examples follow for later pipe segments.



Figure 4. Repair area in the invert of pipe segment 21.

Figure 5 (left) provides an example of the original coal tar epoxy worn-through on the pipe invert in pipe segment 25. The condition shown is typical of the invert where repairs were not conducted. This coating damage may be the result of sediment in the water, standing water in the invert that accelerated coating degradation, or both. The photo also shows the location of the quantitative UT measurements that occurred adjacent to the damage area, as indicated by the five darker-colored dots left by the coupling fluid. The top of the photo also shows the condition of the field joint which had received a grey-colored coating repair. Figure 5 (right) shows the condition of the side wall, also in pipe segment 25, at the location of all quantitative measurements; the three EIS test cells are shown with five UT test locations visible above the test cells. No coating damage is visible on the side wall, suggesting that the pipe invert is experiencing coating damage at a greater rate than the side walls. The coal tar epoxy coating condition was similar on the pipe walls throughout the siphon.

Agua Fria Siphon Coating Inspection and Impedance Analysis



Figure 5. Coating condition in pipe segment 25 at (left) the pipe invert and (right) at side wall where quantitative measurements occurred.

Figure 6 provides an example of a large area of missing coating in the invert of pipe segment 37. The area is approximately 3-ft wide and 5-ft long and allows for uncontrolled corrosion of the steel pipe. Although this condition was not typical of the coating throughout the siphon, it underscores the need for coating maintenance to correct this condition.



Figure 6. Large area of corrosion in the invert near pipe segment 37.

Visual inspection at the lowest elevations of the siphon, approximately pipe segments 37 to 67, was only partially fulfilled due to significant mud along the pipe invert from the monsoon flooding. These pipe segments received quantitative testing as allowable, but several measurements could not be achieved. Figure 7 provides photographs of the typical pipe condition through this section. The side wall of pipe segment 53 is shown in Figure 7 (right); EIS was not possible in the lower side wall due to mud. Pipe segments 38 through 47 were impassible because of deep mud in the invert. A distant examination of these segments was ineffective due to mud on the pipe walls.



Figure 7. Typical pipe condition (right) between pipe segments 37 and 67 with thick mud in the pipe invert and (left) along pipe walls, shown up close for pipe segment 53.

The pipe segments downstream of the lowest siphon elevations have a steep slope as the water begins to flow upward toward the outlet. Figure 8 shows the condition of the invert and pipe joints in this area, at pipe segment 84A. The red- and grey-colored repair areas are present along the invert, but corrosion is prevalent along the invert and rust-through can be seen at the joints.

Agua Fria Siphon Coating Inspection and Impedance Analysis



Figure 8. Coating condition of the invert and pipe joints near pipe segment 84A.

The pipe has a gradual slope between approximately segments 90 and 180, and the water flow is expected to be less turbulent through these areas. Aside from in the invert, no major areas of coating damage were seen in this region. Figure 9 (left) provides an example of the pipe invert at one of the locations where the coal tar epoxy had been repaired in 2003. The photo shows that sediment is abrading the invert coating (center of photo), and that the invert requires coating maintenance. Intact coal tar epoxy with rust-through is at the left, upper edge of the photo. Evidence of water jetting is also visible in the figure. Figure 9 (right) shows the typical coating condition on the pipe walls between segments 90 and 180. The coating appears to be in good condition with no major cracking or corrosion. The field joint coating in the photo has vertically aligned surface defects (fingering) from the spray application, typically the result of a clogged or worn spray tip. These application defects are visible around some joints throughout the siphon but generally do not require repair unless cracking or rust-through is occurring.



Figure 9. Typical condition of (left) invert and joint repair near pipe segment 116 and (right) application defects from brush application of coating near pipe segment 136.

The siphon has a steep upward slope between pipe segment 180 and the end of the siphon, segment 200. Figure 10 shows the typical condition in this region. Corrosion and rust-through are visible along the invert and at the joints, and the pipe walls are heavily covered with dried mud and sediment. Areas of failed coating repair can be seen along the invert. The coating degradation is most likely attributed to sediment abrasion.



Figure 10. Typical joint and invert condition at pipe segment 192.

Electrochemical Impedance Spectroscopy

The impedance magnitude, $|Z|$, is derived from the resulting voltage and current data of the EIS test. Impedance is a measure of how much the circuit resists the current, or the flow of electrons through the coating; the greater the impedance, the greater the corrosion protection. It is a complex resistance that reveals information about the resistive and capacitive behaviors of a material.

Raw EIS data is plotted in the form of a Bode plot, which shows $|Z|$ versus the measurement frequency. Complete Bode plots for all pipe segments tested are in Appendix A – . This plot is useful in analyzing the degree to which a coating prevents water and ions from migrating through to the substrate. The measured values at low frequencies, i.e., $|Z|$ at 0.05 Hz applied frequency ($|Z|_{0.05 \text{ Hz}}$), indicate the overall corrosion resistance. A value greater than 10^8 ohms indicates that the coating is providing good corrosion protection, i.e., resistance to the flow of water and ions. A $|Z|_{0.05 \text{ Hz}}$ greater than 10^8 ohms is especially critical for structures that are in immersion service and are infrequently accessible for inspection or maintenance. When $|Z|_{0.05 \text{ Hz}}$ approaches 10^7 ohms, the coating corrosion protection decreased significantly, and maintenance or replacement should be considered. Figure 11 shows the overall corrosion protection provided at each test location versus pipe segment with a 5-point adjacent averaging trendline included. The figure also has the siphon elevation profile (Figure 2) inset to reference the corrosion protection to the physical location within the siphon.

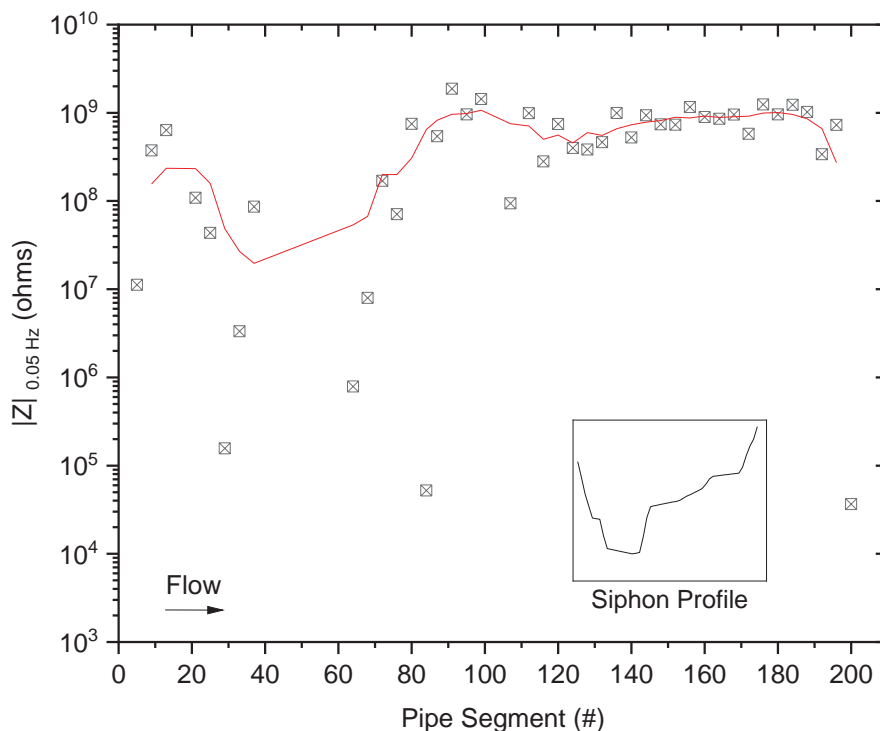


Figure 11. Overall corrosion protection at each pipe segment per EIS testing results with a 5-point adjacent averaging trendline included and siphon elevation profile inset.

The results from pipe segment 1 to 80 are disparate, with most of the $|Z|_{0.05 \text{ Hz}}$ values far lower than the threshold of 10^8 ohm for good corrosion protection. These results may be explained due to the severe service conditions at the siphon's inlet, including turbulent water due to changes in pipe slope and high sediment and debris loads. Direction of water flow also accelerates coating degradation near the inlet by allowing for the development of oxygen-rich regions. In addition, pinholes or cracks in the coating could contribute to the exceptionally low $|Z|$ results; although not yet visible, these coating defects produce low resistance pathways for the current to flow through during EIS testing.

EIS testing could not be performed between pipe segments 37 and 64, which corresponds to the lowest elevations of the siphon. The trendline in Figure 11 suggests that the coating provides poor corrosion protection here. However, these untested pipe segments may be providing excellent corrosion resistance, so the trendline must be interpreted cautiously.

The coal tar epoxy is providing excellent corrosion protection throughout the downstream half of the siphon, specifically from pipe segment 84 to 196, with an average $|Z|_{0.05 \text{ Hz}}$ of 8.2×10^8 ohms. The final data point at pipe segment 200 showed poor corrosion protection, which could be the result of increased turbulence or oxygen in the water. The $|Z|_{0.05 \text{ Hz}}$ values obtained within these pipe segments suggest that another 10 to 20 years of adequate corrosion protection is possible for the visibly undamaged coating.

Dry Film Thickness

The original coating specification specified a minimum DFT of 24 mils. While the coating passed the initial inspection, there is no record of what the final DFT values were prior to the siphon being placed in service. DFT results shown in Figure 12 correspond to EIS findings. The overall DFT is lowest near the inlet of the siphon, while pipe segments 90 to 160 have the highest overall DFT. As expected, throughout the entire length of the siphon, the DFT measured on the pipe's invert is significantly lower than on the pipe's walls. The invert DFT ranged from 40 mils to 4 mils, and its combined average DFT is 15 mils with standard deviation 2.4 mils. DFT on the left-hand side of the pipe was slightly higher than on the right-hand side through the interior portions of the pipe; the left-hand wall was covered with an adhered layer that may have acted as an abrasion-resistant barrier. The left-hand and right-hand walls together measured a combined average DFT of 28 mils with standard deviation 1.8 mils. Standard deviations of the measurements are not shown in the plot but can be determined from the data in Appendix B.

Agua Fria Siphon Coating Inspection and Impedance Analysis

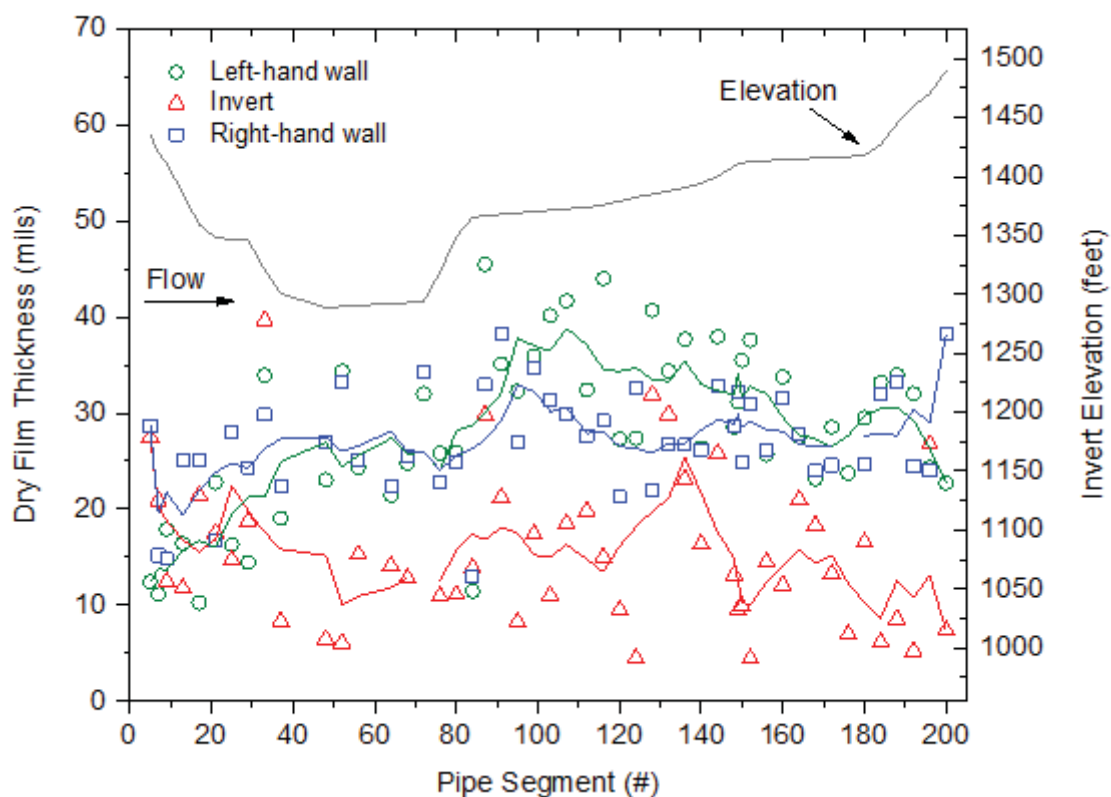


Figure 12. Average DFT at each pipe segment, measured at invert and each wall with a 5-point adjacent averaging trendline included and siphon invert elevation profile inset.

Ultrasonic Thickness

Figure 13 gives the results of the UT testing compared to the thickness values provided on the pipe manufacturer's erection drawings. UT results overwhelmingly matched or exceeded the specified thickness values for each pipe segment tested and for each portion of pipe. Despite the degraded invert coating with low measured DFTs, the UT measurement showed that pipe thinning along the invert is less than 0.001 inches (limit of gauge accuracy). See Appendix C for all UT data.

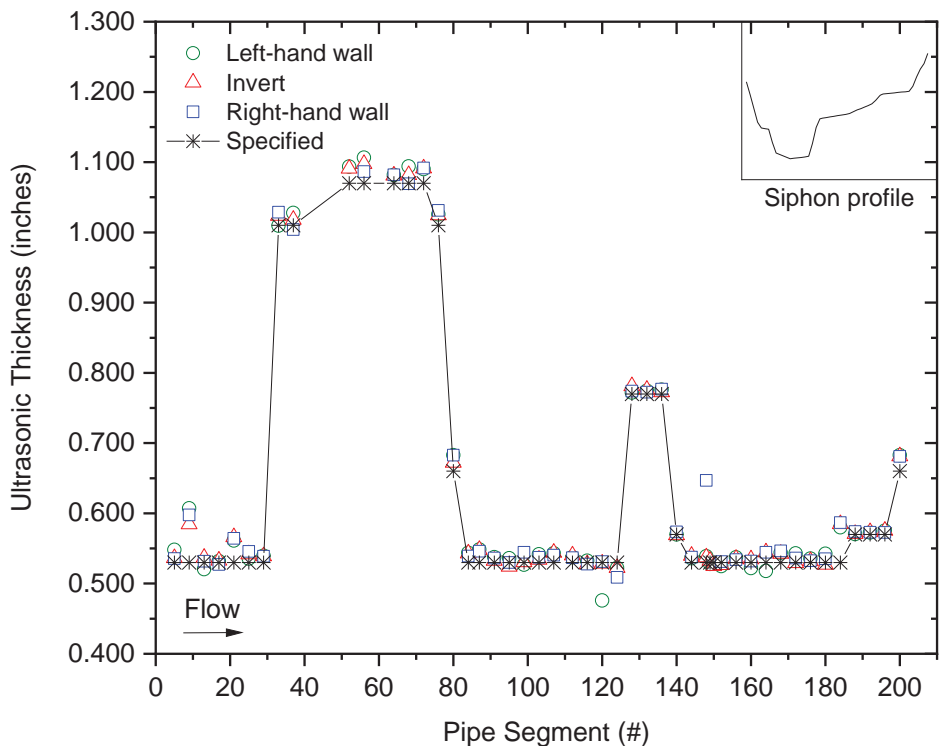


Figure 13. Average UT at each pipe segment, measured at invert and each wall, with specified values also shown and the siphon elevation profile inset.

The few major deviations from the expected value are likely user or equipment error since no obvious signs of metal loss were observed at measurement locations. Multiple instances of discrepancies from the reported value would be expected per measurement area if widespread metal loss is present. However, the presence of a corrosion pit beneath the coating cannot be eliminated and some pitting was visible throughout the siphon where the coating is missing (see Figure 14 and Figures D-1 and D-18 in Appendix D). These pits would need to be further examined for possible repair after cleaning and coating removal and before any coating repair material is applied.

Agua Fria Siphon Coating Inspection and Impedance Analysis



Figure 14: Severe pitting at pipe segment 10.

Appendix A – EIS summary table and Bode plots for all tested pipe segments

Table A-1: Summary of EIS data at $|Z|_{0.05 \text{ Hz}}$ ¹

Pipe segment #	$Z _{0.05 \text{ Hz}}$
5	1.1E+07
9	3.7E+08
13	6.4E+08
21	1.1E+08
25	4.4E+07
29	1.6E+05
33	3.3E+06
37	8.6E+07
64	7.9E+05
68	8.0E+06
72	1.7E+08
76	7.1E+07
80	7.5E+08
84	5.2E+04
87	5.4E+08
91	1.9E+09
95	9.6E+08
99	1.4E+09
107	9.4E+07
112	9.9E+08
116	2.8E+08
120	7.5E+08
124	4.0E+08
128	3.8E+08
132	4.6E+08
136	1.0E+09
140	5.2E+08
144	9.4E+08
148	7.4E+08
152	7.3E+08
156	1.2E+09
160	8.9E+08
164	8.6E+08
168	9.5E+08
172	5.8E+08
176	1.2E+09
180	9.6E+08
184	1.2E+09
188	1.0E+09
192	3.4E+08
196	7.3E+08
200	3.7E+04

¹ Green represents relatively high $|Z|$ and red represents relatively low $|Z|$.

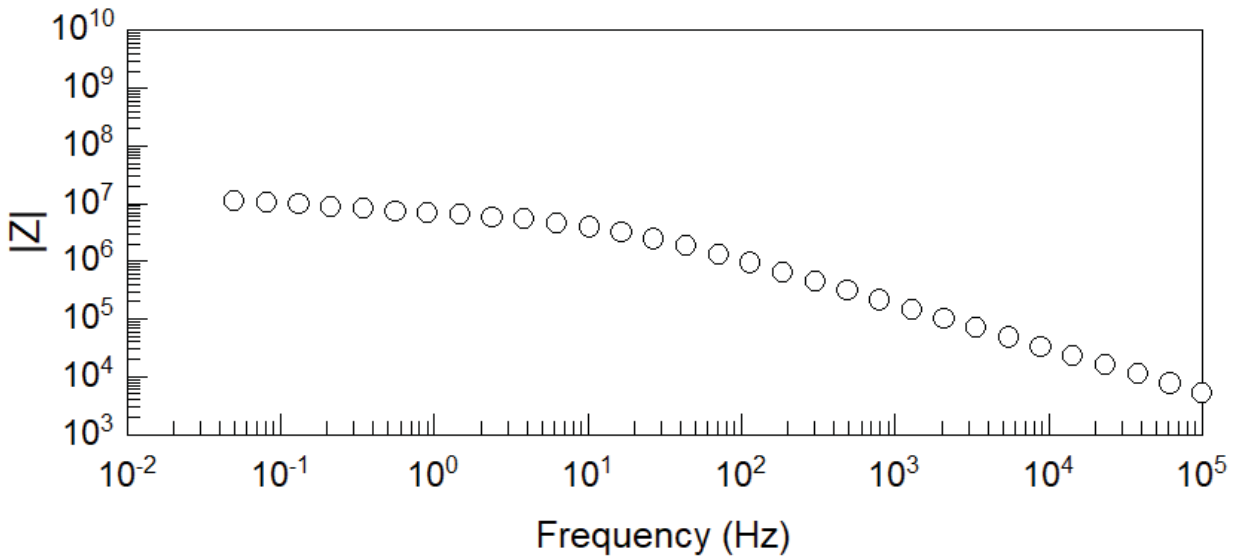


Figure A-1: Bode plot from pipe segment 5.

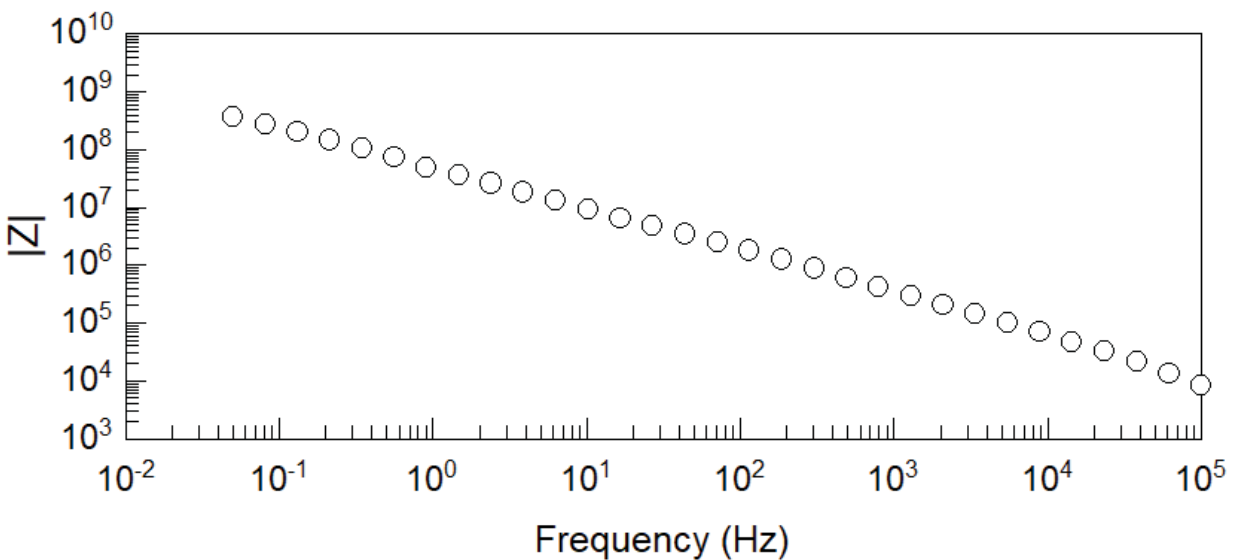


Figure A-2: Bode plot from pipe segment 9.

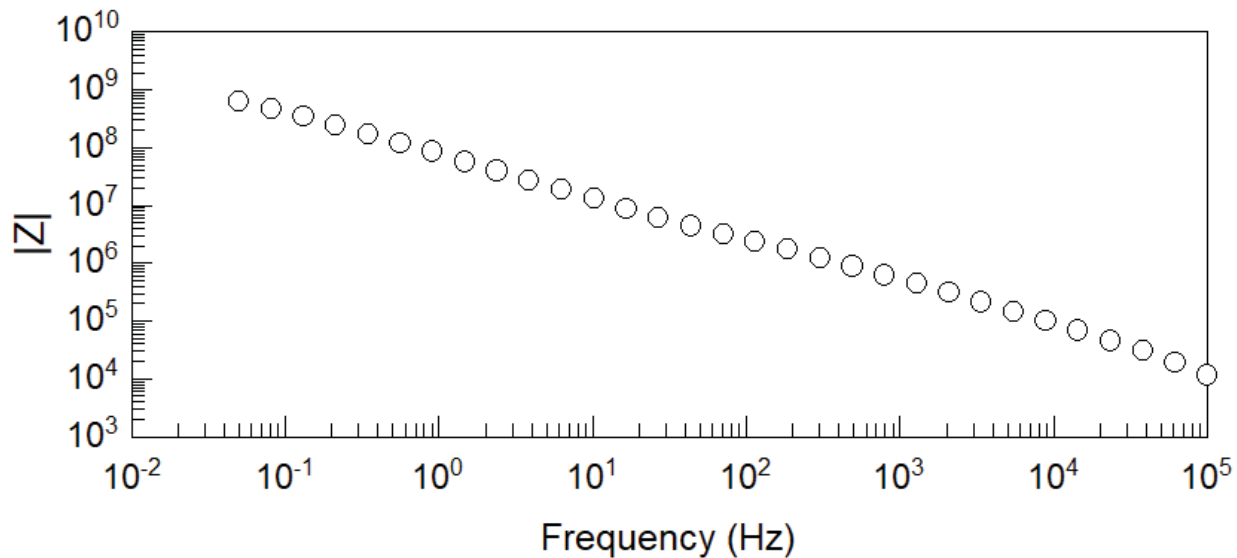


Figure A-3: Bode plot from pipe segment 13.

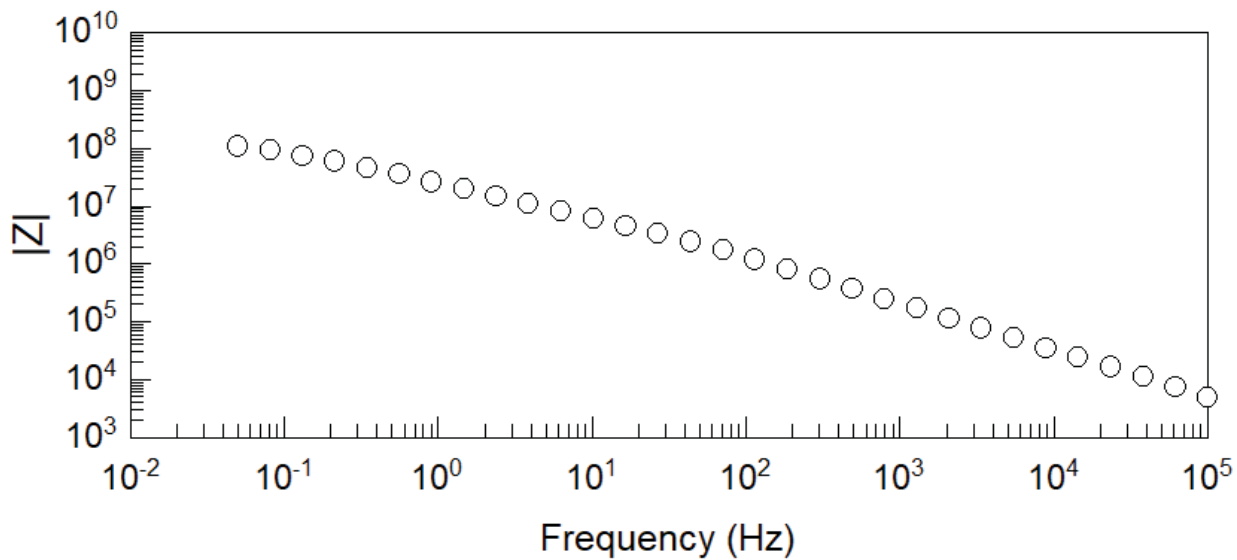


Figure A-4: Bode plot from pipe segment 21.

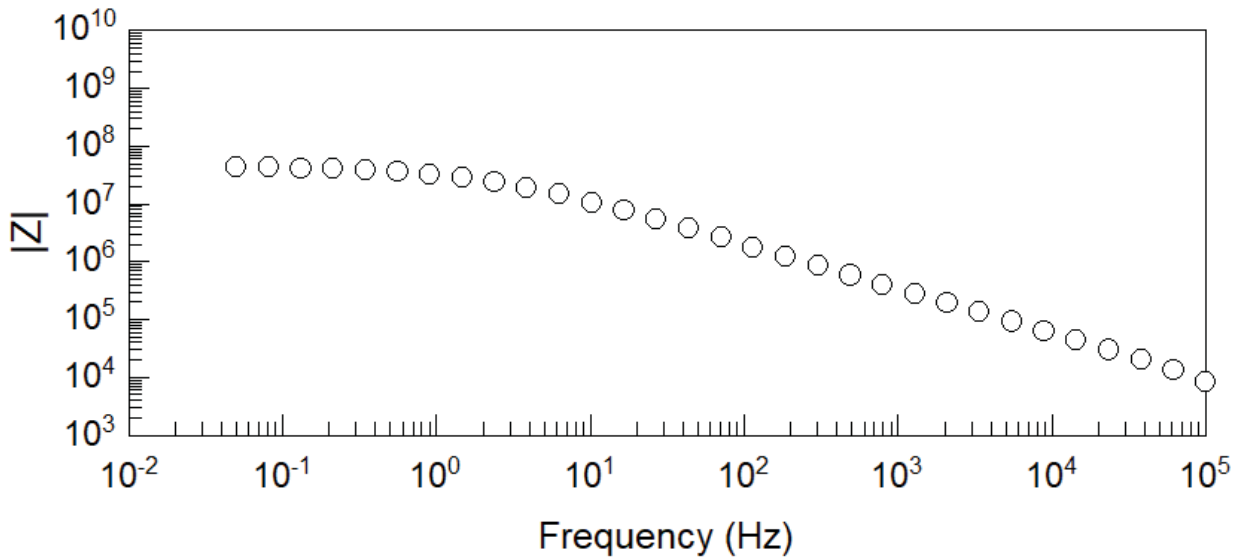


Figure A-5: Bode plot from pipe segment 25.

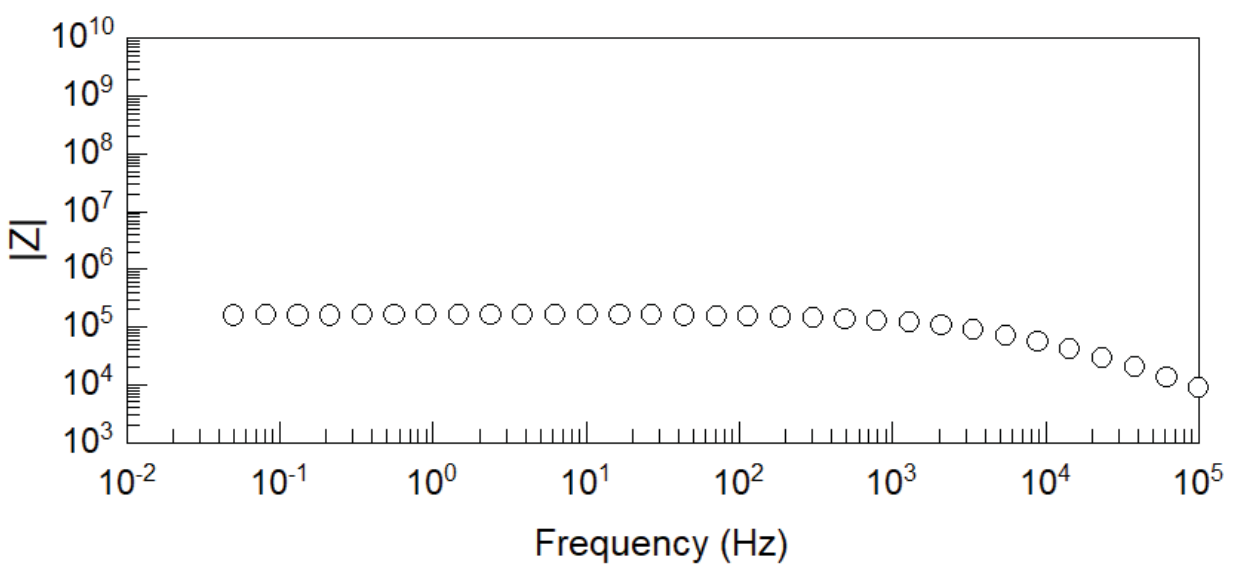


Figure A-6: Bode plot from pipe segment 29.

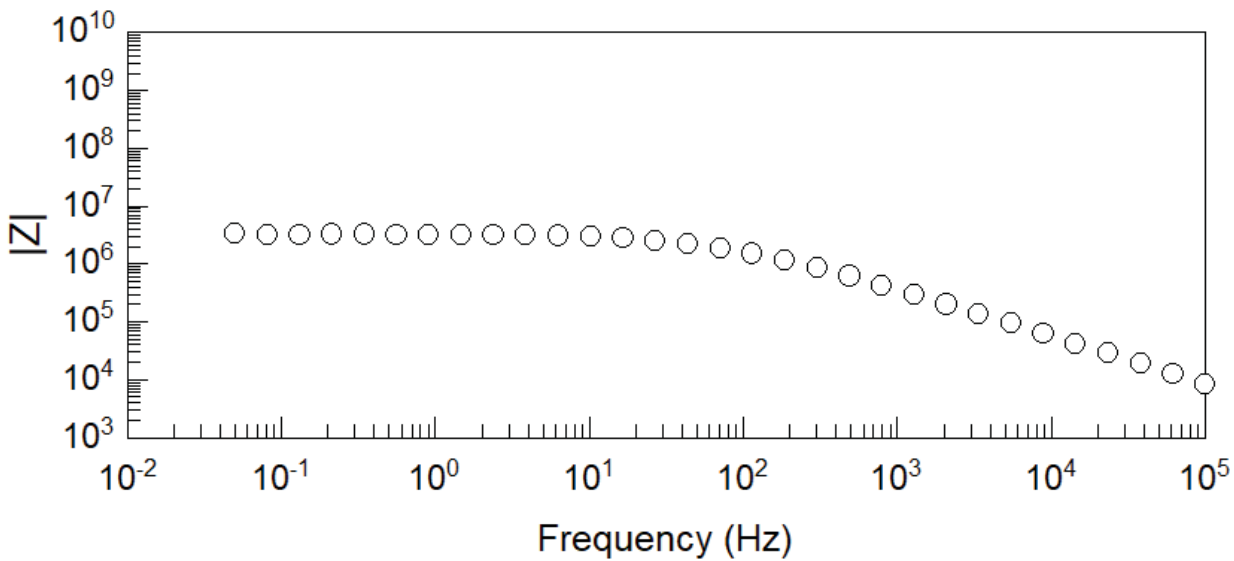


Figure A-7: Bode plot from pipe segment 33.

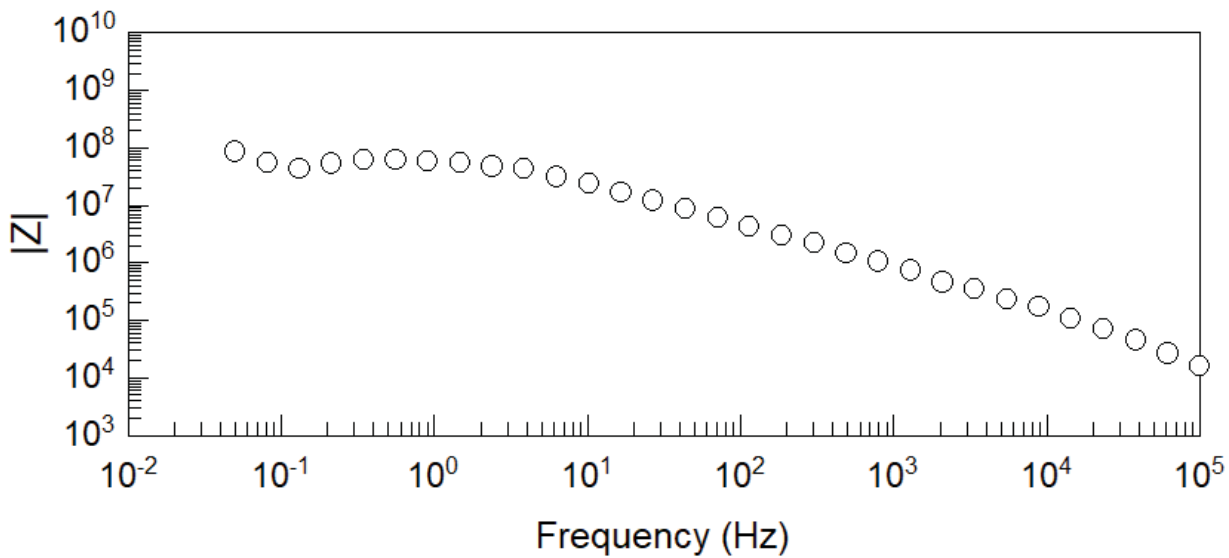


Figure A-8: Bode plot from pipe segment 37.

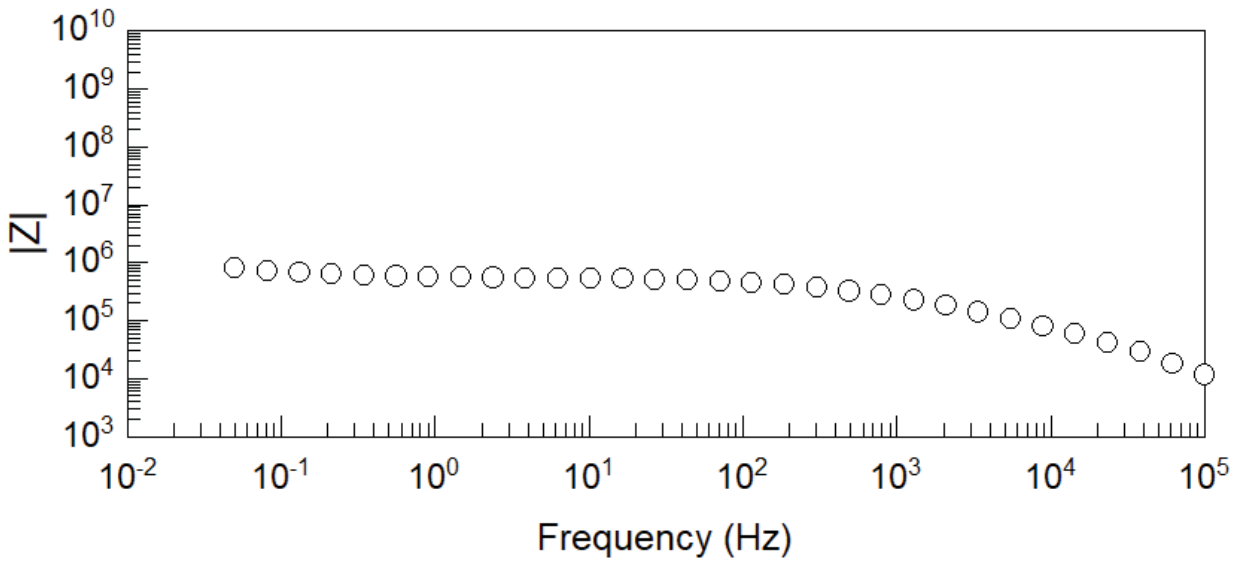


Figure A-9: Bode plot from pipe segment 64.

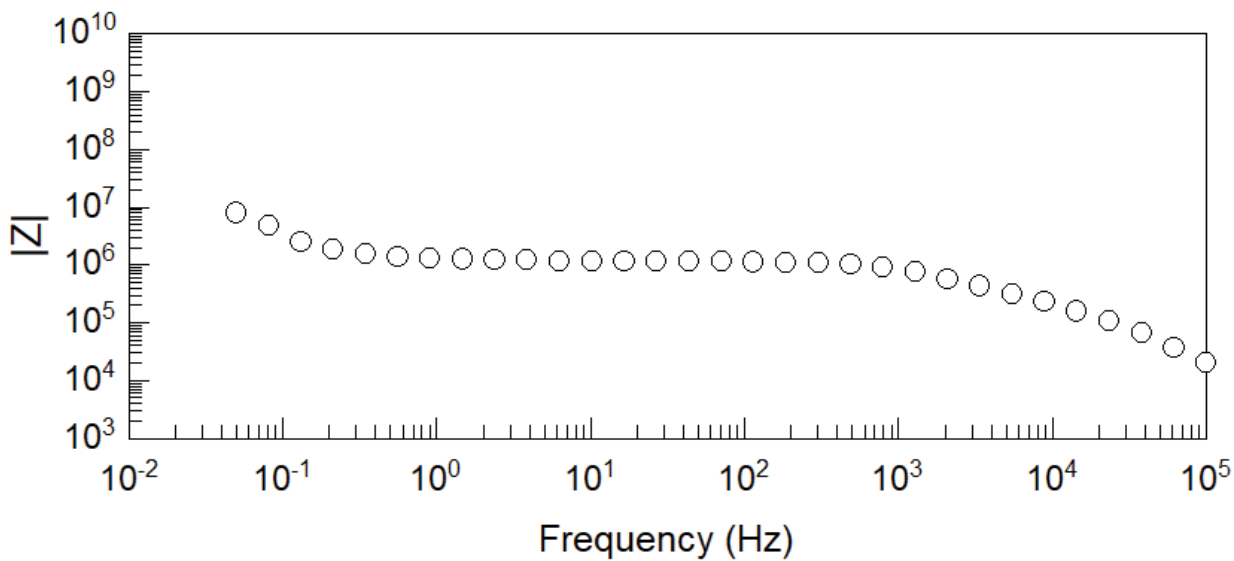


Figure A-10: Bode plot from pipe segment 68.

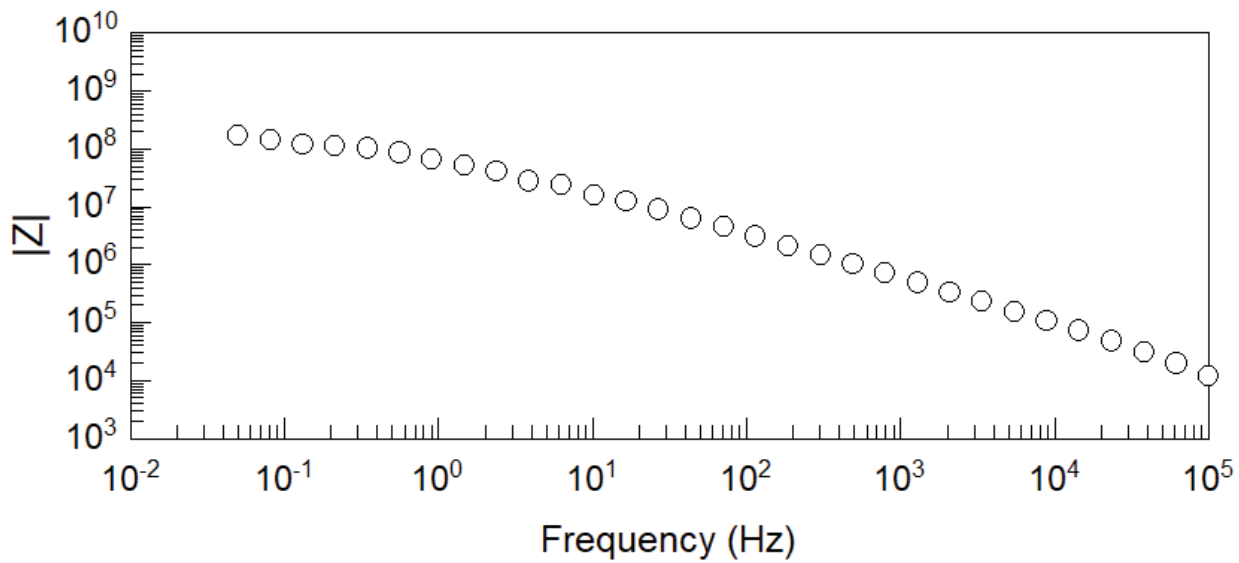


Figure A-11: Bode plot from pipe segment 72.

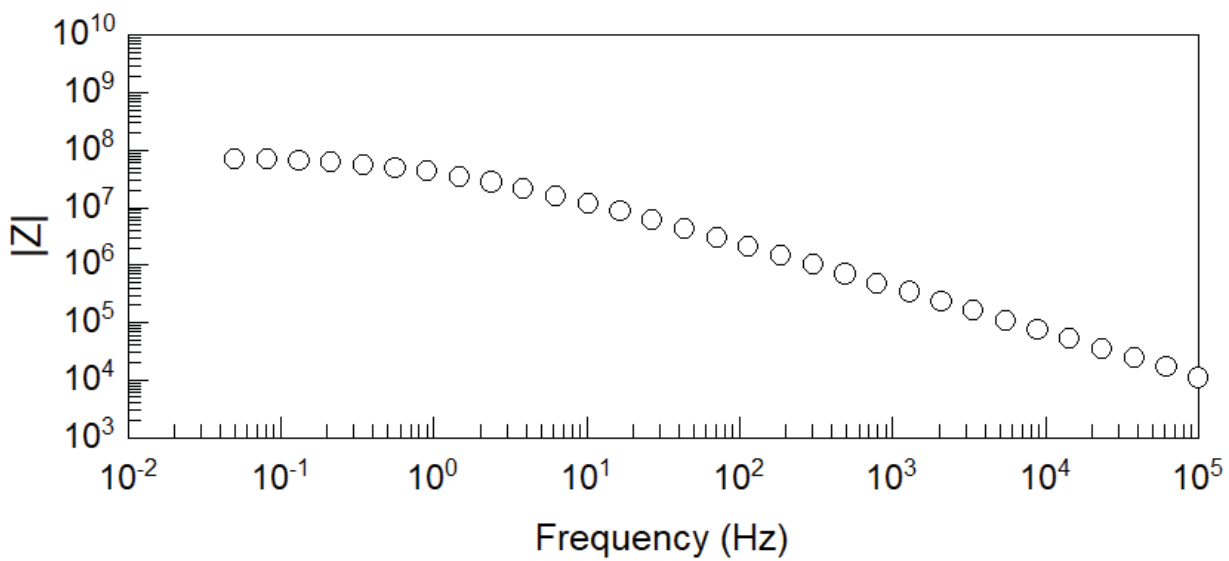


Figure A-12: Bode plot from pipe segment 76.

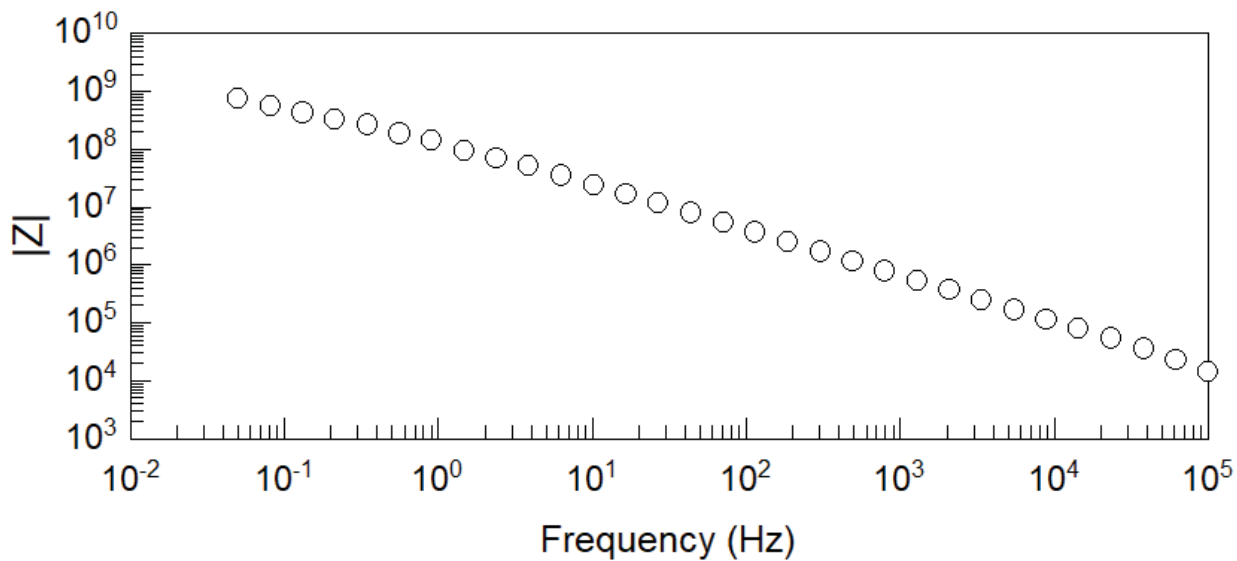


Figure A-13: Bode plot from pipe segment 80.

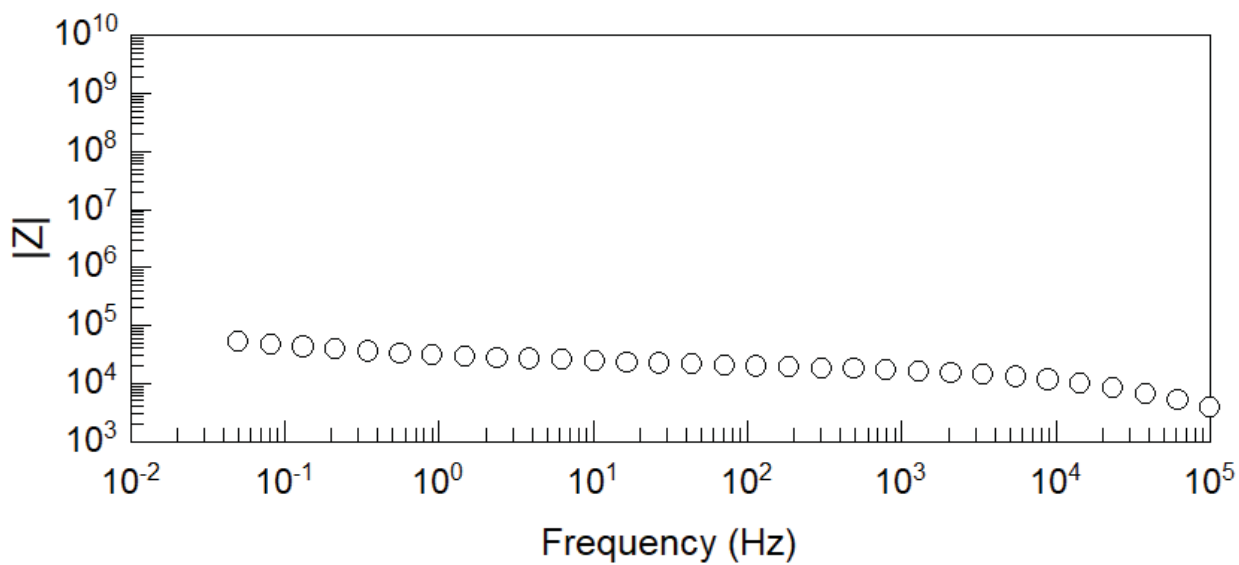


Figure A-14: Bode plot from pipe segment 84.

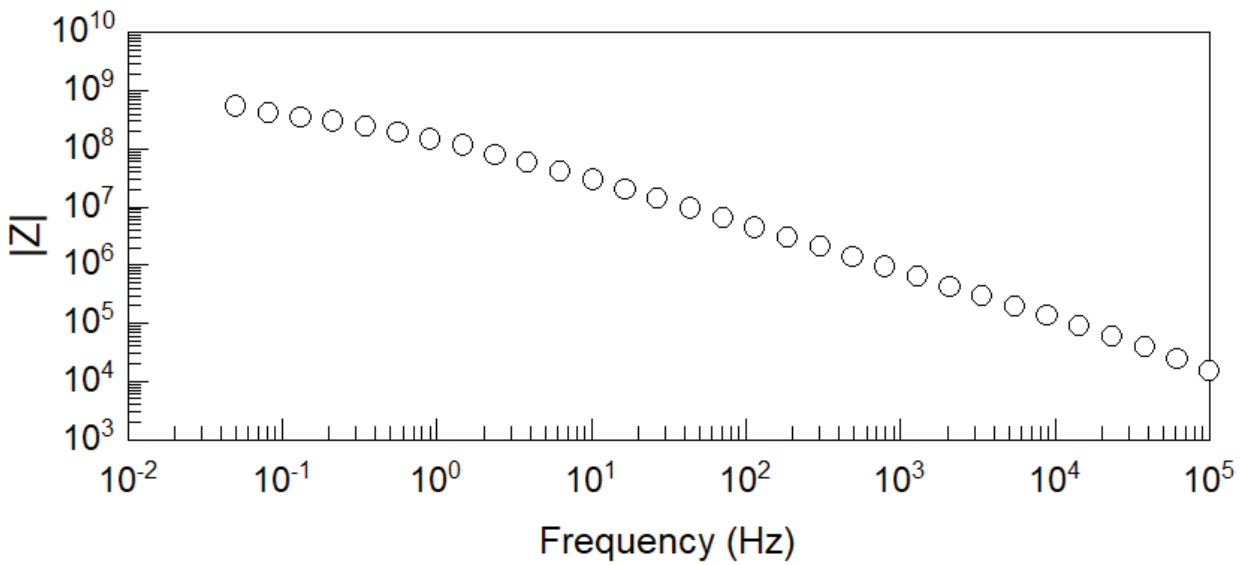


Figure A-15: Bode plot from pipe segment 87.

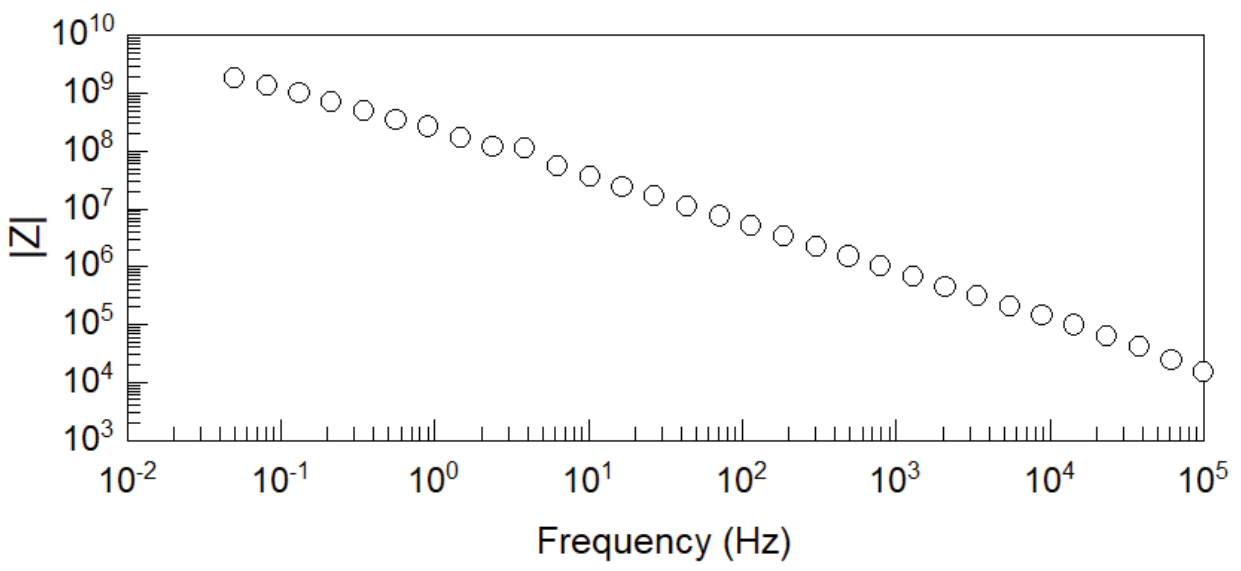


Figure A-16: Bode plot from pipe segment 91.

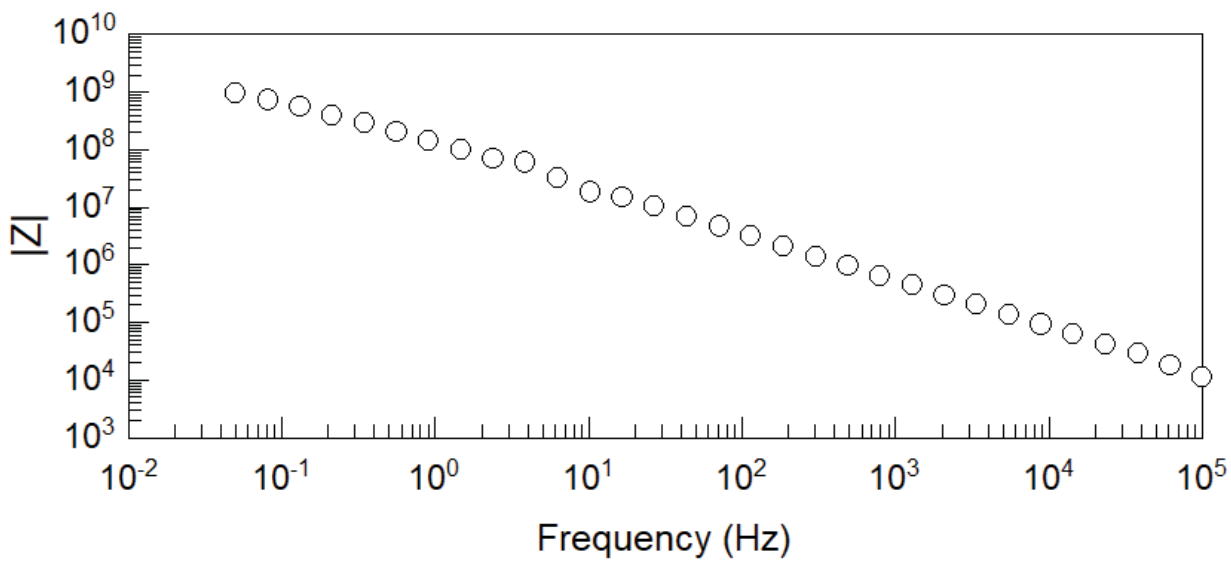


Figure A-17: Bode plot from pipe segment 95.

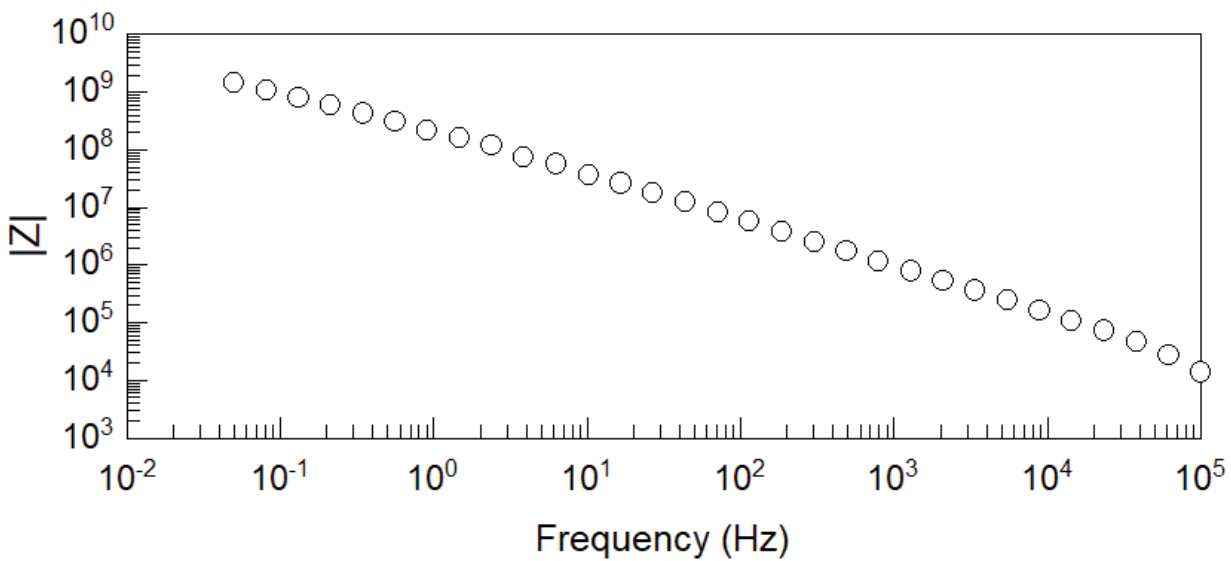


Figure A-18: Bode plot from pipe segment 99.

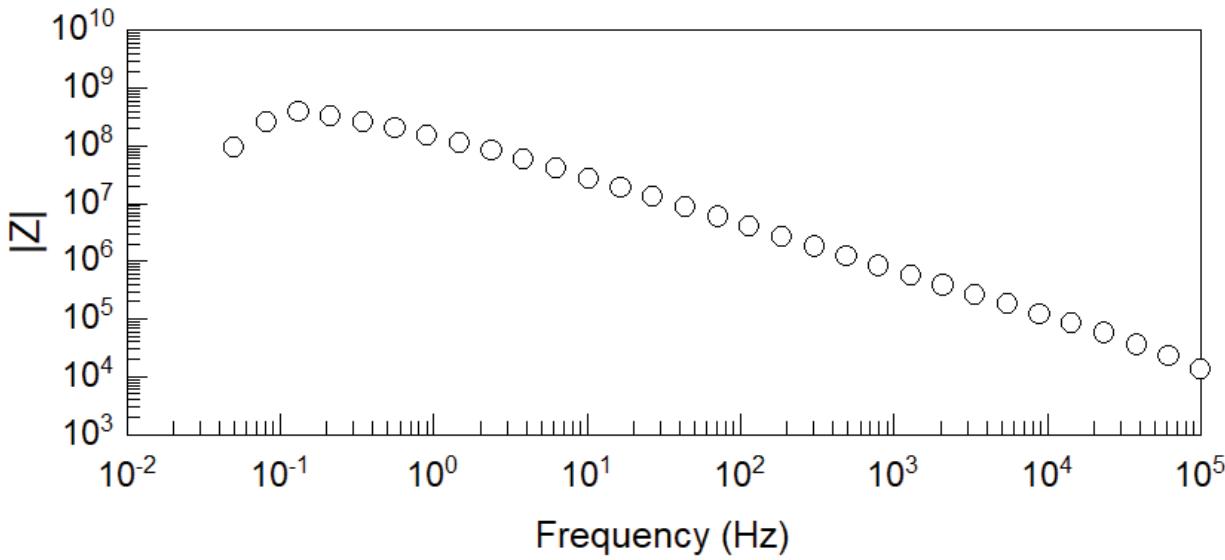


Figure A-19: Bode plot from pipe segment 107.

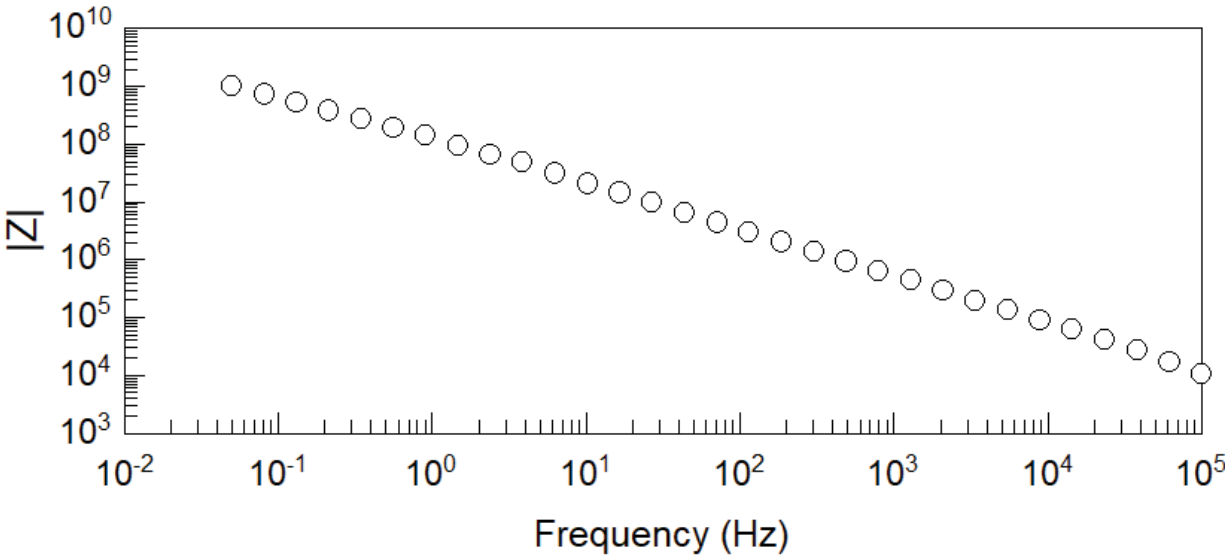


Figure A-20: Bode plot from pipe segment 112.

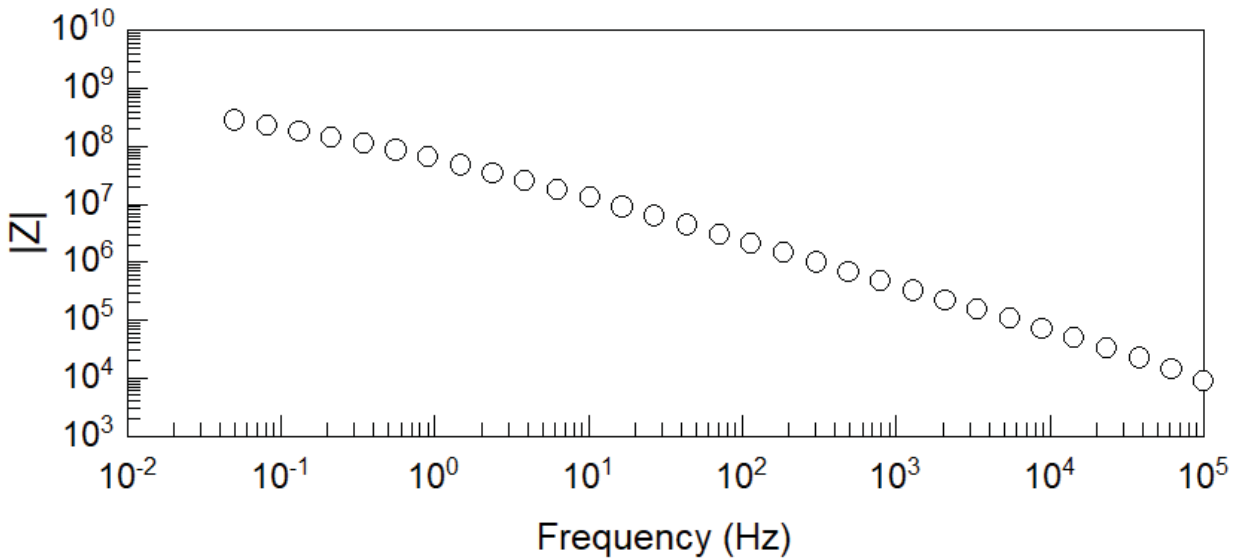


Figure A-21: Bode plot from pipe segment 116.

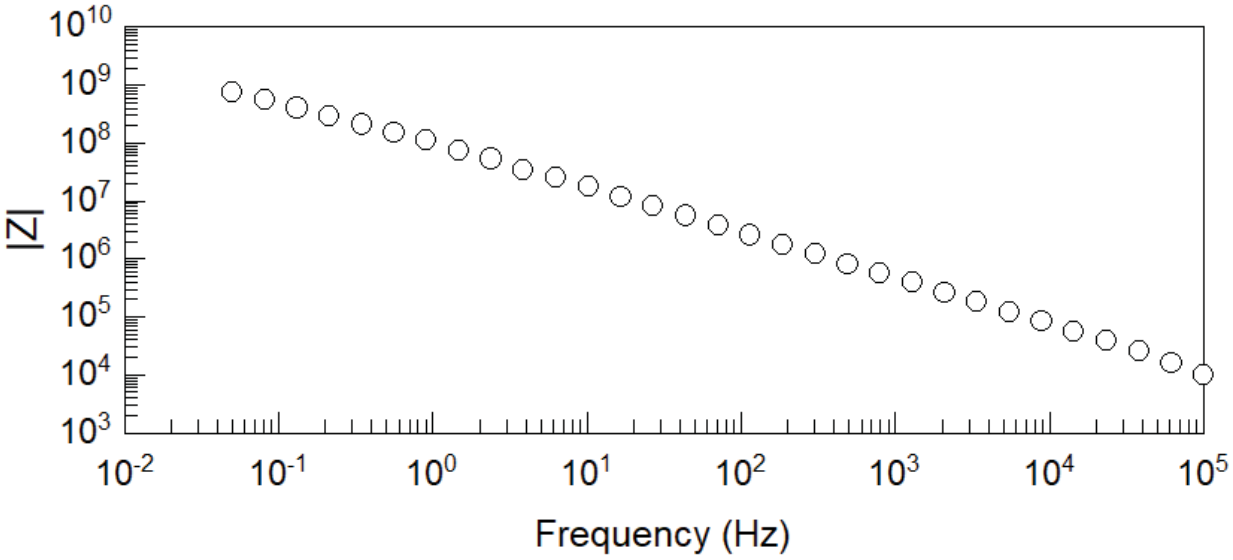


Figure A-22: Bode plot from pipe segment 120.

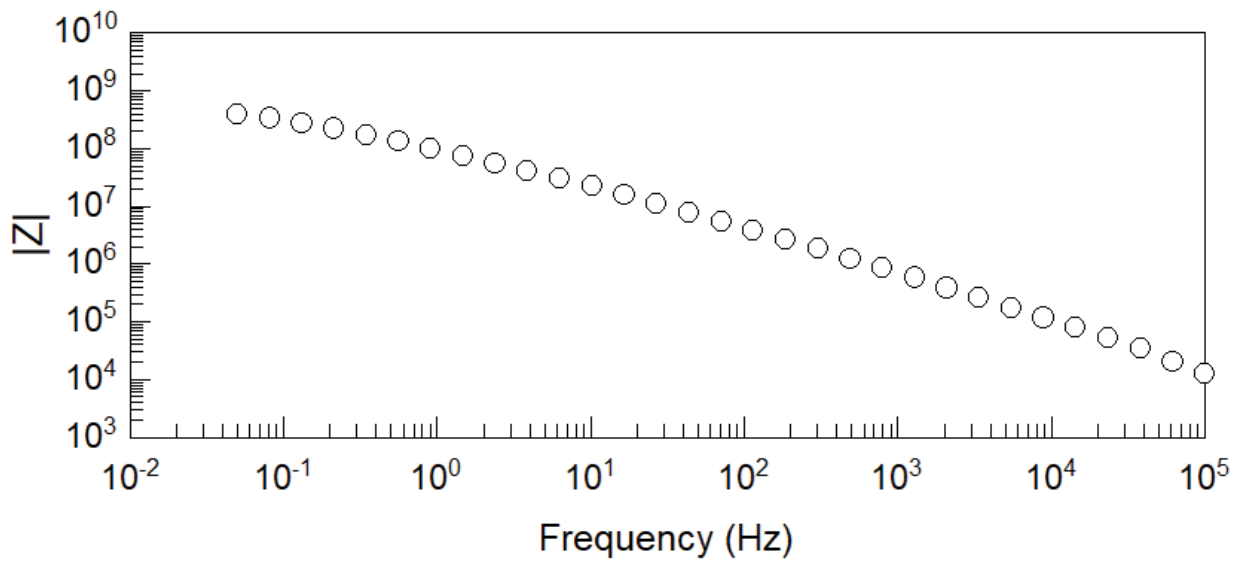


Figure A-23: Bode plot from pipe segment 124.

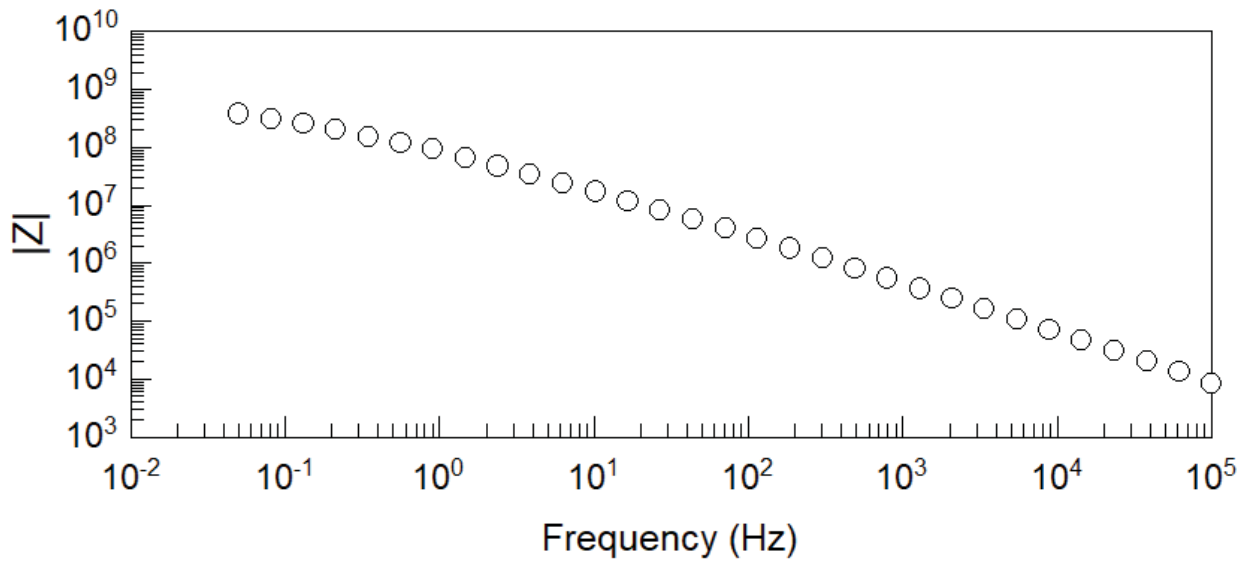


Figure A-24: Bode plot from pipe segment 128.

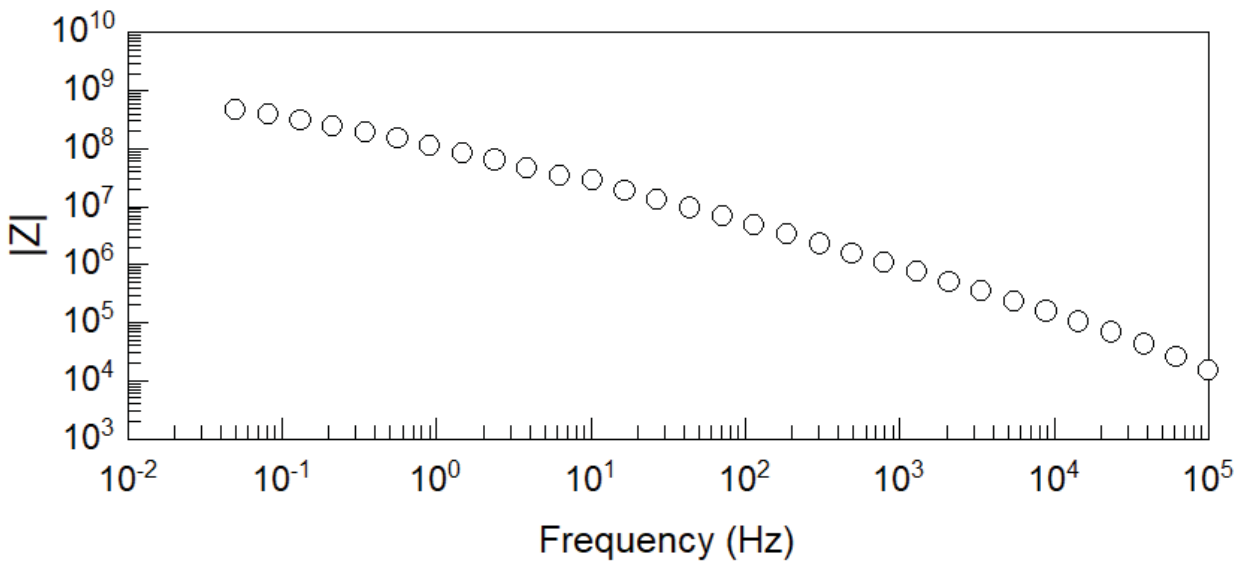


Figure A-25: Bode plot from pipe segment 132.

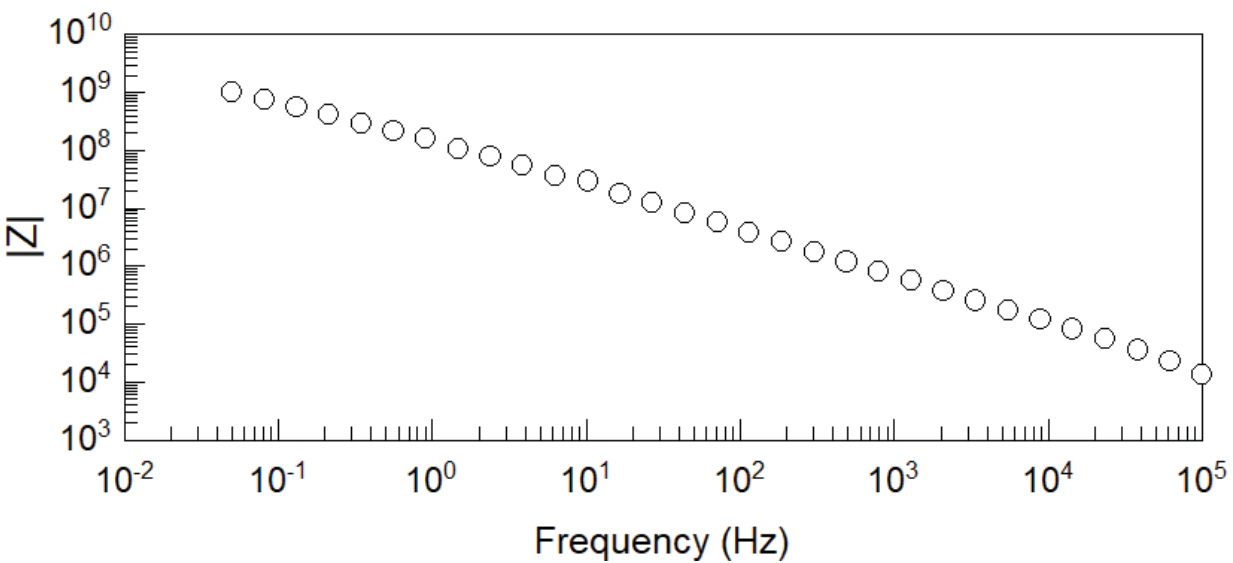


Figure A-26: Bode plot from pipe segment 136.

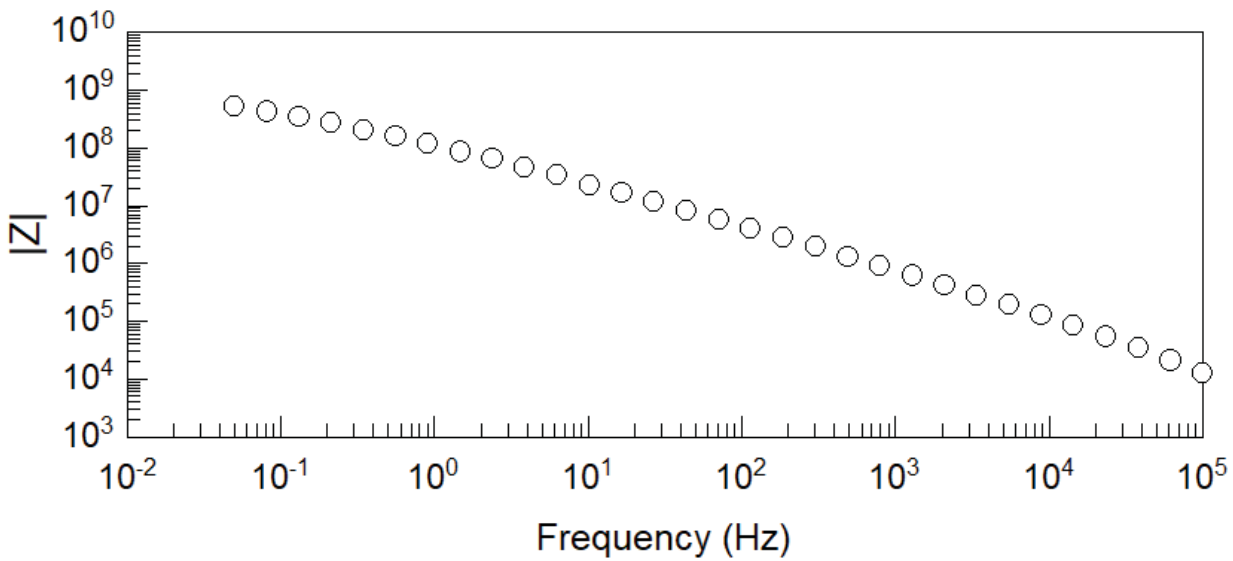


Figure A-27: Bode plot from pipe segment 140.

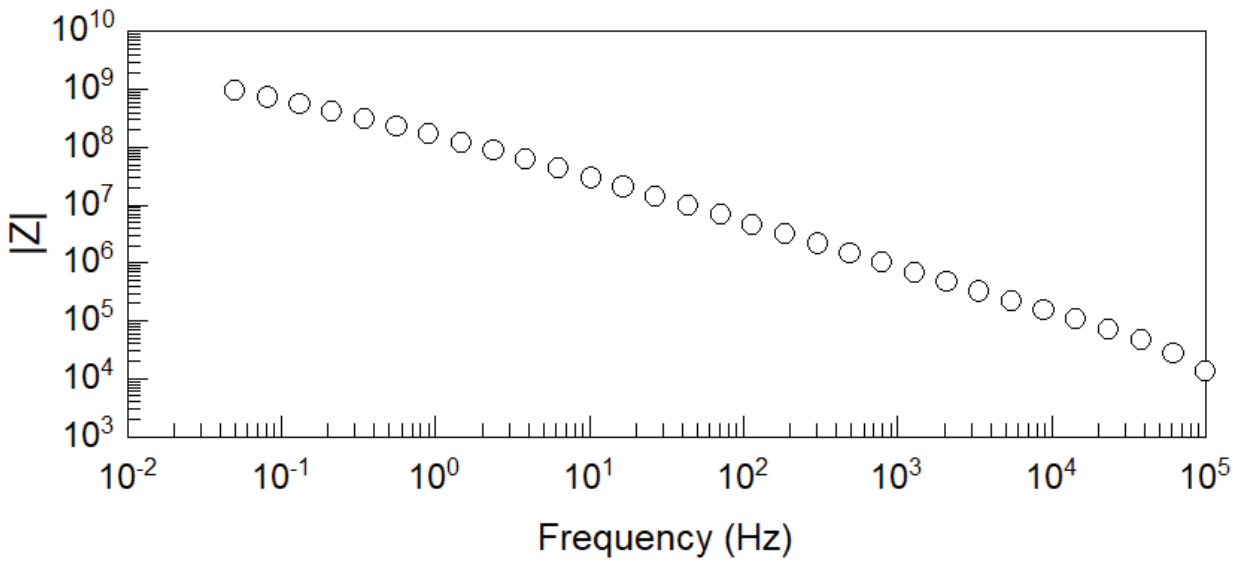


Figure A-28: Bode plot from pipe segment 144.

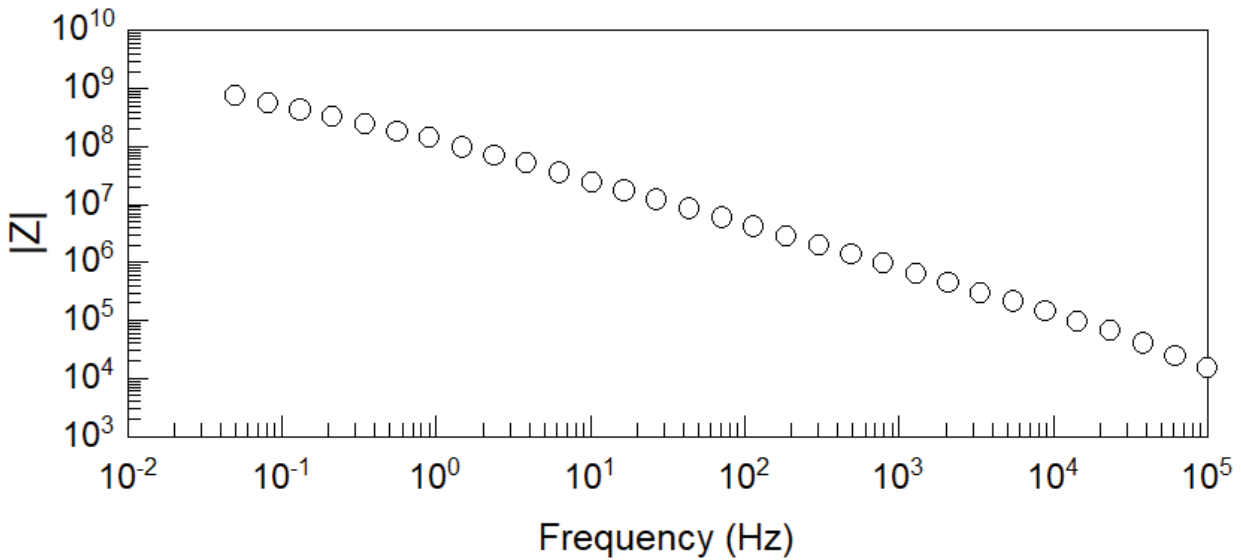


Figure A-29: Bode plot from pipe segment 148.

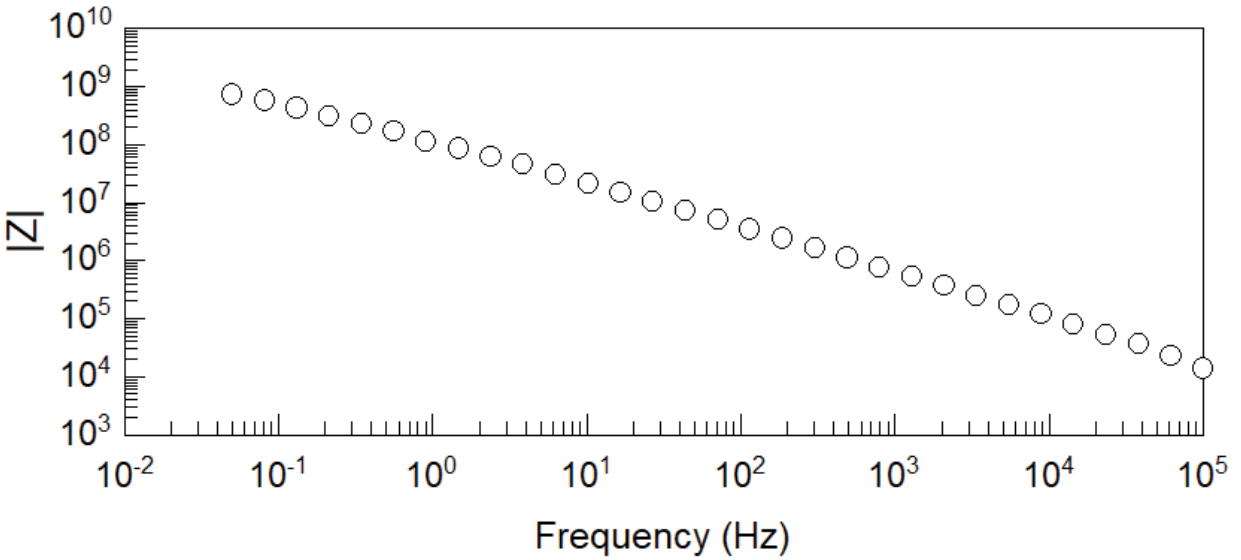


Figure A-30: Bode plot from pipe segment 152.

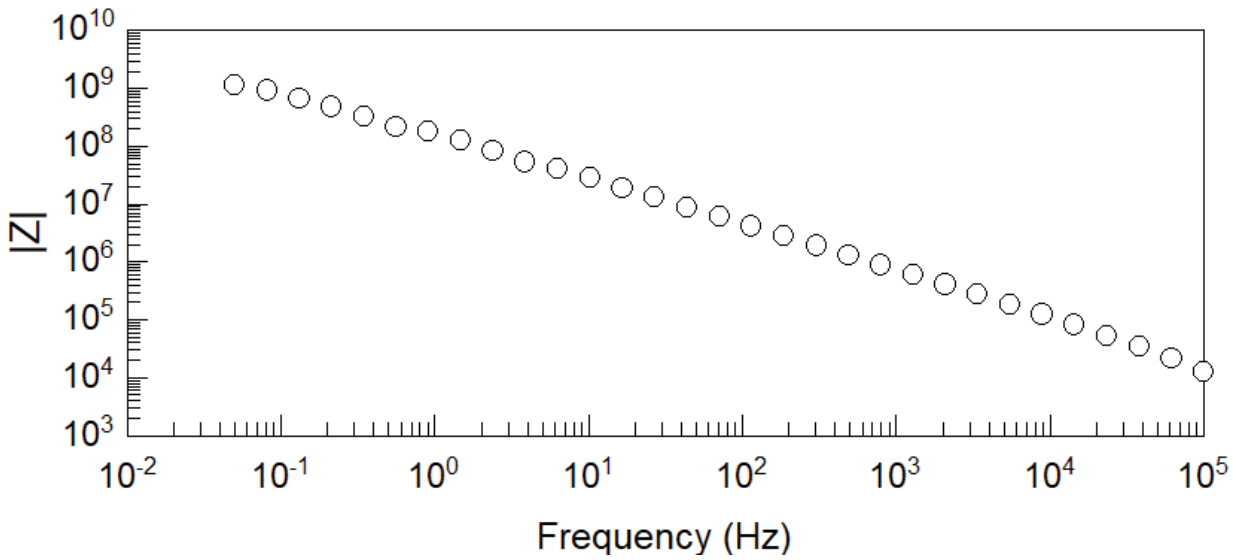


Figure A-31: Bode plot from pipe segment 156.

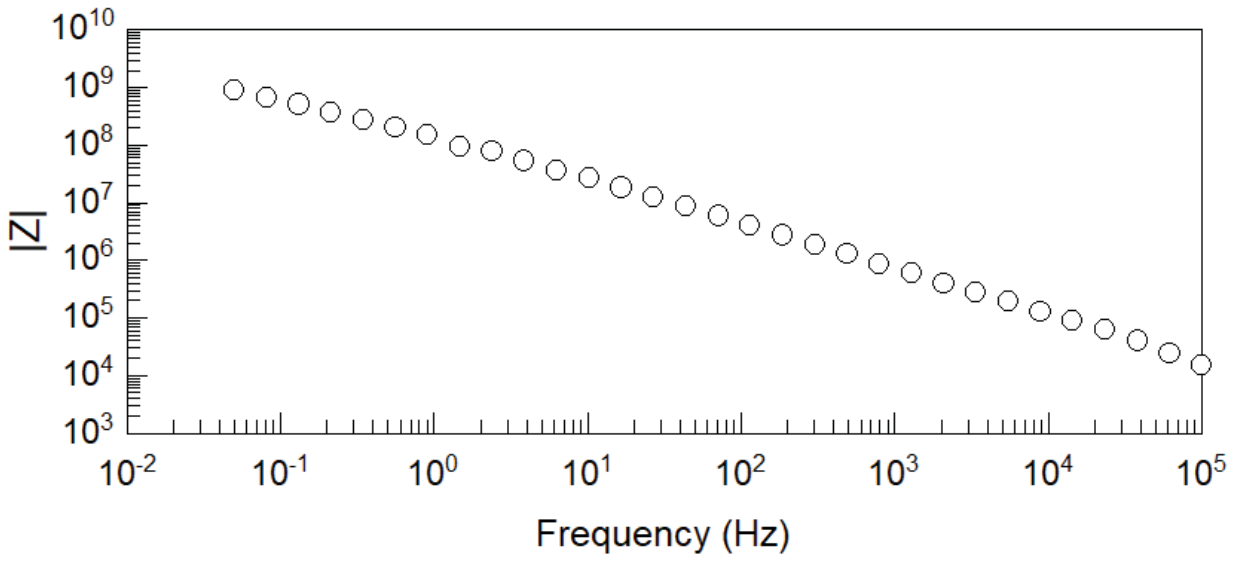


Figure A-32: Bode plot from pipe segment 160.

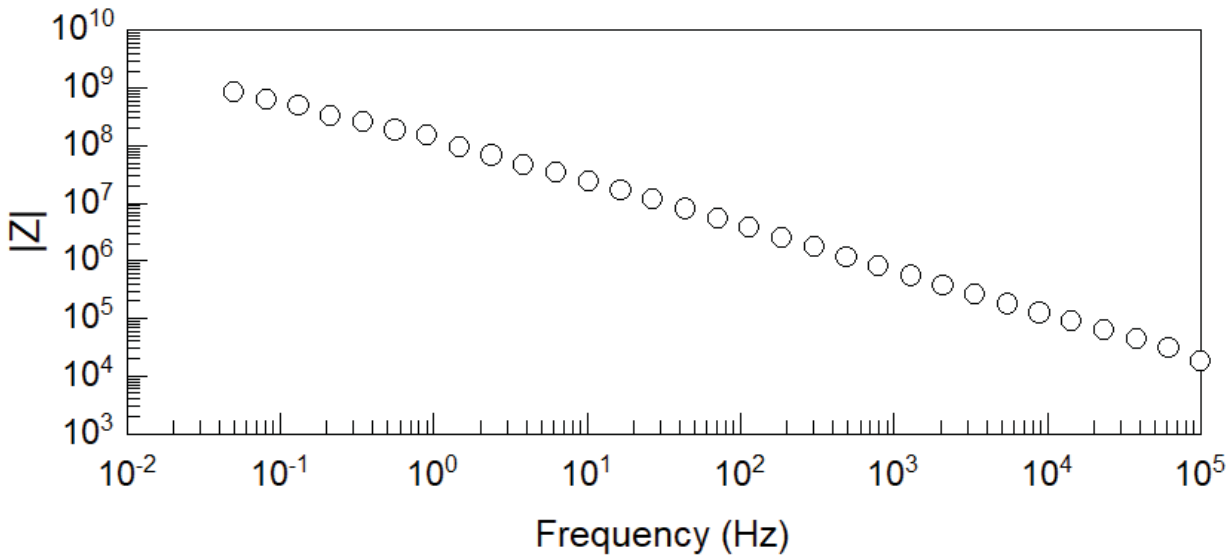


Figure A-33: Bode plot from pipe segment 164.

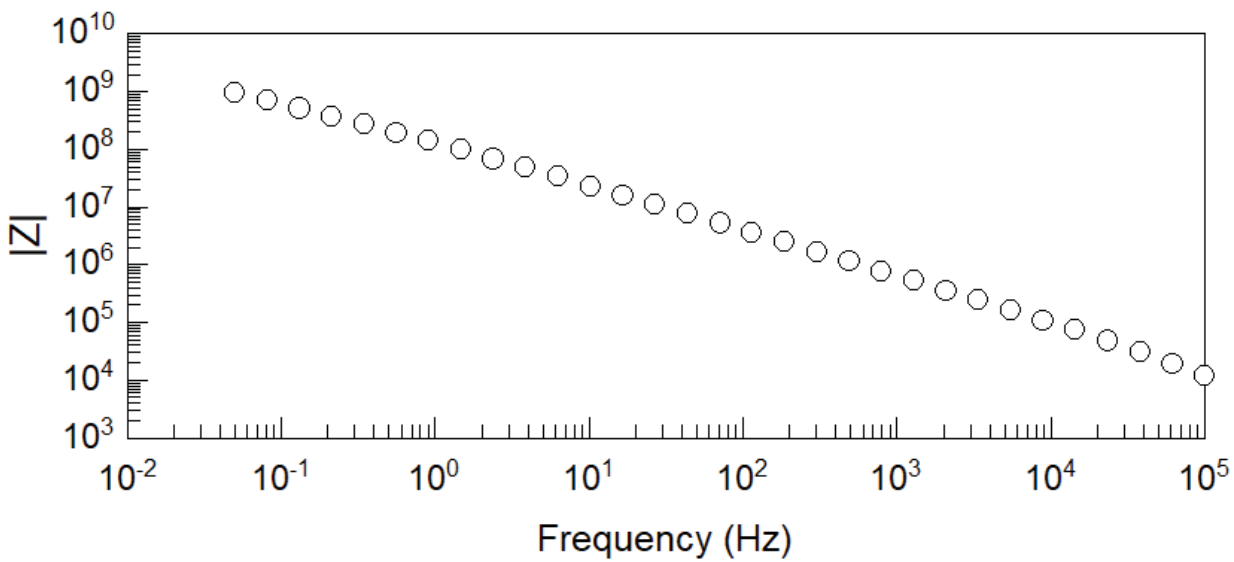


Figure A-34: Bode plot from pipe segment 168.

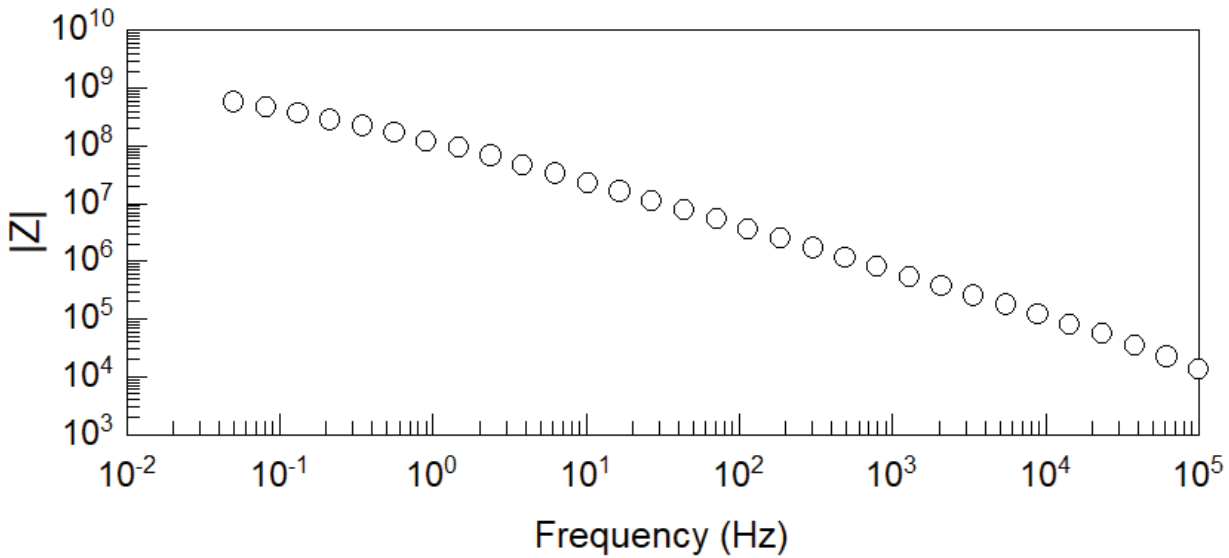


Figure A-35: Bode plot from pipe segment 172.

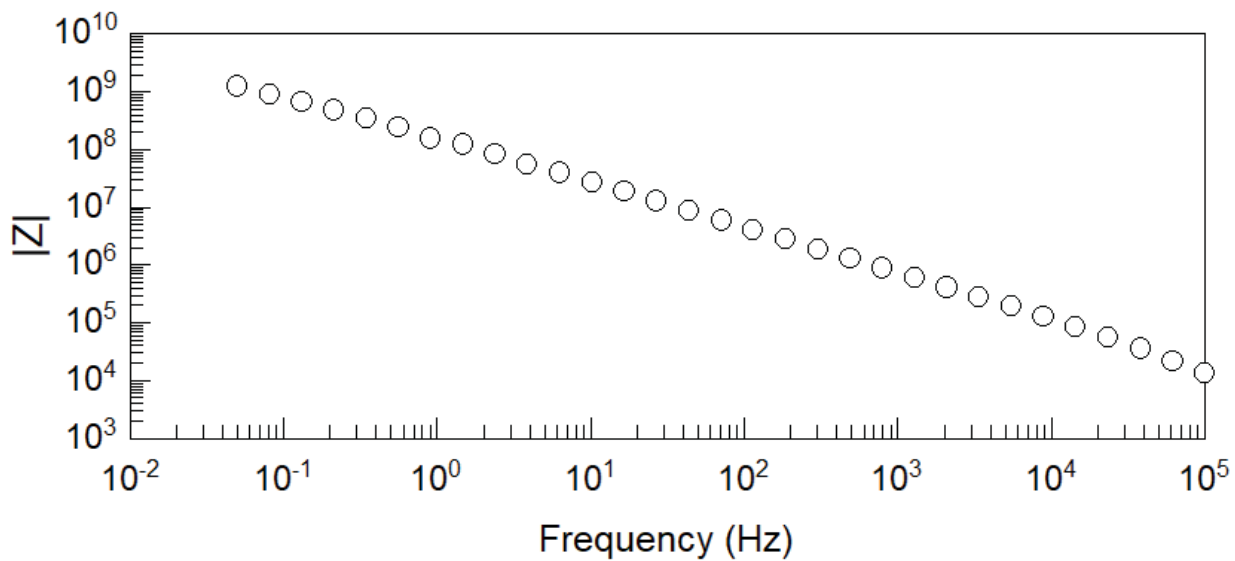


Figure A-36: Bode plot from pipe segment 176.

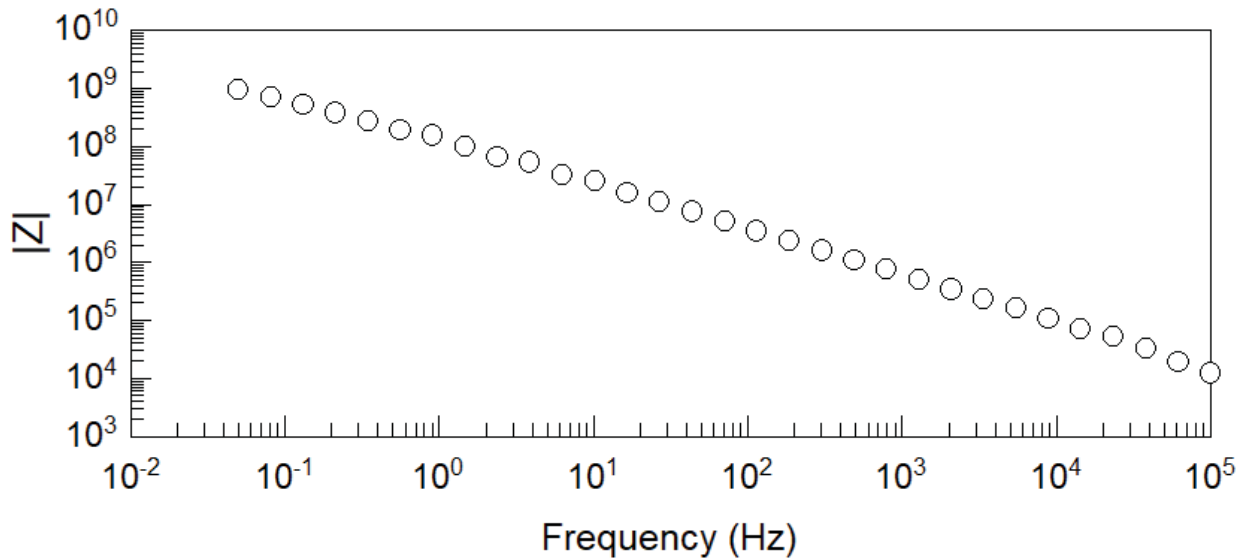


Figure A-37: Bode plot from pipe segment 180.

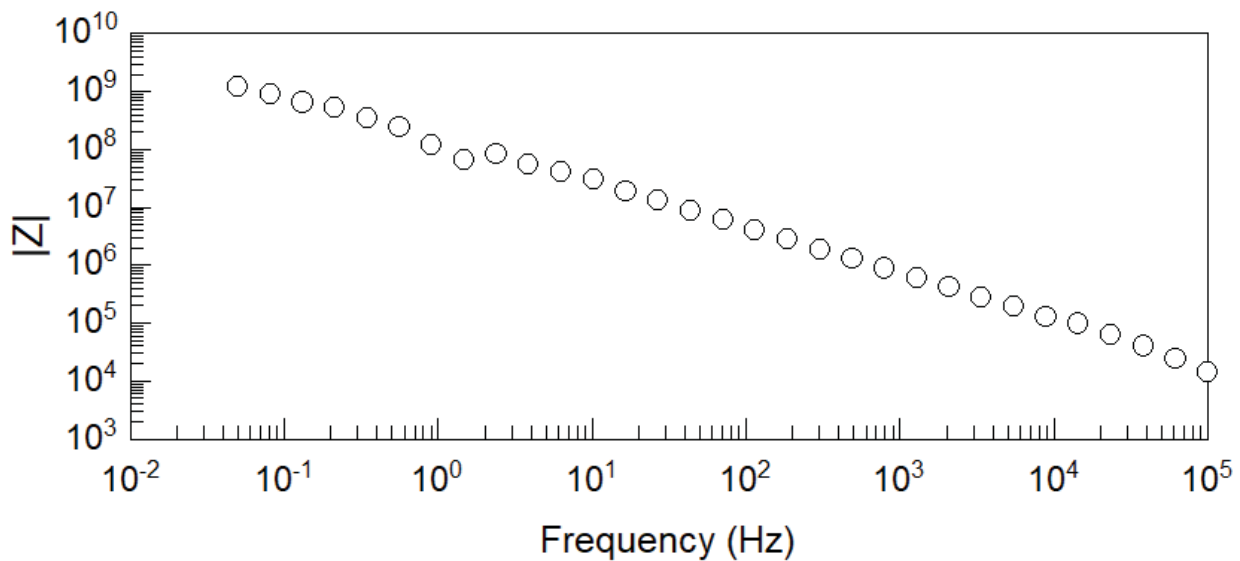


Figure A-38: Bode plot from pipe segment 184.

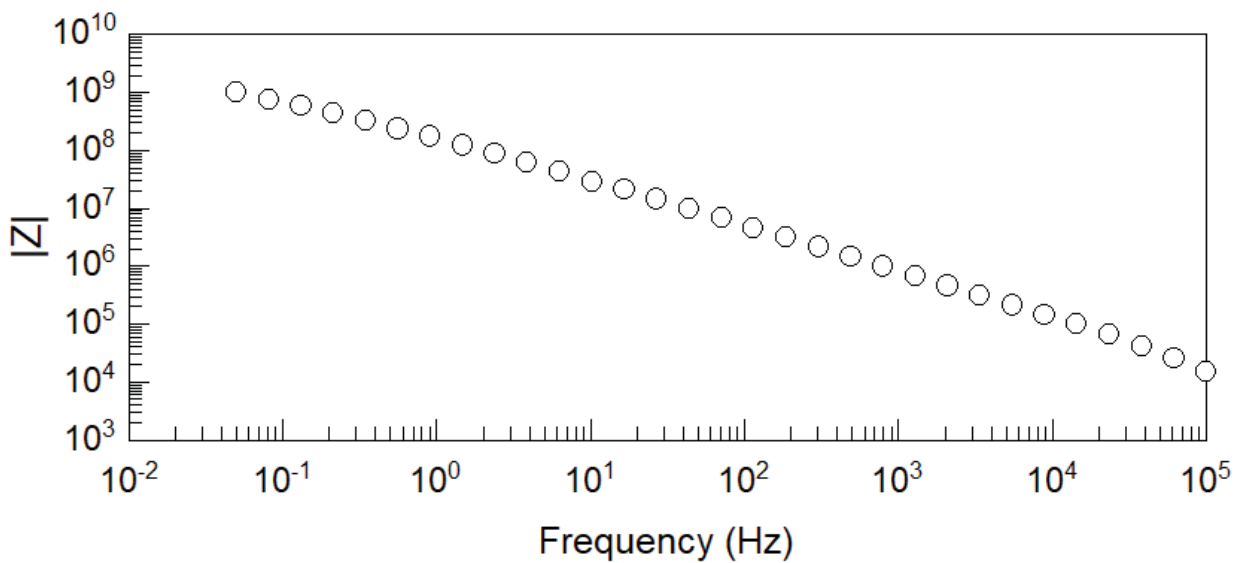


Figure A-39: Bode plot from pipe segment 188.

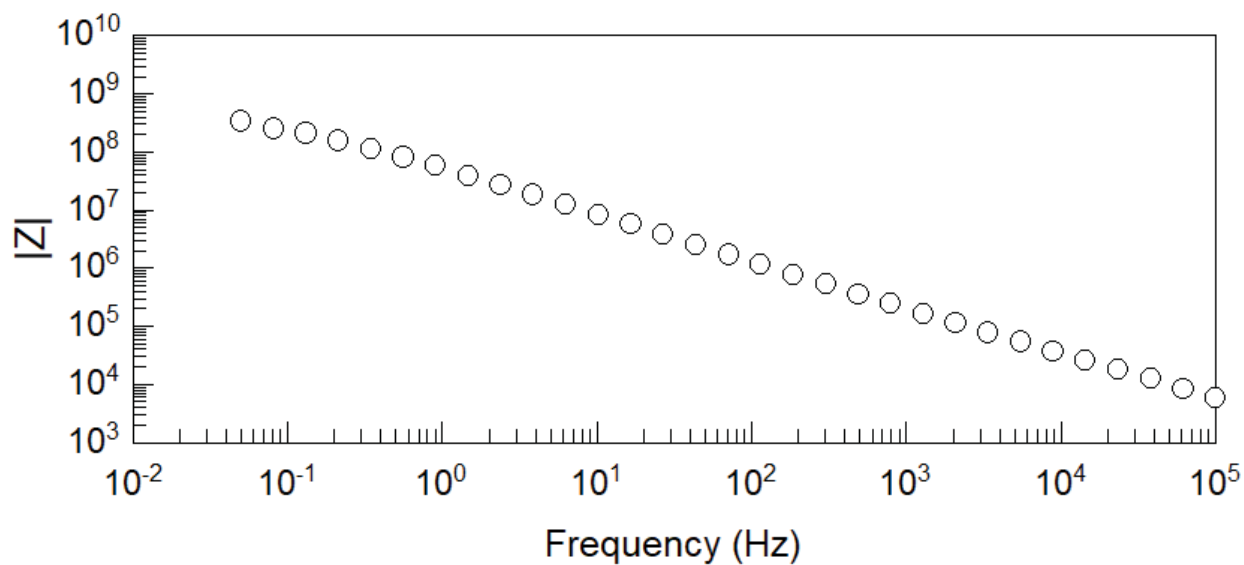


Figure A-40: Bode plot from pipe segment 192.

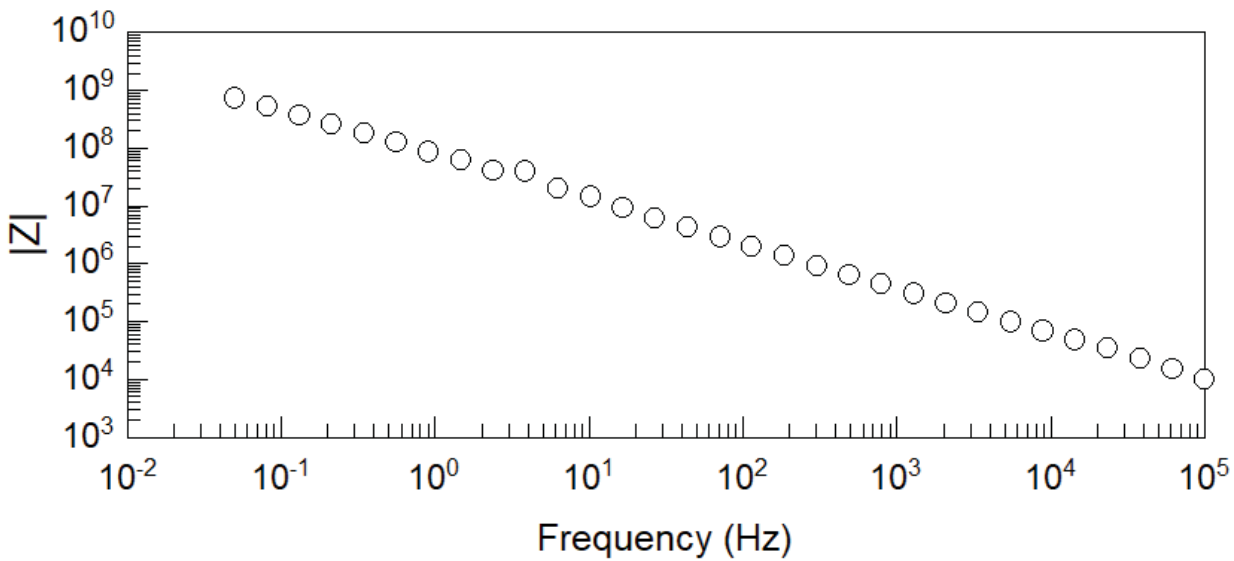


Figure A-41: Bode plot from pipe segment 196.

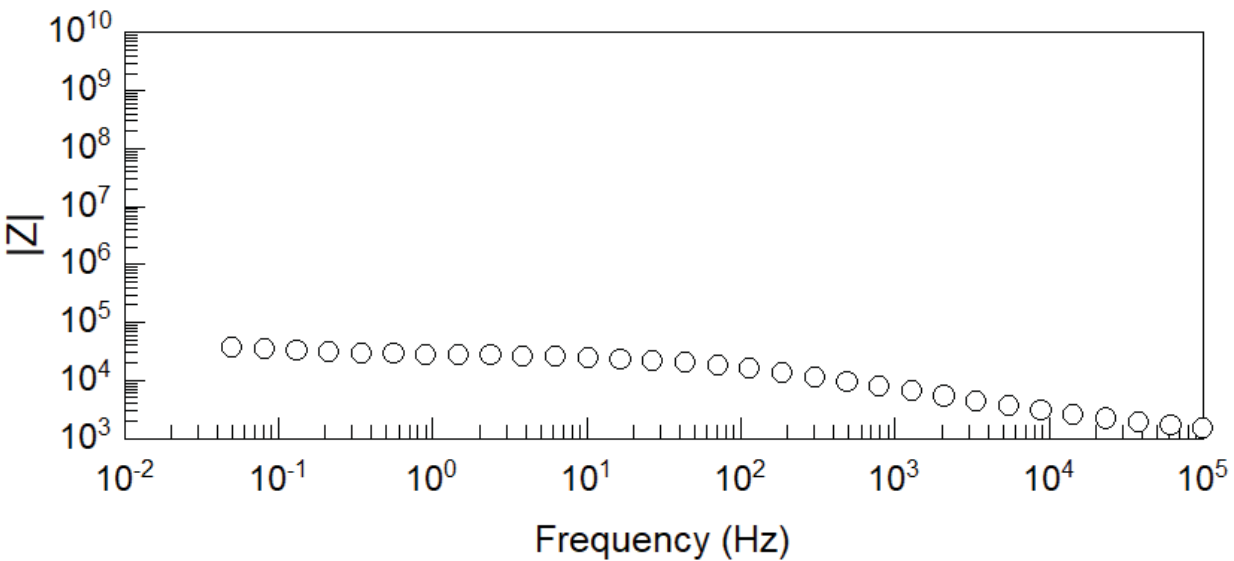


Figure A-42: Bode plot from pipe segment 200.

Appendix B – Dry Film Thickness Raw Data

Table B-1. Coating dry film thickness (DFT) values measured within Agua Fria River Siphon^{1,2}.

Segment	Left-hand wall DFT (mils)					Invert DFT (mils)					Right-hand wall DFT (mils)				
5	12.1	13.5	10.9	13	12.7	26.1	28.2	26.4	26.3	30.5	30	30.5	27.7	27	28.1
7	15.6	8.8	3.8	9.3	18.2	23.5	19.7	22.3	18.4	20.5	15	16.4	16.8	13.1	14.6
9	20.6	22	17.6	16.9	12.4	15.3	13.6	6.8	14.4	12.2	13.5	14.6	18	16.4	11.5
13	17	15.5	17.1	15.1	17.4	12.5	15	8	11.4	11.8	24.5	26.7	26.4	20.4	27.1
17	9.9	6.2	7.7	14.1	13.3	15.7	12.1	27.8	35.5	16	22.6	32.2	17.9	26.2	26.3
21	23.2	26.4	21.9	19.1	23.3	18.9	17	14.6	19.1	18.1	16	18.9	15.3	18	15.7
25	17.4	16	15.1	17	15.9	15.6	10.8	15.8	18.3	13.1	30.6	26.1	28.8	27.5	27.3
29	15.2	13.5	12.9	14.9	15.7	18.9	19.1	19.9	18.7	17.3	25.5	27.3	22.8	23	23.1
33	34.6	35.5	36.5	33.2	29.9	46.3	46.2	41.9	31.8	32.1	30.2	36.8	31.1	26.2	24.9
37	20	17.2	18.6	20.4	19	5.4	8	8.4	8.9	10.8	22.3	22.9	21.6	22.4	22.5
48	23.1	23	23.5	24.4	21.2	7.3	7.7	7.1	6.2	4	26.3	27.8	26.9	27	26.9
52	36.9	33.7	32.5	32.1	36.7	6.5	6.7	6.5	6.1	4.5	37.2	36.7	36.7	28.1	27.4
56	24.9	24.1	23.7	25.4	23.4	16.5	16.5	14.5	13.1	15.8	24	26.1	25.3	25.1	25.3
64	20.9	21	21.3	21.7	22.2	25.5	9.6	12.6	11.9	10.8	24.3	22.3	21.3	22.4	21.4
68	25.1	24.5	24.7	24.3	25.3	14	13.1	10.3	10	16.6	24.8	25.6	25.9	26.2	24.9
72	24.6	40.2	39.6	32.1	23.5	N/A	N/A	N/A	N/A	N/A	31.9	33.4	38.6	34.8	32.7
76	26.4	24.8	27.6	25.5	24.9	10.1	9	11.4	12.7	11.4	22.3	22.1	22.9	23.3	23.4
80	25.7	25.5	25.4	26.8	26.3	13.1	11	11.8	11.6	8	24.3	24.6	23.4	25.7	26.4
84	12.6	11.1	11	11.1	11.6	13.9	11.3	18.1	11.7	14.2	12.4	14.1	12.1	12.5	14
87	47.4	40.3	46.9	47.9	45.2	29.1	30.8	29	28.6	31.6	32.9	33.2	32.2	33.6	32.9
91	35.7	36.3	34	33.9	35.7	23.3	19.6	22.9	18.5	21.8	35.9	46.6	36.2	36.2	36.3
95	30.9	41.1	30.2	28.8	30.4	6.2	8.6	6.8	11.2	8.3	26.6	27.8	28.5	26.6	25.7
99	33.6	37.4	41.4	38.7	28.5	13	21.5	21.5	14.2	16.7	37.2	35.1	33.1	40.1	28.3
103	39.1	42	40.9	40.1	38.8	10.5	11.4	12.5	10.3	10.2	31.3	31.6	30.9	31.9	31.4
107	45.1	40.2	40.7	43.7	38.7	29.4	6.1	27.6	11.6	17.8	29.5	28.5	31.6	30.7	29.6

112	34.8	32.7	31.2	32.9	30.5	19.5	21.9	18.3	19.8	19.5	26.4	27.1	28.8	27.7	28.2
116	43.1	45.4	43.3	43	45.3	13.9	16.6	14.3	16.8	13.3	30.3	27.6	31.9	24.5	31.6
120	26.3	27.6	28.1	27.3	27.2	9.7	10.1	11	10	6.7	21.6	21.4	21.3	20.7	21.3
124	27.2	28	29.4	25.6	26.7	2.9	5.6	5.5	3.2	5.1	33.3	31.5	30.4	31.2	36.4
128	43.4	38.5	39.1	45.5	37	32.7	32.5	30.3	32.2	32	19.4	19	21.5	27	22.9
132	34.5	34	35.1	34	34.4	30	30.9	29.7	29.7	29.1	24.2	26.6	29.1	27.8	26.4
136	38.1	35.9	36.9	40.5	37.1	24.2	23.7	24.9	21	21.8	26.5	26.8	26.6	26.1	27.4
140	26.2	26.4	26	26	27.3	17.6	15.9	16.4	15.6	16.3	26.8	26.4	27	25.5	25.2
144	39.4	37.1	37.3	37.7	38.3	26.4	25.7	20.4	28.7	27.8	31.9	32.2	32.9	33.4	33.6
148	28.7	28.3	28.3	29.2	28.2	13	14.3	13.1	11.5	13.9	29	28.8	28	28.4	29.1
149	30.8	31.5	31.1	30.4	32.1	9	10.8	8.1	9.9	9.4	32.3	31.8	31.9	32.5	32.4
150	35	35.5	32.6	38.8	35.5	8.8	9	10.3	10.1	11	25.5	24.3	24.9	24.6	24.7
152	37.1	39.7	38	36.8	36.4	4	5.5	3.7	5.6	3.2	31.6	31.7	30.8	29.9	30.8
156	26.2	26.4	24.7	25.5	25.8	15.3	15.7	14.3	14.4	12.6	26.4	26.1	26	26.2	26
160	34.3	33	33.7	34	33.8	10.5	10	11.8	12.8	15.2	31.6	31.5	31.7	32.7	30.7
164	26.5	28.3	27.4	27.9	27.4	21.6	22.4	22.7	17.8	20.5	27.9	27.6	27.5	28.1	27.7
168	23	24.2	23.5	22.9	22.1	17.1	17.8	17.2	16.4	22.9	24.4	23.9	24.6	23.3	23.7
172	29.8	28.2	27.7	28.2	28.9	12.7	14.7	17.5	10	11.5	23.2	25.7	24.1	25.4	24.4
176	22.6	23.6	24.9	23.7	23.9	7.5	7.8	8	6.5	5	N/A	N/A	N/A	N/A	N/A
180	24.4	50	24.8	24.1	24.3	14.9	15.7	16.1	17	18.9	25.2	23.8	25	24.3	24.8
184	32.6	32.6	32.8	33.5	34.5	6.6	6	4.4	7.1	6.6	31.4	32.8	30	28.6	37.4
188	33.8	34.1	34	34.4	33.7	7.9	7.9	9.1	7.9	9.8	33.5	35.1	33.3	32.8	31.7
192	32.4	30.8	32.3	32	32.6	6	4.8	5.6	5.5	4.1	25	23.8	25.4	23.5	24.6
196	24.7	24.4	23.6	23.9	25	31.8	28.9	28.4	24.6	20	22.1	27.2	23.9	24.4	22.7
200	16.9	25.5	18.9	24.4	27.8	5.4	12.2	6.5	3.5	9.2	43	35.2	24.2	49.1	40

¹ Green represents relatively high DFT values and red represents relatively low DFT values.

² Originally specified minimum DFT was 24 mils.

Appendix C – Ultrasonic Thickness Raw Data

Table C-1. Steel pipe ultrasonic thickness (UT) values measured within Agua Fria River Siphon¹.

Pipe Segment	Left-hand wall pipe thickness (inches)					Invert pipe thickness (inches)					Right-hand wall pipe thickness (inches)					Specified (inches) ²
5	0.536	0.594	0.538	0.536	0.536	0.536	0.536	0.536	0.538	0.536	0.534	0.532	0.540	0.540	0.532	0.53
9	0.608	0.606	0.608	0.608	0.606	0.596	0.596	0.594	0.540	0.596	0.598	0.598	0.596	0.600	0.600	0.53
13	0.530	0.522	0.532	0.534	0.484	0.538	0.538	0.536	0.536	0.536	0.534	0.528	0.532	0.532	0.532	0.53
17	0.534	0.530	0.530	0.534	0.532	0.532	0.532	0.532	0.534	0.534	0.528	0.530	0.526	0.526	0.526	0.53
21	0.562	0.560	0.562	0.562	0.560	0.560	0.568	0.568	0.566	0.568	0.550	0.612	0.552	0.552	0.556	0.53
25	0.534	0.538	0.538	0.532	0.536	0.532	0.540	0.542	0.542	0.542	0.540	0.544	0.548	0.546	0.550	0.53
29	0.540	0.538	0.540	0.538	0.542	0.540	0.540	0.538	0.538	0.538	0.540	0.540	0.538	0.538	0.538	0.53
33	1.020	1.018	1.018	0.972	1.020	1.026	1.024	1.024	1.022	1.022	1.030	1.028	1.030	1.028	1.028	1.01
37	1.026	1.028	1.028	1.028	1.028	1.018	1.018	1.018	1.018	1.018	1.014	1.016	1.014	1.014	0.962	1.01
52	1.094	1.094	1.094	1.092	1.094	1.092	1.092	1.090	1.090	1.090	N/A	N/A	N/A	N/A	N/A	1.07
56	1.106	1.106	1.106	1.106	1.108	1.102	1.102	1.100	1.100	1.084	1.084	1.088	1.086	1.088	1.086	1.07
64	1.082	1.080	1.082	1.082	1.082	1.082	1.080	1.082	1.080	1.080	1.082	1.082	1.084	1.082	1.080	1.07
68	1.094	1.094	1.094	1.094	1.094	1.082	1.082	1.080	1.082	1.082	1.070	1.070	1.070	1.068	1.068	1.07
72	1.090	1.090	1.090	1.090	1.090	1.092	1.092	1.092	1.090	1.090	1.092	1.092	1.090	1.092	1.092	1.07
76	1.026	1.026	1.024	1.026	1.026	1.024	1.026	1.024	1.024	1.024	1.030	1.030	1.032	1.030	1.034	1.01
80	0.682	0.684	0.684	0.682	0.682	0.684	0.68	0.682	0.68	0.634	0.682	0.682	0.682	0.684	0.684	0.66
84	0.544	0.546	0.542	0.544	0.542	0.542	0.544	0.542	0.542	0.544	0.538	0.540	0.540	0.540	0.538	0.53
87	0.548	0.550	0.548	0.548	0.548	0.548	0.548	0.548	0.548	0.548	0.546	0.544	0.548	0.548	0.544	0.53
91	0.536	0.536	0.540	0.538	0.538	0.526	0.532	0.534	0.536	0.534	0.538	0.536	0.538	0.538	0.532	0.53
95	0.536	0.536	0.536	0.536	0.536	0.478	0.536	0.536	0.534	0.536	0.530	0.530	0.530	0.530	0.530	0.53
99	0.526	0.528	0.526	0.528	0.526	0.530	0.530	0.532	0.528	0.532	0.59	0.534	0.532	0.532	0.534	0.53
103	0.540	0.542	0.542	0.540	0.544	0.534	0.534	0.534	0.534	0.534	0.534	0.538	0.538	0.538	0.538	0.53
107	0.544	0.542	0.544	0.544	0.542	0.544	0.544	0.544	0.544	0.544	0.540	0.540	0.542	0.538	0.542	0.53
112	0.538	0.538	0.536	0.538	0.538	0.540	0.540	0.540	0.540	0.540	0.536	0.536	0.538	0.538	0.536	0.53
116	0.532	0.532	0.534	0.532	0.532	0.530	0.526	0.530	0.526	0.526	0.526	0.528	0.528	0.528	0.528	0.53

120	0.530	0.528	0.528	0.530	0.264	0.530	0.530	0.526	0.530	0.526	0.528	0.532	0.532	0.532	0.532	0.53
124	0.522	0.522	0.522	0.522	0.524	0.522	0.522	0.522	0.522	0.524	0.466	0.518	0.520	0.520	0.520	0.53
128	0.736	0.782	0.780	0.780	0.782	0.782	0.780	0.782	0.780	0.782	0.774	0.774	0.774	0.774	0.774	0.77
132	0.774	0.774	0.774	0.774	0.776	0.776	0.776	0.776	0.776	0.776	0.772	0.774	0.772	0.772	0.772	0.77
136	0.776	0.776	0.776	0.776	0.776	0.772	0.774	0.774	0.772	0.770	0.770	0.778	0.780	0.778	0.778	0.77
140	0.570	0.570	0.570	0.570	0.570	0.570	0.568	0.568	0.570	0.568	0.574	0.574	0.574	0.572	0.574	0.57
144	0.534	0.536	0.536	0.536	0.538	0.534	0.542	0.542	0.540	0.540	0.542	0.536	0.536	0.536	0.538	0.53
148	0.538	0.540	0.540	0.538	0.538	0.540	0.538	0.538	0.534	0.536	1.078	0.536	0.540	0.540	0.540	0.53
149	0.530	0.530	0.530	0.530	0.520	0.530	0.534	0.532	0.534	N/A	N/A	N/A	N/A	N/A	N/A	0.53
150	0.530	0.530	0.530	0.524	0.528	0.526	0.526	0.524	0.524	N/A	N/A	N/A	N/A	N/A	N/A	0.53
152	0.526	0.522	0.526	0.524	0.526	0.528	0.526	0.526	0.524	0.528	0.532	0.532	0.532	0.530	0.530	0.53
156	0.536	0.538	0.538	0.538	0.536	0.534	0.536	0.534	0.536	0.536	0.534	0.534	0.534	0.534	0.534	0.53
160	0.534	0.534	0.532	0.478	0.532	0.534	0.536	0.534	0.534	0.534	0.534	0.53	0.532	0.532	0.532	0.53
164	0.546	0.404	0.548	0.546	0.546	0.546	0.546	0.546	0.54	0.544	0.544	0.544	0.544	0.544	0.546	0.53
168	0.544	0.544	0.544	0.544	0.544	0.544	0.542	0.542	0.542	0.542	0.546	0.546	0.546	0.546	0.548	0.53
172	0.586	0.532	0.532	0.532	0.532	0.53	0.528	0.530	0.528	0.530	0.536	0.536	0.536	0.536	0.538	0.53
176	0.536	0.536	0.536	0.536	0.534	0.53	0.534	0.530	0.532	0.534	0.532	0.532	0.532	0.532	0.534	0.53
180	0.542	0.542	0.542	0.542	0.544	0.538	0.538	0.538	0.538	0.482	0.536	0.534	0.536	0.534	0.536	0.53
184	0.582	0.580	0.578	0.580	0.580	0.586	0.586	0.584	0.584	0.584	0.586	0.588	0.588	0.586	0.586	0.53
188	0.572	0.570	0.570	0.570	0.570	0.570	0.570	0.570	0.572	0.572	0.574	0.574	0.574	0.574	0.574	0.57
192	0.572	0.572	0.572	0.574	0.574	0.572	0.574	0.574	0.574	0.572	0.574	0.572	0.574	0.572	N/A	0.57
196	0.574	0.574	0.576	0.576	0.576	0.574	0.576	0.574	0.576	0.576	0.572	0.572	0.572	0.574	0.574	0.57
200	0.684	0.684	0.682	0.682	0.682	0.68	0.682	0.682	0.682	0.680	0.682	0.680	N/A	N/A	N/A	0.66

¹ Green represents relatively high UT measurements and red represents relatively low UT measurements.

² Obtained from pipe manufacturer's erection drawings.

Appendix D – Inspection Photos



Figure D-1: EIS test cell set-up at pipe segment 5. Four EIS test cells were used in this location due to cell adhesion concerns.



Figure D-2: Pipe wall condition at pipe segment 9. UT test locations visible at lower, right.

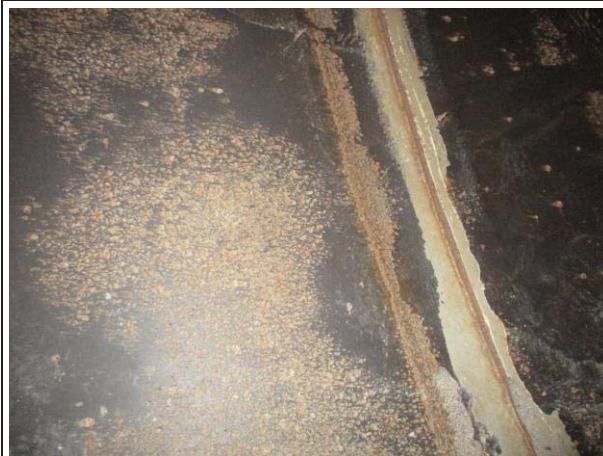


Figure D-3: Corrosion near a joint at pipe segment 9.



Figure D-4: EIS test cell set-up at pipe segment 13. UT test locations are visible above test cells.



Figure D-5: Wall condition near pipe segment 13. UT test locations are visible.

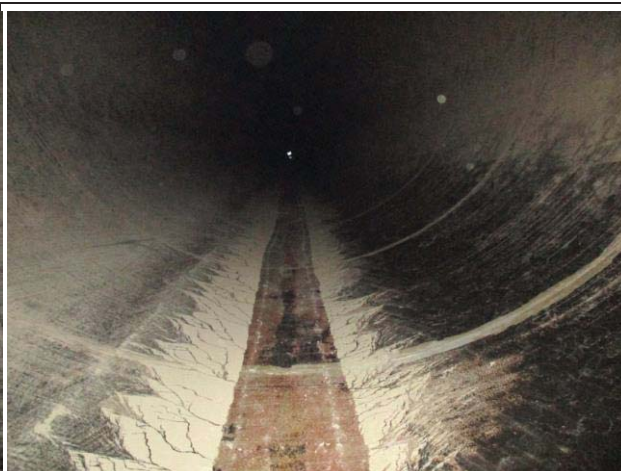


Figure D-6: Condition of invert near pipe segment 13. Rust-through and remnants of repair materials are visible.



Figure D-7: Close-up of rust-through in a joint near pipe segment 13.



Figure D-8: Reclamation inspector performing UT measurements near pipe segment 13.



Figure D-9: EIS test cell set-up and UT test location on pipe segment 17.



Figure D-10: Condition of invert near pipe segment 17. Coating appears to be intact. Sediment is visible to the left and right of invert.



Figure D-11: Defects in the lining at pipe segment 17. Lining appears to be pockmarked with some corrosion within the indentations.



Figure D-12: Defects in the lining at pipe segment 17. Lining appears to be wrinkled near the joint.



Figure D-13: Condition of coating at pipe segment 21. Concentric stripes or wrinkles (fingering) were commonly found near the pipe field joints.



Figure D-14: EIS test cell set-up and UT test location at pipe segment 21. Pipe walls in some areas were covered in thick, dried mud that needed to be scraped away before testing.



Figure D-15: Close up of invert repair. The surface preparation was reported by CAP staff to have been done with water jetting, which resulted in the circular pattern.



Figure D-16: EIS test cell set-up and UT test location at pipe segment 25.



Figure D-17: Close-up of EIS test cell set-up and UT test location at pipe segment 25.



Figure D-18: Visible corrosion along the invert of pipe segment 25.



Figure D-19: Corrosion and rust-through near a joint at pipe segment 25.



Figure D-20: A coating repair area in the invert of pipe segment 25. The repair in this area looks to be in good condition, but corrosion is visible adjacent to the repaired area.



Figure D-21: Repaired spots on pipe segment 29.



Figure D-22: EIS test cell set-up and UT test location at pipe segment 29.



Figure D-23: Close-up of EIS test cell set-up and UT test location at pipe segment 29. The center test cell leaked water and could not be used.



Figure D-24: General condition of pipe segment 29. Areas of corrosion and areas of repair are visible throughout.



Figure D-25: Condition of the EIS test cell set-up at pipe segment 33.



Figure D-26: Condition of the wall near pipe segment 33.



Figure D-27: Condition of the wall at pipe segment 37. A small amount of rust-through is visible within the field joint repair area.



Figure D-28: The inspection team working near pipe segment 37.



Figure D-29: A small repair patch near pipe segment 37. Mud is visible on the pipe wall.



Figure D-30: A field joint repair near pipe segment 37.



Figure D-31: Condition of the wall of pipe segment 53. Large areas of corrosion are visible. The failed field joint repair shows rust-through.



Figure D-32: Condition of the wall near pipe segment 53. This area represented one of the largest areas of widespread corrosion rust-through found in the siphon.



Figure D-33: Wall condition of pipe segment 84A.



Figure D-34: Condition of the siphon near pipe segment 84A. Joint and invert repairs have failed and rust-through and corrosion are visible.



Figure D-35: Condition of the wall near pipe segment 84A. Coating wrinkles and potential cracks are abundant.



Figure D-36: Condition of the pipe wall of segment 91.



Figure D-37: EIS test cell set-up and UT test location at segment 91. Dried mud covered both sides of the wall and needed to be scraped away to perform testing.



Figure D-38: Condition of the pipe invert near segment 91. An area of severe corrosion extends nearly three feet wide across the invert.



Figure D-39: An access point near pipe segment 91.



Figure D-40: Condition of the wall of pipe segment 95.



Figure D-41: Condition of the invert at pipe segment 95. Widespread corrosion is visible.



Figure D-42: Condition of a previously-repaired joint at pipe segment 95. The repair material has been abraded in some areas to reveal multiple layers of coating. Rust-through and evidence of water jetting are visible.

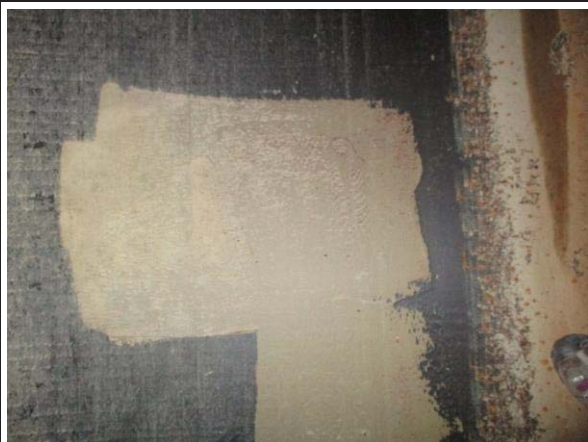


Figure D-43: An area of repair on the pipe wall near segment 95 that appears to be in good condition.



Figure D-44: Condition of the wall at pipe segment 99.

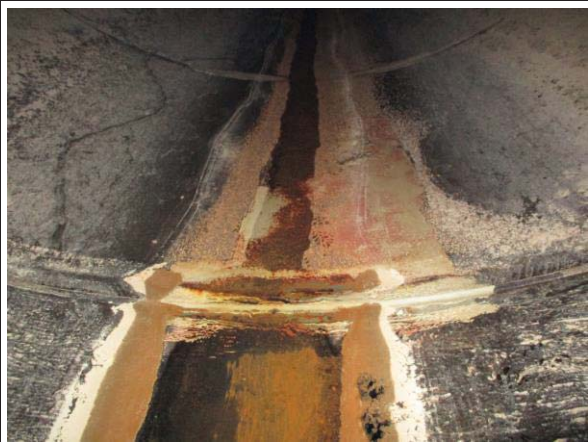


Figure D-45: Condition of the invert at pipe segment 99. Corrosion and rust-through are prevalent throughout.



Figure D-46: Condition of the wall at pipe segment 103. Dried mud and sediment on the walls were almost plaster-like.



Figure D-47: Condition of the invert at pipe segment 103.



Figure D-48: Condition of the walls near pipe segment 103. Both sides were covered in difficult-to-remove dried mud.



Figure D-49: Condition of the invert and pipe joint at segment 107. Coating repair has failed and significant rust-through and corrosion is visible.

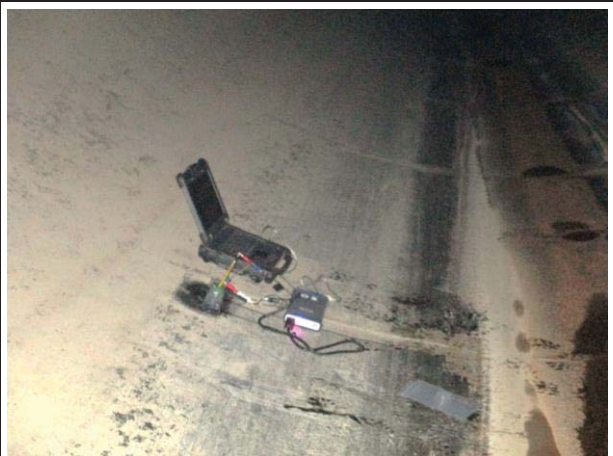


Figure D-50: EIS test set-up at segment 107. The siphon's curvature was shallow enough to allow for the equipment to be set directly onto the pipe wall.



Figure D-51: Condition at pipe segment 112.



Figure D-52: Reclamation inspector programming UT gage while waiting for EIS to finish. Each test took between 2 and 3 minutes to complete.

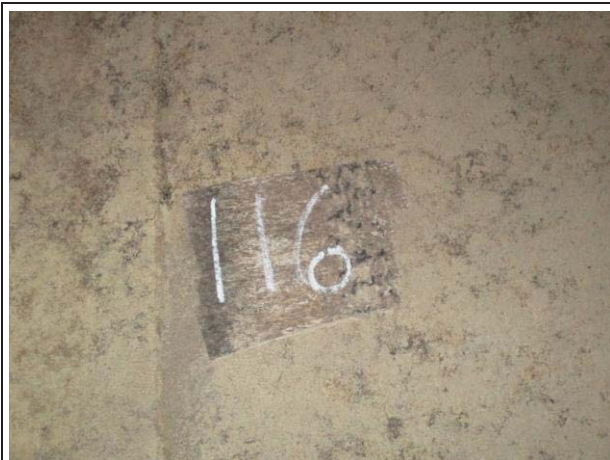


Figure D-53: Condition of pipe segment 116.

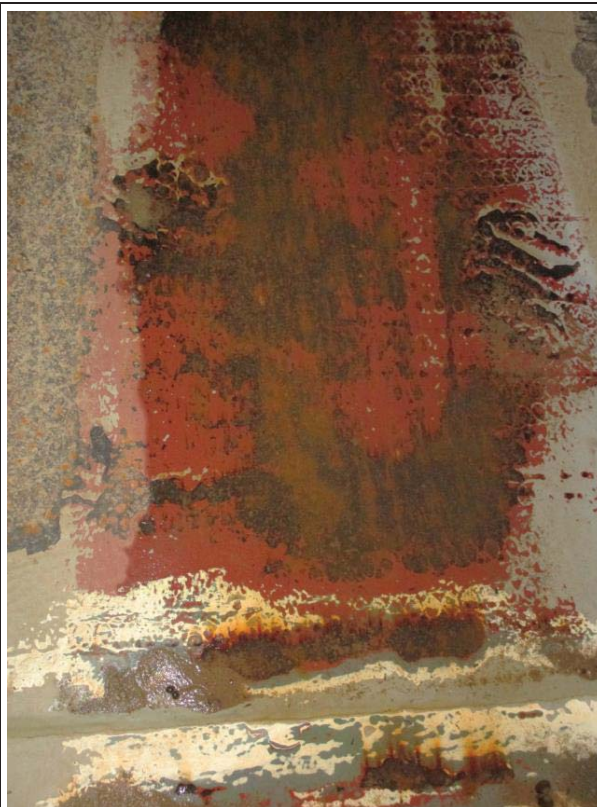


Figure D-54: Condition of the invert at pipe segment 116. A large coating repair area has been abraded away to reveal evidence of water jetting. Corrosion and rust-through is also visible.



Figure D-55: Condition of pipe segment 120.



Figure D-56: An area of mud accumulation (left), cleaned coal tar enamel (center), and corrosion within invert (far right) near pipe segment 120.

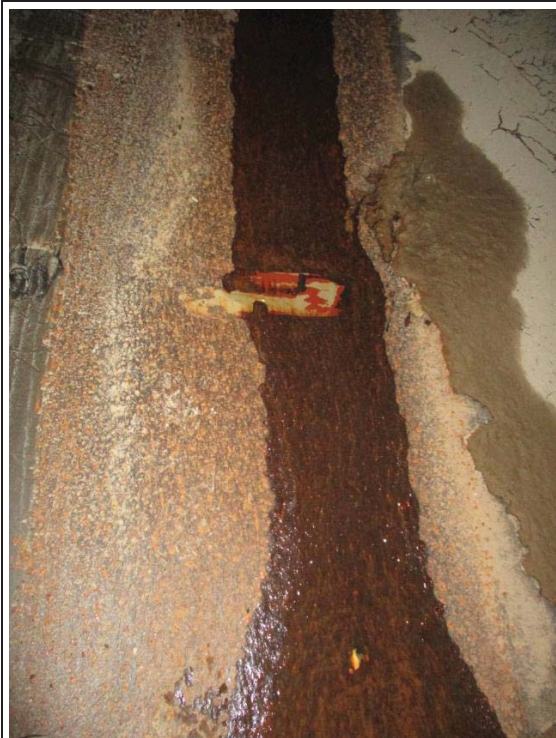


Figure D-57: Severe corrosion in the invert near pipe segment 124.



Figure D-58: Brush marks from application defects around joints near segment 132.

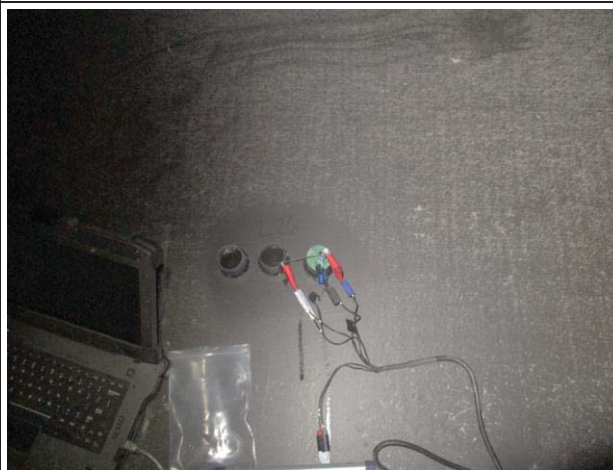


Figure D-59: General condition of the pipe near segment 136 within EIS test equipment and measurement in progress at right.



Figure D-60: Close-up of EIS test cell set-up at pipe segment 136.



Figure D-61: General condition of pipe wall and invert near pipe segment 140.



Figure D-62: Failed field joint repair near pipe segment 140. Multiple layers of coating material are visible and evidence of water jetting is present.



Figure D-63: Invert and wall condition near pipe segment 140.



Figure D-64: Pipe invert condition near pipe segment 148.





Figure D-65: General condition of the pipe walls and invert near segment 152. Commonly, one side of the wall would be covered with much more dried mud than the other.



Figure D-66: General condition of the invert and walls near pipe segment 192. Severe corrosion and rust-through is visible in the invert.

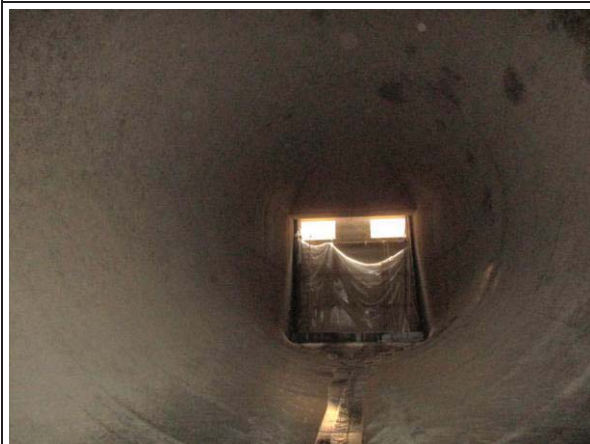


Figure D-67: View of the outlet from pipe segment 200.



Figure D-68: EIS test cell set-up at pipe segment 200. The coating is riddled with defects, visible at right. Segment 200 had among the worst EIS results of all tested segments.

Appendix E – CAP’s detailed inspection notes

Table E-1: Detailed inspection notes for each pipe segment provided by CAP

Segment #	Length (feet)	Thickness (inches)	Joint ¹	Inspection Notes	Miscellaneous Observations
1	39.82	0.57	Joint OK	Shop welds ² rusty ~5-7 o'clock (~10' length), some blistering on invert (~10' length)	Temp ~ 85° F, Humidity ~70%
2	14.04	0.57	Joint Rusty ~ 10'	Shop welds rusty ~5-7 o'clock (~10' length), some blistering on invert (~10' length)	
3	39.82	.57 to .53	Joint Rusty ~ 10'	Shop welds rusty ~5-7 o'clock (~10' length), some blistering on invert (~10' length)	shop welds not quite as rusty as previous piece
4	39.82	0.53	Joint Rusty ~ 15'	Shop welds rusty ~5-7 o'clock (~10' length), some blistering on invert (~10' length)	shop welds about as rusty as previous piece
5	39.82	.53 to .57	Joint Rusty ~ 15'	Blistering ~6-9 o'clock 15', 22', & 38' - see Jennifer's data & photo	EIS left ³
6	39.82	0.57	Joint Rusty ~ 20'	Blistering ~6-8 o'clock extensive first 20', widespread entire length of pipe	DFT ~20 mils 7 o'clock, 30'
7	14.89	0.57	Joint Rusty ~ 20'	Blistering ~5-8 o'clock - full length of elbow - see Jennifer's data & photo	
8	7.62	0.53	Joint Rusty ~ 15'	Blistering ~4-6 o'clock - full length of elbow	
9	59.84	0.53	Joint Rusty ~ 3-9	Invert Rust	Fall Protection Anchor Lugs, EIS right
10	59.83	0.53	Joint Rusty ~ 3-6	Joint Rusty ~3-6 o'clock, rust throughout invert, blisters and pitting	DFT ~20 mils & UT ~.51" ~7 o'clock, 55' - Hollow Sound ~7 o'clock, ~55'
11	59.79	0.53	Joint Rusty ~ 5-7	Spot rusting and pitting at invert throughout pipe	DFT ~15 mils - invert ~50'
12	59.82	0.53	Joint Rusty ~ 5-7	Rust entire length at invert, the epoxy patch to protect the joint is eroding - see photo	DFT ~20 mils inv 20', DFT of repair 30-60 mils
13	59.82	0.53	Joint Rusty ~ 4-7	Epoxy repair at joint flaking and eroding, rust along invert throughout pipe	EIS left
14	59.83	0.53	Joint Rusty ~ 4-8	Epoxy repair at joint flaking and eroding, rust along invert throughout pipe	DFT ~13 mils inv and ~20 mils 5 o'clock 3'
15	59.82	0.53	Joint Rusty ~ 5-8	Invert Rust	15' - Hollow Spot in invert - sides felt solid
16	59.82	0.53	Joint Rusty ~ 4-9	Mild invert rusting throughout pipe	DFT ~33 mils Inv 3'

17	59.82	0.53	Joint Rusty ~ 5-9	Little Rust upstream half of pipe - heavy rust 6-7 o'clock ~35' to end of pipe	EIS left
18	59.82	0.53	Joint Rusty ~ 5-9	Epoxy repair at joint flaking and eroding, slight rust along invert throughout pipe	
19	29.82	0.53	Joint Rusty ~ 5-8	Invert Rust - spot rust 6 to 8 sprodaic throughout pipe	
20	10.88	0.53	Joint Rusty ~ 5-8	Invert Rust	
21	59.82	0.53	Joint Rusty ~ 5-8	Invert Rust	EIS right
22	59.83	0.53	Joint Rusty ~ 5-8	Invert Rust - but little in this piece	
23	59.82	0.53	Joint Rusty ~ 5-8	Repair epoxy flaking at joint - invert repair missing from ~5' to 20' - rust throughout invert	Repair intact ~6:30 to 7 o'clock
24	59.82	0.53	Joint Rusty ~ 6-8	Repair epoxy flaking at joint - rust throughout invert - see Photo for Piece 25	DFT ~12-13mils inv ~1'
25	59.82	0.53	Joint Rusty ~ 5-8	Rust entire length at invert - see photo	
26	59.82	0.53	Joint Rusty ~ 5-7	Rust entire length at invert, some repair patches are intact - Anchor lugs installed near downstream joint	EIS left
27	32.90	0.53	Joint Rusty ~ 5-7	Rust entire length at invert, some repair patches are intact - wear in the invert	
28	8.54	0.53	Joint Rusty ~ 6-8	Rust entire length at invert	
29	59.81	.53 to .66	Joint Rusty ~ 6-8	Rust entire length at invert - sediment on the wall and invert	EIS right
30	59.83	0.66	Joint Rusty ~ 5-9	Little Rust on this piece - shop weld patches are mostly intact - some sediment deposition in pipe	
31	59.82	0.66	Joint Rusty ~ 6-8	Little Rust on this piece - shop weld patches are mostly intact - some sediment deposition in pipe	
32	25.20	0.66	Joint Rusty ~ 6-8	Little Rust on this piece	
33	17.14	.66 to 1.01	Joint Rusty ~ 6-7	Little Rust on this piece	EIS left

34	39.90	1.01	Joint Rusty ~ 6-7	Little Rust on this piece - shop weld patches are worn and welds rusty	Photo shows pipe with ladder at blowoff structure in distance and Reclamation Engineers at Piece 37 for EIS test
35	39.81	1.01	Joint Rusty ~ 6-7	Little Rust on this piece - patches of rust - as compared to complete invert as typically seen elsewhere	Photo shows spot rusting in invert near the downstream joint
36	39.84	1.01	Joint Rusty - Invert	Little Rust on this piece - patches of rust - as compared to complete invert as typically seen elsewhere	
37	39.79	1.01	Joint Rusty ~ 4-9	Spot Rusting in invert pipe - 20' to 30' spot rust and repair worn	DFT 6.5 mils to 10 mils 25' in invert, EIS right
38	39.80	1.01	Joint Rusty ~ 6-7	Significant rust - patches are wearing and rusting in repaired areas	Photo is mid-pipe
39	39.80	1.01 to 1.07	Joint Rusty ~ 6-8	Rust in invert - but little compared to what typically seen	
40	24.80	1.07	Joint Rusty ~ 6-8	15' from Upstream joint 2' wide blistering 360° - some rust is present in invert - some of the old patches are intact	Blowoff Structure
41	6.07	1.07	Joint Rusty	Not able to see invert due to flooding	Short piece between blowoff and manhole
42	39.81	1.07	Joint Rusty	Not able to see invert due to flooding - about 14" of water still in pipe	Manhole Access
43	40.00	1.07	Joint Rusty	Not able to see invert due to flooding	
44	39.80	1.07	Joint Rusty	Not able to see invert due to flooding - fingering on walls begin 30' to piece 45	
45	39.81	1.07	Joint Rusty	Not able to see invert due to flooding - fingering on walls from upstream joint to ~30' - begins again near d/s joint	DFT measured ~30 mils 30' from u/s joint
46	39.81	1.07	Joint Rusty	Fingering first ~10' of pipe, rust most of pipe piece	DFT measured ~11 to 17 mils 30' from u/s joint
47	39.80	1.07	Joint Rusty	Rust downstream of joint - both sides of pipe - fingering of lining	
48	39.81	1.07	Joint Rusty	Rust downstream of joint - both sides of pipe - fingering of lining	DFT measured ~11 to 14 mils 1' from u/s joint
49	39.81	1.07	Joint Rusty	Rust downstream of joint - both sides of pipe - fingering of lining	
50	39.80	1.07	Joint Rusty	Rust downstream of joint - both sides of pipe - fingering of lining	
51	39.81	1.07	Joint Rusty	Rust downstream of joint - both sides of pipe - fingering of lining - last 10' of pipe rust spots up to 9 o'clock	DFT ~21 mils
52	39.81	1.07	Joint Rusty	Rust spot downstream of joint - up to 9 o'clock 5' long - fingering of lining - last 10' of pipe rust 3 to 9 o'clock	

53	39.80	1.07	Joint Rusty	2' wide rust 360° immediately downstream of joint - fingering of lining - some "coating slides" on this pipe	
54	39.81	1.07	Joint Rusty	Welds rusty - fingering of lining	
55	39.81	1.07	Joint Rusty ~ 4-7	Fingering of lining - mud starting to clear	
56	39.80	1.07	Joint Rusty	Mud beginning again - not able to perform EIS - BoR measured DFT & UT	
57	39.81	1.07	Joint Rusty	Only ~2' width of inv visible due to mud - picture of rusty joint	
58	39.81	1.07	Joint Rusty	Only ~2' width of inv visible due to mud	
59	39.80	1.07	Joint Rusty	Only ~2' width of inv visible due to mud - rust spots visible in mud	
60	39.81	1.07	Joint Rusty	Only ~2' width of inv visible due to mud	
61	39.81	1.07	Joint Rusty	Only ~2' width of inv visible due to mud	
62	39.81	1.07	Joint Rusty	Only ~2' width of inv visible due to mud	
63	39.80	1.07	Joint Rusty	Only ~2' width of inv visible due to mud	
64	39.81	1.07	Joint Rusty	~3' width of invert visible	EIS test indicated low values, EIS right
65	39.81	1.07	Joint Rusty	~3' width of invert visible	
66	39.82	1.07	Joint Rusty ~4'	Downstream 25' of pipe visible - no mud - invert rusted and pitted	
67	41.84	1.07	Joint Rusty ~4'	Invert rusted and pitted	DFT 4.5-10 mils in 39'
68	37.81	1.07	Joint Rusty	Invert Rusted length of pipe	DFT 7 o'clock 1' ~37 mils, 5 o'clock 1' ~44 mils - EIS test indicated low values, EIS left
69	39.84	1.07	Joint Rusty ~3'	Invert Rusted length of pipe	
70	39.88	1.07	Joint Rusty ~3'	Inverted Rusted length of pipe - ~3' wide path in sediment	DFT 5 o'clock 38' 15-20 mils
71	29.83	1.07	Joint Rusty ~3'	Invert Rusted length of pipe - Fingering of lining	
72	11.24	1.07 to 1.01	Joint Rusty	Invert Rusted length of pipe	DFT 6 o'clock 1' ~9-10 mils, - EIS test indicated low values, EIS right
73	39.81	1.01	Joint Rusty	Invert Rusted length of pipe - Devoe flaking off welds	DFT 6 o'clock 13 mils

74	39.80	1.01	Joint Rusty ~5-6	Invert Rusted length of pipe ~5 to 6 o'clock with sediment 5 to 7 o'clock - ~2' path in invert - rusty	DFT 6 o'clock 10' 10-15 mils, & 6 o'clock 39' 10 mils
75	39.81	1.01	Joint Rusty ~5-6	Invert Rusted length of pipe ~5 to 6 o'clock with sediment 5 to 7 o'clock - ~2' path in invert - rusty	DFT 4 o'clock 21-22 mils, 8 o'clock 21-22 mils, 6 o'clock 8-12 mils - all at 39'
76	39.80	1.01	Joint Rusty ~5-7	Invert Rusted length of pipe ~5 to 7 o'clock with sediment 5 to 7 o'clock - ~2' path in invert - rusty	EIS left
77	39.80	1.01 to .77	Joint Rusty ~5-7	Invert Rusted length of pipe ~5 to 7 o'clock with sediment 5 to 7 o'clock - ~2' path in invert - rusty	DFT 6 o'clock 35' 6-10 mils
78	49.83	.77 to .66	Joint Rusty ~5-7	Invert Rusted length of pipe ~5 to 7 o'clock with sediment 5 to 7 o'clock - ~2' path in invert - rusty	
79	49.83	0.66	Joint Rusty ~5-7	Invert Rusted length of pipe ~5 to 7 o'clock with sediment 5 to 7 o'clock - ~2' path in invert - rusty	
80	41.87	.66 to .53	Joint Rusty ~5-7	Invert Rusted length of pipe ~5 to 7 o'clock with sediment 5 to 7 o'clock - ~2' path in invert - rusty	DFT 6 o'clock 3' 6.5-10 mils, EIS right
81	159.28	0.53	Joint Rusty ~5-7	Invert Rusted length of pipe ~5 to 7 o'clock with sediment 5 to 7 o'clock - ~2' path in invert - rusty	
82	44.70	0.53	Joint Rusty ~5-7	Invert Rusted length of pipe ~5 to 7 o'clock with sediment 5 to 7 o'clock - ~2' path in invert - rusty	DFT ~7 o'clock 2' 38-40 mils
83	20.40	0.53	Joint Rusty ~5-7	Invert Rusted length of pipe ~5 to 7 o'clock - ~2' path in invert - rusty	Less Sediment accumulation at elbow, inv rusted ~3' wide, epoxy patch is worn and rust beneath patch
84A	29.82	0.53	Joint Rusty ~5-7	Invert Rusted length of pipe ~5 to 7 o'clock - ~2' path in invert - rusty	DFT Inv on Closure piece - 9.5-11 mils, 4 o'clock 5' 22.5-24 mils, EIS left
84B	29.83	0.53	Joint Rusty ~5-7	Invert Rusted length of pipe ~5 to 7 o'clock - ~2' path in invert - rusty	Anchor Lugs at Downstream End of piece
85	60.00	0.53	Joint Rusty ~5-7	Invert Rusted length of pipe ~5 to 7 o'clock - ~2' path in invert - rusty	DFT ~7 o'clock 35' 7.5-20 mils
86	59.82	0.53	Joint Rusty ~5-7	Invert Rusted length of pipe ~5 to 7 o'clock - ~2' path in invert - rusty	~25' invert sounds hollow
87	59.82	0.53	Joint Rusty ~5-7	Invert Rusted length of pipe ~5 to 7 o'clock - ~2' path in invert - rusty	DFT 5 o'clock 38' 34-35 mils, 7 o'clock 38' 23-28 mils, EIS right
88	59.82	0.53	Joint Rusty ~5-7	Invert Rusted length of pipe ~5 to 7 o'clock - ~2' path in invert - rusty	
89	59.82	0.53	Joint Rusty ~5-7	Invert Rusted length of pipe ~5 to 7 o'clock - ~2' path in invert - rusty	DFT ~6:30, 12' 23.5-25 mils
90	59.83	0.53	Joint Rusty ~5-7	Invert Rusted length of pipe ~5 to 7 o'clock - ~2' path in invert - rusty	

91	59.81	0.53	Joint Rusty ~5-7	Invert Rusted length of pipe ~5 to 7 o'clock - ~2' path in invert - rusty	DFT Inv 38' 11.5-15 mils 36-inch MH this piece at Sta 40+00, EIS left
92	59.83	0.53	Joint Rusty ~5-7	Invert Rusted length of pipe ~5 to 7 o'clock - ~2' path in invert - rusty	
93	59.82	0.53	Joint Rusty ~5-7	Invert Rusted length of pipe ~5 to 7 o'clock - ~2' path in invert - rusty	
94	59.83	0.53	Joint Rusty ~5-7	Invert Rusted length of pipe ~5 to 7 o'clock - ~2' path in invert - rusty	
95	59.82	0.53	Joint Rusty ~5-7	Invert Rusted length of pipe ~5 to 7 o'clock - ~2' path in invert - rusty	
96	59.82	0.53	Joint Rusty ~5-7	Invert Rusted length of pipe ~5 to 7 o'clock - ~2' path in invert - rusty	EIS right
97	59.82	0.53	Joint Rusty ~5-7	Invert Rusted length of pipe ~5 to 7 o'clock - ~2' path in invert - rusty	
98	59.82	0.53	Joint Rusty ~5-7	Invert Rusted length of pipe ~5 to 7 o'clock - ~2' path in invert - rusty	
99	59.83	0.53	Joint Rusty ~5-7	Invert Rusted length of pipe ~5 to 7 o'clock - ~2' path in invert - rusty	EIS left
100	59.82	0.53	Joint Rusty ~5-7	Invert Rusty 2-3 ft width - rest of pipe appears ok, dirt from ~4 to 8 o'clock	
101	59.82	0.53	Joint Rusty ~5-7	Invert Rusty 2-3 ft width - rest of pipe appears ok, dirt from ~4 to 8 o'clock	DFT 5 o'clock, 37' 35 mils, Inv 39' 10 mils
102	59.82	0.53	Joint Rusty ~5-7	Invert Rusty 2-3 ft width - rest of pipe appears ok, dirt from ~4 to 8 o'clock	
103	59.82	0.53	Joint Rusty ~5-7	Invert Rusty 2-3 ft width - rest of pipe appears ok, dirt from ~4 to 8 o'clock	EIS left

104	59.83	0.53	Joint Rusty ~5-7	Invert Rusty 2-3 ft width - rest of pipe appears ok, dirt from ~4 to 8 o'clock	
105	59.82	0.53	Joint Rusty ~5-7	Invert Rusty 2-3 ft width - rest of pipe appears ok, dirt from ~4 to 8 o'clock	
106	59.82	0.53	Joint Rusty ~5-7	Invert Rusty 2-3 ft width - rest of pipe appears ok, dirt from ~4 to 8 o'clock	~ 40' to 45' - full circumference delamination & blistering DFT where intact ~25 mils, ~15 mils where delaminating, 2 mils lowest
107	59.82	0.53	Joint Rusty ~5-7	Invert Rusty 2-3 ft width - rest of pipe appears ok, dirt from ~4 to 8 o'clock	EIS left

E-7

108	59.83	0.53	Joint Rusty ~5-7	Invert Rusty 2-3 ft width - rest of pipe appears ok, dirt from ~4 to 8 o'clock	
109-110	59.82	0.53	Joint Rusty ~5-8	Invert Rusty 2-3 ft width - rest of pipe appears ok, dirt from ~4 to 8 o'clock	
111	59.82	0.53	Joint Rusty ~5-9	Invert Rusty 2-3 ft width - rest of pipe appears ok, dirt from ~4 to 8 o'clock	
112	59.82	0.53	Joint Rusty ~5-10	Invert Rusty 2-3 ft width - rest of pipe appears ok, dirt from ~4 to 8 o'clock	EIS right
113	59.82	0.53	Joint Rusty ~5-11	Invert Rusty 2-3 ft width - rest of pipe appears ok, dirt from ~4 to 8 o'clock	
114	59.83	0.53	Joint Rusty ~5-12	Invert Rusty 2-3 ft width - rest of pipe appears ok, dirt from ~4 to 8 o'clock	About 10' into pipe, coating "slide" very thick coating ~5 to 7 o'clock
115	59.86	0.53	Joint Rusty ~5-13	Invert Rusty 2-3 ft width - rest of pipe appears ok, dirt from ~4 to 8 o'clock	
116	59.88	0.53	Joint Rusty ~5-14	Invert Rusty 2-3 ft width - rest of pipe appears ok, dirt from ~4 to 8 o'clock	EIS left
117	59.70	0.53	Joint Rusty ~5-15	Invert Rusty 2-3 ft width - rest of pipe appears ok, dirt from ~4 to 8 o'clock	
118	59.96	0.53	Joint Rusty ~5-16	Invert Rusty 2-3 ft width - rest of pipe appears ok, dirt from ~4 to 8 o'clock	
119	59.76	0.53	Joint Rusty ~5-17	Invert Rusty 2-3 ft width - rest of pipe appears ok, dirt from ~4 to 8 o'clock	
120	59.89	0.53	Joint Rusty ~5-18	Invert Rusty 2-3 ft width - rest of pipe appears ok, dirt from ~4 to 8 o'clock	EIS right
121	59.83	0.53	Joint Rusty ~5-19	Invert Rusty 2-3 ft width - rest of pipe appears ok, dirt from ~4 to 8 o'clock	
122	59.62	0.53	Joint Rusty ~5-20	Invert Rusty 2-3 ft width - rest of pipe appears ok, dirt from ~4 to 8 o'clock	~ 50' into pipe, 2' wide delamination - full circumference
123	59.82	0.53	Joint Rusty ~5-21	Invert Rusty 2-3 ft width - rest of pipe appears ok, dirt from ~4 to 8 o'clock	
124	60.03	.53 to 66	Joint Rusty ~5-22	Invert Rusty 2-3 ft width - rest of pipe appears ok, dirt from ~4 to 8 o'clock	A couple "slides" on pipe left downstream end of piece, EIS left
125	14.03	0.66	Joint Rusty	Rust in pipe ~ 5 to 6 o'clock, slightly up on right side wall	
126	59.49	0.66	Joint Rusty	Rust entire length of pipe ~ 4 to 5 o'clock - spotty last 10' of piece	DFT ranging 3 to 30 mils inv ~2'
127	50.15	.66 to .77	Joint Rusty	Beginning ~ 10' into this piece and continuing d/s, little to no rust -	DFT ~5 o'clock 2', 2.5-5 mils

				though there are a few minor spots of rust	
128	49.82	0.77	Joint Rusty	Little to no rust - though there are a few minor spots of rust	~33', Rt side, slide w/ spot rusting, DFT 5.5-10 mils, EIS right
129	49.83	0.77	Joint Rusty ~3-6	Some spot rusting in pipe	DFT ~5 o'clock ~25', 15 mils
130	49.83	0.77	Joint Rusty	Minor rust spots at joint ~5 o'clock	
131	49.82	0.77	Joint Rusty ~3-6	Some spot rusting in pipe, fingering of lining with rust	Fingering 40' to 50' - perhaps solvent in coating
132	49.83	0.77	Joint Rusty ~3-6	Some spot rusting in pipe, fingering of lining with rust	Spot rusting in inv ~45' - impact damage? EIS left
133	49.82	0.77	Joint Rusty ~3-6	Spot rusting throughout invert - impact damage? Fingering with rust on side walls - slide most of pipe length	
134	49.82	0.77	Joint Rusty ~3-6	Spot rusting downstream of each shop weld	
135	49.84	0.77	Joint Rusty ~4-6		
136	49.20	.77 to .57	Joint Rusty ~4-6	Beginning ~10' rust 5 o'clock 18" wide length of pipe & fingering right side last 10' of pipe	EIS right
137	60.45	0.57	Joint Rusty ~4-6	Rusting of invert - most significant d/s of welds	~ halfway into pipe, invert rust is continuous about 3'
138	59.82	0.57	Joint Rusty ~5-7	Invert rust ~ 3' wide	
139	59.83	0.57	Joint Rusty ~5-7	Invert rust ~ 3' wide	
140	59.63	0.57	Joint Rusty ~5-7	Invert rust ~ 3' wide	EIS left
141	60.07	0.57	Joint Rusty ~5-7	Invert rust ~ 3' wide	
142	59.89	0.57	Joint Rusty ~5-7	Invert rust ~ 3' wide	
143	59.88	.57 to .53	Joint Rusty ~5-7	Invert rust ~ 3' wide	
144	58.95	0.53	Joint Rusty ~5-7	Invert rust ~ 3' wide	EIS right

145	60.82	0.53	Joint Rusty ~5-7	Invert rust ~ 3' wide	
146	59.84	0.53	Joint Rusty ~5-7	Invert rust ~ 3' wide - inv patches sporadic	DFT ~5 o'clock 50' 32-35 mils
147	59.79	0.53	Joint Rusty ~4'	Invert rust ~ 3' wide - inv patches sporadic	
148	59.77	0.53	Joint Rusty ~4'	Invert rust ~ 3' wide - inv patches sporadic	EIS left
149	59.78	0.53	Joint Rusty ~4'	Invert rust ~ 3' wide - inv patches sporadic	
150	59.77	0.53	Joint Rusty ~4'	Invert rust ~ 3' wide - inv patches sporadic	
151	59.78	0.53	Joint Rusty ~4'	Invert rust ~ 3' wide & Slides 10', 15', & 20' - sporadic inv patches	~40' small slide & "snake" ~8 o'clock (DFT ~30 mils), DFT ~4 o'clock 25' 22 mils
152	59.77	0.53	Joint Rusty ~4'	Invert rust ~ 3' wide - inv patches sporadic	EIS right
153	59.78	0.53	Joint Rusty ~4'	Invert rust ~ 3' wide - inv patches sporadic	
154	57.82	0.53	Joint Rusty ~4'	Invert rust ~ 3' wide - inv patches sporadic	
155	61.83	0.53	Joint Rusty ~4'	Invert rust ~ 3' wide - inv patches sporadic	
156	59.82	0.53	Joint Rusty ~4'	Invert rust ~ 3' wide - inv patches sporadic	EIS left

157	59.82	0.53	Joint Rusty ~4'	Invert rust ~ 3' wide - inv patches sporadic	
158	59.83	0.53	Joint Rusty ~4'	Invert rust ~ 3' wide - inv patches sporadic	Rust ~6' wide in places, more on right side, d/s half of pipe piece
159	59.82	0.53	Joint Rusty ~4'	Invert rust ~ 3' wide - inv patches sporadic	
160	59.82	0.53	Joint Rusty ~4'	Invert rust ~ 3' wide - inv patches sporadic	~25' Large "glob" area w/ DFT 30-156 mils; DFT ~5 o'clock ~55' 25-30 mils, EIS right
161	59.82	0.53	Joint Rusty ~4'	Invert rust ~ 3' wide - inv patches sporadic	
162	59.83	0.53	Joint Rusty ~4'	Invert rust ~ 3' wide - inv patches sporadic	
163	59.82	0.53	Joint Rusty ~4'	Invert rust ~ 3' wide - inv patches sporadic	
164	59.82	0.53	Joint Rusty ~4'	Invert rust ~ 3' wide - inv patches sporadic	EIS left
165	59.83	0.53	Joint Rusty ~4'	Invert rust ~ 3' wide - inv patches sporadic	
166	59.82	0.53	Joint Rusty ~4'	Invert rust ~ 3' wide - inv patches sporadic	
167	59.82	0.53	Joint Rusty ~4'	Invert rust ~ 3' wide - inv patches sporadic	
168	57.10	0.53	Joint Rusty ~4'	Invert rust ~ 3' wide - inv patches sporadic	EIS right
169	62.55	0.53	Joint Rusty ~4'	Invert rust ~ 3' wide - inv patches sporadic	

170	59.82	0.53	Joint Rusty ~4'	Invert rust ~ 3' wide - inv patches sporadic	
171	59.82	0.53	Joint Rusty ~4'	Invert rust ~ 3' wide - inv patches sporadic	
172	59.82	0.53	Joint Rusty ~4'	Invert rust ~ 3' wide - inv patches sporadic	EIS left
173	59.83	0.53	Joint Rusty ~4'	Invert rust ~ 3' wide - inv patches sporadic	DFT ~5 o'clock, 59' 25-27.5 mils
174	59.82	0.53	Joint Rusty ~4'	Invert rust ~ 3' wide - inv patches sporadic	
175	56.93	0.53	Joint Rusty ~4'	Invert rust ~ 3' wide - inv patches sporadic	
176	62.71	0.53	Joint Rusty ~4'	Invert rust ~ 3' wide - inv patches sporadic	7 o'clock ~35' spot rust at 57' & slides on both sides of pipe, EIS right
177	59.83	0.53	Joint Rusty ~4'	Invert rust ~ 3' wide - inv patches sporadic	Slides 10' & 15' both sides of pipe
178	59.82	0.53	Joint Rusty ~4'	Invert rust ~ 3' wide - inv patches sporadic	
179	59.82	0.53	Joint Rusty ~4'	Invert rust ~ 3' wide - inv patches sporadic	
180	59.83	0.53	Joint Rusty ~4'	Invert rust ~ 3' wide - inv patches sporadic	EIS left
181	22.98	0.53	Joint Rusty ~4'	Invert rust ~ 3' wide - inv patches sporadic	
182	10.53	0.53	Joint Rusty ~4'	Invert rust ~ 3' wide - inv patches sporadic	
183	59.83	0.53	Joint Rusty ~4'	Invert rust ~ 3' wide - inv patches sporadic	
184	59.82	0.53	Joint Rusty ~4'	Invert rust ~ 3' wide - inv patches sporadic	EIS right
185	59.14	0.53	Joint Rusty ~4'	Invert rust ~ 3' wide - inv patches sporadic	
186	60.51	0.53	Joint Rusty ~4'	Invert rust ~ 3' wide - inv patches sporadic	
187	59.83	0.53	Joint Rusty ~4'	Invert rust ~ 3' wide - inv patches sporadic	5 o'clock ~ 40' delamination - slight - near weld
188	59.82	.53 to .57	Joint Rusty ~4'	Invert rust ~ 3' wide - inv patches sporadic	5 o'clock ~ 40' delamination, blisters, an dspot rust - ~45' slide area both sides of pipe - rusting on edges of slide, EIS left
189	59.83	0.57	Joint Rusty ~4'	Invert rust ~ 3' wide - inv patches sporadic	
190	59.82	0.57	Joint Rusty ~4'	Invert rust ~ 3' wide - inv patches sporadic	
191	59.83	0.57	Joint Rusty ~4'	Invert rust ~ 3' wide - inv patches sporadic	Delaminating slide area - 5' 2-ft width & 10' 4-ft width
192	18.59	0.57	Joint Rusty ~4'	Invert rust ~ 3' wide	EIS right
193	9.90	0.57	Joint Rusty ~5-6	Invert rust 5-6 o'clock	DFT inside bend 10-20.5 mils

194	39.82	0.57	Joint Rusty ~5- 7	Rust ~4 o'clock full length 1' to 3' wide	DFT 5-10 mils
195	39.81	0.57	Joint Rusty ~3- 4	Minor spot rust 3 - 5 o'clock	
196	39.81	.57 to .66	Joint Rusty ~3- 5	5' to 20' pitting , spot rust ~ 5 o'clock	DFT 4 o'clock 5-31 mils, EIS right
197	39.81	0.66	Joint Rusty ~4- 5	Rusty 4-6 o'clock	
198	42.83	0.66	Joint Rusty ~4- 6	~4 o'clock 2' pitting and 15' pitting	DFT 14.5-19 mils
199	11.69	0.66	Joint Rusty ~4- 6	Rusty 4-6 o'clock	
200	41.31	0.66	Joint Rusty ~4- 6		EIS right

¹ A distance indicates total feet of rust centered on the invert, while two numbers indicate a clock face boundary of rust.

² With few exceptions, shop welds were rusty throughout the entire pipeline, in particular 4 to 8 o'clock.

³ EIS tests performed about 3 feet from upstream joint, ~5 or 7 o'clock.

Appendix C – Salt River Siphon Report (2018)

RECLAMATION

Managing Water in the West

Salt River Siphon Coating Inspection and Impedance Analysis

Materials and Corrosion Laboratory, 8540-2018-73

Salt River Siphon, Hayden-Rhodes Division—Arizona



Mission Statements

The U.S. Department of the Interior protects America’s natural resources and heritage, honors our cultures and tribal communities, and supplies the energy to power our future.

The mission of the Bureau of Reclamation is to manage, develop, and protect water and related resources in an environmentally and economically sound manner in the interest of the American public.

Disclaimer:

Information in this report may not be used for advertising or promotional purposes. The data and findings should not be construed as an endorsement of any product or firm by the Bureau of Reclamation, Department of Interior, or Federal Government. The products evaluated in the report were evaluated for purposes specific to the Bureau of Reclamation mission. Reclamation gives no warranties or guarantees, expressed or implied, for the products evaluated in this report, including merchantability or fitness for a particular purpose.

Salt River Siphon Coating Inspection and Impedance Analysis

REPORT DOCUMENTATION PAGE			Form Approved OMB No. 0704-0188		
T1. REPORT DATE December 2018		T2. REPORT TYPE Technical Memorandum		T3. DATES COVERED	
T4. TITLE AND SUBTITLE Salt River Siphon Coating Inspection and Impedance Analysis			5a. CONTRACT NUMBER XXXR4079V4-RX122553011000000		
			5b. GRANT NUMBER		
			5c. PROGRAM ELEMENT NUMBER		
6. AUTHOR(S) Stephanie Prochaska, M.S., sprochaska@usbr.gov, 303-445-2323 Bobbi Jo Merten, Ph.D., bmerten@usbr.gov, 303-445-2380			5d. PROJECT NUMBER		
			5e. TASK NUMBER		
			5f. WORK UNIT NUMBER 86-68540		
7. PERFORMING ORGANIZATION NAME(S) AND ADDRESS(ES) Bureau of Reclamation Technical Service Center, Materials and Corrosion Lab 6 th and Kipling St, Denver, CO 80225-0007			8. PERFORMING ORGANIZATION REPORT NUMBER 8540-2018-73		
9. SPONSORING / MONITORING AGENCY NAME(S) AND ADDRESS(ES) Central Arizona Project P.O. Box 43020 Phoenix, AZ 85080-3020			10. SPONSOR/MONITOR'S ACRONYM(S) BOR/USBR: Bureau of Reclamation DOI: Department of the Interior		
			11. SPONSOR/MONITOR'S REPORT NUMBER(S)		
12. DISTRIBUTION / AVAILABILITY STATEMENT Final report can be downloaded from Reclamation's website: https://www.usbr.gov/research/					
13. SUPPLEMENTARY NOTES					
14. ABSTRACT The Salt River Siphon, a [REDACTED] steel pipe near Phoenix, AZ, is operated and maintained by the Central Arizona Project (CAP). Investigators from the Bureau of Reclamation's Technical Service Center inspected the siphon's coal tar epoxy lining by traditional visual inspection techniques as well as dry film thickness (DFT), steel thickness, and electrochemical impedance spectroscopy analysis (EIS). The visual inspection results show that the lining and Devgrip 238 repair material require maintenance for pipe segments approaching the outlet and in spots along the invert and pipe field joints. EIS results show that the coal tar epoxy is providing excellent corrosion protection overall. However, pipe segments 48 to 84 show reduced protection (10^8 ohms at 0.1 Hz), and pipe segments 155 to the outlet show insufficient corrosion protection (10^5 ohms at 0.1 Hz). DFT results show lining abrasion at distinct locations, including a 50% DFT loss at the invert of pipe segments 44-84. Steel thickness values exceed the pipe manufacturer's erection drawings by 0.02 inches, except for pipe segments 174 to 192, which should be monitored for pipe thinning. Repairs to all damaged areas is recommended and may result in satisfactory corrosion protection for the entire pipe for at least another 10-20 years.					
15. SUBJECT TERMS Coatings, coal tar epoxy, coatings survey, electrochemical impedance spectroscopy, film thickness, ultrasonic thickness					
16. SECURITY CLASSIFICATION OF:			17. LIMITATION OF ABSTRACT U	18. NUMBER OF PAGES 100	19a. NAME OF RESPONSIBLE PERSON Stephanie Prochaska
a. REPORT U	b. ABSTRACT U	c. THIS PAGE U			19b. TELEPHONE NUMBER 303-445-2323

BUREAU OF RECLAMATION

Materials and Corrosion Laboratory

Report Number 8540-2018-73

Salt River Siphon Coating Inspection and Impedance Analysis

STEPHANIE PROCHASKA Digitally signed by STEPHANIE PROCHASKA
Date: 2019.01.23 09:34:40 -07'00'

Prepared by: Stephanie Prochaska, M.S.
Materials Engineer, Materials and Corrosion Lab

ALLEN SKAJA Digitally signed by ALLEN SKAJA
Date: 2019.01.23 09:41:51 -07'00'

Checked by: Allen Skaja, Ph.D.
Coatings Specialist, Materials and Corrosion Lab

BOBBI JO MERTEN Digitally signed by BOBBI JO
MERTEN
Date: 2019.01.23 15:15:34 -07'00'

Technical Approval: Bobbi Jo Merten, Ph.D.
Coatings Specialist, Materials and Corrosion Lab

WILLIAM KEPLER Digitally signed by WILLIAM
KEPLER
Date: 2019.01.23 14:20:00 -07'00'

Peer Review: William Kepler, Ph.D., P.E.
Manager, Materials and Corrosion Lab

Salt River Siphon Coating Inspection and Impedance Analysis

Acronyms and Abbreviations

CAP	Central Arizona Project
CE	counter electrode
DFT	dry film thickness
EIS	electrochemical impedance spectroscopy
PCCP	prestressed concrete cylinder pipe
RE	reference electrode
Reclamation	Bureau of Reclamation
TSC	Technical Service Center
UT	ultrasonic thickness
WE	working electrode

Symbols

°	degrees
ft	foot
Hz	hertz
kHz	kilohertz
mV	millivolt
$ Z $	impedance magnitude
$ Z _{0.1 \text{ Hz}}$	impedance magnitude at 0.1 hertz applied frequency
%	percent

Executive Summary

The Salt River Siphon is a [REDACTED] steel pipe near Phoenix, AZ, that is operated and maintained by the Central Arizona Project (CAP). The structure was originally constructed as prestressed concrete cylinder pipe (PCCP). The PCCP was replaced with a steel pipe in 1997, which received an Amercoat 78HB coal tar epoxy interior lining. The lining and underlying steel require occasional inspection to evaluate their condition and plan for maintenance or replacement in a timely manner.

Investigators from the Bureau of Reclamation's Technical Service Center (TSC) travelled to the CAP's Salt River Siphon to evaluate the condition of the interior lining. Investigators conducted traditional visual inspection techniques as well as dry film thickness (DFT), ultrasonic/steel thickness (UT), and electrochemical impedance spectroscopy (EIS).

The visual inspection showed that the coal tar epoxy was in generally good condition except for much of the pipe invert, sections of the field joints, and full pipe segments leading up to the outlet. The condition of the field-repaired pipe joints performed in 2001 paralleled that of the surrounding coal tar epoxy, with some appearing in good condition and others showing signs of abrasion or corrosion along the lower half of the pipe cross-section.

Sediment and debris appear to be the major contributors to damaged and abraded coating as well as the turbulence resulting from pipe elevation and directional changes. The upper half of the pipe walls and crown also received limited inspection because close-up access was not possible, and the surfaces contained a significant amount of mud and dirt. Quantitative testing confirmed abrasion of the invert coating but also showed that much of the intact coating, i.e. showing no visible damage, is providing excellent corrosion protection. The ladders and handrails at the deep well access point were found to be corroded.

The investigators recommend spot repairs of missing or degraded coating in the following areas:

- First priority: Possible full circumference of the siphon from pipe segment 155 to the outlet,
- First priority: Pipe invert, approximately 4- to 6-ft of pipe cross-section, particularly for pipe segments 130 through 162,
- First priority: Pipe joints, approximately lower half of pipe cross-section,
- Second priority: the entire pipe invert of the siphon from pipe segment 48 to 84.

Recommended coating materials include coal tar epoxy, 100% solids epoxy, or a coating with enhanced abrasion resistance. Spot repairs, if performed, should use an array of these materials to determine the optimum material for a future full recoating of the Salt River Siphon. In addition, the corroded ladders and handrails at the deep well access point should be replaced with composite materials. Pipe segments 174 to 192 should be monitored for steel thinning. Contact the TSC for any assistance required with the project specification.

Salt River Siphon Coating Inspection and Impedance Analysis

Contents

Salt River Siphon Coating Inspection and Impedance Analysis	iii
Acronyms and Abbreviations	iv
Symbols	iv
Executive Summary	v
Background	1
Conclusions and Recommendations	1
Inspection Methods	2
General Observations	2
Electrochemical Impedance Spectroscopy	2
Dry Film Thickness	4
Ultrasonic Thickness	4
Results, Analyses, and Discussion	4
General Observations	4
Electrochemical Impedance Spectroscopy	13
Dry Film Thickness	15
Ultrasonic Thickness	16

Background

The Salt River Siphon, a [REDACTED] Central Arizona Project (CAP) pipeline near Phoenix, AZ, was installed from 1975-78. Originally constructed out of prestressed concrete cylinder pipe (PCCP), the siphon was abandoned in place and a new steel pipe was constructed from 1996-1997. The steel pipeline is composed of 166 individual pipe pieces, joined in the field, with the last 507-ft of the original PCCP sliplined with 39 individual steel liners for a total of 205 pieces. The interior of the steel is lined with Amercoat 78HB coal tar epoxy. Warranty work was performed on the lining in 1999, and CAP made lining repairs, predominantly to the siphon's invert, in 2001 using grey and red coats of Devgrip 238.

CAP invited corrosion mitigation specialists from the Bureau of Reclamation's (Reclamation's) Technical Service Center (TSC) to assess the condition of the coal tar epoxy lining and perform quantitative field inspection techniques within the pipe. The TSC's Stephanie Prochaska and Bobbi Jo Merten conducted the inspection from November 5-8, 2018, along with several CAP engineers and inspectors.

Conclusions and Recommendations

Overall, the coal tar epoxy throughout the siphon appeared to be in visually good condition. In addition, the quantitative results from electrochemical impedance spectroscopy (EIS), dry film thickness (DFT), and ultrasonic thickness (UT) testing show the lining to be in good condition throughout most of the siphon with measured values meeting or exceeding specified values.

In general, most of the lining damage that was observed is limited to the pipe invert and field joints. Sediment in the water and elevation and directional changes along the pipe alignment are the major contributors to the coating damage observed. Lining removal and replacement with an abrasive-resistant lining should be performed at damaged areas of the invert and on damaged pipe joints. The Devgrip 238 repair material on the pipe joints was successful, but areas of pipe corrosion are visible along the invert and side walls, approximately up to the springline. These field repairs are showing light-to-medium abrasion of the repair material. Limited EIS measurements of the Devgrip 238 repair material suggest that it is providing good corrosion protection.

The highest priority lining degradation is found between pipe segments 155 and the outlet (pipe segment 205). Heavy abrasion is evident for both the coal tar epoxy and the Devgrip 238 repair material. The coal tar epoxy on the siphon walls is very rough and covered with tightly adherent mud or biofilm that is difficult to remove. In this area, EIS results show that the lining is providing the insufficient corrosion resistance. In addition, the left-hand wall showed reduced DFT, and UT measurements were slightly lower than specified. Pipe segments 174 to 192 should be monitored for steel thinning. Removal and replacement of the full circumference of lining from pipe segments 155 to the outlet should be considered. A detailed inspection of the inaccessible areas, i.e., the pipe side walls and crown, could confirm this need.

High priority spot repairs should also be conducted between pipe segment 130 and 162, where areas of pitting and blisters were observed. Often, the pitting was found on one side of the invert with numerous, small blisters less than two feet away on the other side. The lining should be removed and replaced in these areas to prevent the pitting and blistering from progressing. The pitting may require further inspection for weld repairs after coating removal and before recoating.

A lower priority area for repairs is the invert from pipe segment 48 to 84. In this area, EIS results show that the lining is still providing sufficient corrosion protection, but the values are lower than those of the surrounding areas and are nearing the threshold for needing maintenance. In addition, the DFT measurements from the invert are the lowest of the entire siphon and are less than half of the specified value, suggesting that the lower half of the lining from pipe segment 48 to 84 will soon need repair.

Spot repairs can be performed by abrasive blast, water jetting, or power tool surface preparation to remove the existing coating. The surface preparation should impart an angular profile on the steel surface and lightly abrade the adjacent 2- to 3-inches of intact coating. Apply new coating to the freshly prepared surfaces. Recommendations for a spot repair material include coal tar epoxy, 100% solids epoxy, or a coating with enhanced abrasion resistance. This approach could delay the recoating of the entire pipe interior by as much as 10 to 20 years.

Ladders and handrails near pipe segment 124 (deep well) should be removed and replaced with composite materials.

Inspection Methods

General Observations

The visual inspection documents all defects that are visible, such as missing and damaged lining, i.e., cracks, blisters, rust-through, etc. TSC investigators worked alongside CAP staff to collect visual inspection data. The pipe entrants observed each pipe segment at least twice while conducting quantitative analysis.

Electrochemical Impedance Spectroscopy

The lining surface was wiped clean of mud with a rag and then wiped dry to prepare the lining surface for EIS testing. Disposable, 2.25-inch diameter test cells were affixed to the coal tar epoxy over an area absent of visible defects or cracks. A fast-curing aquarium-grade silicone adhesive provided a seal for attachment of each test cell to the lining. Tap water containing approximately 1 tablespoon of salt (approximately 20 grams of NaCl) per liter was added to the test cells as an electrolyte. The filled test cells were left for at least one hour to equilibrate before testing.

Each prepared test location comprised of at least two test cells. At some test sites, a third test cell was added in case of inadequate adhesion resulting in cell leakage. The test cell positions were along the lower side wall, approximately four feet up the pipe wall and adjacent to the upstream pipe joint. In most cases, the test sites alternated between the left-hand (north) and right-hand (south) pipe wall, referenced to facing downstream.

EIS measurements were performed using an Ivium Compactstat portable potentiostat that was powered by a ruggedized laptop (Figure 1). The laptop also provided the necessary software to run the measurements. Each measurement utilized two test cells: one containing a copper/copper sulfate reference electrode (RE) and a platinum mesh counter electrode (CE) and the other containing a platinum mesh working electrode (WE). This arrangement allows for a 4-electrode measurement of current and voltage through a circuit to evaluate the lining beneath each test cell. The current and voltage leads are separate in the RE/CE test cell and together in the WE test cell. These two parameters allow for interrogation of the complex resistance, i.e., impedance of the lining; all other resistances in the circuit are assumed to be negligible by comparison.



Figure 1. Typical EIS set-up during measurement at pipe segment 160 with ruggedized laptop connected to a portable potentiostat (not shown, behind the laptop).

During the test, a 50 millivolt (mV) amplitude (root mean squared) sinusoidal voltage perturbation is applied, and the current required to achieve the desired voltage is measured. The

evaluated perturbation frequencies were 100 kilohertz (kHz) to 0.1 hertz (Hz) at five points per decade, resulting in an array of data points during a test time of approximately two to three minutes.

Dry Film Thickness

DFT measurements were taken on the coal tar epoxy using a PosiTector 6000 coating thickness gauge. Fifteen measurements were recorded for each pipe segment where EIS testing occurred: five measurements each on the right-hand side of the pipe wall, the pipe invert, and the left-hand side of the pipe wall. DFT was measured in the clean area adjacent to the EIS test cells as applicable.

Repaired areas in the invert were not measured for DFT. In addition, areas with missing lining or visible lining damage were also not measured. Rather, measurements were taken at the most proximate area of visually sound coal tar epoxy lining.

Ultrasonic Thickness

UT measurements were taken using a Cygnus Instruments M5-C4+ UT gauge and coupling fluid. Fifteen total measurements were recorded for each pipe segment where EIS was performed: five measurements each on the right-hand side of the pipe wall, the pipe invert, and the left-hand side of the pipe wall. UT was measured in the clean area adjacent to the EIS test cells where applicable; spots of coupling fluid from the measurement locations are seen around the test cells in Figure 1.

Results, Analyses, and Discussion

General Observations

The cursory visual inspection performed by TSC investigators resulted in photo-documentation of approximately every fourth pipe segment and evaluation of visible coating damage. Additional inspection photos are in Appendix D. CAP staff produced systematic visual inspection data at every pipe segment which can be found in Appendix E.

A sequential evaluation of the visual inspection data follows, beginning at the upstream end of the pipe. The actual inspection occurred in the order by which the sections of siphon were dewatered and prepared for inspection as well as the steep elevation changes that made entering and exiting in certain locations more favorable. Instead, inspectors progressed by entering and exiting from various manholes as well as the upstream and downstream end of the siphon. The entire length of the siphon was inspected. The siphon elevation profile is shown in Figure 2.

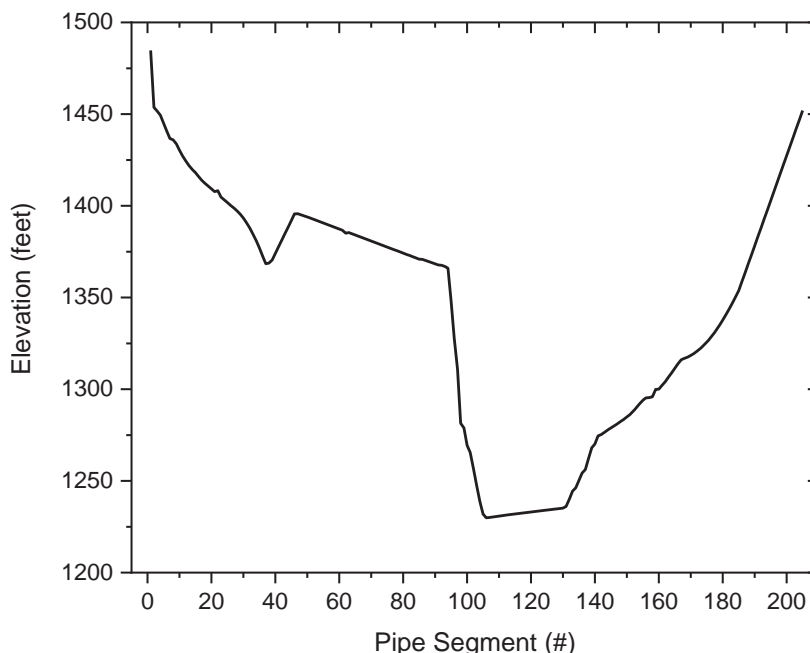


Figure 2. Siphon elevation profile.

The siphon contains significant pipe slope changes with several steep declines and inclines. Most notably, there is an approximate 24 percent (%) decline, approximately 14 degrees ($^{\circ}$), from pipe segments 1 to 4, a 26% decline (15°) from segments 95 to 106, and a 30% incline (17°) from segments 175 to 205. Rope access techniques were used for inspecting the steepest sections of the pipe. The inspection’s route was such that all inspections occurred while descending a slope.

The condition of the coal tar epoxy and the Devgrip 238 repair material near the siphon’s inlet was found to be good on the pipe walls and invert, as seen in Figure 3. The coal tar epoxy is smooth and undamaged, and the joint repair areas do not show signs of abrasion. Repair material abrasion is visible in some areas of the invert near pipe segment 4. In this area, the grey top coat is missing, revealing the red mid-coat.



Figure 3: Pipe wall and joint repairs near pipe segment 4 are in good condition (left). Abrasion of repair material in the invert was commonly found throughout the siphon (right).

Invert damage of varying severity was commonly found throughout the siphon. In some of the most severe cases, the repair material has been abraded down to bare steel and corrosion is present. Figure 4 shows one such example of a large area of corrosion in the invert near pipe segment 12.

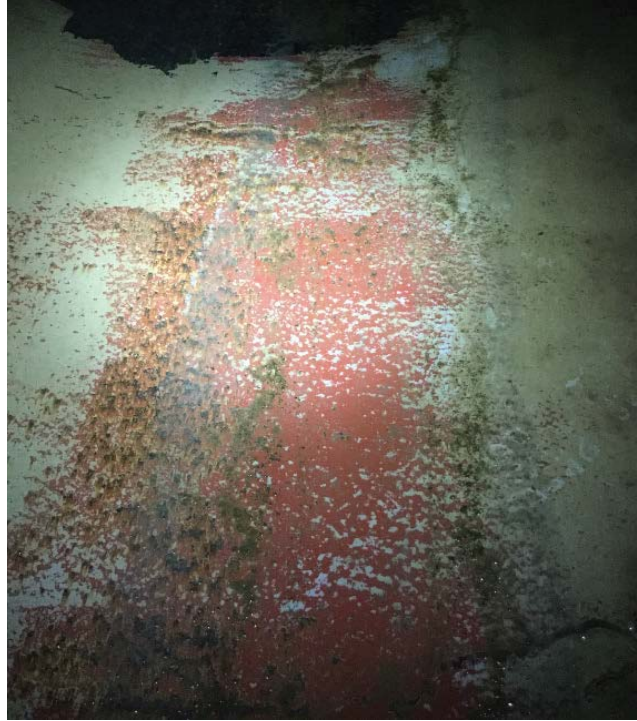


Figure 4: Large area of abraded repair material and corrosion in the invert near pipe segment 12.

The first drop in elevation ends near pipe segment 40 where there is a short incline for approximately 10 segments. Despite the possibility for turbulence in this area, the coating is in good condition with few visible defects. Small, unbroken blisters were found near the test cells at pipe segment 40 (Figure 5), and an orange-peeled surface is seen at pipe segment 48.



Figure 5: Coating condition at pipe segment 40 (left) and 48 (right). Small blisters are visible in the coating around the test cells at segment 40. UT coupling fluid is seen around the blisters.

Between pipe segments 50 and 94, the siphon's downward slope is at its most shallow angle. In general, the coal tar epoxy is in good condition with only a few noted defects. Near pipe segment 80 a small area of corrosion above a joint repair area was found. The corrosion, seen in Figure 6, is located directly on the welded joint interface.



Figure 6: Corrosion near pipe segment 80 at a joint interface directly above repair material (white).

One notable irregularity in the pipe wall is a bulge to the left of the pipe invert at pipe segment 95. The bulge, seen in Figure 7, is approximately two feet in diameter and protrudes approximately six inches into the pipe at its center.



Figure 7: 2'x2'x6" bulge found on the left-hand wall of pipe segment 95.

Between pipe segments 94 and 108, the elevation decreases by approximately 140 feet into the deep well. No major lining defects of either the coal tar epoxy or repair material were noted throughout this section. Mud and sediment was wiped away to reveal the condition of the repair material at pipe segment 108, as seen in Figure 8.



Figure 5: Intact repair material at pipe segment 108.

Between segments 108 and 130, the siphon's elevation increases slightly before beginning a steep incline to the outlet. Pipe defects are abundant between segments 130 and 160, with areas of blisters and pitting adjacent to the pipe invert being the main concerns. Figure 9 shows the blisters and pitting and provides a scale using a 6-inch yellow ruler.



Figure 6: Large blisters near pipe segment 136 (left) and pitting near pipe segment 140 (right).

The invert throughout this portion of the siphon is also in poor condition. Abraded repair material and corrosion were found at a joint near pipe segment 144. In addition, pitting and blisters were found on opposite sides of the invert in multiple pipe segments. Figure 10 shows an example of pitting corrosion on one side of the invert and blisters on the other side. An additional large area of blistering was found near pipe segment 162.



Figure 7: Highly abraded repair material on either side of the invert near pipe segment 144. Pitting is on the left and blisters are on the right of the invert.

In general, the coal tar epoxy appeared to be in poorest condition from approximately pipe segment 160 to the outlet. The incline is very steep and long, and sediment and debris was prevalent throughout. The repair coating in the invert was significantly abraded to the red mid-coat and, in some instances, to the bottom, primer coat. The coating along the pipe walls appeared rough and tightly adhered biofilm was very difficult to remove. Figure 11 shows the extent of the invert abrasion at the outlet and a close up of rough coating at an EIS test location.



Figure 8: Abraded repair coating visible in the invert with mud and sediment nearby (left). Rough coating visible with tightly adherent mud at an EIS test location at pipe segment 180 (right).

In addition to inspecting the coating in the siphon, inspectors also noted severe corrosion and wear on the ladders and guardrails leading out from the deep well. As seen in Figure 12, thinning due to corrosion is visible on the ladder rungs and the bolt holding the ladder to the wall. Corrosion is also present near the interface between the guardrail and the concrete floor, likely exacerbated by pH concentration cell.



Figure 9: Severe corrosion on the ladder, bolts, and guardrail in the access point leading to the deep well.

Electrochemical Impedance Spectroscopy

Figure 13 gives the results from the EIS testing with a 5-point adjacent averaging trendline. Results are reported as impedance magnitude, $|Z|$, at 0.1 Hz—a value derived from voltage and current data indicating the resistance to the flow of electrons through the coating—versus pipe segment number. Impedance magnitudes can aid in prioritizing maintenance of a pipeline. Impedance magnitudes over 10^8 ohms indicate good corrosion protection with a potential for 10 to 20 more years of adequate coating performance. Between 10^7 and 10^8 ohms, lining maintenance may be required much sooner. Below 10^7 ohms, the lining is providing poor corrosion protection, and maintenance or replacement should be a high priority.

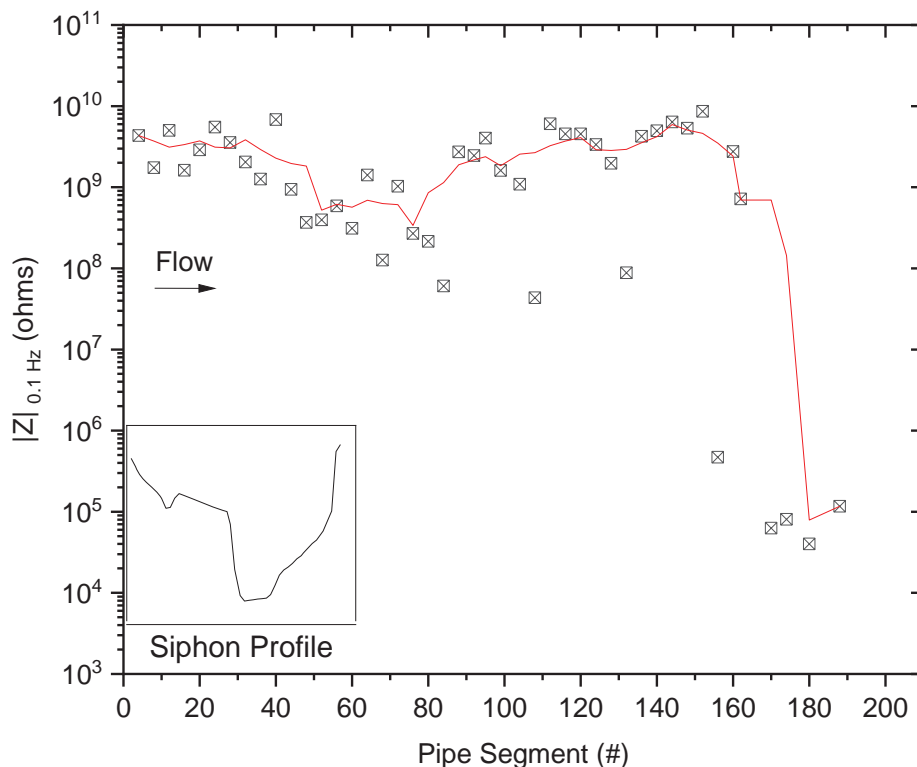


Figure 10. Overall corrosion protection at each pipe segment per EIS testing results with a 5-point adjacent averaging trendline included and siphon elevation profile inset.

In general, the coating on the lower pipe walls throughout the siphon is providing good corrosion protection with an average $|Z|_{0.1 \text{ Hz}}$ greater than 10^9 Hz. Between the inlet and pipe segment 152, only three measurements fell slightly below the 10^8 -ohm threshold, with no measurements below 10^7 ohms. A subset of this section, from pipe segment 48 to 84 shows a notable reduction in the average $|Z|_{0.1 \text{ Hz}}$, indicating the need for coating maintenance sooner here than in the surrounding sections. The test result at pipe segments 108 and 132 also show a reduction in corrosion protection.

From segment 156 to the outlet, there is a significant reduction in corrosion protection, with most measurements between 10^4 and 10^5 ohms, suggesting that there are non-visible cracks or pinholes in the coating that necessitate its removal and replacement. In this area of the siphon, the elevation changes drastically from the deep well to the outlet (see siphon profile in Figure 13 inset), and turbulent water is possible. In addition, sediment and other debris that collects in the deep well may be abrading the coating as it is forced up and out of the siphon.

Testing in the area near the outlet was extremely difficult due to the slope and necessity of using ropes to safely inspect the area and to tie off the equipment. Therefore, frequency of measurements was reduced from every four pipe segments to every eight pipe segments.

EIS measurements were taken at seven repair locations to evaluate the performance of the Devgrip 238 repair material. All test sites were located on the lower pipe wall of the siphon,

with the majority being between pipe segments 86 and 91. All $|Z|_{0.1 \text{ Hz}}$ for the tested repair areas were above 10^8 ohms, except one that was 1.15×10^7 ohms. A repair area at pipe segment 166 is providing good corrosion protection (more than 10^8 ohms) while the coal tar epoxy on nearby segments was found to be in very poor condition (less than 10^5 ohms). EIS summary tables and Bode plots, which show the $|Z|$ versus measurement frequency raw data, for all tested pipe segments and repair areas are in Appendix A.

Dry Film Thickness

According to the CAP, the specified lining thickness for the coal tar epoxy in the siphon was 24 mils.

Figure 14 shows the DFT for the left-hand wall, invert, and right-hand wall at each pipe segment with a dashed line representing the specified thickness. The average DFT for these regions are 25.8 mils, 27.8 mils, and 22.2 mils, respectively. The standard deviation for the average left- and right-hand wall calculation is 8 mils while the invert is 11 mils. Although it is difficult to visually discern abraded coal tar epoxy, lining thinning due to abrasion is likely occurring throughout the siphon as represented by lower-than-specified DFT measurements.

Most of the measurements in the invert did not meet the specified DFT. Pipe segments 36 through 84 had the lowest DFT in the invert, with an average DFT of 12.2 mils. This corresponds to poorer EIS results throughout these segments.

The average DFT of the right-hand wall and left-hand wall are very similar throughout the pipe, except near the outlet. The left-hand wall DFT was 17.2 mils from pipe segments 160 to 188. The lowest EIS results of the entire siphon were recorded throughout these segments.

Changes in DFT loosely correspond to siphon elevation changes. DFT immediately near the inlet and in the deep well are markedly higher than average. A significant spike in DFT at pipe segment 99 may be due to extra coating material applied on the steep slope.

Due to accessibility difficulties, DFT measurements were not taken at some locations nearest to the outlet. A summary table of all raw DFT data is in Appendix B.

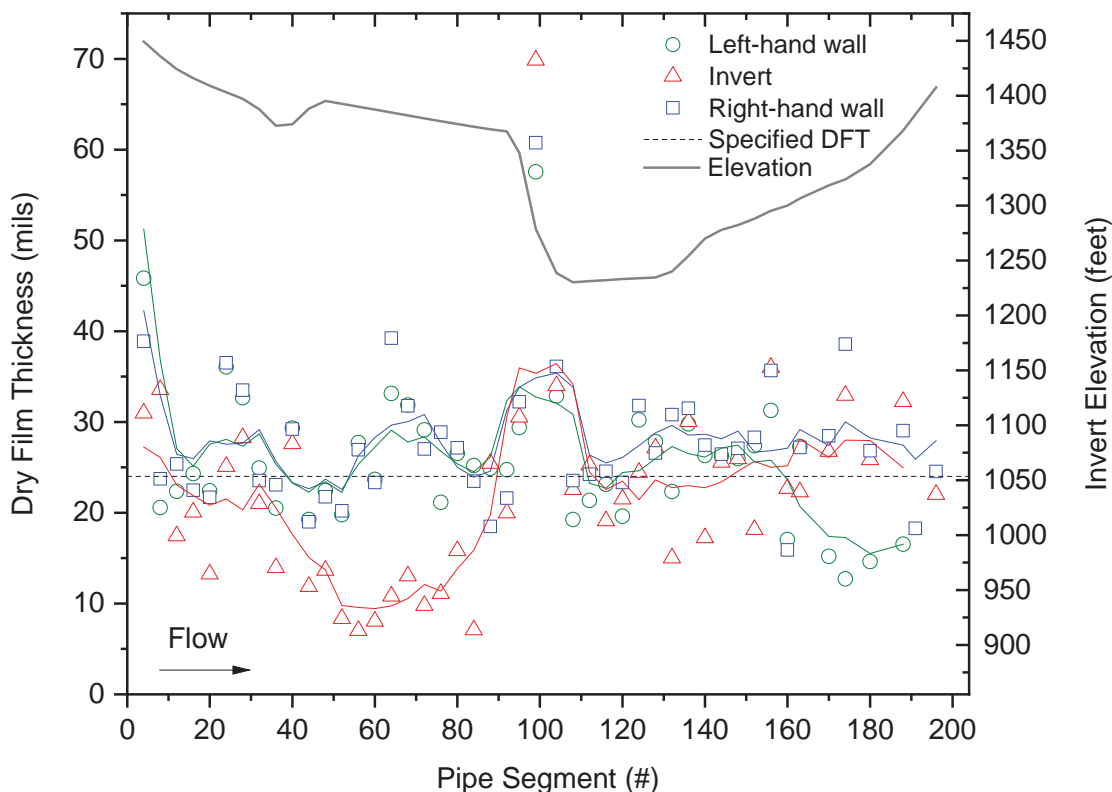


Figure 11. Average DFT at each pipe segment, measured at invert and each wall with a line indicating 80% of the specified DFT and siphon invert elevation profile inset.

Ultrasonic Thickness

Figure 15 shows the average UT for the left-hand wall, invert, and right-hand wall of each inspected pipe segment. Expected values (from construction specifications provided by the CAP) are also included in the figure. The UT measurements indicate that the pipe wall thickness is approximately 0.02 inches thicker than the specified value for most pipe segments. The right-hand wall at pipe segment 4 and the invert at pipe segment 8 had two individual spots that measured nearly 0.50 inches lower than the specified value. Further inspection should determine if these values are a result of a pipe anomaly or measurement error.

Another notable area is pipe segment 124 (the deep well) where wall thickness at the invert matches the specified value, and the left- and right-hand wall measurements exceed it by 0.02 inches.

Pipe segments approaching the siphon outlet have several trends to investigate further. Pipe segments 170 and 196 exceed the specified value by 0.10 inches, which may suggest that the segments have a higher tolerance for pipe thinning. However, pipe segments 174, 188, and 192 are approximately equivalent to the specified value, and pipe segment 180 is 0.02 inches thinner than the specified value. The above-specified values elsewhere in the siphon suggest that pipe

thinning may be occurring from pipe segments 174 to 192. Further inspection is necessary to determine if, unlike the rest of the pipe, the segments in question were constructed to the specified thickness or if there has been actual metal loss in these areas.

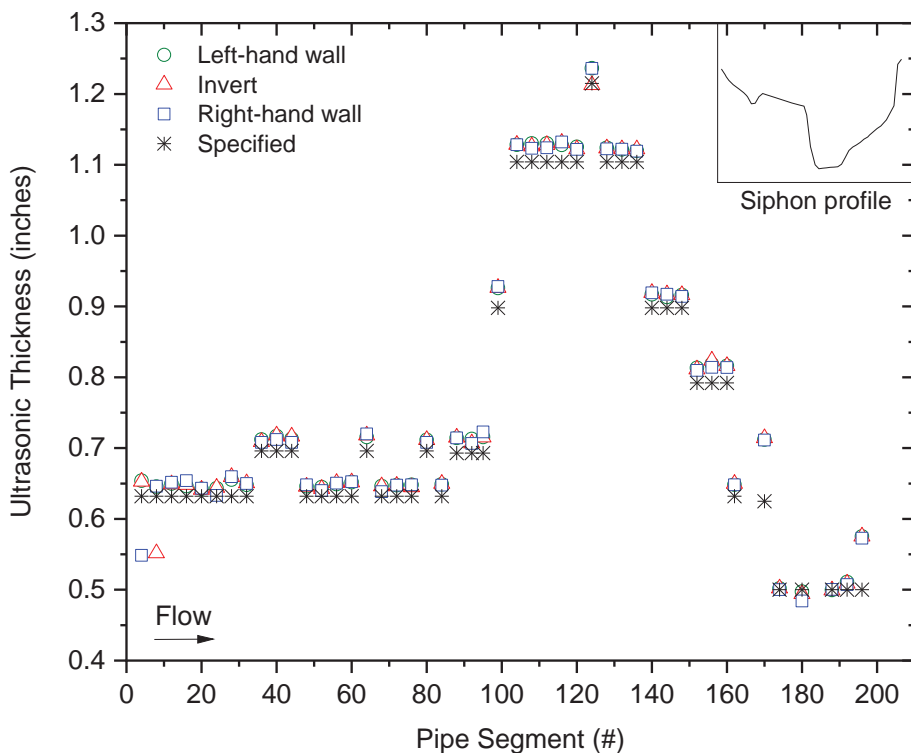


Figure 12. Average UT at each pipe segment, measured at invert and each wall, with specified values also shown and the siphon elevation profile inset.

Isolated areas of pitting and corrosion were found throughout the pipe, as seen in Figure 16, but pit depth was not measured directly on the pits via UT or a pit gauge.



Figure 13: Areas of pitting near pipe segment 60 (left) and 140 (right).

Although pits and corrosion were found on bare metal, inspectors did not find any evidence to suggest systematic pipe wear. The extensive amount of abraded coating, particularly in the invert, suggests that without a good coating system in place, accelerated pipe thinning could occur. A table of raw UT data for each pipe segment is in Appendix C.

Appendix A – EIS summary table and Bode plots for all tested pipe segments

Table A-1: Summary of coal tar epoxy EIS data at $|Z|_{0.1 \text{ Hz}}^1$

Pipe segment #	$ Z _{0.1 \text{ Hz}}$ (ohms)
4	4.33E+09
8	1.74E+09
12	5.02E+09
16	1.62E+09
20	2.88E+09
24	5.52E+09
28	3.55E+09
32	2.04E+09
36	1.26E+09
40	6.83E+09
44	9.38E+08
48	3.67E+08
52	3.97E+08
56	5.90E+08
60	3.12E+08
64	1.41E+09
68	1.26E+08
72	1.03E+09
76	2.69E+08
80	2.15E+08
84	6.07E+07
88	2.72E+09
92	2.45E+09
95	4.02E+09
99	1.61E+09
104	1.09E+09
108	4.34E+07
112	6.05E+09
116	4.55E+09
120	4.54E+09
124	3.35E+09
128	1.97E+09
132	8.80E+07
136	4.25E+09
140	4.97E+09
144	6.36E+09
148	5.34E+09
152	8.64E+09
156	4.70E+05
160	2.76E+09
162	7.18E+08
170	6.29E+04
174	8.07E+04
180	4.00E+04
188	1.17E+05

¹ Green represents no maintenance needed, yellow represents mid-to-low priority maintenance, and red represents high priority maintenance needed.

Table A-2: Summary of Devgrip 238 EIS data at $|Z|_{0.1 \text{ Hz}}$

Pipe segment #	$Z _{0.1 \text{ Hz}}$ (ohms)
86	1.27E+09
87	1.15E+07
88	4.97E+08
89	5.26E+09
90	1.34E+09
91	1.59E+09
166	2.48E+08

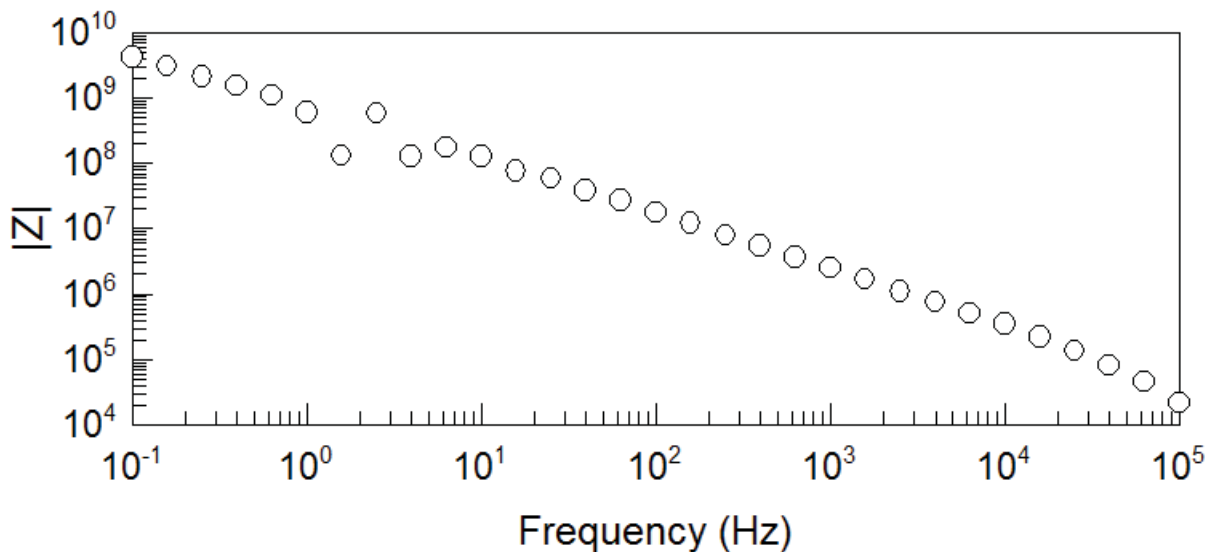


Figure A-1: EIS Bode plot from pipe segment 4, coal tar epoxy.²

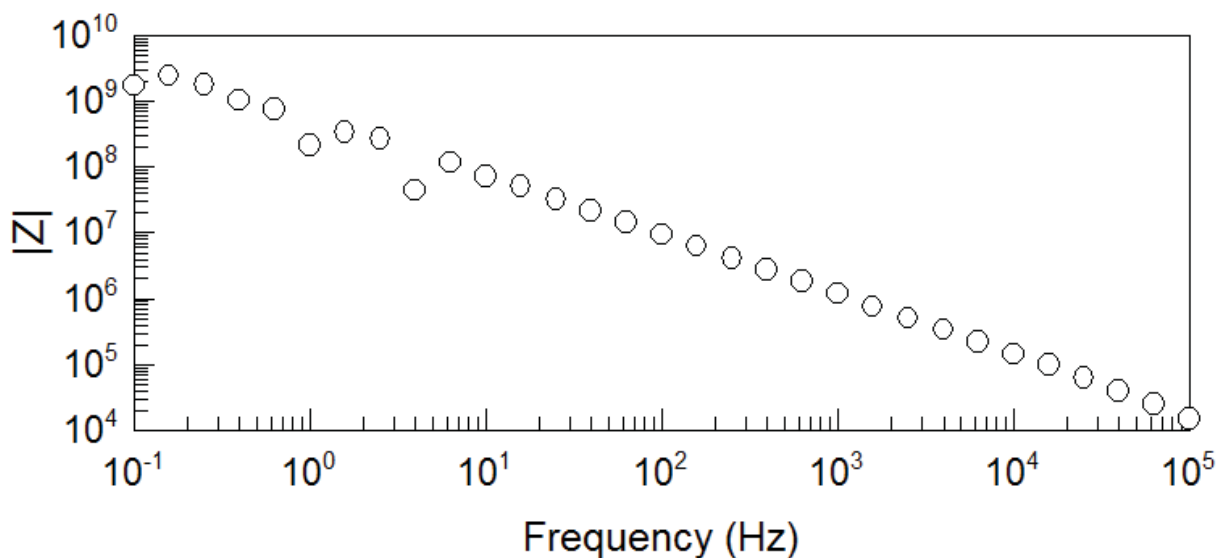


Figure A-2: EIS Bode plot from pipe segment 8, coal tar epoxy.

² Data scatter (noise) between 1 Hz and 50 Hz in some of the Bode plots could have been caused by outside electromagnetic signals, e.g. phones or tablets not being off or in airplane mode during the measurement, other testing devices, etc.

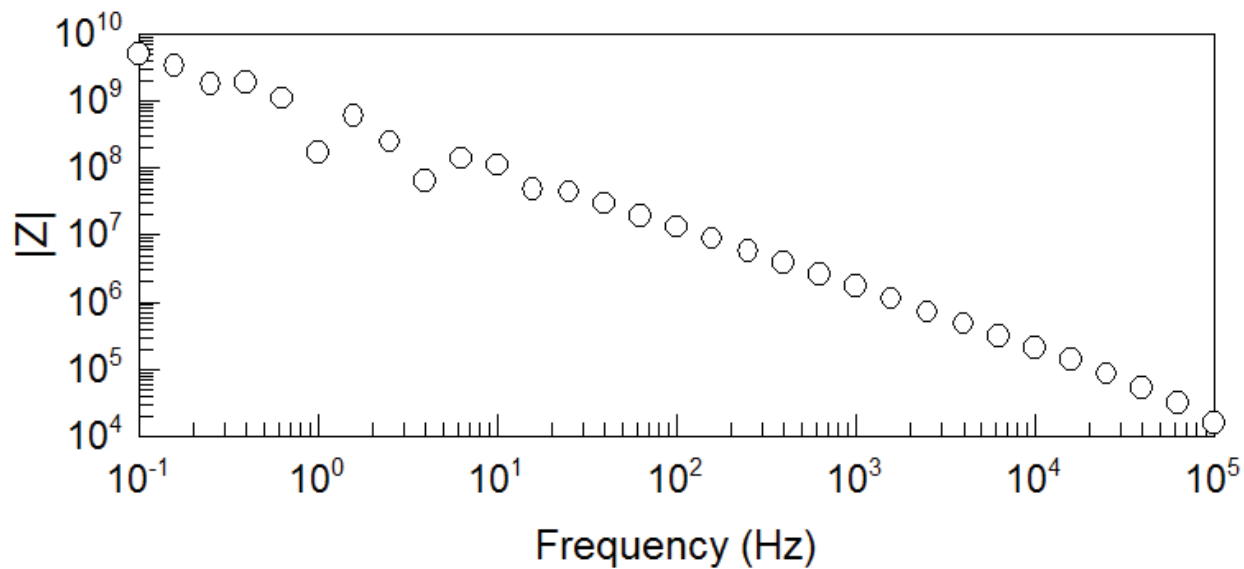


Figure A-3: EIS Bode plot from pipe segment 12, coal tar epoxy.

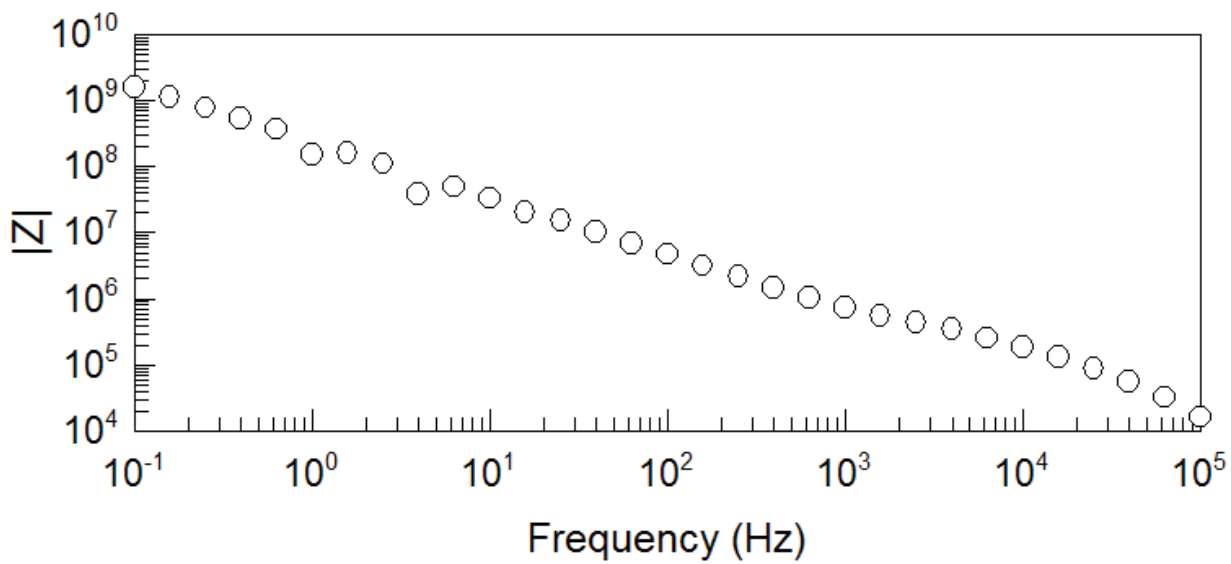


Figure A-4: EIS Bode plot from pipe segment 16, coal tar epoxy.

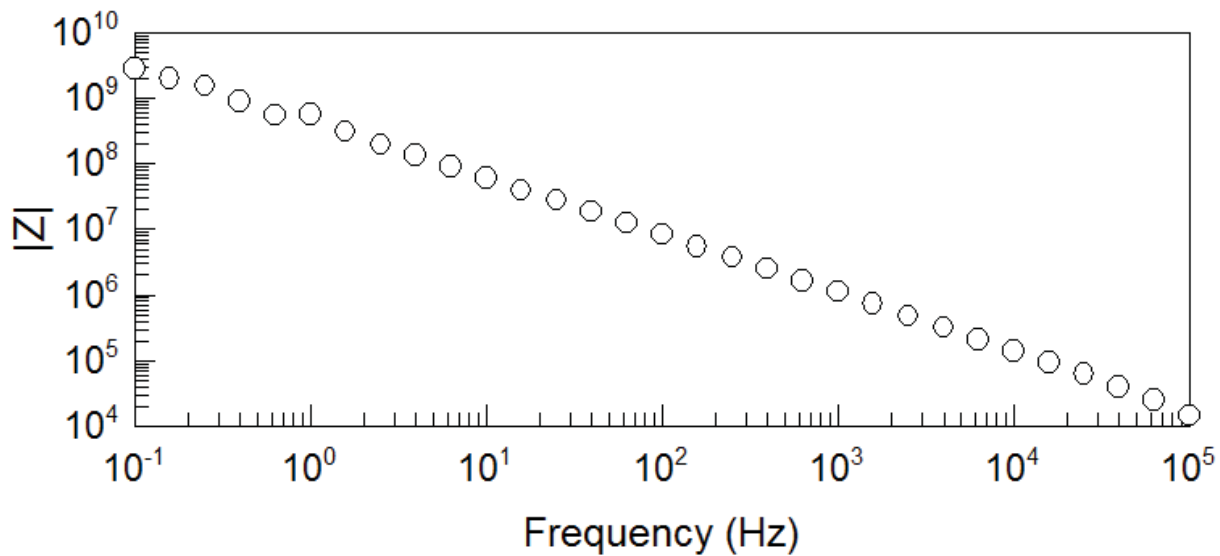


Figure A-5: EIS Bode plot from pipe segment 20, coal tar epoxy.

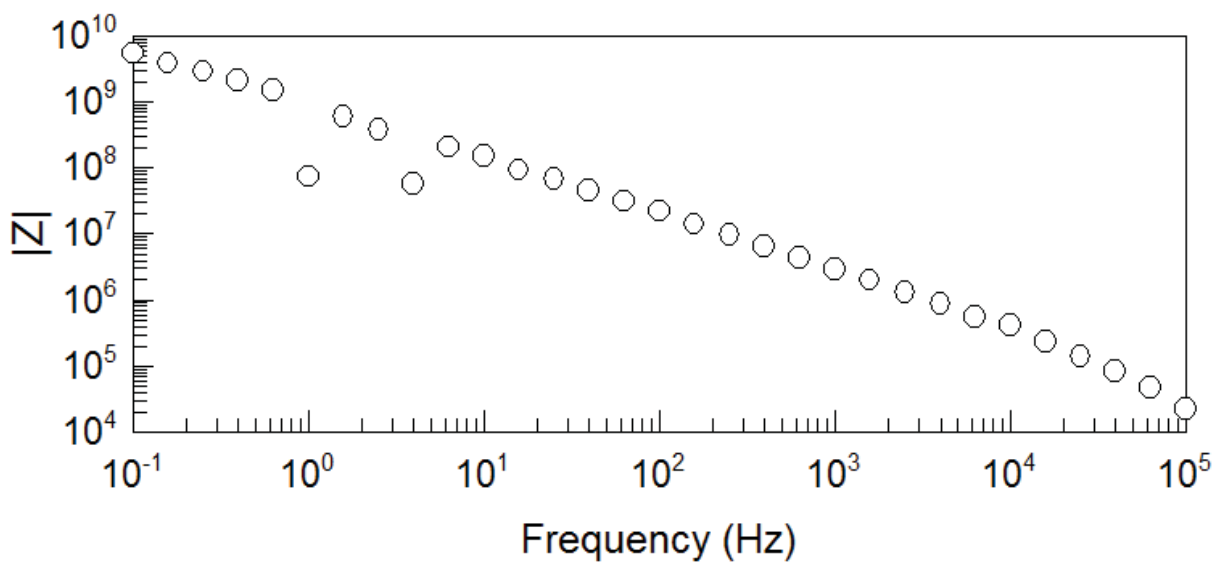


Figure A-6: EIS Bode plot from pipe segment 24, coal tar epoxy.

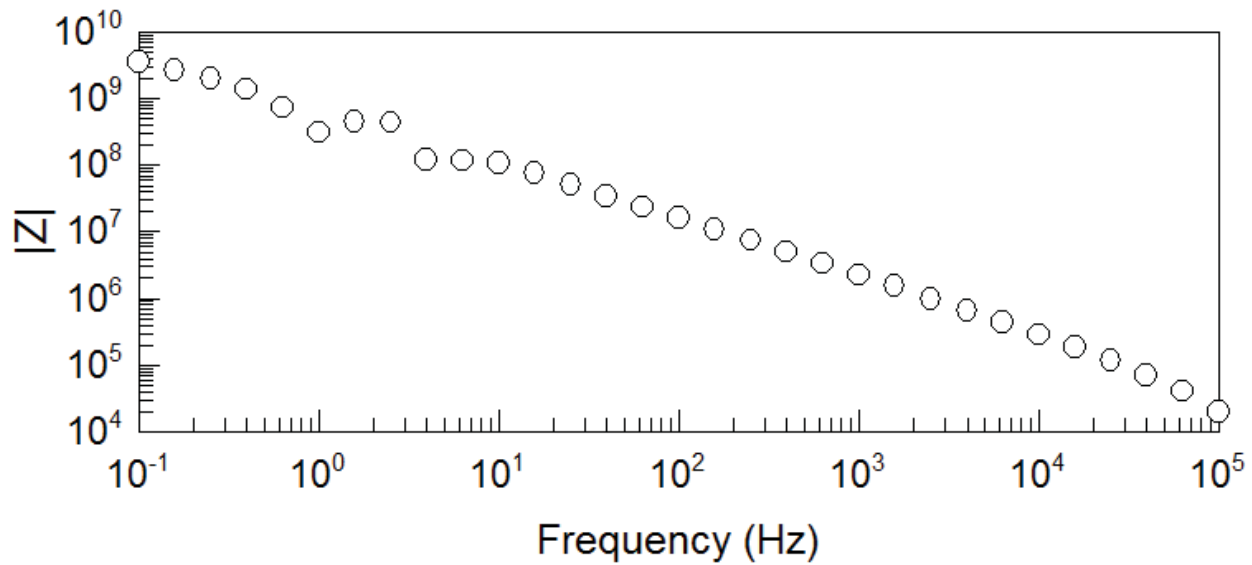


Figure A-7: EIS Bode plot from pipe segment 28, coal tar epoxy.

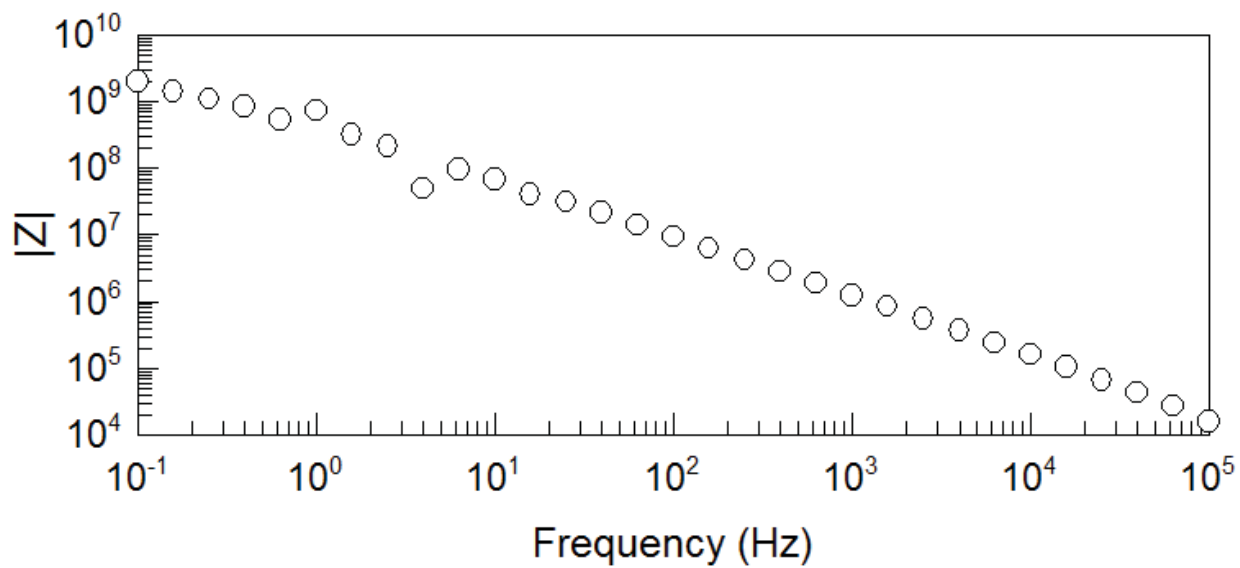


Figure A-8: EIS Bode plot from pipe segment 32, coal tar epoxy.

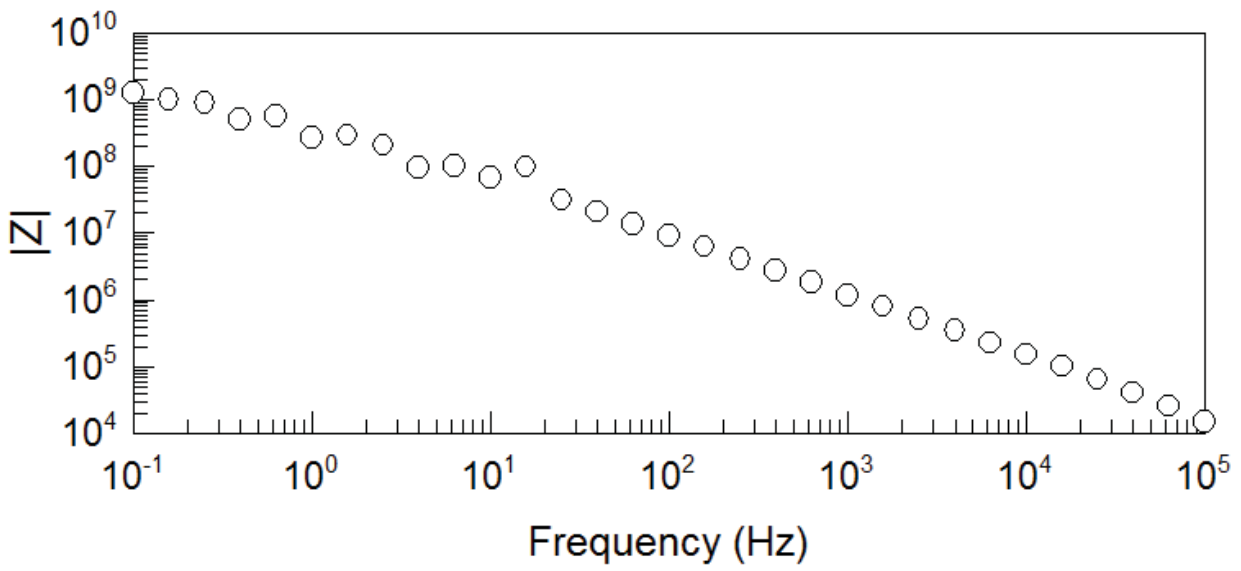


Figure A-9: EIS Bode plot from pipe segment 36, coal tar epoxy.

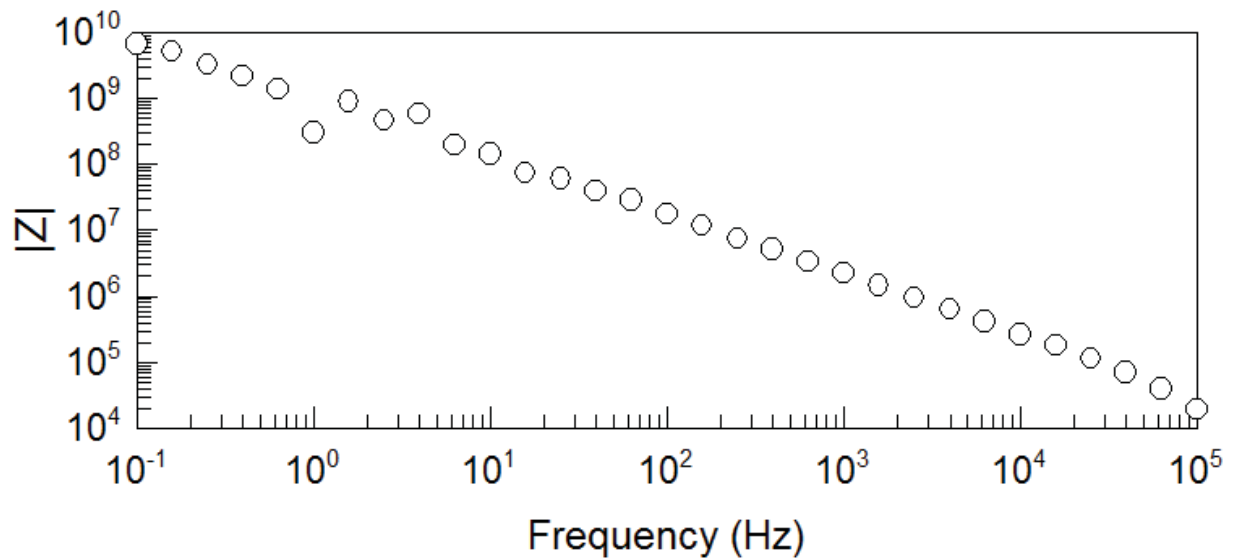


Figure A-10: EIS Bode plot from pipe segment 40, coal tar epoxy.

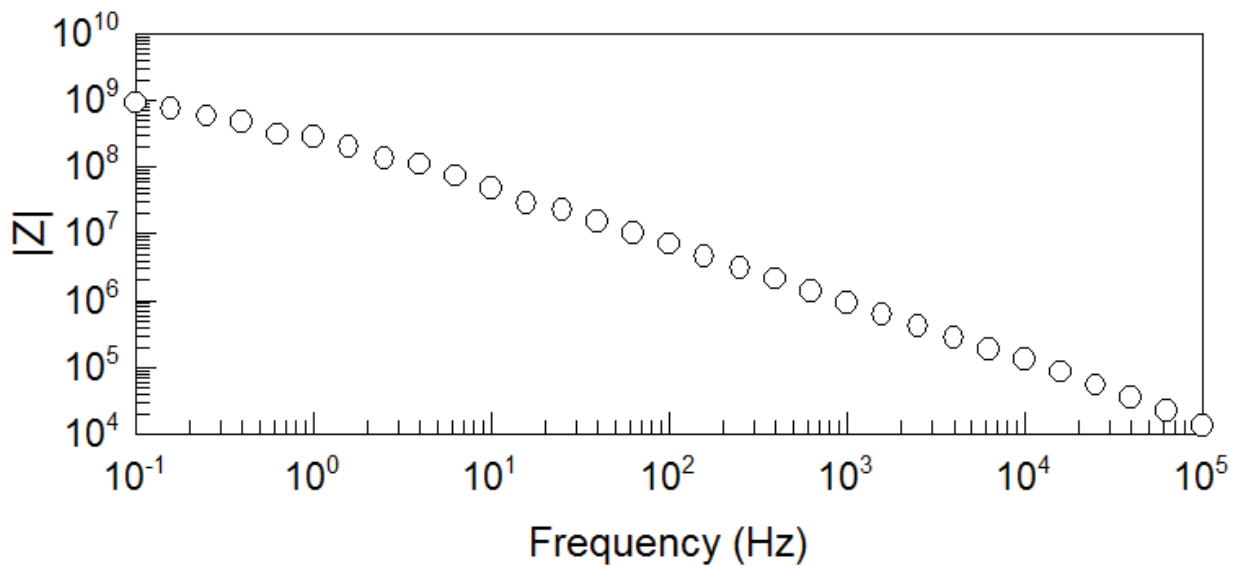


Figure A-11: EIS Bode plot from pipe segment 44, coal tar epoxy.

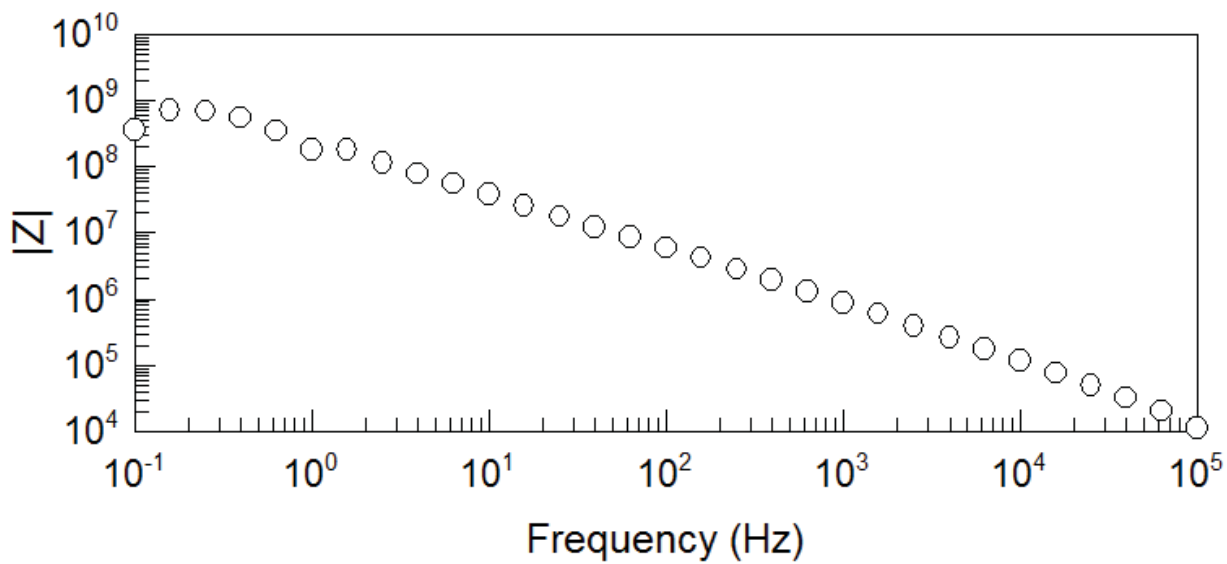


Figure A-12: EIS Bode plot from pipe segment 48, coal tar epoxy.

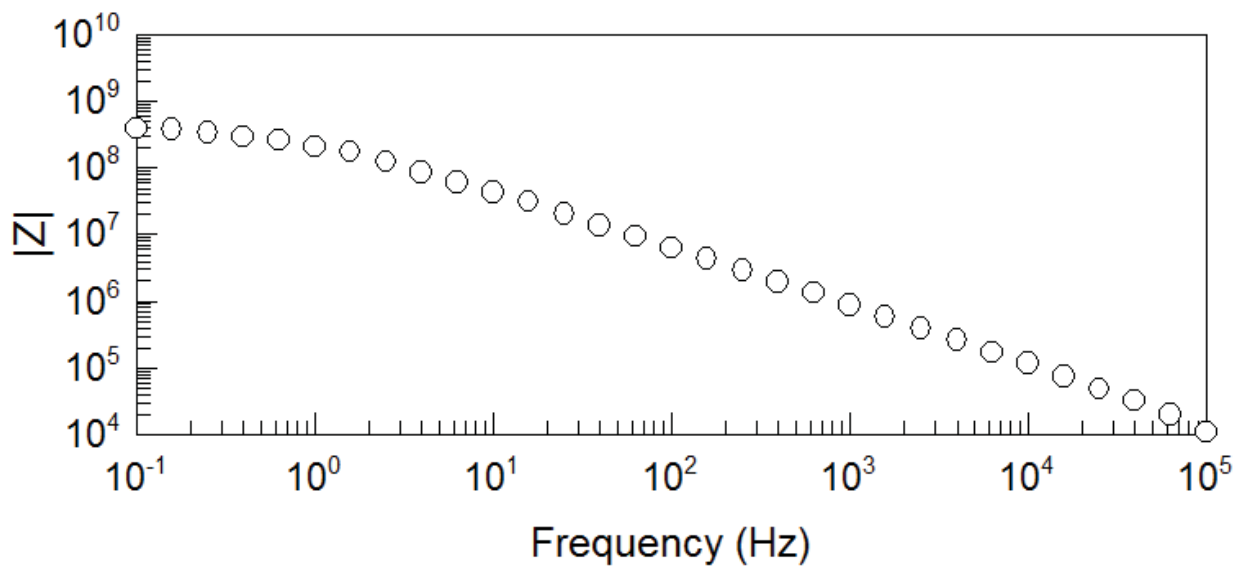


Figure A-13: EIS Bode plot from pipe segment 52, coal tar epoxy.

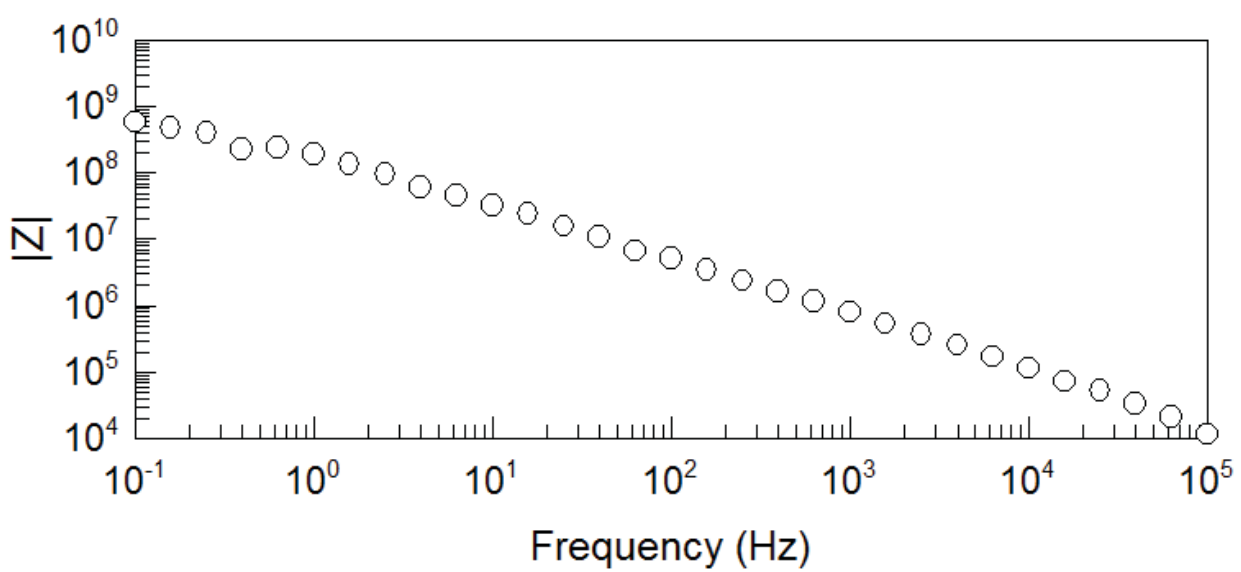


Figure A-14: EIS Bode plot from pipe segment 56, coal tar epoxy.

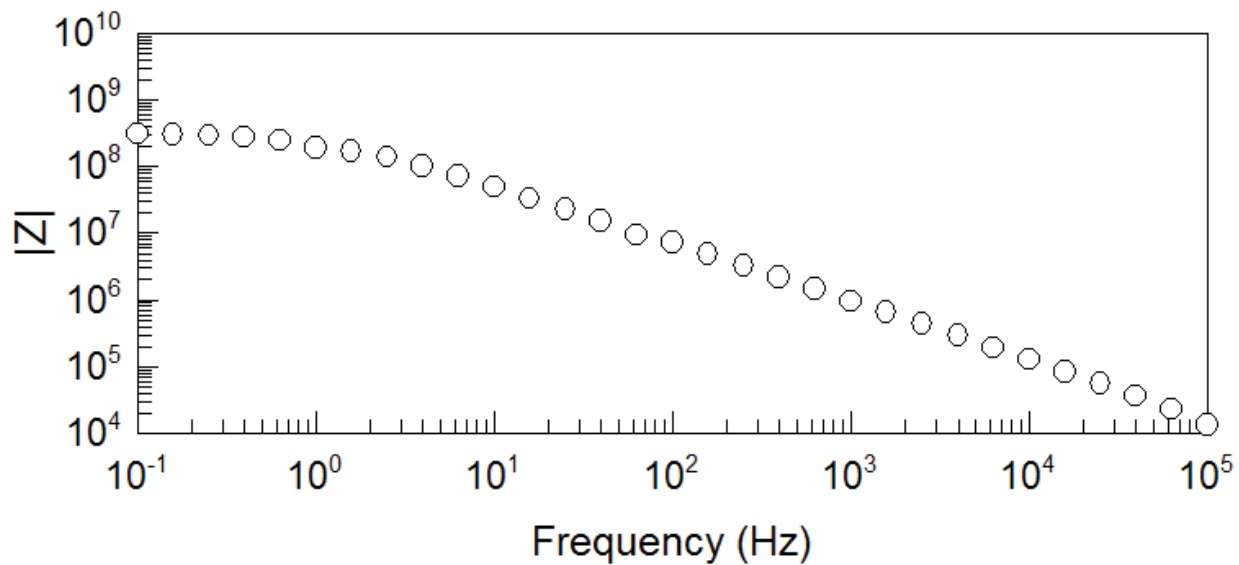


Figure A-15: EIS Bode plot from pipe segment 60, coal tar epoxy.

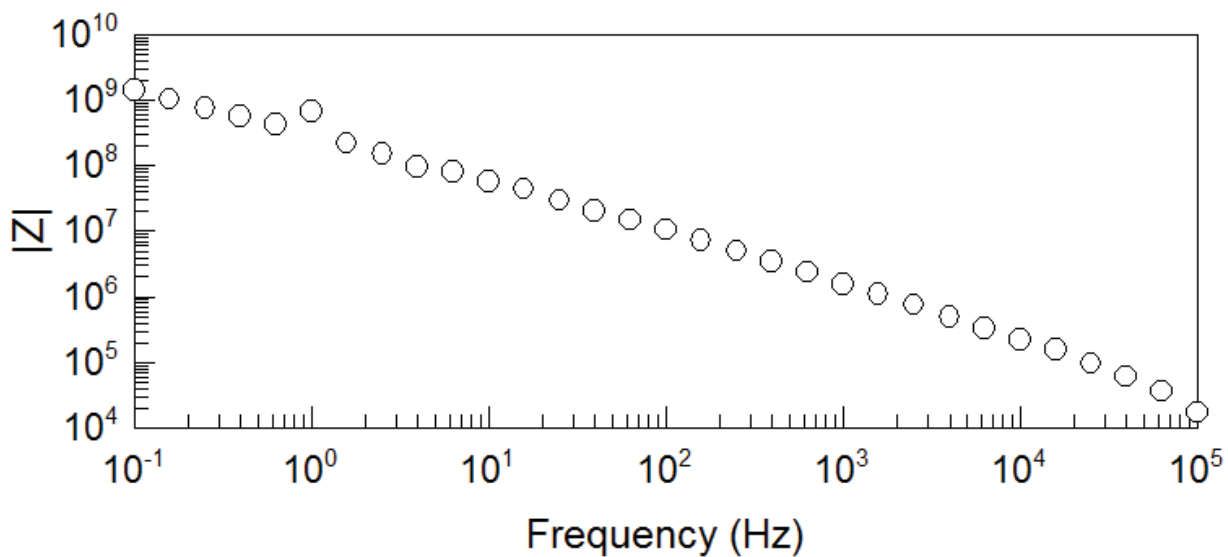


Figure A-16: EIS Bode plot from pipe segment 64, coal tar epoxy.

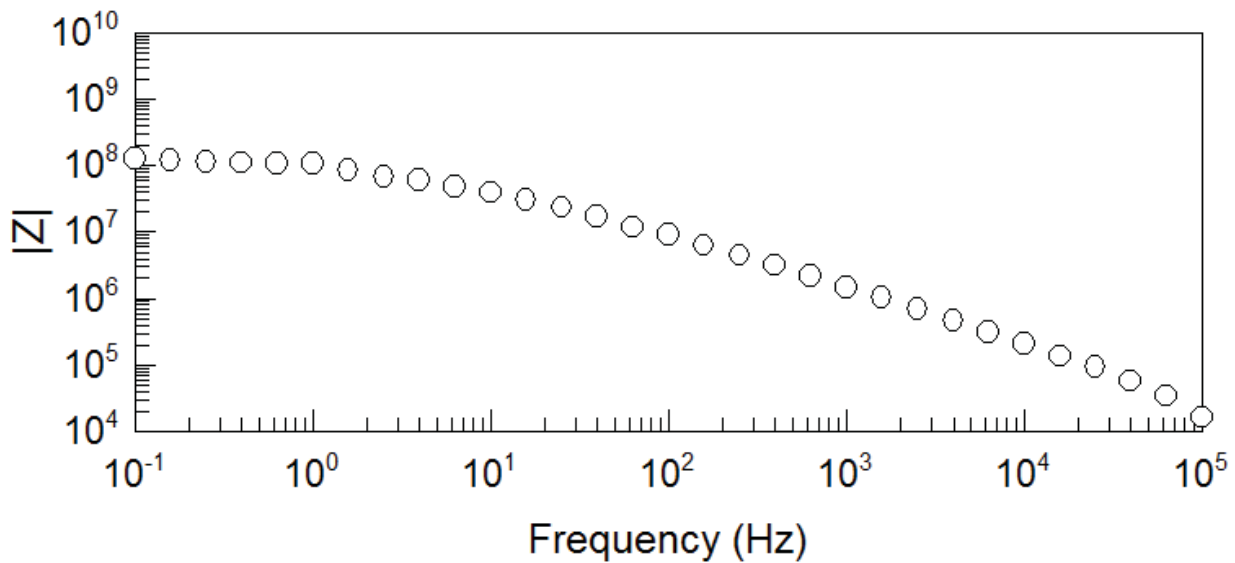


Figure A-17: EIS Bode plot from pipe segment 68, coal tar epoxy.

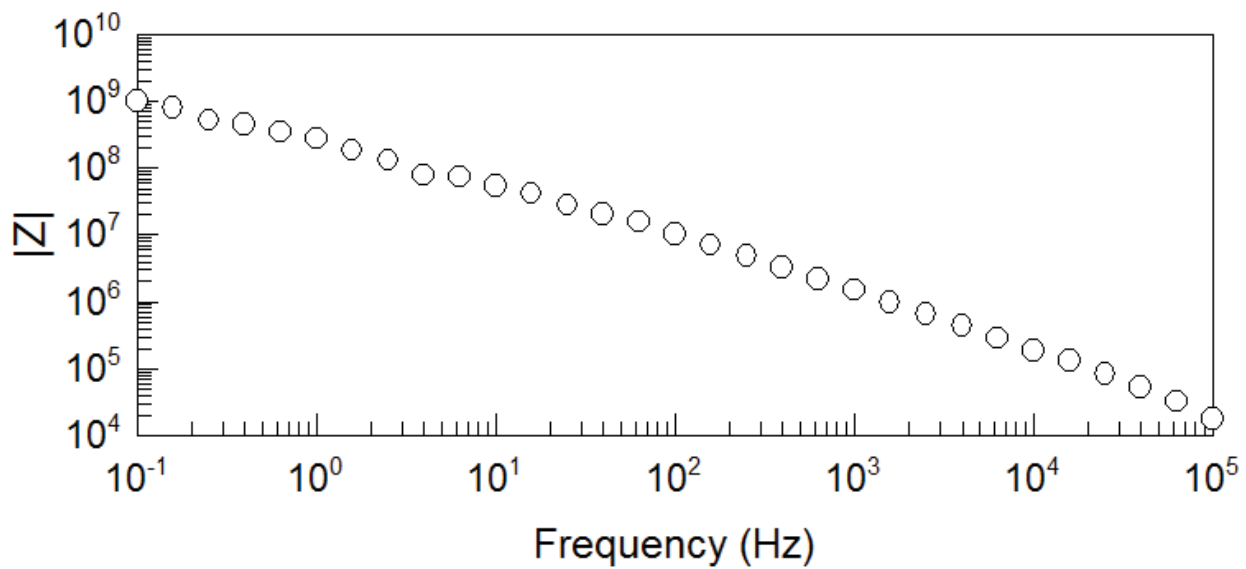


Figure A-18: EIS Bode plot from pipe segment 72, coal tar epoxy.

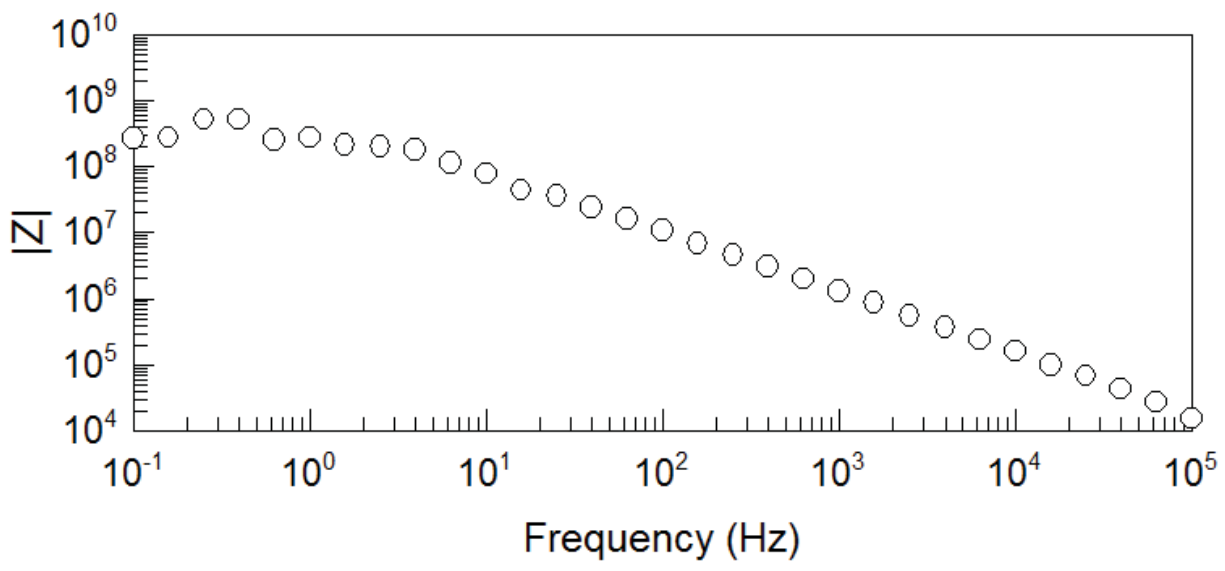


Figure A-19: EIS Bode plot from pipe segment 76, coal tar epoxy.

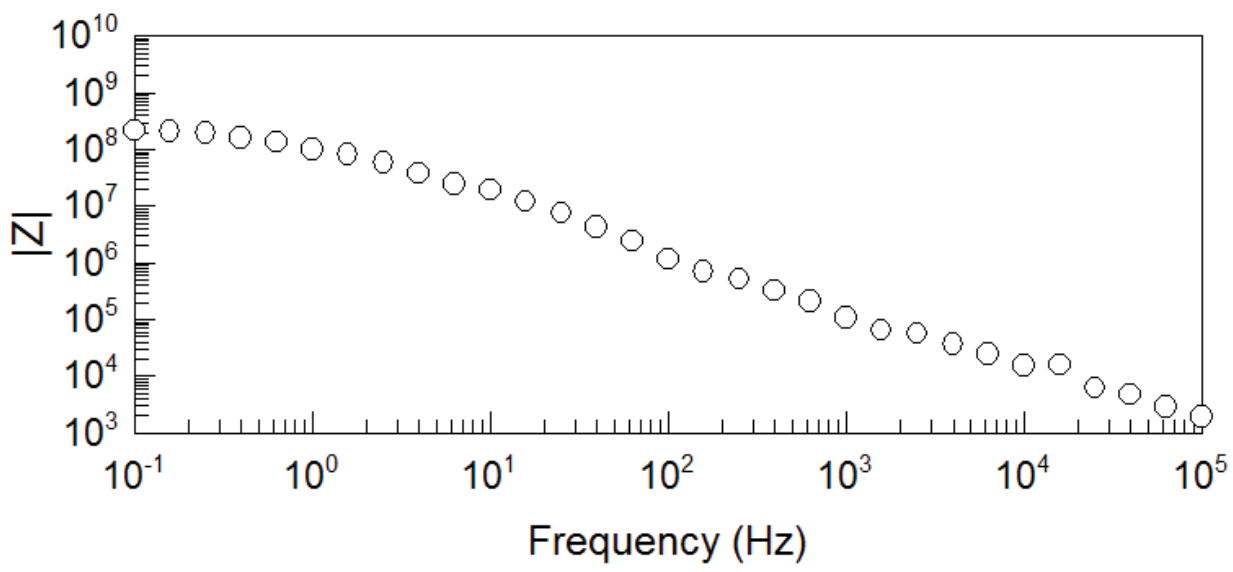


Figure A-20: EIS Bode plot from pipe segment 80, coal tar epoxy.

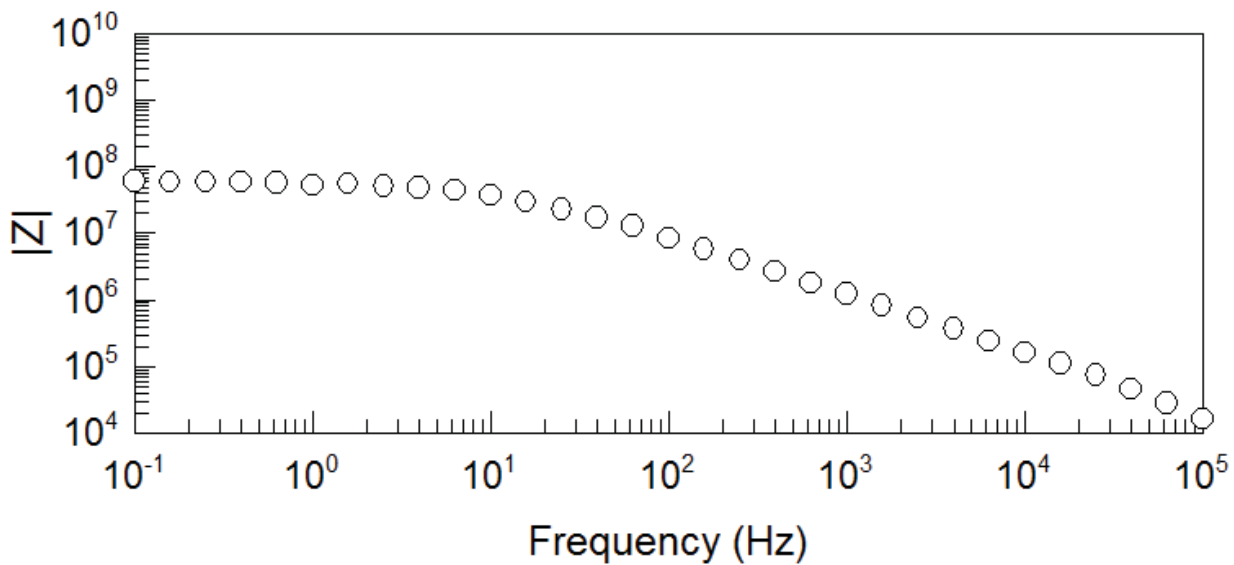


Figure A-21: EIS Bode plot from pipe segment 84, coal tar epoxy.

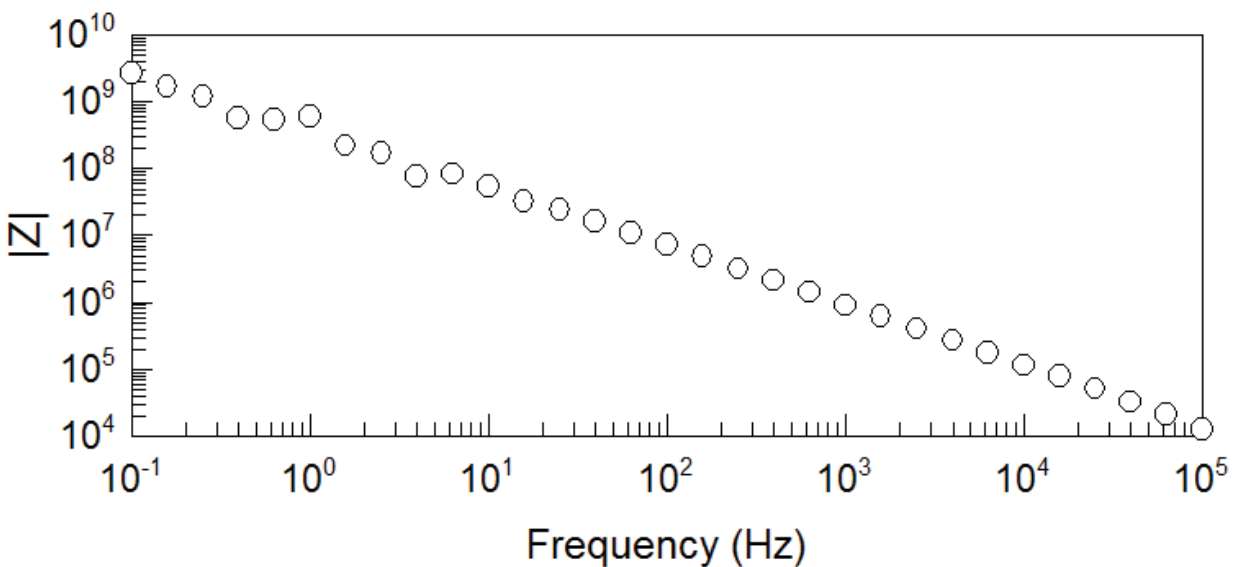


Figure A-22: EIS Bode plot from pipe segment 88, coal tar epoxy.

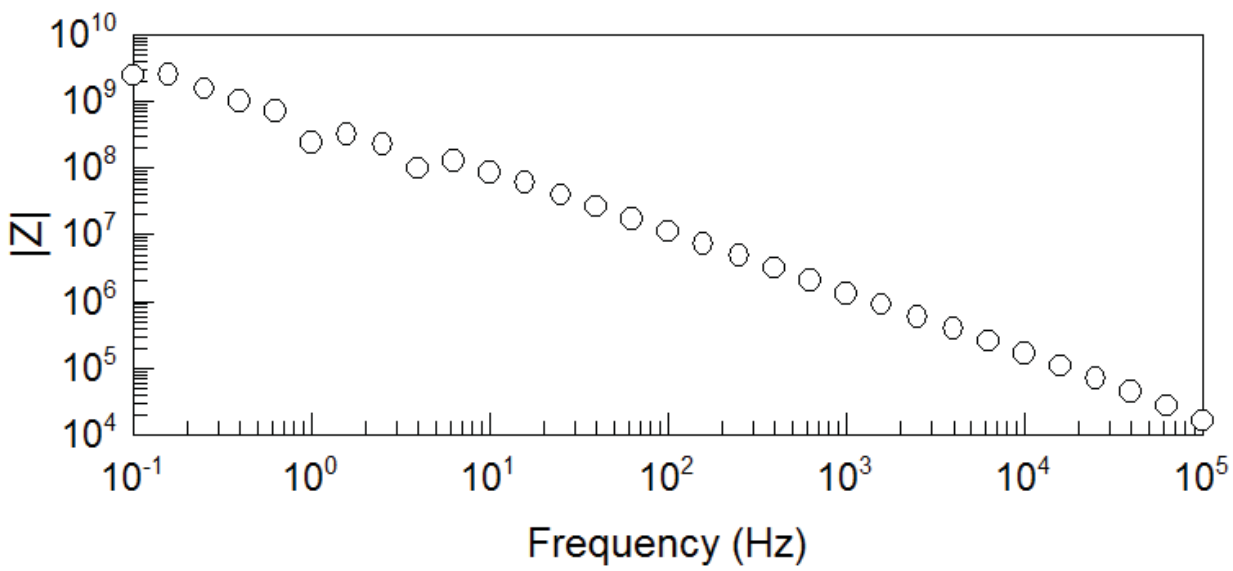


Figure A-23: EIS Bode plot from pipe segment 92, coal tar epoxy.

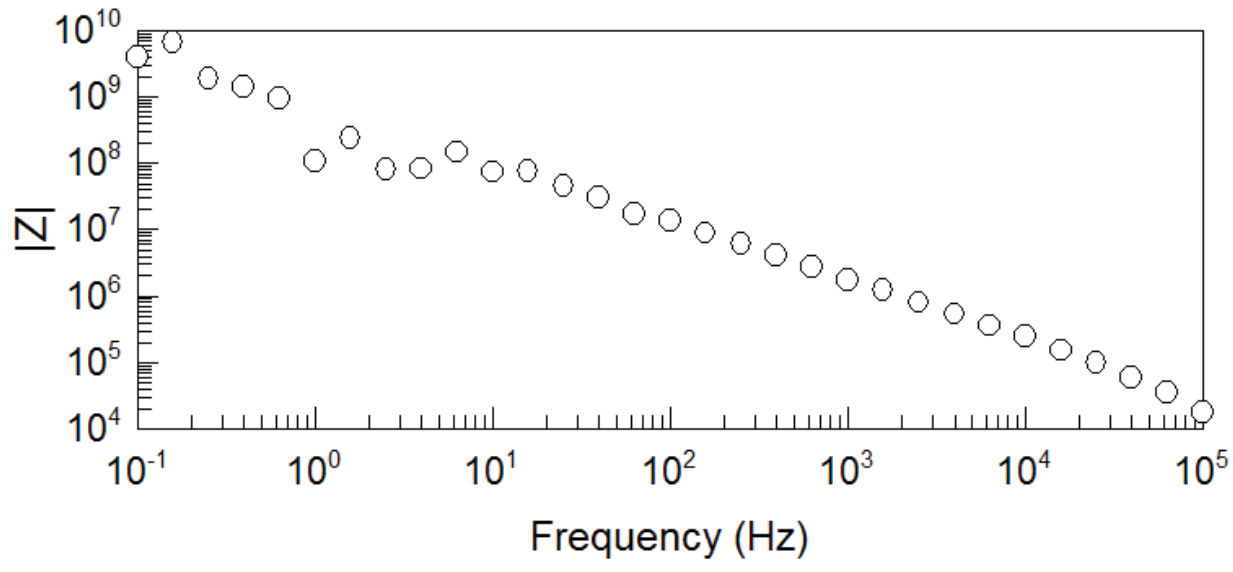


Figure A-24: EIS Bode plot from pipe segment 95, coal tar epoxy.

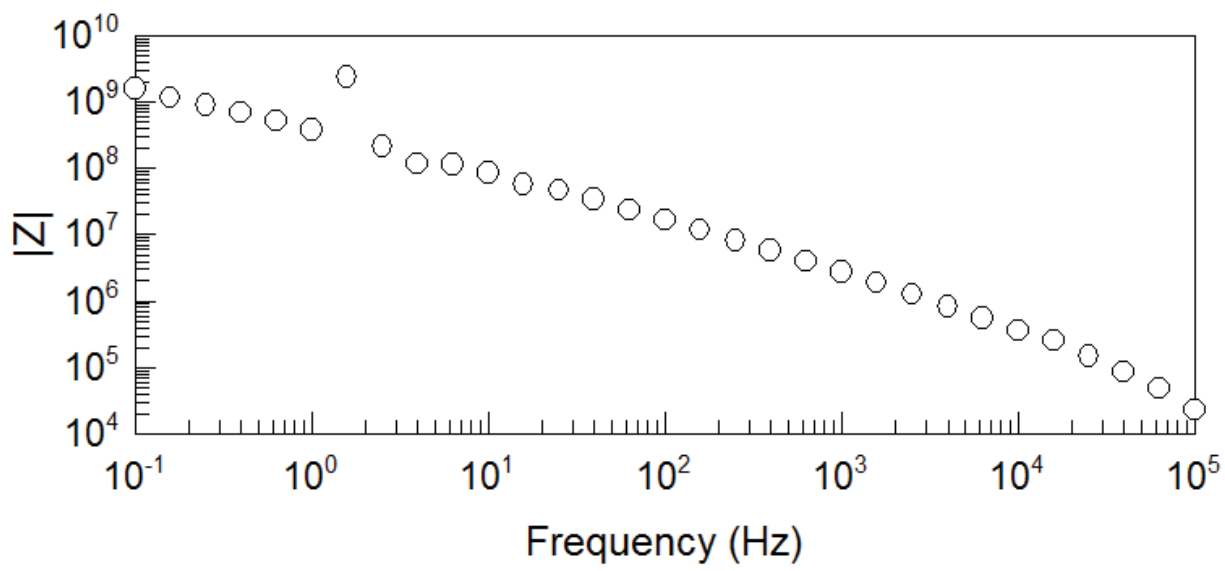


Figure A-25: EIS Bode plot from pipe segment 99, coal tar epoxy.

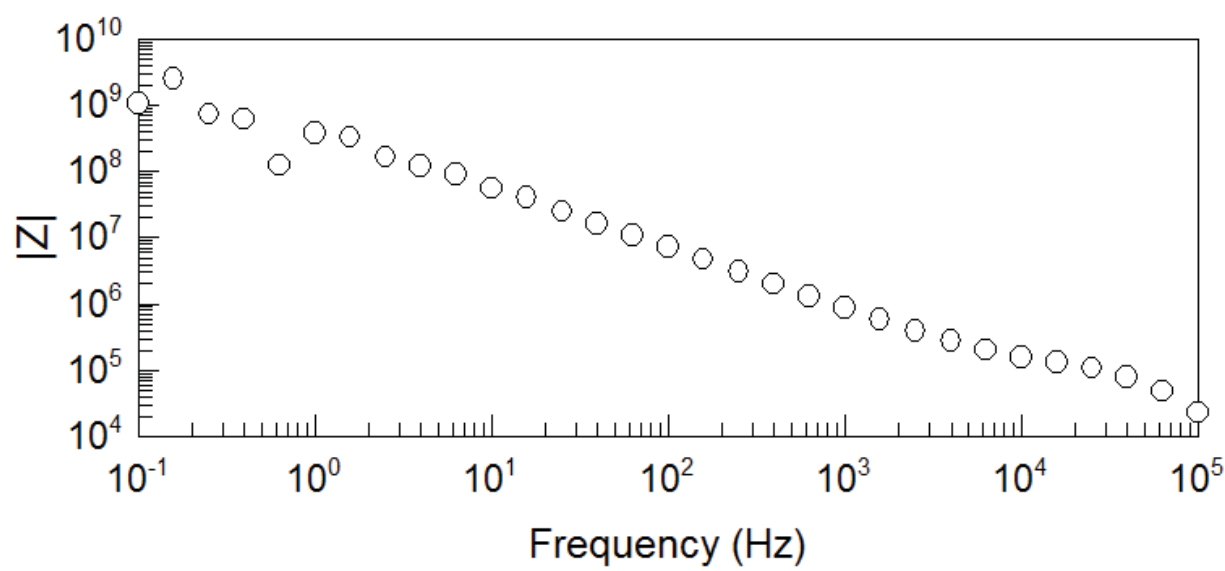


Figure A-26: EIS Bode plot from pipe segment 104, coal tar epoxy.

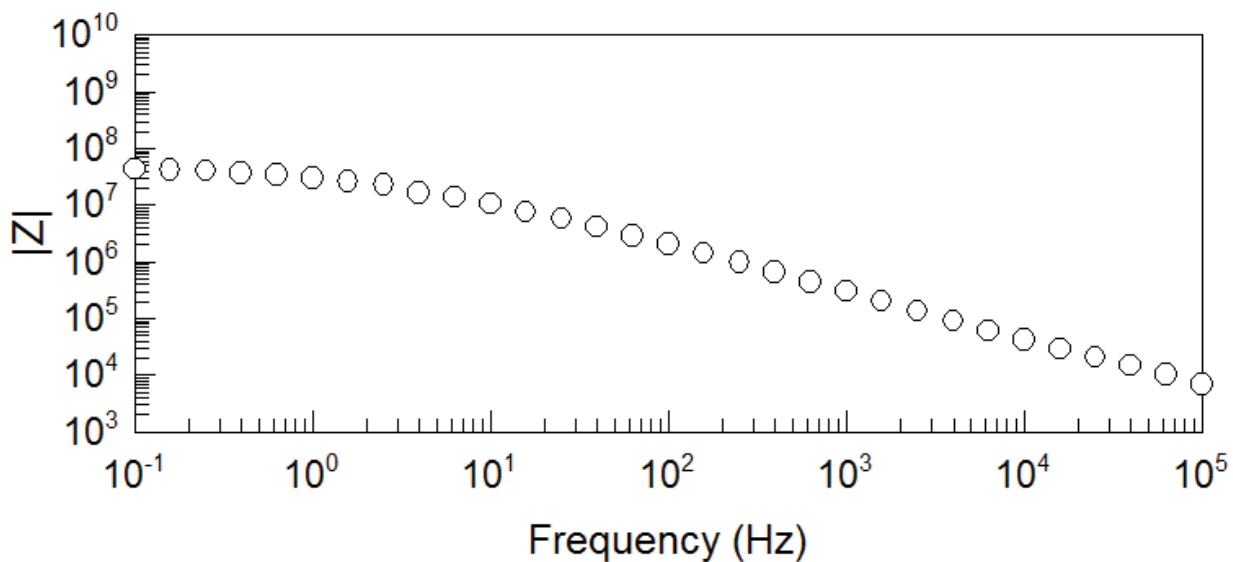


Figure A-27: EIS Bode plot from pipe segment 108, coal tar epoxy.

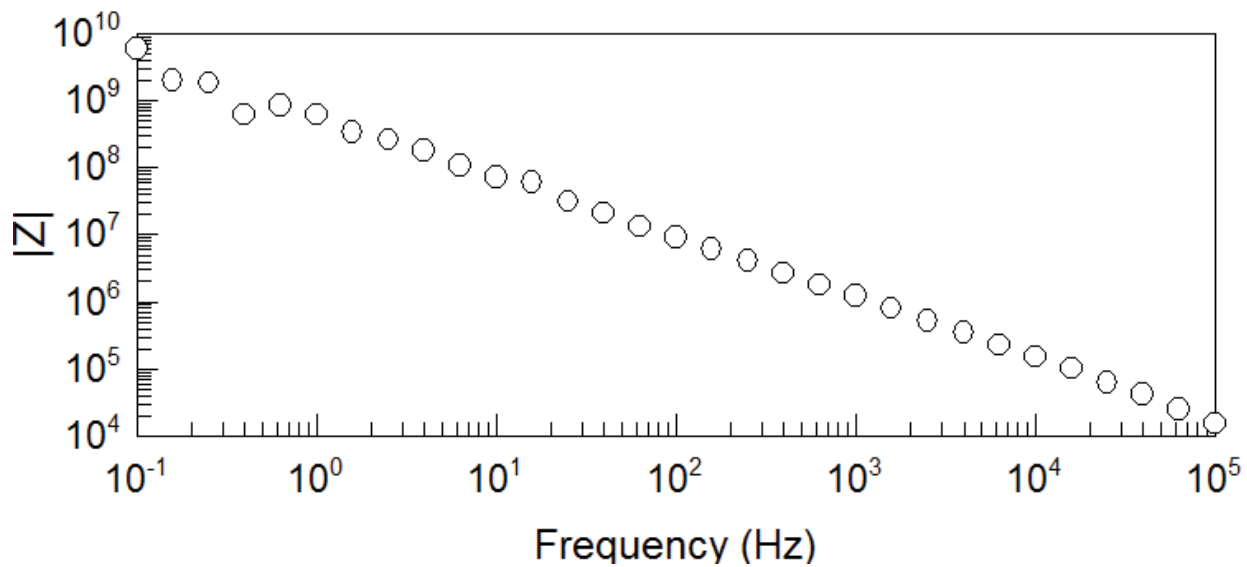


Figure A-28: EIS Bode plot from pipe segment 112, coal tar epoxy.

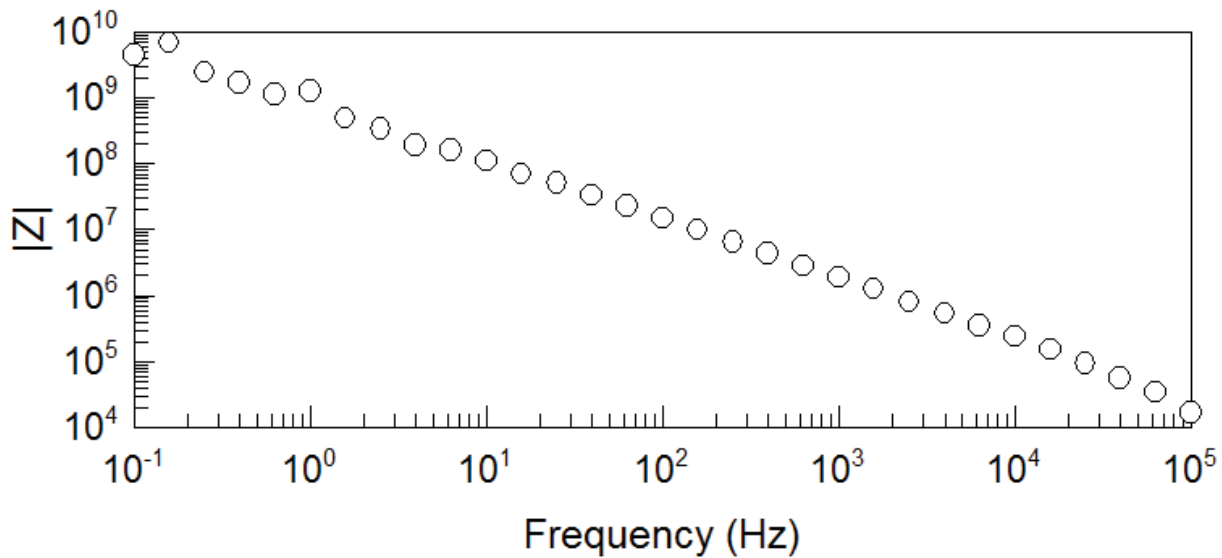


Figure A-29: EIS Bode plot from pipe segment 116, coal tar epoxy.

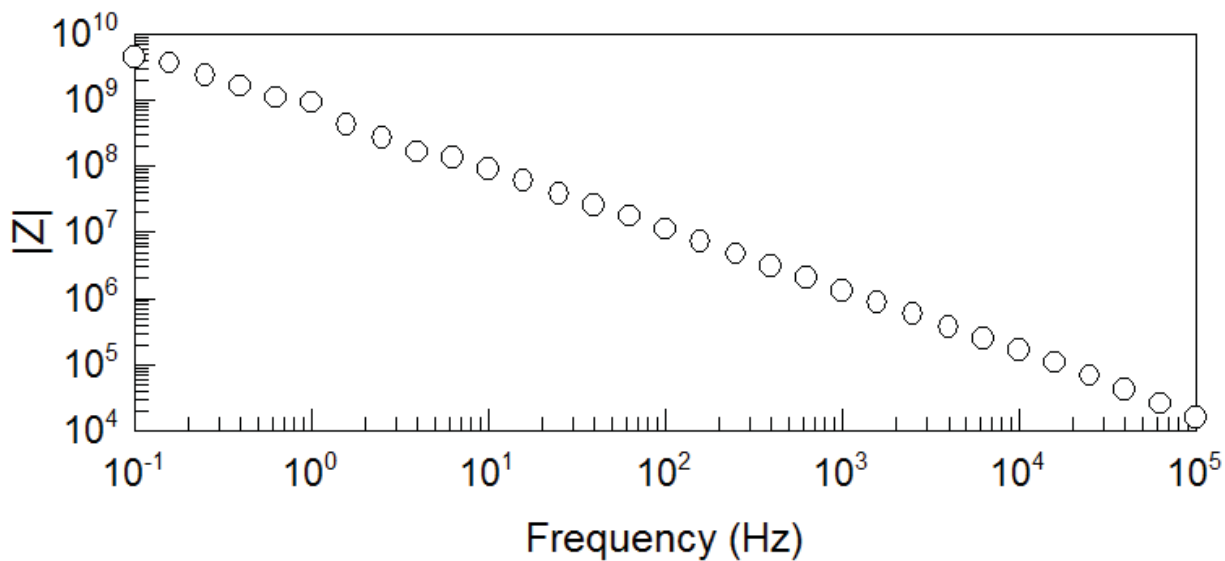


Figure A-30: EIS Bode plot from pipe segment 120, coal tar epoxy.

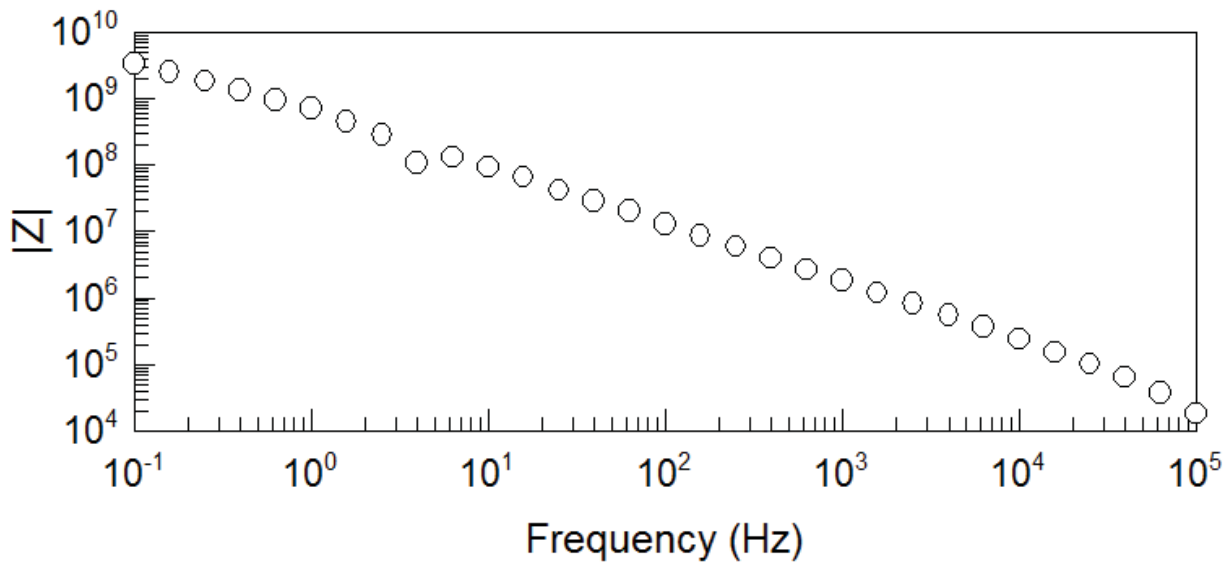


Figure A-31: EIS Bode plot from pipe segment 124, coal tar epoxy.

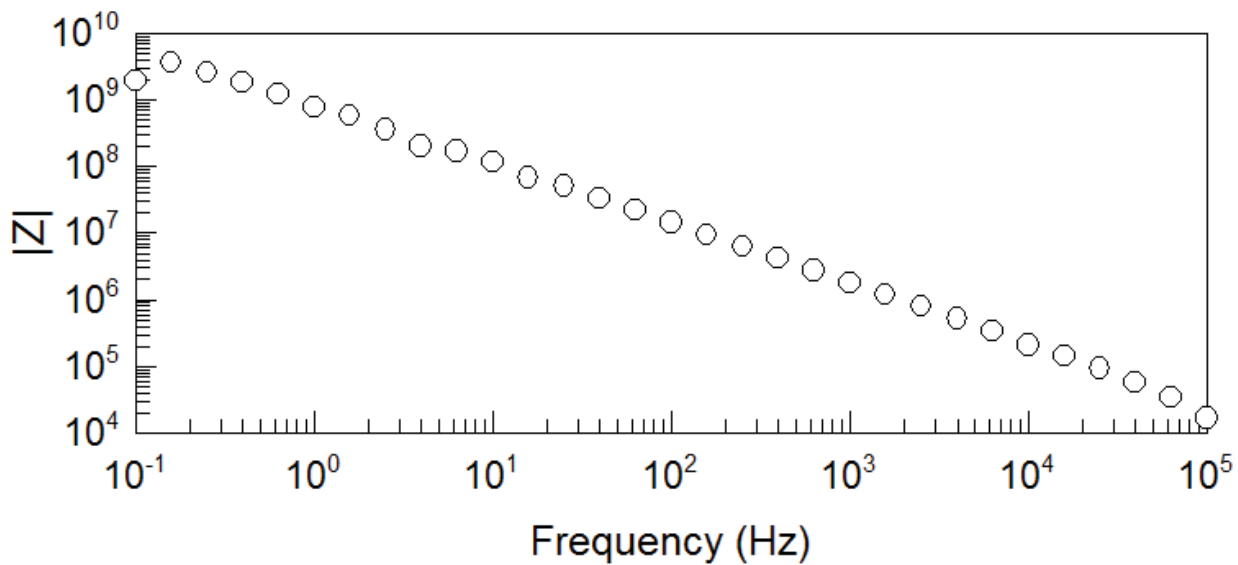


Figure A-32: EIS Bode plot from pipe segment 128, coal tar epoxy.

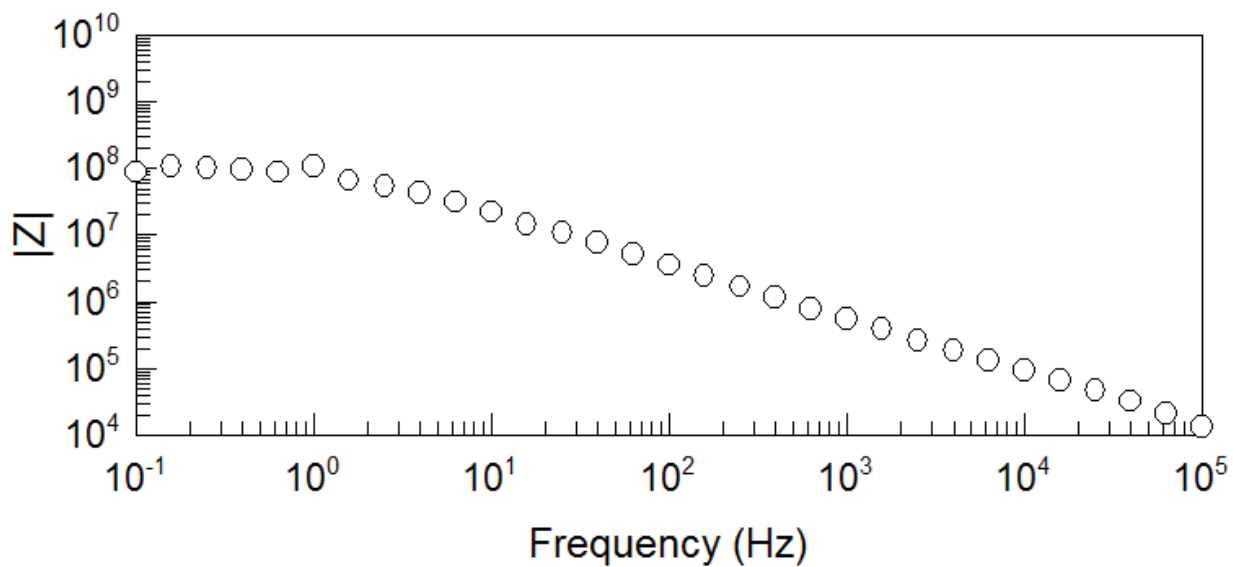


Figure A-33: EIS Bode plot from pipe segment 132, coal tar epoxy.

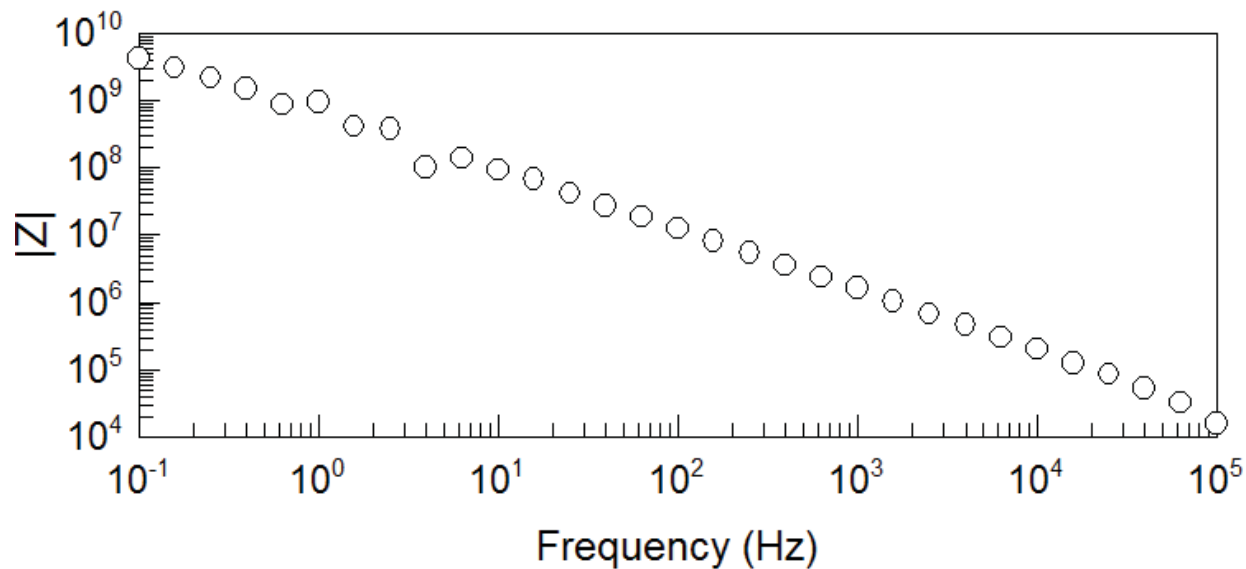


Figure A-34: EIS Bode plot from pipe segment 136, coal tar epoxy.

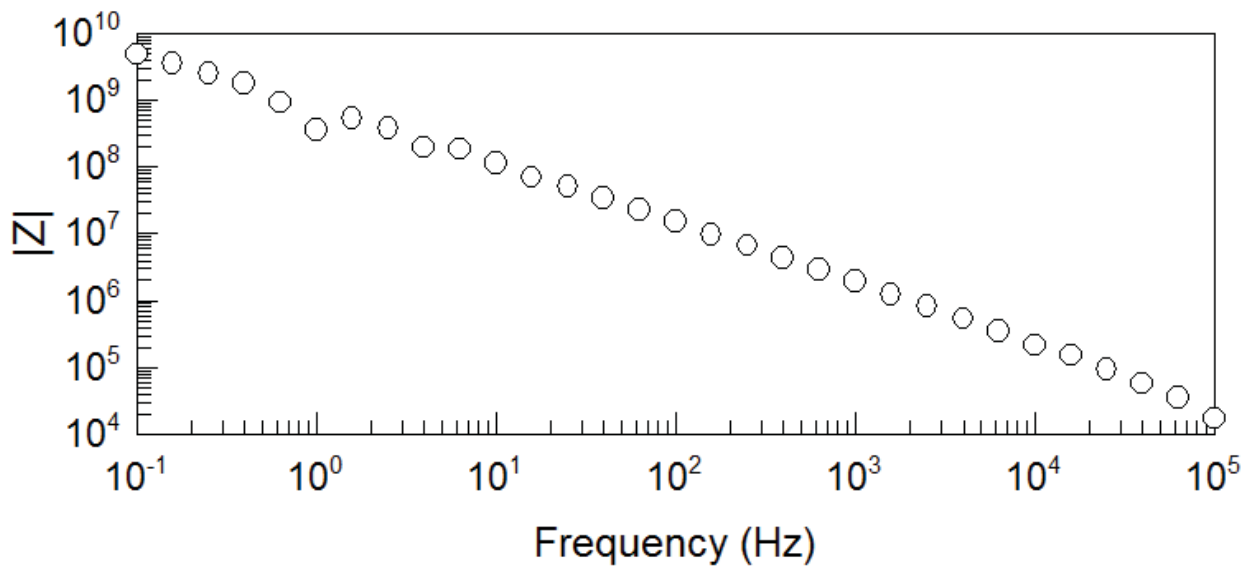


Figure A-35: EIS Bode plot from pipe segment 140, coal tar epoxy.

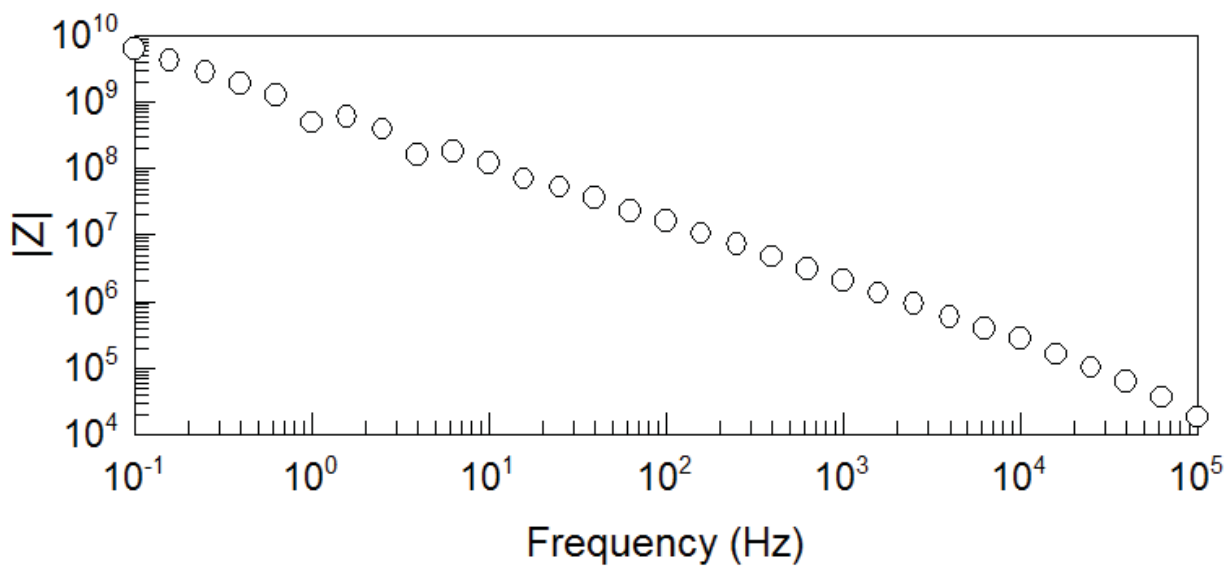


Figure A-36: EIS Bode plot from pipe segment 144, coal tar epoxy.

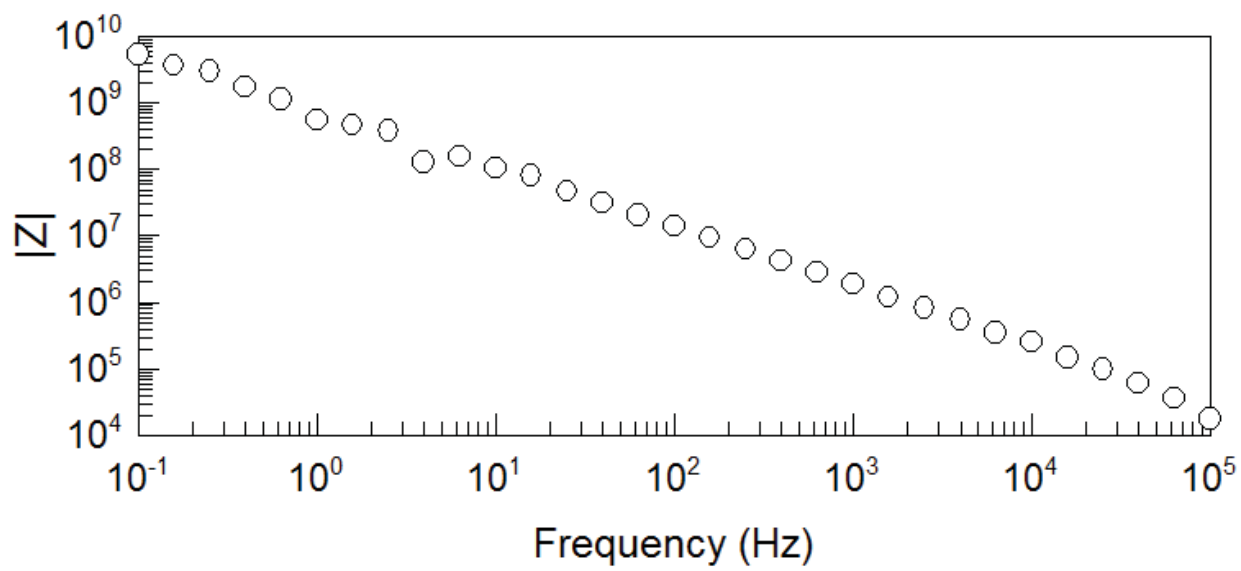


Figure A-37: EIS Bode plot from pipe segment 148, coal tar epoxy.

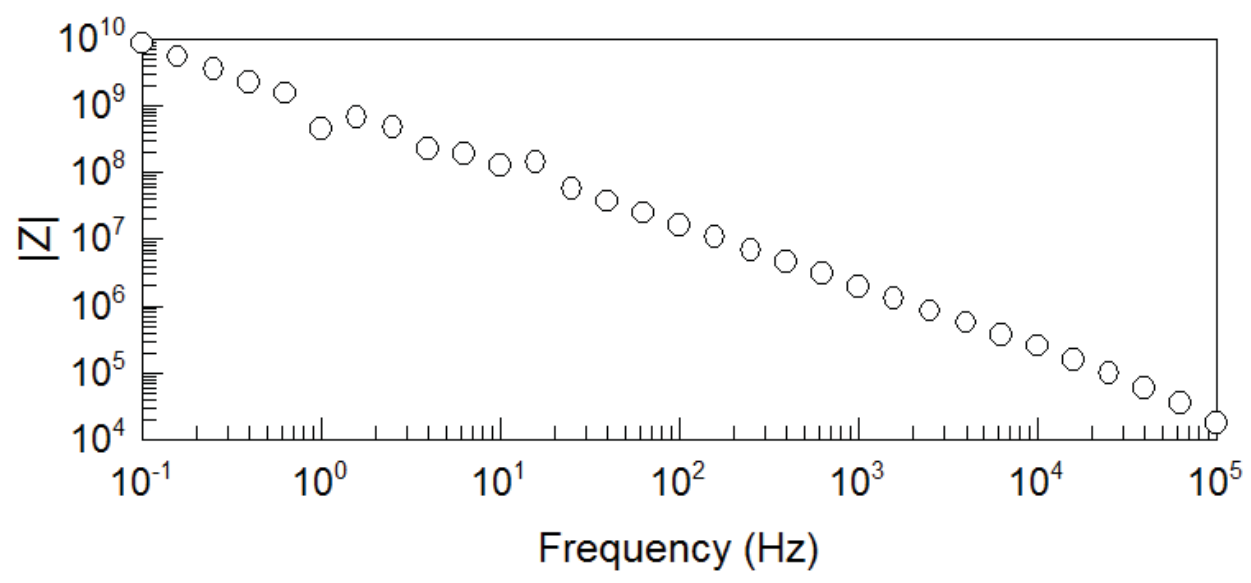


Figure A-38: EIS Bode plot from pipe segment 152, coal tar epoxy.

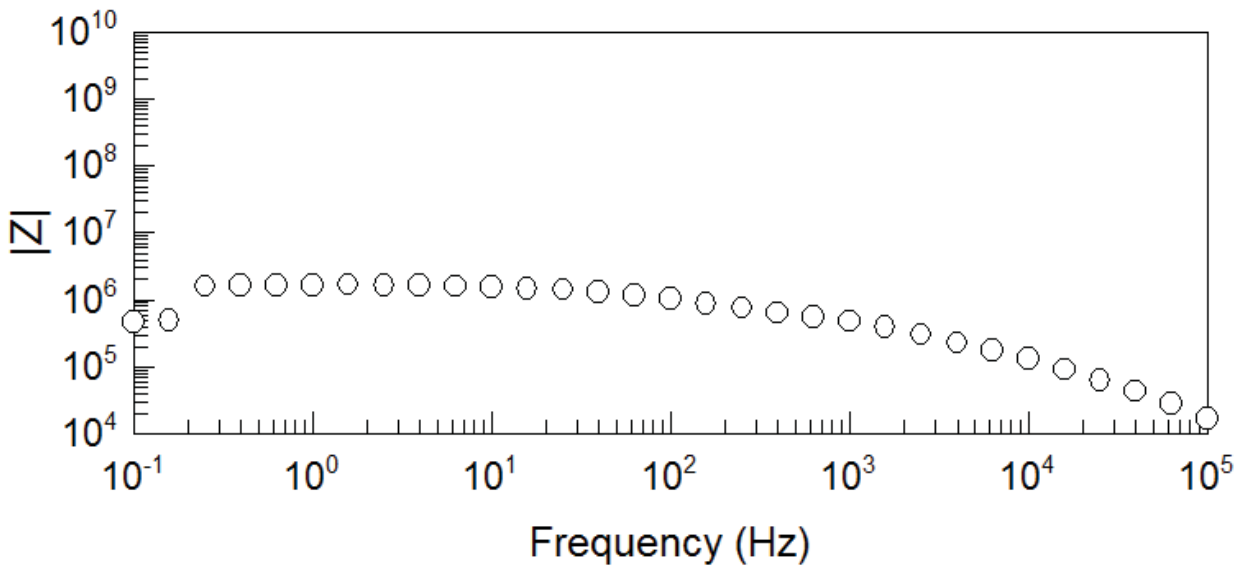


Figure A-39: EIS Bode plot from pipe segment 156, coal tar epoxy.

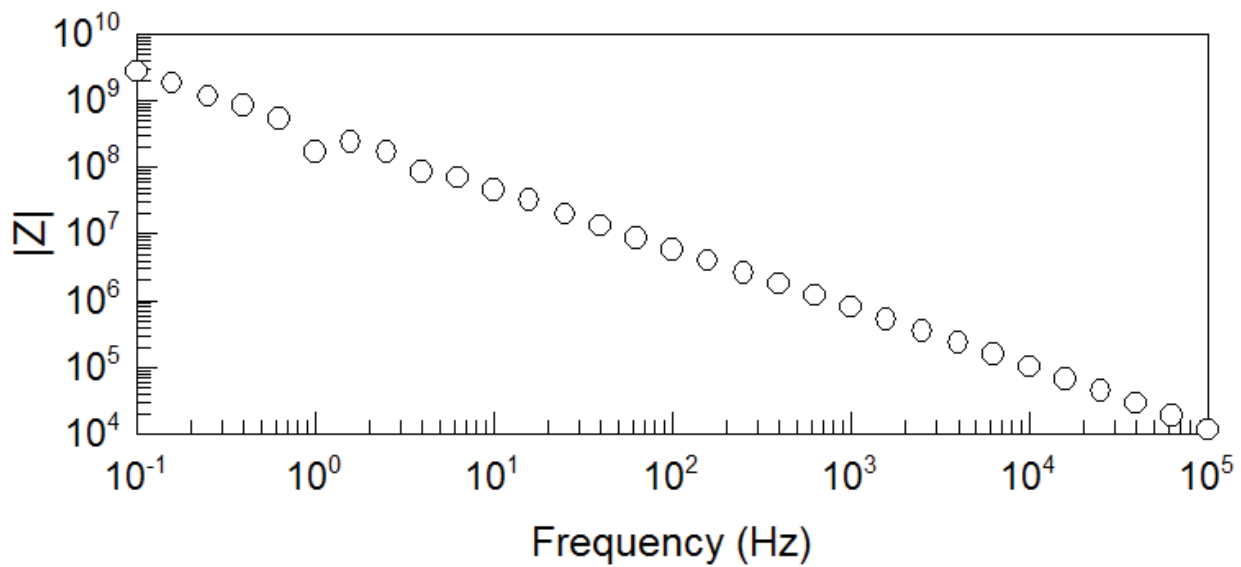


Figure A-40: EIS Bode plot from pipe segment 160, coal tar epoxy.

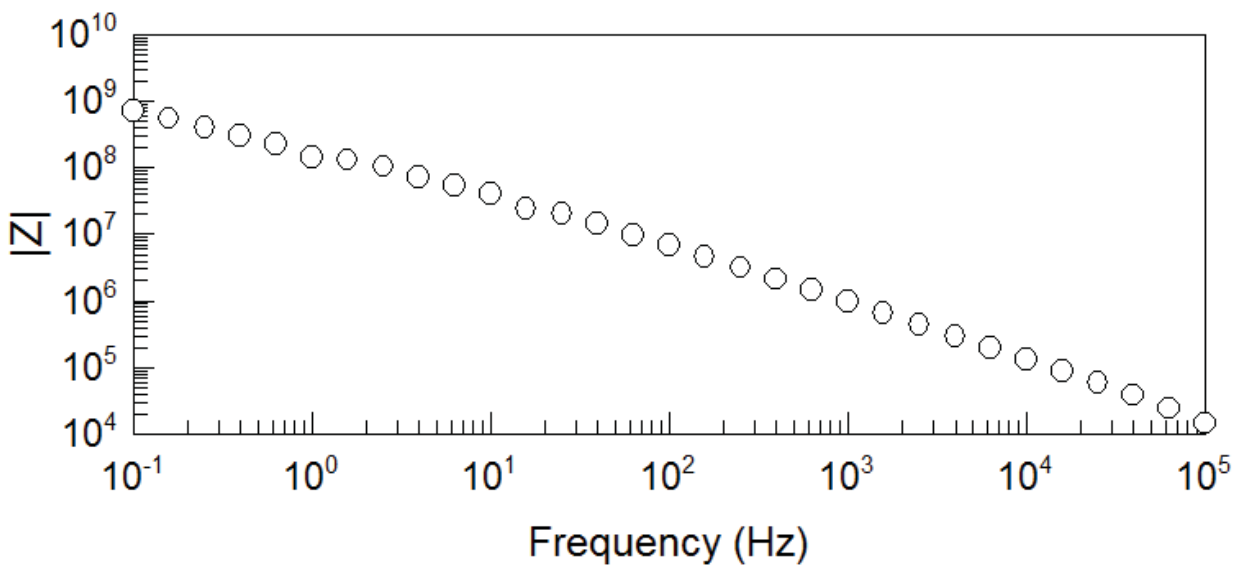


Figure A-41: EIS Bode plot from pipe segment 162, coal tar epoxy.

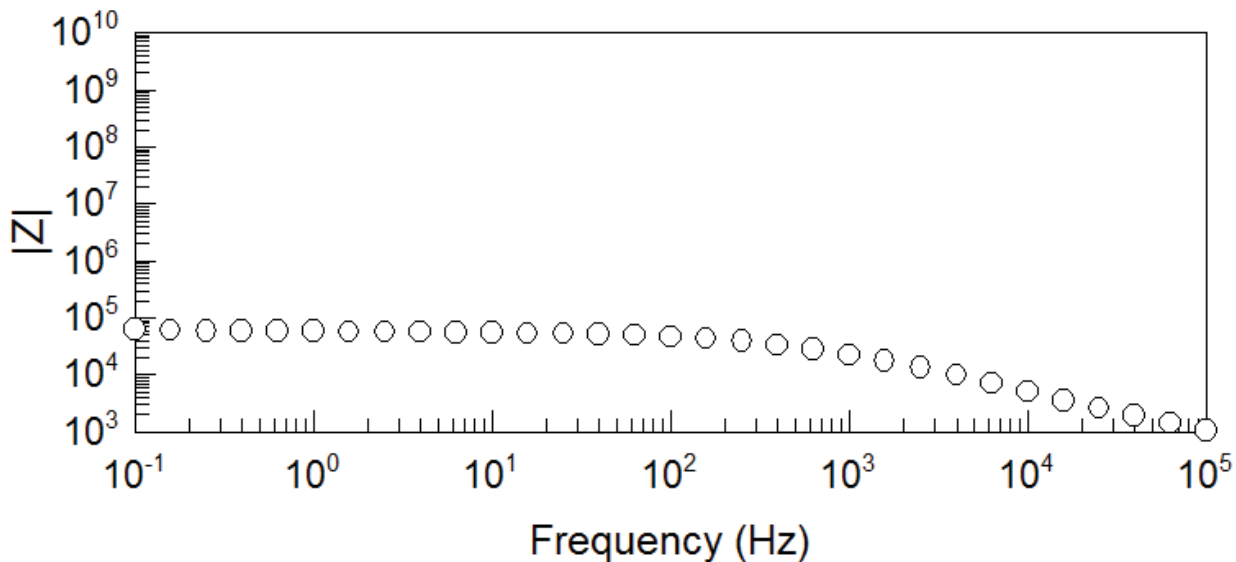


Figure A-42: EIS Bode plot from pipe segment 170, coal tar epoxy.

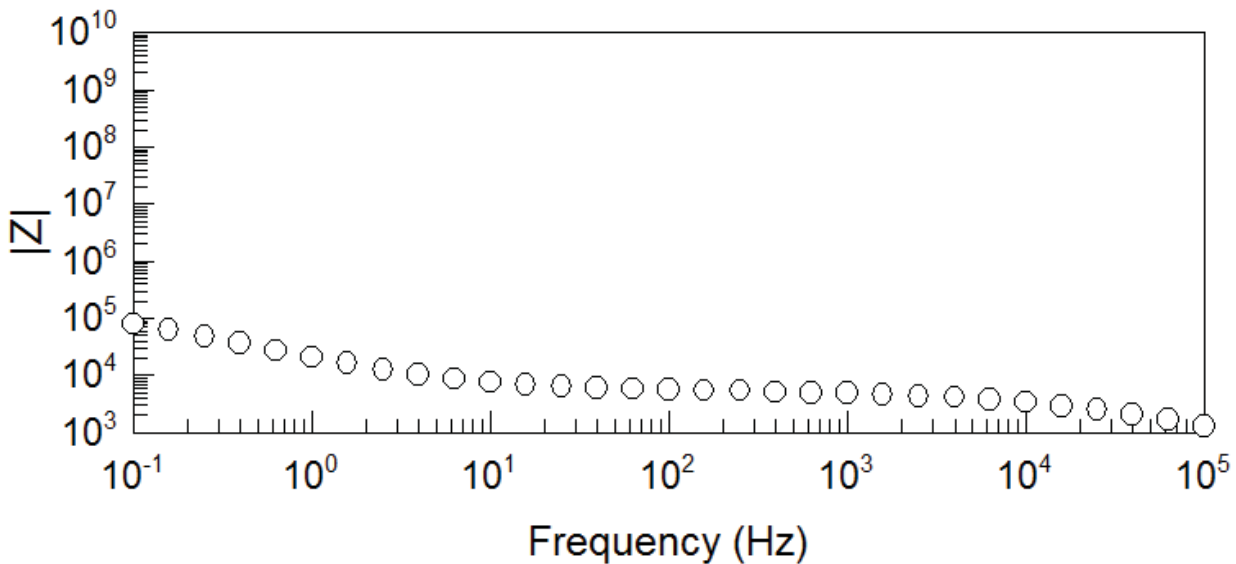


Figure A-43: EIS Bode plot from pipe segment 174, coal tar epoxy.

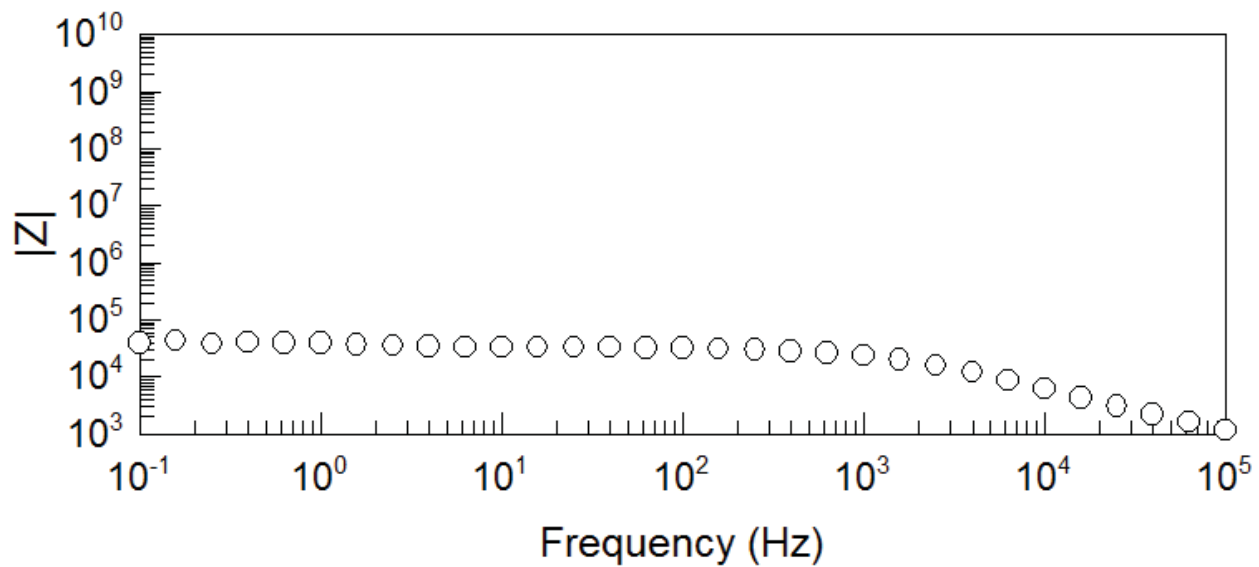


Figure A-44: EIS Bode plot from pipe segment 180, coal tar epoxy.

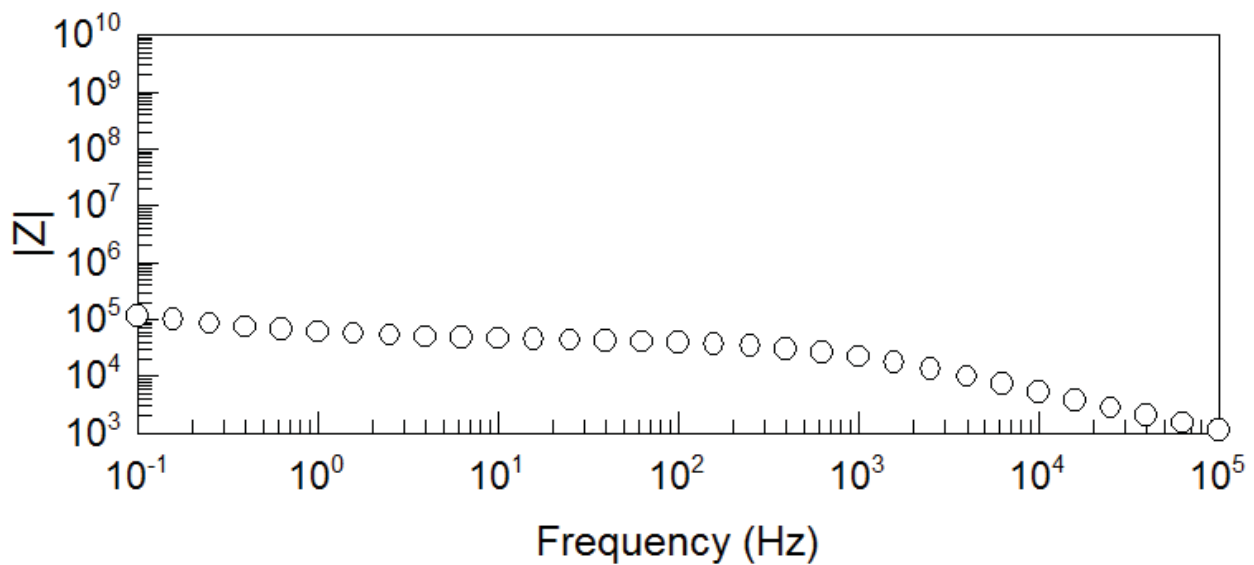


Figure A-45: EIS Bode plot from pipe segment 188, coal tar epoxy.

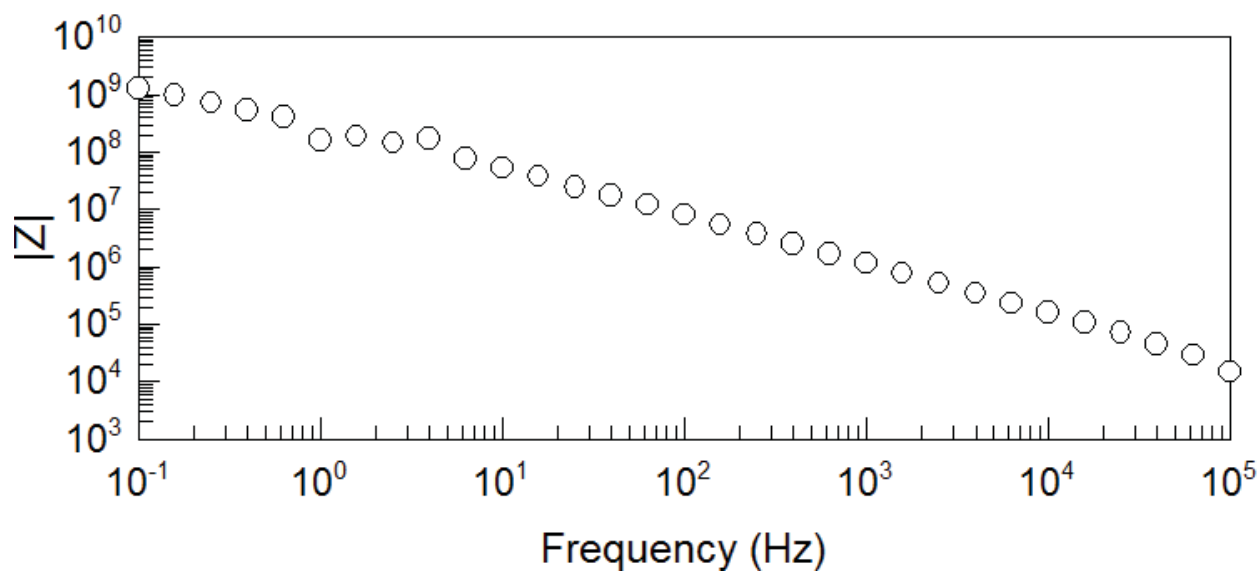


Figure A-46: EIS Bode plot from pipe segment 86, Devgrip 238.

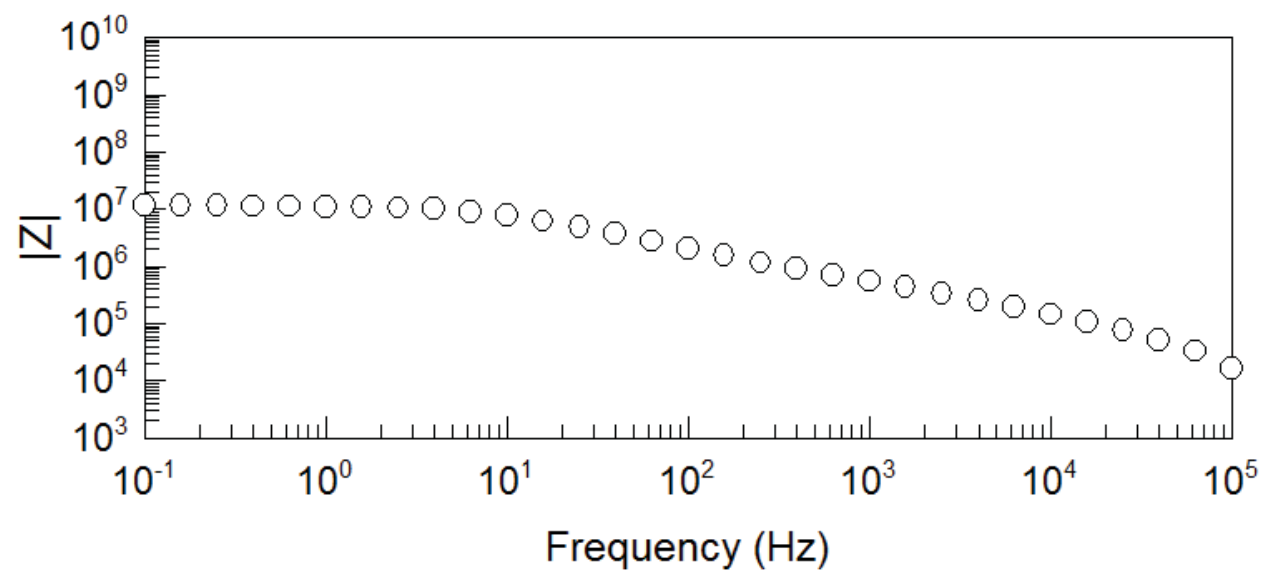


Figure A-47: EIS Bode plot from pipe segment 87, Devgrip 238.

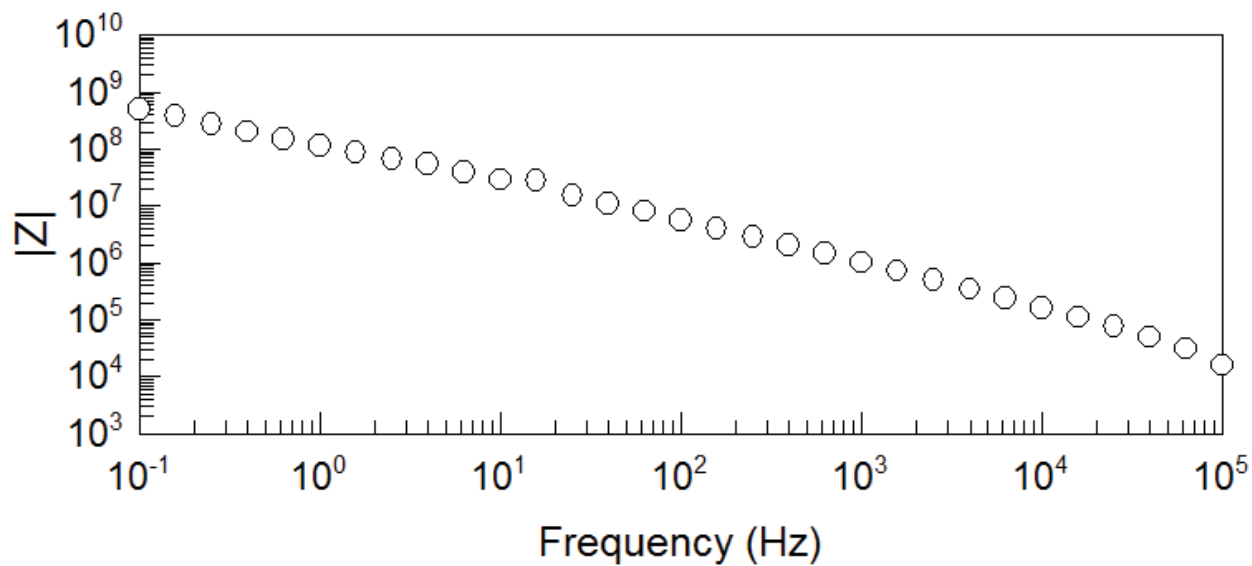


Figure A-48: EIS Bode plot from pipe segment 88, Devgrip 238.

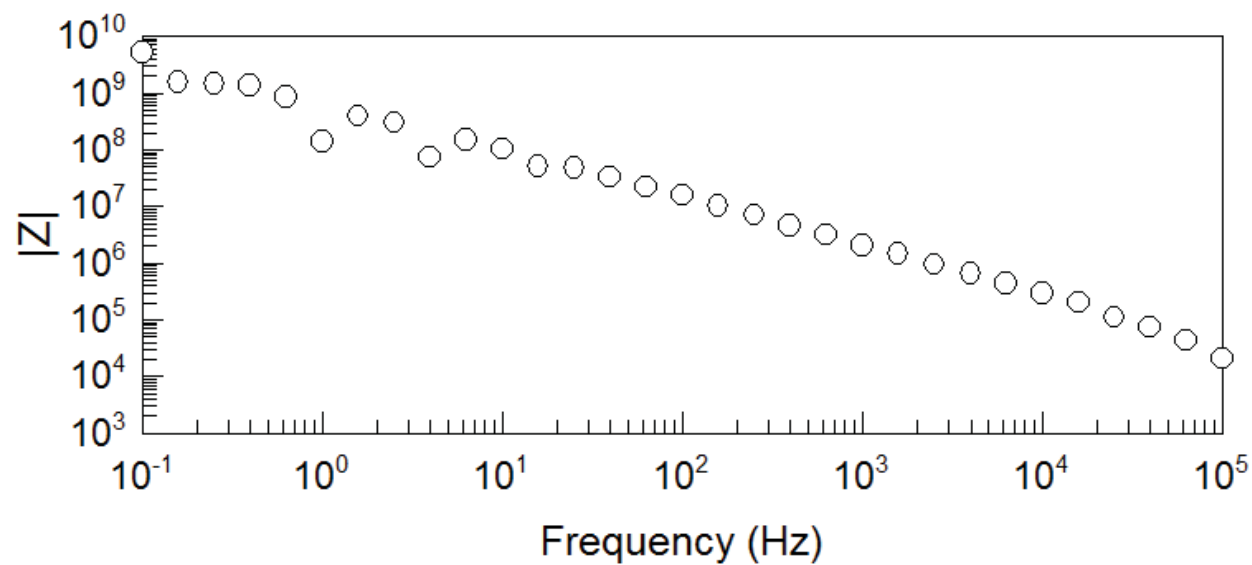


Figure A-49: EIS Bode plot from pipe segment 89, Devgrip 238.

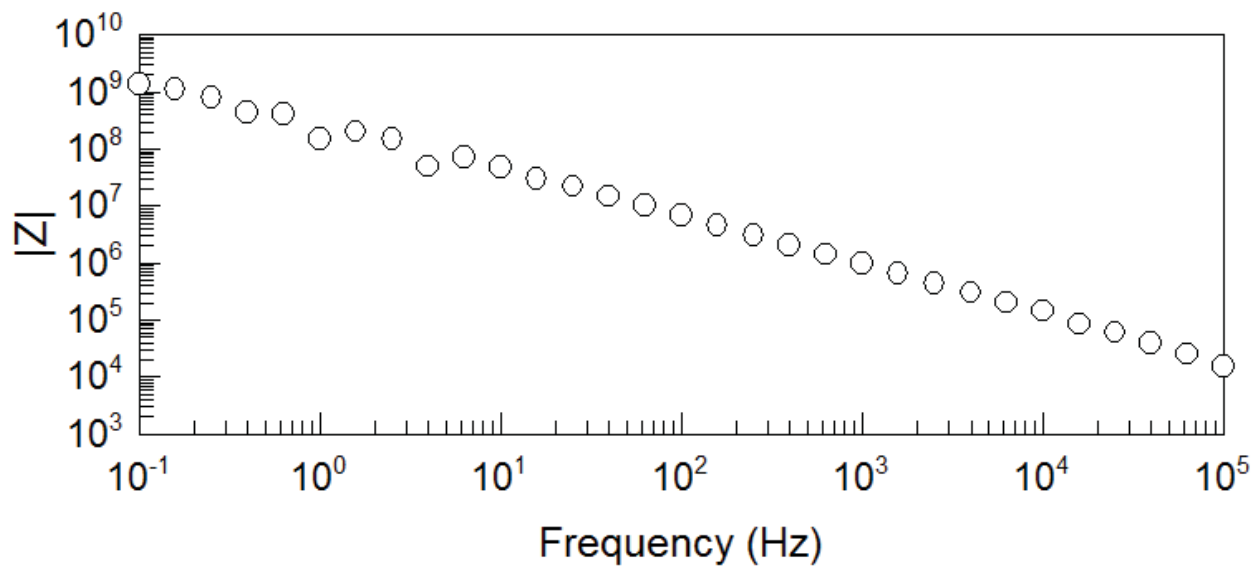


Figure A-50: EIS Bode plot from pipe segment 90, Devgrip 238.

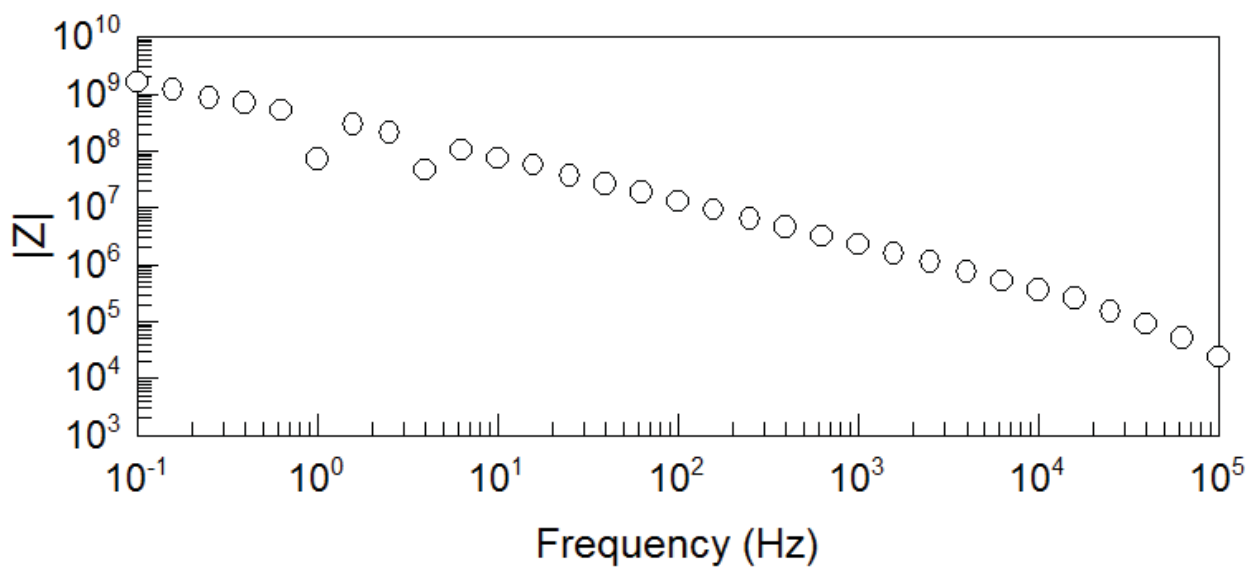


Figure A-51: EIS Bode plot from pipe segment 91, Devgrip 238.

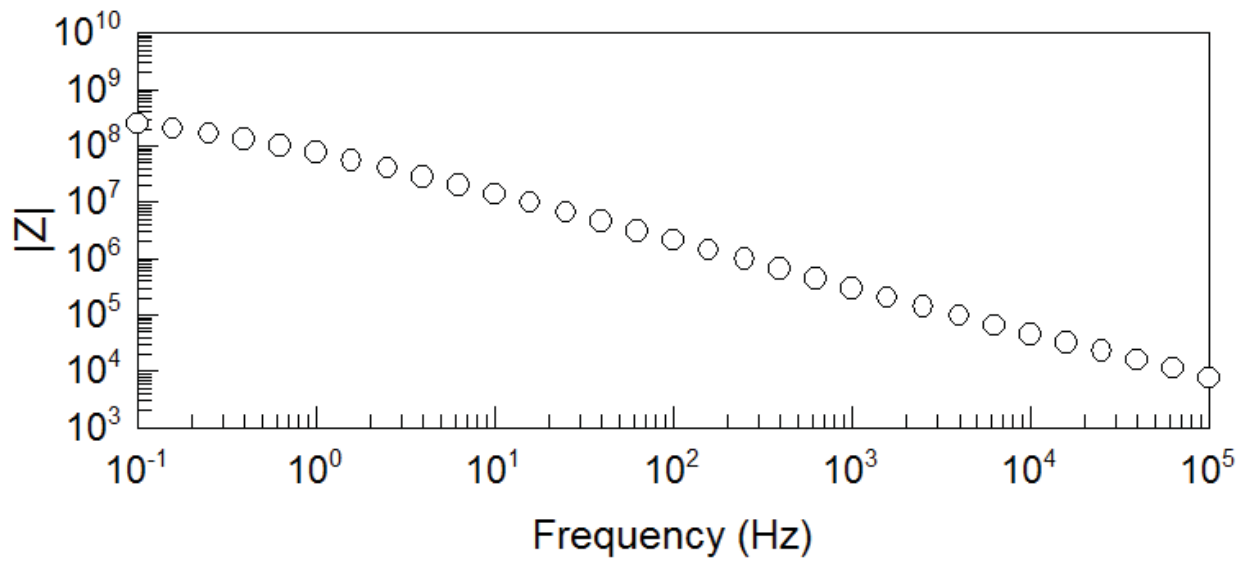


Figure A-52: EIS Bode plot from pipe segment 166, Devgrip 238.

Appendix B – Dry Film Thickness Raw Data

Table B-1. Coating dry film thickness (DFT) values measured within the Salt River Siphon.³

Segment	Right-hand wall DFT (mils)					Invert DFT (mils)					Left-hand wall DFT (mils)				
4	31.8	40	40.9	42.4	39.4	31.1	30.6	32.2	30.2	30.8	47	46.9	46	43	46.3
8	22.9	23.8	24	23.5	24.5	27.5	23.6	41.9	38.3	36.5	21.2	18.5	22.9	22.1	18.1
12	26.2	27	25.9	25	22.7	15.5	16.5	17.1	19.2	18.9	22.4	22.3	22.9	22.7	21.5
16	22.6	22.9	23.1	21.9	21.9	22.3	19	19.7	19	20.3	22.7	23	25.6	24.7	25.5
20	21.7	22.5	21.1	21.8	21.4	12.2	11.4	13.1	13.9	15.6	22.7	20.1	23	23.2	23.1
24	38.6	33.2	37.6	37.3	35.9	25.2	25.3	25.2	26.6	23.2	35.8	37	36.5	35.7	35.3
28	32.4	28.9	34.5	36.3	35.4	25.5	28.7	30.8	28.8	27.5	30.9	32.9	34.1	31.7	33.8
32	21.4	22.9	25.3	24.4	23.7	23.2	20	18.6	23.4	19.8	25.8	24.9	23.6	23.3	27
36	22.6	24.9	22	22.4	23.5	10.9	14.5	12.5	17.3	14.5	21.1	20.8	19.6	20.6	20.4
40	29.1	28.8	28.5	29	30.6	27.3	25.9	28.1	27.9	28.8	30.1	30.7	28.3	28.4	29.1
44	19.3	18.3	17.9	18.4	21.1	14.4	12	12.4	9.4	11.1	18.3	18.7	19.5	19.8	20
48	22.2	21.7	21.1	21.8	22	14	15.9	12.7	13.3	12.4	23.1	21.6	20.9	24.8	21.8
52	19.3	20.3	21.3	19.1	21.1	9	7.2	9.5	5.4	10.6	18.5	21.7	20.1	19.6	19
56	25.7	28.1	27.1	25.4	28.4	5.9	6.8	7.5	5.5	9.4	27.1	27.9	28	27	28.6
60	23.5	22.3	23.5	23.2	24.1	7.4	6.2	8.3	8.5	9.8	23.9	23.1	22.6	25.2	23.5
64	40	40.7	40.4	37.7	37.4	11.4	11.8	10.6	9.4	10.8	33.3	32.8	32	33.9	33.7
68	32.8	30.8	30.9	32.1	32.3	11	14.1	12.8	14	13.3	32	32.4	30.9	32.7	31.3
72	21.8	29	27.9	27.6	28.8	8.2	9	12	9.3	10.4	29.1	29.2	29.5	28.7	29.1
76	27.7	28.2	28.4	30	30.1	7.9	13.3	15.3	13.8	5.2	20.2	20.9	21.6	20.6	22.4
80	25.8	27.9	27	27.4	27.7	16.2	13.7	12.1	18.5	18.6	26.2	28.9	25.1	26.8	25.7
84	24	23.2	23	22.6	24.6	11.8	5.5	7.6	5.4	5.2	25.3	24.2	25.8	24.9	25.8
88	18.3	18.7	18.4	19.9	17.1	27.2	25.2	22.6	26	26.2	24.9	24.6	25.4	25.2	24.4

³The specified minimum DFT was 24 mils. Shaded green cells represent DFT that meets or exceeds specified DFT, yellow cells are 75% or less of specified DFT, and red cells are 50% or less of the specified DFT.

92	30.3	16.3	14.9	25.7	20.8	20.2	20	9.9	22.3	27.5	17.3	25	31.1	24.3	26
95	31.4	32	30.8	32.8	34.1	29.3	29.9	30.8	31.5	31.1	28.2	30.8	29.1	28.8	30
99	61	64.2	61.1	62	55.5	79.1	65.1	69.9	61.8	73.3	62.3	50.8	44.8	57.1	72.8
104	43	35	34.8	34.6	33.2	35.6	33.9	33.7	35	31.7	33.9	33.2	31.6	29.7	35.9
108	22.3	22.9	24	25	N/A	24.9	18	24.4	23.1	22.3	22	18.3	17.8	18.7	19.5
112	24.1	23.3	24.1	24.5	25.2	27.2	24.6	25.7	24	24.7	26.4	19.6	19.1	21.7	20
116	24.4	24.5	24.2	24.2	25.5	22.7	18.3	16.9	20.1	17.5	24	21.3	22.9	23.3	24.2
120	21	29.2	23.5	21.5	21.4	23.8	21.1	20.5	22.3	19.8	18.9	17.7	19.8	21.8	19.9
124	33.6	32.7	32	31.5	29.2	22.9	23.9	25.7	27.8	21.9	31.8	29.8	28.9	30.8	29.8
128	26.5	26.6	27.6	26.4	25.8	26.5	28.4	26.5	29.7	24.6	27.3	29.5	26.9	28.4	27.1
132	35.1	32.3	29	29.3	28.3	17.7	13.6	13.3	16.5	13.9	22.5	21	21.7	22.5	24
136	33.9	32.5	29.2	30	31.9	31.1	30.9	29	29.2	30	30	29.6	28.4	30.6	30.3
140	27.1	27	27.1	26.6	29.4	15.1	17.1	17.5	18.3	18.2	26.5	26.2	28.3	25.3	25.2
144	27.9	24.8	28.3	26.4	24.9	25.1	26	25.9	24.8	26	26.5	26.9	26.6	25.2	26.2
148	27.8	26.8	26	27.2	27.6	26	25.3	25.7	26.3	26.4	25.8	25.8	26.3	26	25.9
152	27.9	27.9	28.1	28.7	28.9	16.3	17.5	18.4	19.7	18.8	27.9	26.9	28.5	26.3	27.3
156	33.4	38.8	35.7	35.5	34.9	35.4	35.6	35.1	39.9	34	31.7	31.2	29.7	32.1	31.7
160	14.6	19.2	14.3	16.7	14.7	23.4	21.8	22.4	23.1	22.7	20.1	15.2	18.3	15.2	16.4
163	29.7	28.4	25.8	24.2	27.9	22.2	22.4	22.6	21.6	22.6	26.8	27.2	29.8	27.3	25.4
170	31.4	28.1	26.5	28.6	27.7	26.9	26	25.6	26.4	28.8	12.7	16.8	14.2	15.9	16.4
174	39.5	41.3	41.5	33.8	36.8	33.1	32.4	33.9	28.6	36.6	12.4	11.3	12.9	11.1	15.9
180	28.1	26.1	25.5	25.6	28.9	26.4	24.2	26.9	25	26.7	13.6	14.5	15.2	15.6	14.2
188	29.4	32.1	28.1	28.7	26.9	32.3	31.5	32.1	34.9	30.4	17.5	16.7	14.1	14.2	20.2
191	20.2	17.6	18.5	16.7	18.4										
196	25.9	24.2	24.4	24.4	23.8	22.3	24.8	22.4	19.3	21.3	N/A				

Appendix C – Ultrasonic Thickness Raw Data

Table C-1. Steel pipe ultrasonic thickness (UT) values measured within the Salt River Siphon.⁴

Pipe Segment	Right-hand wall pipe thickness (inches)					Invert pipe thickness (inches)					Left-hand wall pipe thickness (inches)					Specified (inches) ⁵
4	0.654	0.654	0.654	0.652	0.128	0.652	0.652	0.652	0.654	0.654	0.654	0.654	0.654	0.654	0.654	0.632
8	0.646	0.646	0.646	0.646	0.646	0.65	0.648	0.648	0.646	0.166	0.648	0.646	0.646	0.646	0.642	0.632
12	0.652	0.652	0.652	0.65	0.652	0.648	0.648	0.65	0.65	0.648	0.65	0.65	0.65	0.65	0.65	0.632
16	0.658	0.654	0.654	0.652	0.652	0.648	0.648	0.648	0.648	0.648	0.646	0.646	0.646	0.646	0.648	0.632
20	0.644	0.644	0.644	0.642	0.642	0.644	0.64	0.64	0.642	0.64	0.642	0.642	0.644	0.64	0.644	0.632
24	0.644	0.642	0.644	0.642	0.594	0.644	0.646	0.644	0.642	0.644	0.644	0.642	0.644	0.642	0.644	0.632
28	0.66	0.66	0.66	0.66	0.658	0.66	0.658	0.66	0.658	0.66	0.656	0.654	0.656	0.656	0.656	0.632
32	0.65	0.652	0.648	0.65	0.65	0.652	0.65	0.65	0.65	0.65	0.648	0.648	0.648	0.648	0.648	0.632
36	0.708	0.708	0.708	0.708	0.708	0.708	0.708	0.708	0.71	0.71	0.712	0.712	0.712	0.712	0.712	0.696
40	0.712	0.712	0.712	0.712	0.712	0.718	0.718	0.718	0.718	0.718	0.716	0.716	0.716	0.718	0.718	0.696
44	0.702	0.71	0.712	0.71	0.706	0.716	0.718	0.716	0.716	0.716	0.712	0.712	0.714	0.714	0.714	0.696
48	0.648	0.648	0.648	0.648	0.648	0.646	0.646	0.646	0.644	0.646	0.644	0.648	0.646	0.646	0.646	0.632
52	0.64	0.64	0.64	0.64	0.64	0.644	0.642	0.642	0.642	0.642	0.644	0.646	0.644	0.646	0.644	0.632
56	0.65	0.65	0.65	0.65	0.652	0.65	0.654	0.65	0.65	0.65	0.648	0.65	0.65	0.65	0.648	0.632
60	0.652	0.652	0.652	0.652	0.654	0.65	0.652	0.652	0.652	0.652	0.652	0.652	0.652	0.652	0.652	0.632
64	0.72	0.72	0.72	0.72	0.72	0.718	0.718	0.718	0.718	0.718	0.716	0.716	0.714	0.716	0.716	0.696
68	0.648	0.648	0.648	0.6	0.648	0.646	0.648	0.646	0.646	0.644	0.646	0.646	0.646	0.648	0.646	0.632
72	0.648	0.648	0.646	0.648	0.648	0.646	0.648	0.648	0.646	0.646	0.648	0.648	0.646	0.648	0.648	0.632
76	0.648	0.646	0.648	0.648	0.65	0.646	0.646	0.644	0.644	0.644	0.648	0.648	0.648	0.648	0.648	0.632
80	0.708	0.708	0.708	0.708	0.708	0.712	0.71	0.712	0.712	0.712	0.712	0.71	0.712	0.712	0.712	0.696
84	0.648	0.646	0.648	0.648	0.648	0.65	0.652	0.648	0.65	0.648	0.646	0.65	0.65	0.65	0.648	0.632

⁴ Shaded green cells represent UT measurements that meet or exceed the specified UT value, yellow cells are measurements that are slightly lower than specified, and red cells are measurements much lower than specified.

⁵ Specified values obtained from pipe manufacturer’s erection drawings.

88	0.716	0.714	0.714	0.714	0.714	0.716	0.714	0.714	0.716	0.714	0.714	0.714	0.714	0.714	0.716	0.693
92	0.708	0.708	0.704	0.704	0.708	0.706	0.704	0.708	0.708	0.708	0.714	0.712	0.712	0.714	0.712	0.693
95	0.712	0.714	0.76	0.716	0.712	0.716	0.716	0.714	0.716	0.714	0.716	0.716	0.716	0.716	0.714	0.693
99	0.928	0.928	0.928	0.928	0.928	0.926	0.926	0.926	0.928	0.926	0.926	0.926	0.926	0.926	0.926	0.898
104	1.128	1.128	1.128	1.13	1.128	1.128	1.128	1.128	1.128	1.13	1.128	1.128	1.128	1.128	1.13	1.104
108	1.124	1.124	1.122	1.124	1.122	1.126	1.126	1.126	1.126	1.126	1.13	1.13	1.13	1.13	1.13	1.104
112	1.124	1.124	1.124	1.124	1.124	1.128	1.128	1.128	1.128	1.128	1.13	1.13	1.13	1.13	1.13	1.104
116	1.132	1.132	1.132	1.132	1.132	1.13	1.132	1.132	1.13	1.132	1.128	1.128	1.128	1.128	1.128	1.104
120	1.122	1.12	1.122	1.122	1.122	1.122	1.122	1.122	1.122	1.122	1.124	1.126	1.126	1.124	1.126	1.104
124	1.236	1.236	1.236	1.236	1.236	1.236	1.123	1.234	1.236	1.234	1.236	1.236	1.236	1.238	1.236	1.215
128	1.122	1.122	1.122	1.122	1.124	1.124	1.122	1.122	1.124	1.124	1.124	1.124	1.124	1.124	1.124	1.104
132	1.122	1.122	1.122	1.122	1.122	1.122	1.122	1.122	1.122	1.122	1.122	1.122	1.122	1.122	1.12	1.104
136	1.12	1.118	1.12	1.118	1.12	1.122	1.122	1.122	1.122	1.122	1.12	1.12	1.12	1.12	1.12	1.104
140	0.918	0.92	0.92	0.92	0.918	0.918	0.918	0.92	0.92	0.92	0.916	0.916	0.918	0.918	0.918	0.898
144	0.916	0.918	0.918	0.918	0.916	0.916	0.916	0.918	0.918	0.918	0.914	0.914	0.912	0.914	0.912	0.898
148	0.914	0.914	0.914	0.914	0.914	0.914	0.918	0.916	0.916	0.916	0.916	0.916	0.916	0.916	0.916	0.898
152	0.81	0.808	0.81	0.81	0.81	0.814	0.81	0.81	0.81	0.812	0.812	0.814	0.812	0.814	0.814	0.792
156	0.814	0.814	0.814	0.814	0.814	0.824	0.824	0.824	0.822	0.824	0.82	0.82	0.818	0.818	0.818	0.792
160	0.814	0.812	0.814	0.814	0.814	0.816	0.816	0.816	0.816	0.816	0.816	0.816	0.816	0.816	0.816	0.792
163	0.65	0.65	0.648	0.646	0.646	0.65	0.65	0.65	0.65	0.648	0.648	0.648	0.648	0.65	0.648	0.632
170	0.712	0.712	0.71	0.71	0.712	0.714	0.714	0.714	0.714	0.714	0.712	0.712	0.712	0.712	0.712	0.625
174	0.5	0.5	0.5	0.5	0.5	0.502	0.502	0.502	0.502	0.502	0.502	0.502	0.502	0.502	0.502	0.5
180	0.496	0.496	0.438	0.496	0.494	0.494	0.496	0.49	0.496	0.494	0.496	0.496	0.498	0.498	0.498	0.5
188	0.498	0.5	0.5	0.504	0.5	0.498	0.498	0.5	0.5	0.5	0.498	0.5	0.5	0.5	0.5	0.5
196	0.508	0.508	0.506	0.508	0.506	0.508	0.508	0.51	0.51	0.508	0.51	0.51	0.51	0.512	0.512	0.5

Appendix D – Inspection Photos

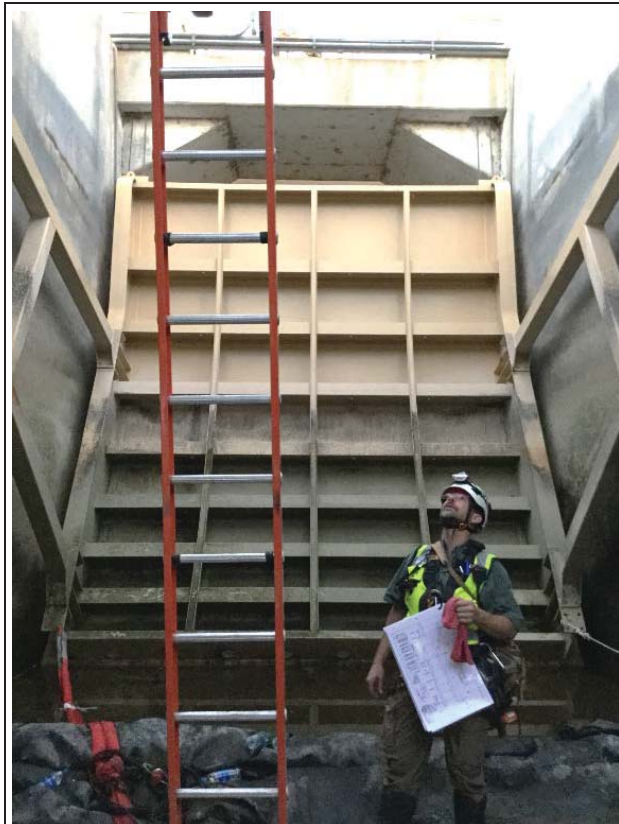


Figure D-1: Downstream side of the radial gate [REDACTED]



Figure D-2: View into the siphon inlet.

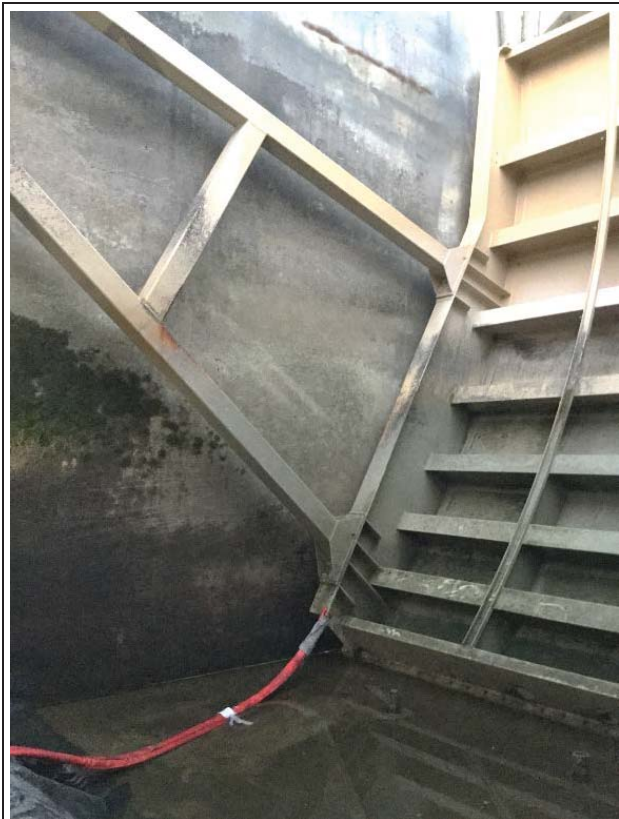


Figure D-3: Small amounts of corrosion visible on the radial gate arm near the inlet of the [redacted]



Figure D-4: Pipe segment 4. Image of pipe wall and joint; joint contains repair material.



Figure D-5: Pipe segment 4. EIS cups set above a circular area of Devgrip 238 repair.



Figure D-6: Near pipe segment 4. Image of pipe joints repaired with Devgrip 238. Repair material appears to be in good condition.



Figure D-7: Near pipe segment 4. Image shows repair material along the pipe joint in the pipe's crown.

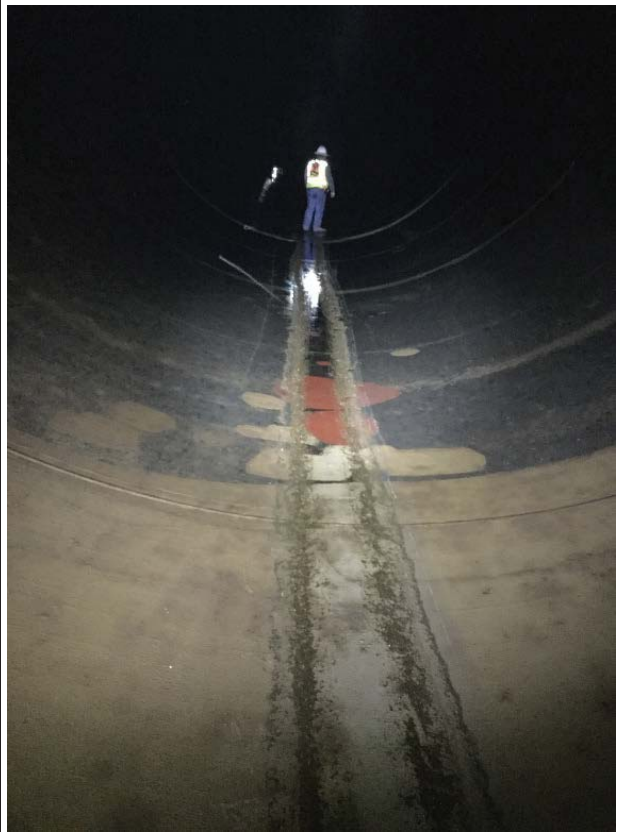


Figure D-8: Near pipe segment 4. Image of repairs in the invert. In some areas, the top coat (grey) of the repair material had been omitted when doing the repair.



Figure D-9: EIS test cell set-up at pipe segment 12.

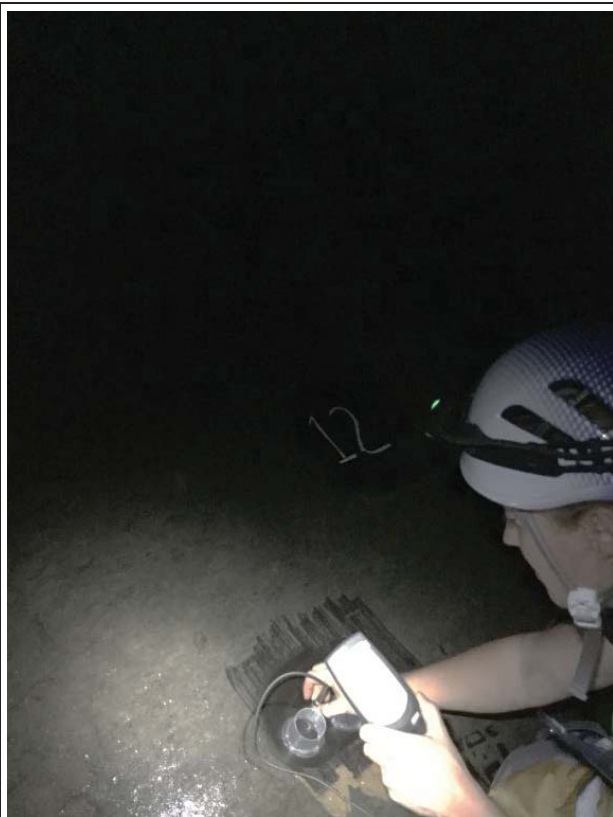


Figure D-10: Inspector measuring DFT within the EIS test location at pipe segment 12.



Figure D-11: Pipe segment 12. Image of the invert and pipe wall. Joint and invert repairs are visible.

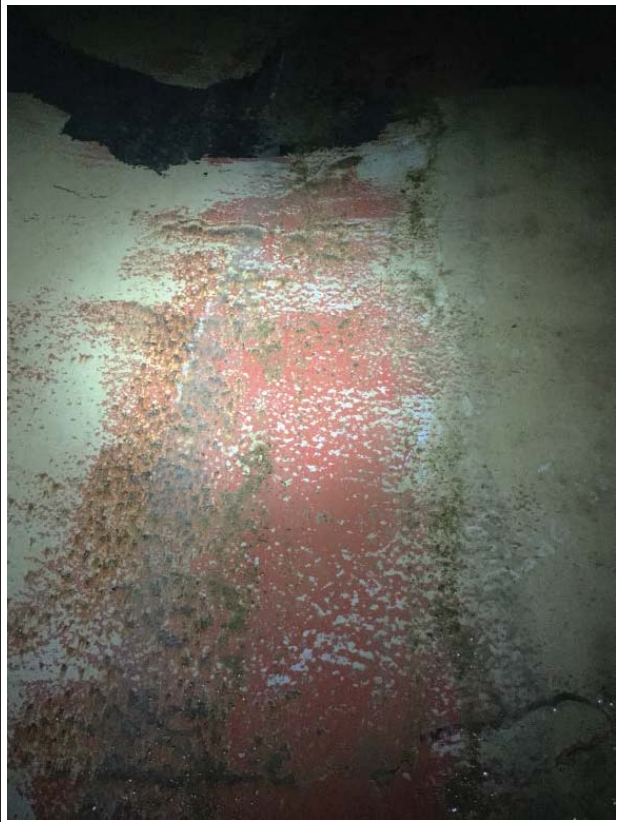


Figure D-12: Area of abraded repair material and corrosion in the invert near pipe segment 12.



Figure D-13: Area of abraded repair material and corrosion in the invert near pipe segment 12.



Figure D-14: Pipe segment 16. Image of the invert and EIS test cell set-up.

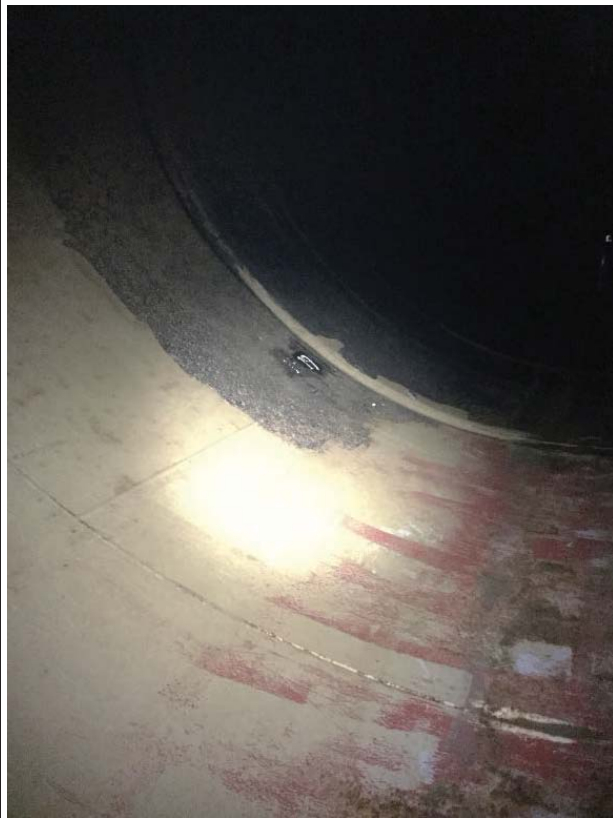


Figure D-15: Invert and wall condition near pipe segment 19. Abraded Devgrip 238 is seen near the invert



Figure D-16: Bare steel visible in a portion of coal tar epoxy near pipe segment 19. Steel does not appear to be corroded.



Figure D-17: Pipe wall near segment 19. Repair material, mud, and coal tar epoxy are all visible.

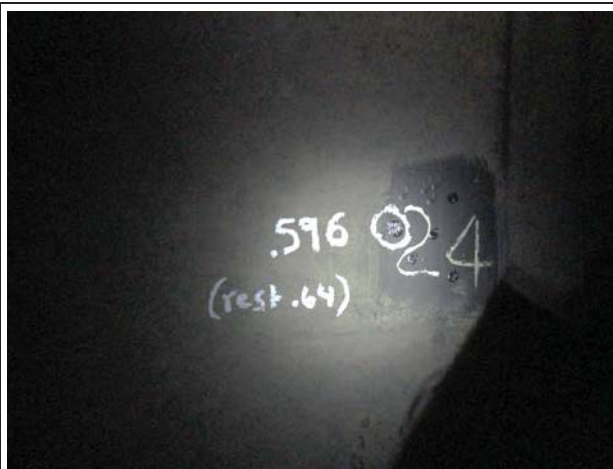


Figure D-18: Record of UT measurements at pipe segment 24 highlighting one area of lower-than-expected wall thickness, 0.596-inch instead of 0.640-inch.



Figure D-19: EIS test in progress at pipe segment 24.



Figure D-20: Near pipe segment 24. Image of a pipe joint as it crosses the invert. Repair material is abraded in the very center of the invert.



Figure D-21: Pipe segment 28. Image of pipe wall, including joint. EIS test cell set-up is at bottom left.



Figure D-22: Near pipe segment 28. Image of a pipe joint crossing the invert. Mud and other sediment has accumulated in the joint resulting in abrasion to the repair material.



Figure D-23: Pipe segment 32. Image of pipe wall and EIS test cell set-up. At this location, the EIS test time was 1 hour, from gluing the test cells to test completion.



Figure D-24: Pipe segment 36. Image of UT measurement results; UT measured 0.708 inch.



Figure D-25: EIS test cell set-up at pipe segment 36. The pipe walls were covered with a thick layer of mud.



Figure D-26: EIS test cell set up showing blisters (circled) at pipe segment 40.



Figure D-27: Close-up of blisters at pipe segment 40. Blisters can be seen throughout the area. The EIS test cells were placed to avoid the blisters. The UT measurements were taken around the blisters.



Figure D-28: Wall and joint condition of pipe segment 44. Repair material is seen a few feet up the wall of the pipe. Corrosion is visible in the interface between the two pipe sections.



Figure D-29: UT measurements near pipe segment 44; circled measurement area is 0.664 inch and all others are 0.710. Abraded repair coating is visible at the pipe joint at bottom left.



Figure D-30: Pipe segment 46. Pipe wall is covered with mud and sediment.



Figure D-31: Pipe segment 48. Coal tar epoxy looks to be in excellent condition.



Figure D-32: EIS test cell set-up at pipe segment 48. Coal tar epoxy has an orange-peeled surface.



Figure D-33: Near pipe segment 48. Image of pipe invert. The repair material is highly abraded with areas of corrosion throughout the invert.



Figure D-34: Areas of corrosion adjacent to repair material on a pipe joint near pipe segment 48.



Figure D-35: EIS test cell set-up at pipe segment 60. Thick mud was prevalent through this area.



Figure D-36: Isolated area of corrosion near pipe segment 60.



Figure D-37: Pipe segment 80. Coal tar epoxy is in visually good condition.



Figure D-38: Pipe segment 85. Image of invert and pipe wall. Repair material is abraded and corrosion is prevalent throughout the invert.

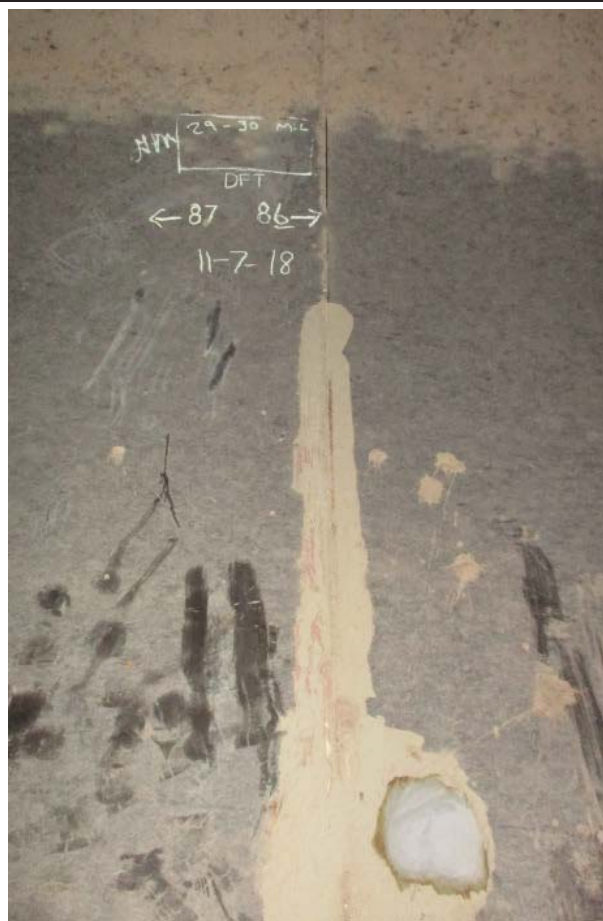


Figure D-39: Repair material at a pipe joint between pipe segments 86 and 87. Repair material is lightly abraded.



Figure D-40: Inspector affixing EIS test cell to the pipe wall at pipe segment 88. Adjacent joint has abraded repair material and light corrosion at interface of pipe segments.

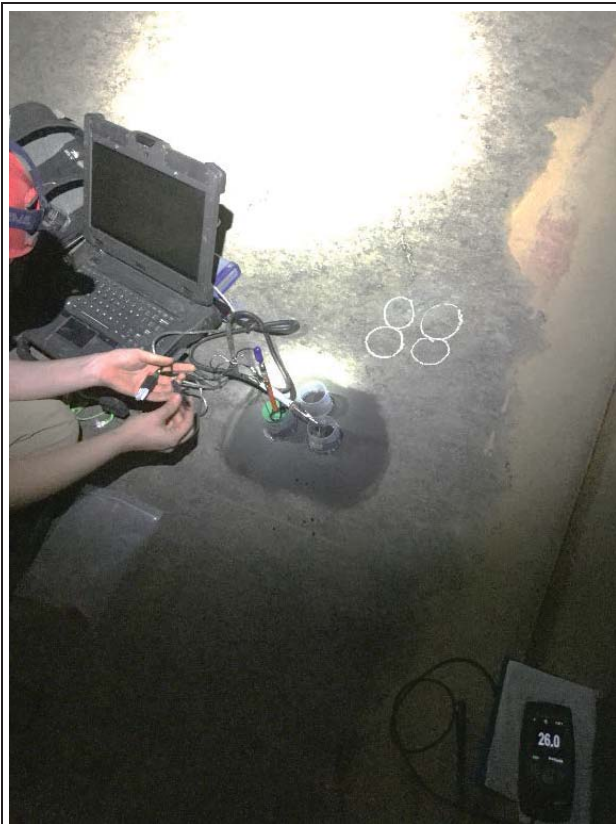


Figure D-41: EIS set-up at pipe segment 88.



Figure D-42: Abraded repair area near pipe segment 88. Grey top coat has been abraded away to reveal the red mid-coat.



Figure D-43: A large area of abraded repair material near pipe segment 88.



Figure D-44: Pipe segment 92. A large area of repair material is lightly abraded through the topcoat to the midcoat.



Figure D-45: Pipe segments 92 and 93. Image of a bend in the pipe near a point of elevation change.

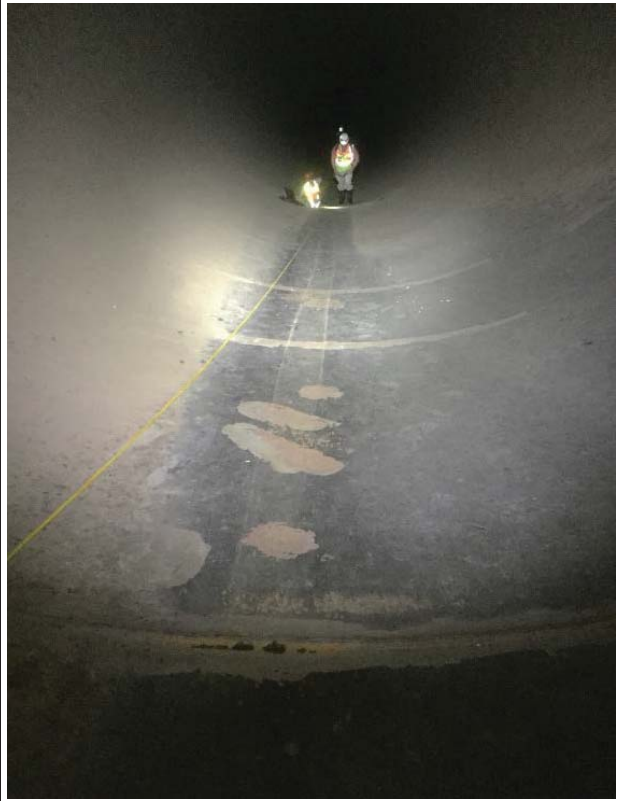


Figure D-46: Near pipe segment 93. Image of invert and pipe walls. Pipe is at a 26% grade through this section.



Figure D-47: Pipe segment 95. Image shows widespread sediment coverage on the pipe wall.



Figure D-48: Large bulge in the pipe wall near pipe segment 95. Bulge is approximately 2-ft. x 2-ft.



Figure D-49: Pipe segment 99. Image of pipe wall and joint.



Figure D-50: Pipe segment 104. Image of pipe wall, UT measurement test location, and pipe joint. Pipe joint has been repaired.



Figure D-51: Pipe segment 108. Image of abraded repair material and repair material in good condition a few feet up the pipe wall.



Figure D-52: Near pipe segment 108. Image of invert and pipe walls. EIS test cells are visible on right.



Figure D-53: Inspectors analyzing EIS data at pipe segment 112.



Figure D-54: Pipe segment 116.



Figure D-55: EIS test cell set-up at pipe segment 120.



Figure D-56: Near pipe segment 124. Mud is visible in and around the invert.



Figure D-57: Pipe segment 128. Image of EIS test cell set-up and UT measurement sites.



Figure D-58: Pipe segment 132. Image of wall and repaired joint.



Figure D-59: EIS test cell set-up at pipe segment 132. The coating at the test location had a notably rough surface.



Figure D-60: Near pipe segment 132. Pipe walls, crown, and invert are covered in mud and sediment.



Figure D-61: Pipe segment 136. Image of pipe wall and EIS test cell set-.



Figure D-62: Large blisters visible near pipe segment 136.

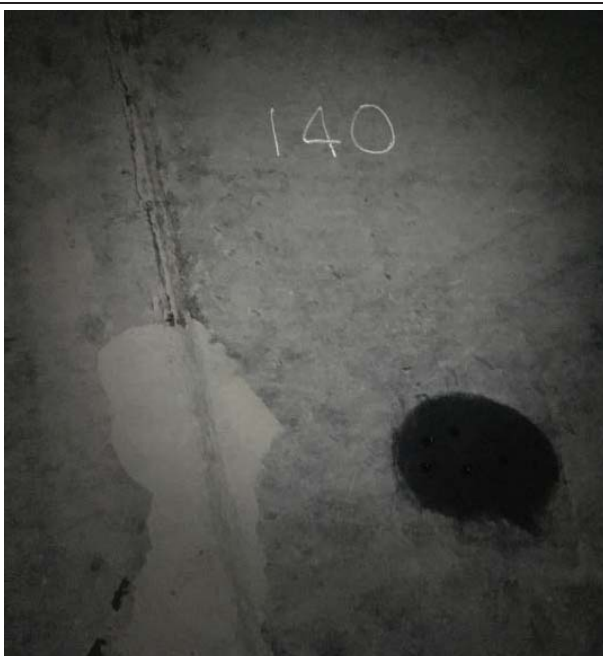


Figure D-63: Pipe segment 140. Image of pipe wall and joint with joint repair material.



Figure D-64: Large area of pitting and blistering near pipe segment 140.



Figure D-65: Near pipe segment 140. Image of invert with abrasion of repair material topcoat.



Figure D-66: Pipe segment 144. Image of pipe wall and EIS test cell set-up.

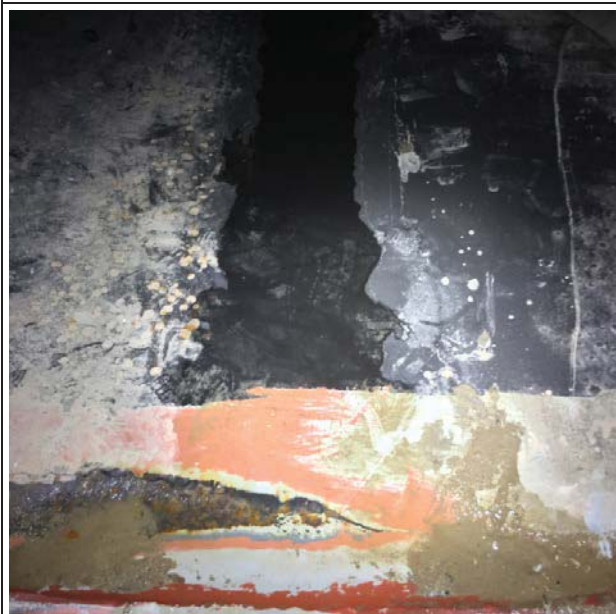


Figure D-67: Near pipe segment 144. Image of invert. Pitting is seen on left side of the invert and blisters are visible on the right.



Figure D-68: Large area of blisters near pipe segment 144; boot footprint provides scale.



Figure D-69: Large blisters near pipe segment 144, invert water is at left.

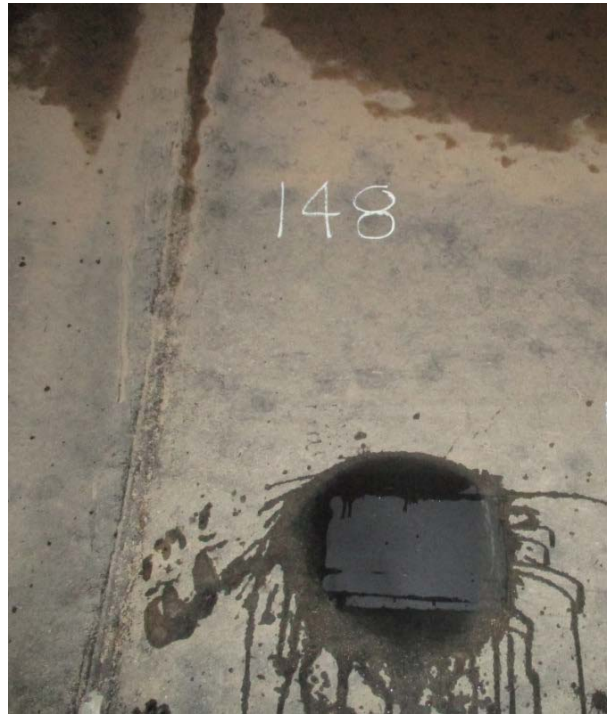


Figure D-70: Pipe segment 148. Blisters were prevalent adjacent to invert.



Figure D-71: Blistering adjacent to the invert of pipe segment 148.



Figure D-72: Blistering (circled top) and large pits (circled bottom) near pipe segment 148.



Figure D-73: EIS test cell set-up at pipe segment 152.



Figure D-74: Inspector measuring DFT at pipe segment 156.

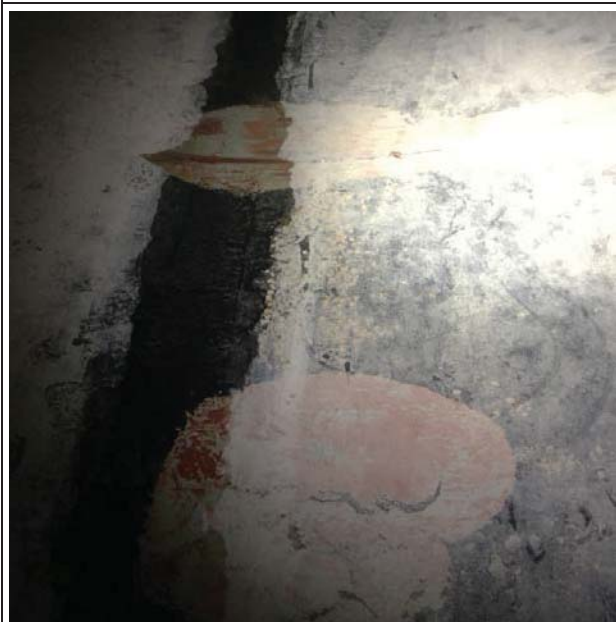


Figure D-75: Near pipe segment 156. Areas of abraded repair coating are visible at and around the joint and at the invert.



Figure D-76: Near pipe segment 158. Image of pipe wall and bend in pipe.



Figure D-77: EIS test set-up at pipe segment 160.



Figure D-78: Close-up of EIS test cells at pipe segment 160. Paint drips and a rough surface finish of the coating are present in this segment.



Figure D-79: Pipe segments 162 and 163. EIS test cell set-up visible on pipe wall.



Figure D-80: Near pipe segment 162. Mud accumulation is present in the invert and at pipe joint.



Figure D-81: Blistering of the repair material in the invert near pipe segment 162.

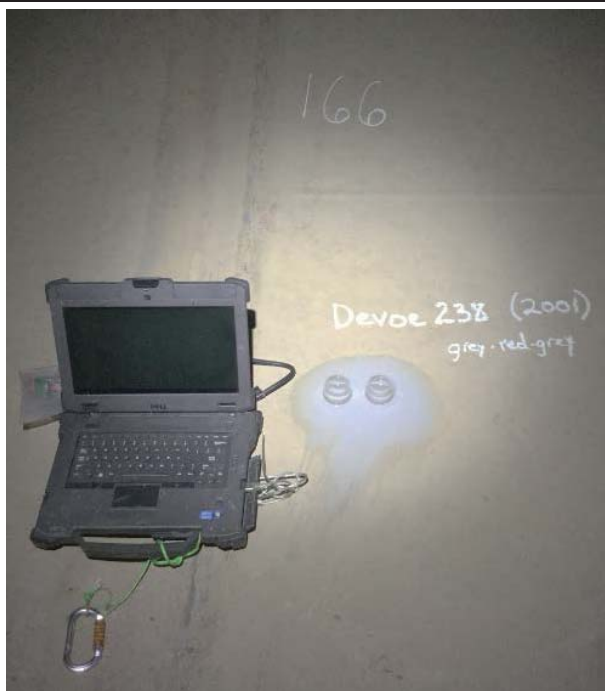


Figure D-82: EIS test cell set-up at a repair material location at pipe segment 166.



Figure D-83: EIS set-up within 30° slope at pipe segment 170.

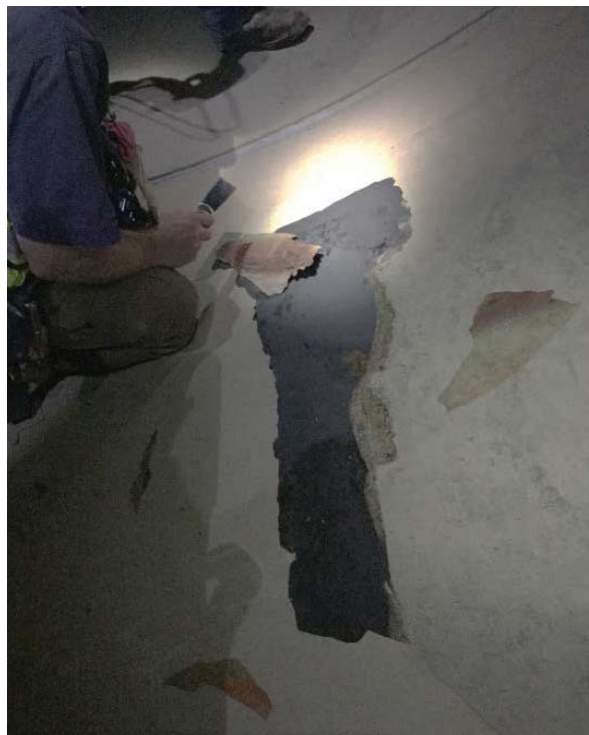


Figure D-84: Delaminated repair material with underlying coal tar epoxy in good condition near pipe segment 170.



Figure D-85: EIS in progress at pipe segment 174.

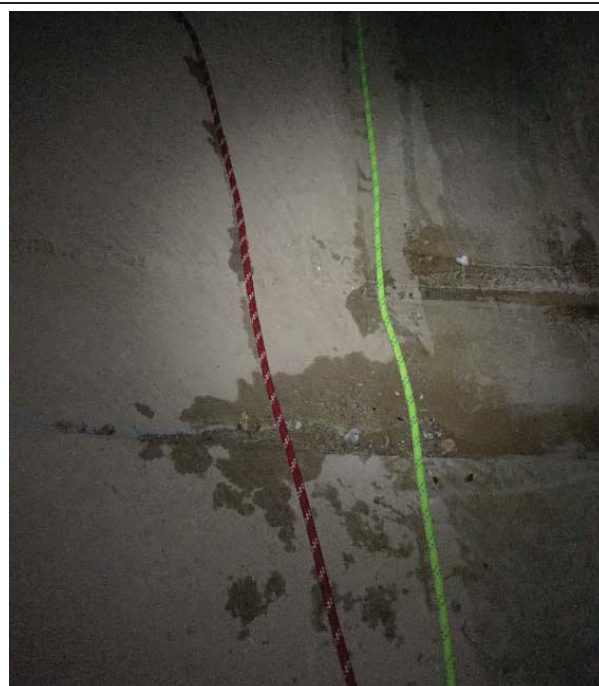


Figure D-86: Near pipe segment 174. Image of pipe joint with sediment in the joint. The 30° slope of the pipe in this area necessitated the use of ropes.



Figure D-87: Pipe segment 180. Image of pipe wall and EIS test cell set-up.



Figure D-88: Test cell set-up at pipe segment 180. The coating in this area could not be cleaned sufficiently for EIS test cells to hold electrolyte.



Figure D-89: Near pipe segment 180.



Figure D-90: Pipe segment 188. Coal tar epoxy was found to be rough.

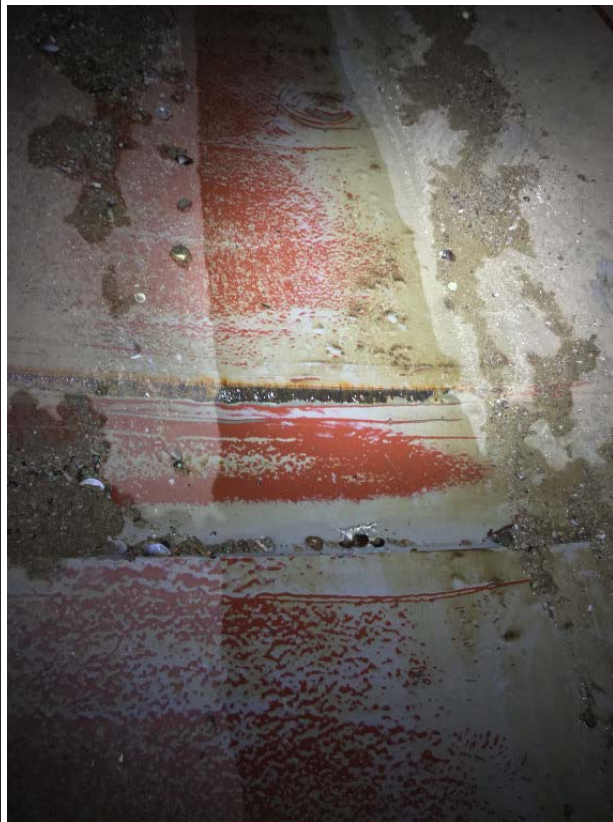


Figure D-91: Near pipe segment 188. Image of the invert. Repair coating was heavily abraded and mud and sediment were present.



Figure D-92: Near pipe segment 194. Mud and sediment in the invert coupled with the extreme slope made the inspection difficult.



Figure D-93: EIS test cell set-up at pipe segment 196.

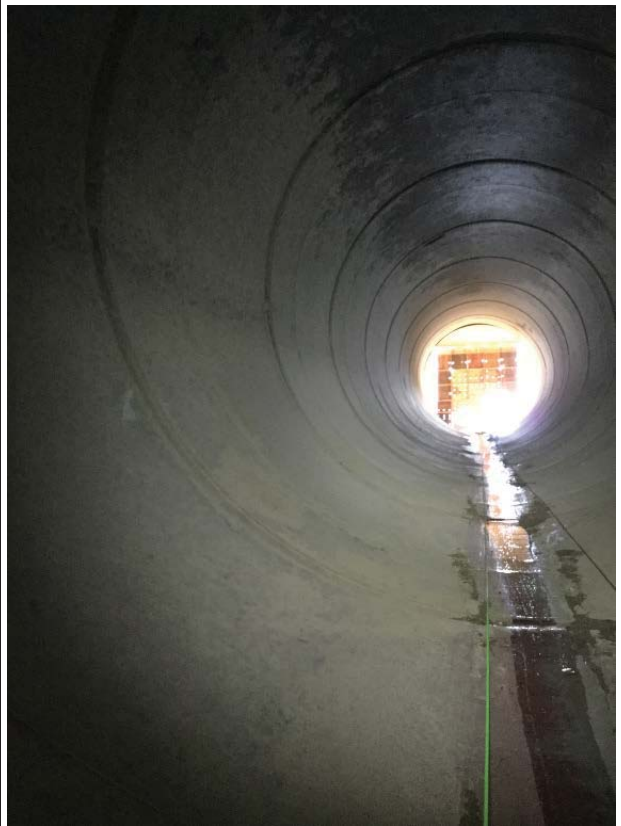


Figure D-94: Image of pipe wall near the outlet.



Figure D-95: View downstream of the outlet.



Figure D-96: Corroded ladders and railings at the deep-well access point.



Figure D-97: Corroded ladders and railings at the deep-well access point.



Figure D-98: Corroded ladders and railings at the deep-well access point.

Appendix E – CAP’s Detailed Inspection Notes

Table E-1: Detailed inspection notes for each pipe segment provided by CAP

Appendix D – Agua Fria River Siphon Report (2019)

BUREAU OF RECLAMATION
Technical Service Center
Denver, Colorado

TRAVEL REPORT

86-68540

Code: 86-68540 **Date:** Nov 27, 2019
To: Jessica Torrey, Manager, Materials and Corrosion Lab
From: Matthew Jermyn, Daryl Little, 86-68540
Subject: Inspection and field EIS analysis of the Salt River Siphon at the Central Arizona Project

Personnel on Site: Matthew Jermyn, Daryl Little: 86-68540; Jim Geisbush, Jennifer Jia: Central Arizona Project.

1. **Inspection period:** November 18-21, 2019
2. **Site visited:** Salt River Siphon, Phoenix, AZ
3. **Purpose of trip:** The purpose of the trip was to perform visual, dry film thickness (DFT), and ultrasonic thickness (UT) inspections of the [REDACTED] siphon, and to set up and perform field electrochemical impedance spectroscopy (EIS). The inspection was conducted by Matthew Jermyn, Materials Engineer, and Daryl Little, Materials Engineer.

4. **Background:**
The Salt River Siphon, a [REDACTED] siphon near Phoenix, AZ, was installed in 1975-78. Originally constructed out of Prestressed Concrete Cylinder Pipe (PCCP), the siphon was replaced with a steel pipe and returned to service in 1997. The interior of the siphon is coated with Amercoat 78HB coal tar epoxy. Warranty work was performed on the coating in 1998, and the Central Arizona Project (CAP) made coating repairs, predominantly to the siphon's invert, in 2001.

CAP invited coatings specialists from the Bureau of Reclamation's (Reclamation's) Technical Service Center to inspect the coal tar epoxy lining and perform field electrochemical impedance spectroscopy (EIS) on November 18-21, 2019. Field EIS testing provides a non-destructive method which aids in determining the degree of coating degradation prior to visible damage being observed. The data helps to determine the remaining service life of the coating system and when coating

replacement should be considered in order to prevent severe damage of the steel due to corrosion.

5. Method:

EIS

Matthew Jermyn and Daryl Little (Inspection Team) affixed disposable EIS test cells to the coal tar epoxy at the following pipe segments starting from the inlet: 3, 5, 8, 9, 11, 13, 15, 17, 19, 21, 23, 25, 27, 29, 31, 33, 35, 37, 39, 41, 43, 45. Facing down stream, the test cell positions were either at the 1:30 or 10:30 clock positions; for segments 3,5,9, and 11 cells were placed at both 1:30 and 10:30 clock.

Each test location was prepared by wiping or scraping mud from the surface and using a rag to dry the area. An aquarium-grade silicone adhesive provided a seal for attachment of each 2.25-inch diameter test cell to the lining. Each location was comprised of three to four test cells. The adhesive cured for at least two hours before adding tap water to the test cells. Due to the overhead nature of the testing positions, parafilm was placed over the test cells and water was added by injection through ports on the sides of the cells. To ensure that the coating was re-saturated before testing, the filled cells were left overnight.

EIS measurements were performed using an Ivium Compactstat potentiostat powered by a laptop. The laptop also provided the necessary software to run the measurements. Each measurement required only two test cells: one containing a copper/copper sulfate reference electrode and a platinum mesh counter electrode, and one containing platinum mesh that acts as a working electrode. The third and fourth cells were used for insurance purposes in case one of the cells did not completely adhere, and leakage occurred.

During the test, a 50 mV amplitude (root mean squared) sinusoidal voltage perturbation was applied, and the current required to achieve the desired voltage was measured. The phase angle, θ , is the difference, or lag, between the sinusoidal current response and the applied voltage. When the current response and applied voltage are in phase, $\theta = 0$ degrees, and the system displays characteristics of a pure resistor; when the applied voltage and current response are completely out of phase, $\theta = -90$ degrees, and the system displays characteristics of a pure capacitor. The impedance, Z , is calculated from the voltage and current output. Impedance is a measure of how much the circuit resists the current, or the flow of electrons through the coating. The test frequencies applied were 100 kHz to 0.1 Hz at five points per decade, resulting in an array of points during a test time of approximately two to three minutes.

Dry Film Thickness (DFT)

DFT measurements were taken by CAP staff, Jim Guisbush, and not included as part of this report. Multiple measurements were recorded for each pipe segment at which EIS was performed.

Ultrasonic Thickness (UT)

UT measurements were taken using a Cygnus Instruments M5-C4+ UT gauge and coupling fluid. Multiple measurements were recorded around a single location for each pipe segment in which EIS was performed. The average of the replicant measurements for each location were then calculated.

6. Results:

EIS

Raw EIS data is plotted in the form of a Bode plot which shows impedance magnitude, $|Z|$, versus the measurement frequency. A Bode plot is useful in analyzing how the coating prevents water and ions from migrating through to the substrate. At low frequencies, high $|Z|$ values suggest the coating is providing good corrosion resistance since it is resisting the flow of water and ions. Especially for structures that are in immersion service and are infrequently accessible for inspection or maintenance, $|Z| > 10^8$ Ohms at the lowest frequency indicates good corrosion resistance. When $|Z| < 10^7$ at lowest frequencies, the coating is providing poor corrosion resistance and maintenance should be considered.

Figure 1 shows the plot of $|Z|$ at 0.1 Hz versus pipe segment. Complete Bode plots for all pipe segments tested are in Appendix 1.

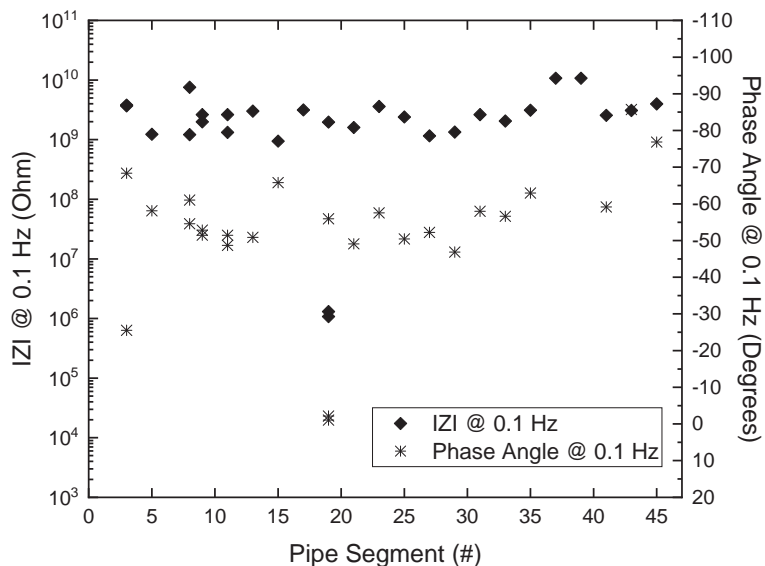


Figure 1 Impedance magnitude and phase angle at low frequencies versus pipe segment.

Changes in phase angle, θ , can be used to indicate the capacitive/resistive nature of the electrical circuit. This in turn provides an indication of whether corrosion is occurring at the substrate. Where corrosion processes are not occurring, current is stored at the interface between the coated surface and the substrate, and the system behaves as a pure capacitor. Where corrosion processes are occurring,

current has the option to flow through the interface via the corrosion charge transfer mechanism. With consideration to the electrical circuit, this behaves as a second parallel resistor-capacitor in series with the coating resistor, and causes phase angle, θ , to increase from -90 degrees towards 0 degrees. The effect of corrosion is observed at lower frequencies. Coatings that are performing well have phase angles more negative than -50 to -60 degrees at the lowest frequencies. Phase angle data is incorporated in the graphs shown in Figure 1 and in Appendix 1.

The coal tar epoxy is providing good corrosion protection throughout the section of the siphon tested at the 10:30 and 1:30 positions. Substantial noise was observed in the EIS results at section 3 near the outlet; however, impedance magnitudes at low frequencies were still recorded above the 10^7 ohm threshold. Phase angle data at this location was unreliable. With exception to section 19 at the 10:30 position, all EIS results exceeded the 10^7 Ohm threshold and hovered in the range of -50 to -60 degrees for phase angle. Overall, this indicates the coal tar epoxy at the 10:30 and 1:30 positions at the tested pipe segments is still offering excellent protection. As shown in Figure 2, it was observed in section 19 at the 10:30 position that there was substantial blistering where the test was conducted; this accounts for the 10^6 ohm impedance magnitude and zero degree phase angle observed. The coating at this location and elsewhere where similar blistering is observed will need to be repaired.



Figure 2 Blistering observed at EIS test cell location on pipe section#19 at 10:30 position.

UT

Table 1 gives the results of the UT testing. UT results compared favorably with the expected thickness values reported on the original drawings from each of the sections. The increase in the average thickness values starting at segment 37 are due to an increase in the wall thickness of the pipe. No obvious signs of metal loss were observed at measurement locations. In addition, multiple instances of discrepancies from the reported value would be expected per measurement area if major metal loss had occurred.

Pipe Segment #	Clock Position	Average Thickness (in)
3	10:30	0.652
5	12:00	0.654
8	10:30	0.645
9	7:30	0.651
11	7:30	0.652
13	7:30	0.649
15	7:30	0.647
19	7:30	0.640
21	7:30	0.632
23	7:30	0.653
25	7:30	0.640
27	7:30	0.617
29	7:30	0.649
31	7:30	0.650
33	7:30	0.649
35	7:30	0.655
37	7:30	0.703
39	7:30	0.715
41	7:30	0.719
43	7:30	0.717

7. Recommendations

Overall, results indicate the coal tar epoxy at the tested positions is still offering excellent protection. Where blistering is observed, as in Section 19 at the 10:30 position, coating repair is recommended.

SIGNATURES AND SURNAMENES FOR:

Travel to: Salt River Siphon, Phoenix, AZ

Dates of Inspection: November 18-22, 2019

Names and Codes of Travelers: Matthew Jermyn, Daryl Little, Ph.D., 86-68540

Author

Date

MATTHEW JERMYN

Digitally signed by MATTHEW JERMYN
Date: 2020.03.06 12:12:08 -07'00'

Matthew Jermyn
Materials Engineer, Materials and Corrosion Laboratory (MCL)



Digitally signed by DARYL LITTLE
Date: 2020.03.06 15:11:35 -07'00'

Daryl Little, Ph.D.
Materials Engineer, Materials and Corrosion Laboratory (MCL)

Peer Review

Date

STEPHANIE PROCHASKA

Digitally signed by STEPHANIE PROCHASKA
Date: 2020.03.06 13:30:57 -07'00'

Stephanie Prochaska, M.S.
Materials Engineer, Materials and Corrosion Laboratory (MCL)

Appendix 1 – EIS Results

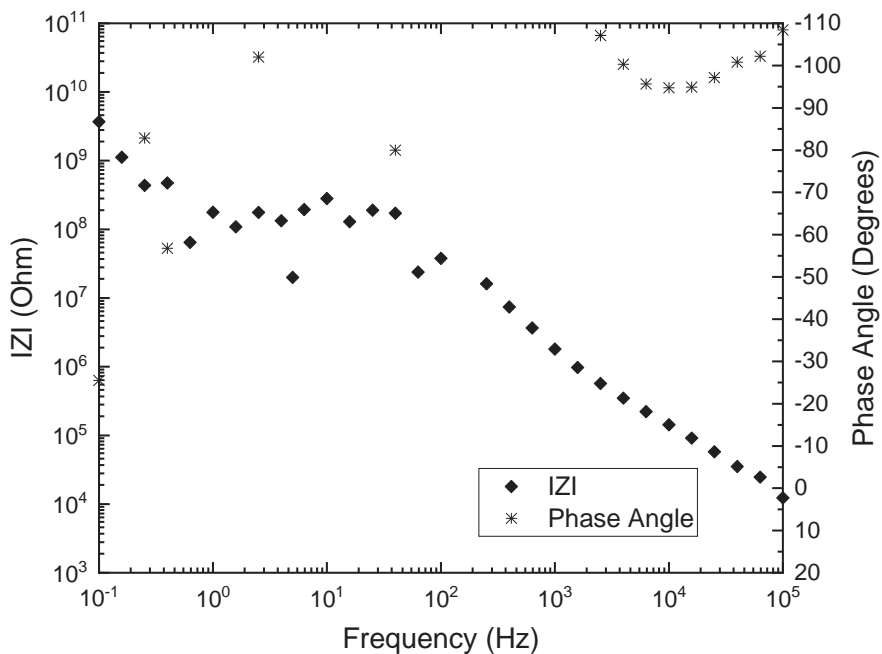


Figure 3 Pipe segment #3 EIS results at the 1:30 position.

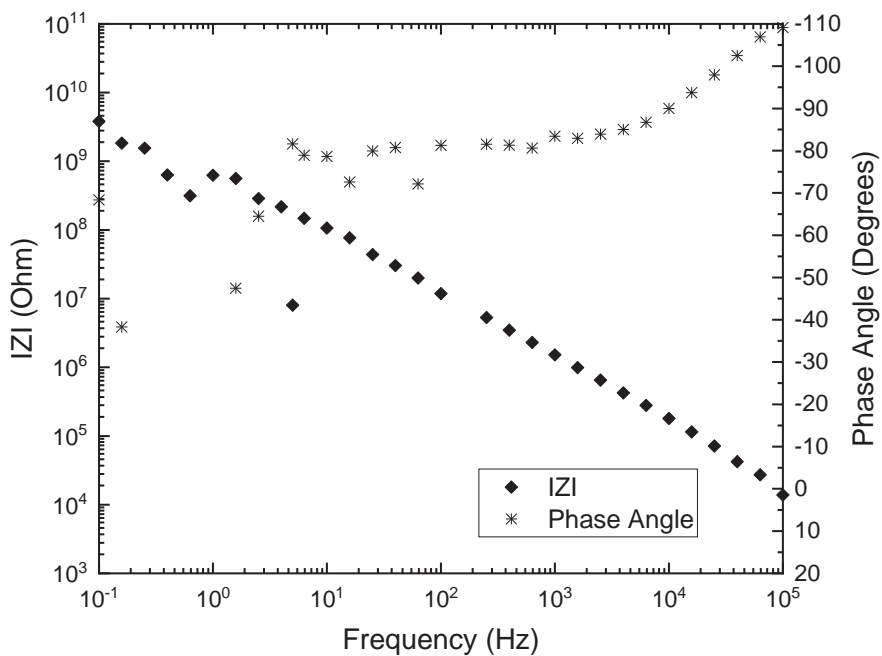


Figure 4 Pipe segment #3 EIS results at the 10:30 position.

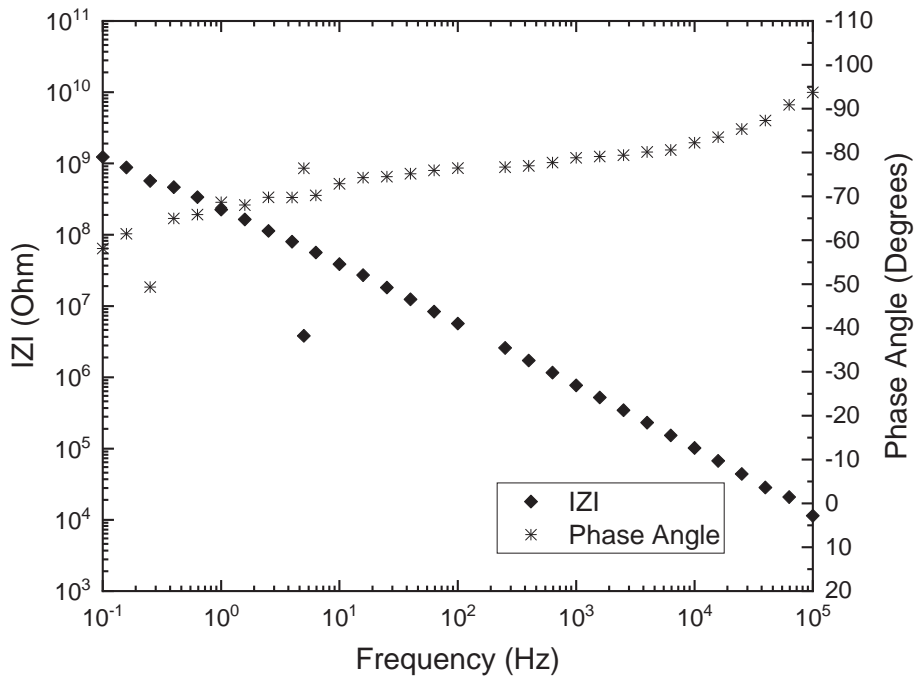


Figure 5 Pipe segment #5 EIS results at the 1:30 position.

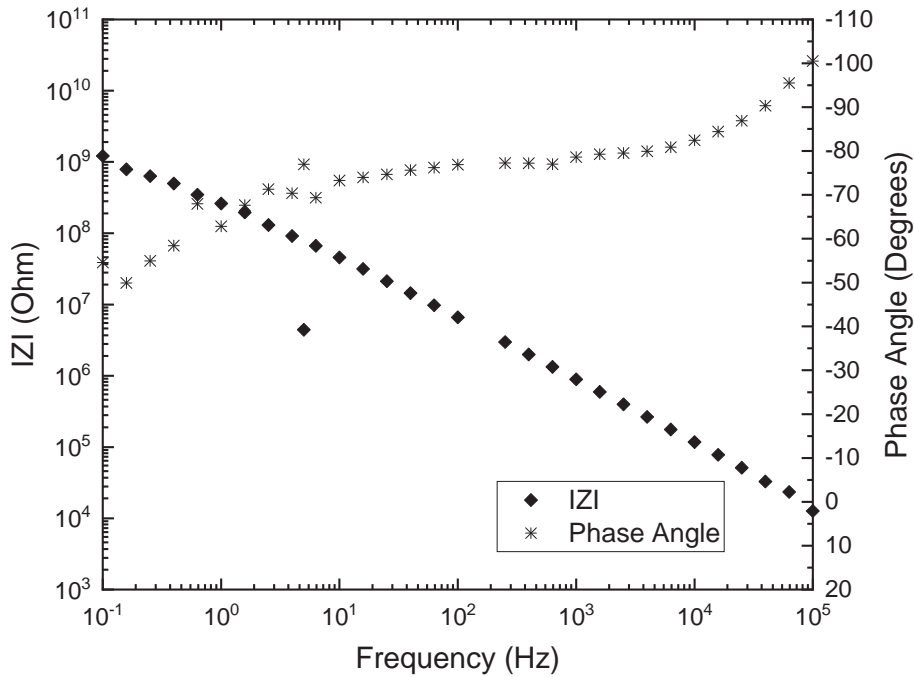


Figure 6 Pipe segment #8 EIS results at the 1:30 position.

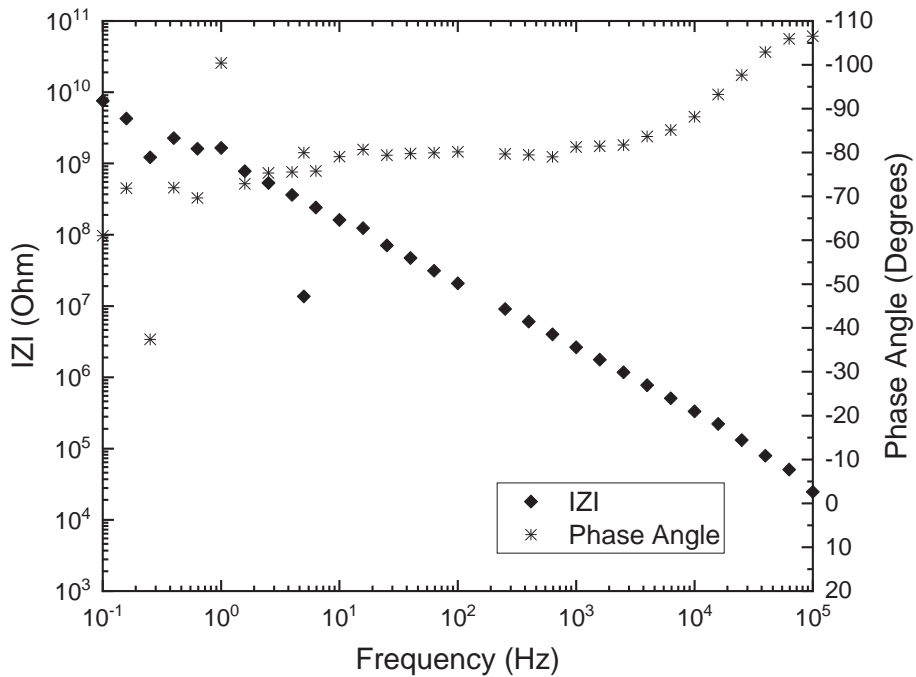


Figure 7 Pipe segment #8 EIS results at the 10:30 position.

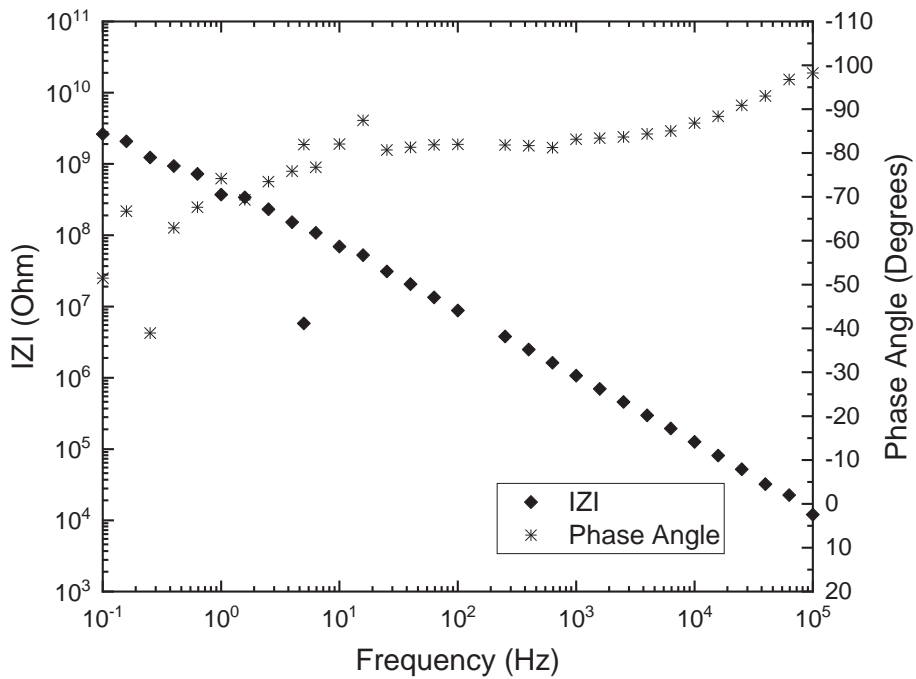


Figure 8 Pipe segment #9 EIS results at the 1:30 position.

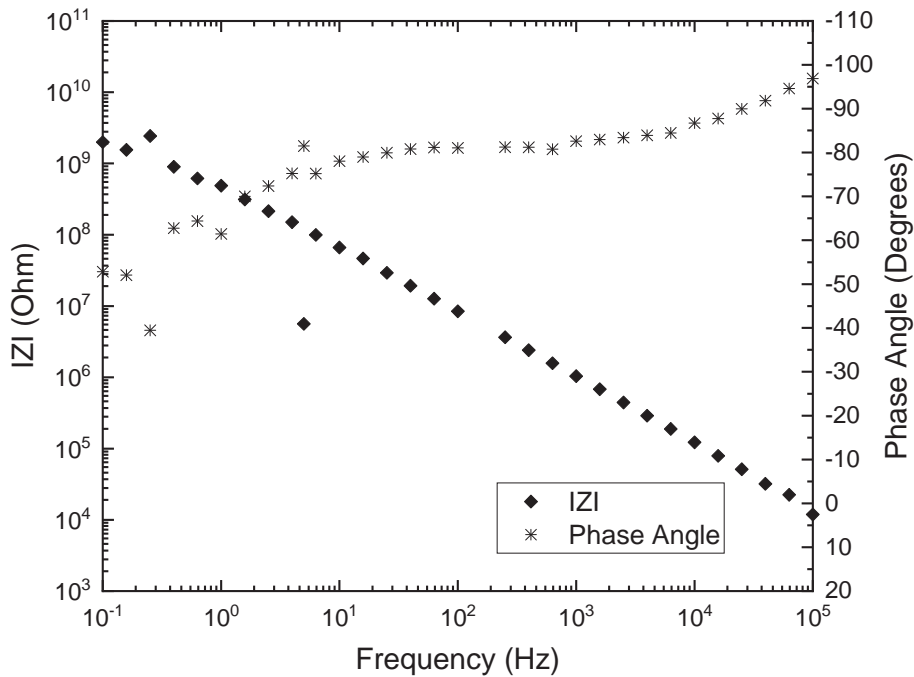


Figure 9 Pipe segment #9 EIS results at the 10:30 position.

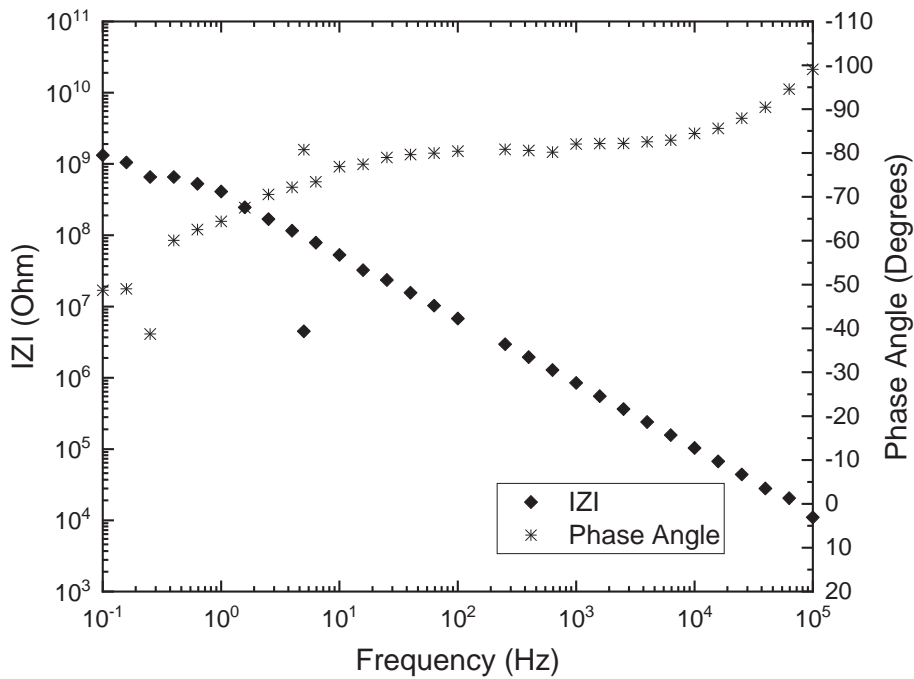


Figure 10 Pipe segment #11 EIS results at the 1:30 position.

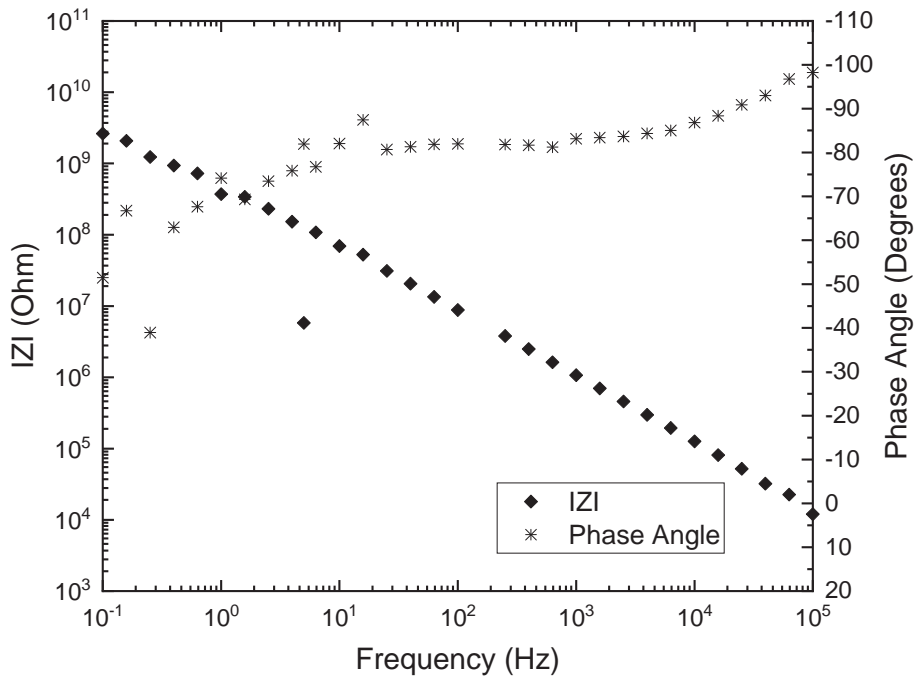


Figure 11 Pipe segment #11 EIS results at the 10:30 position.

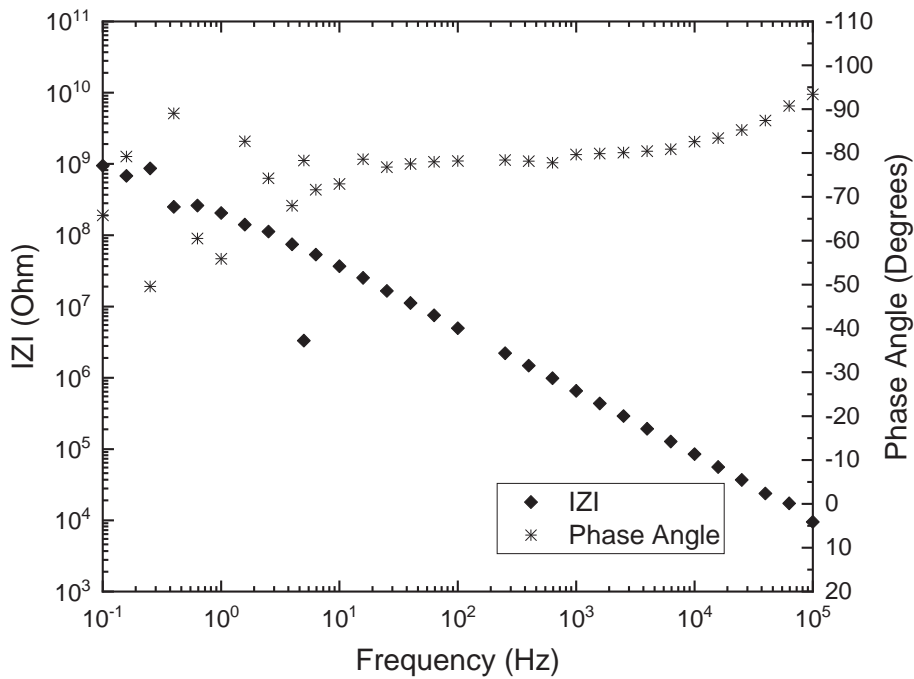


Figure 12 Pipe segment #13 EIS results at the 1:30 position.

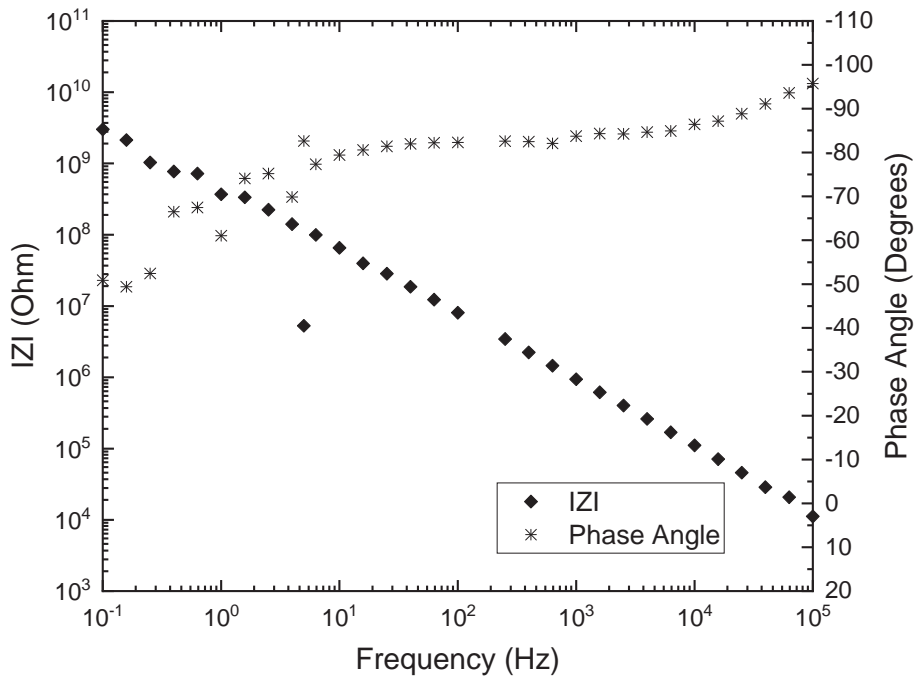


Figure 13 Pipe segment #15 EIS results at the 1:30 position.

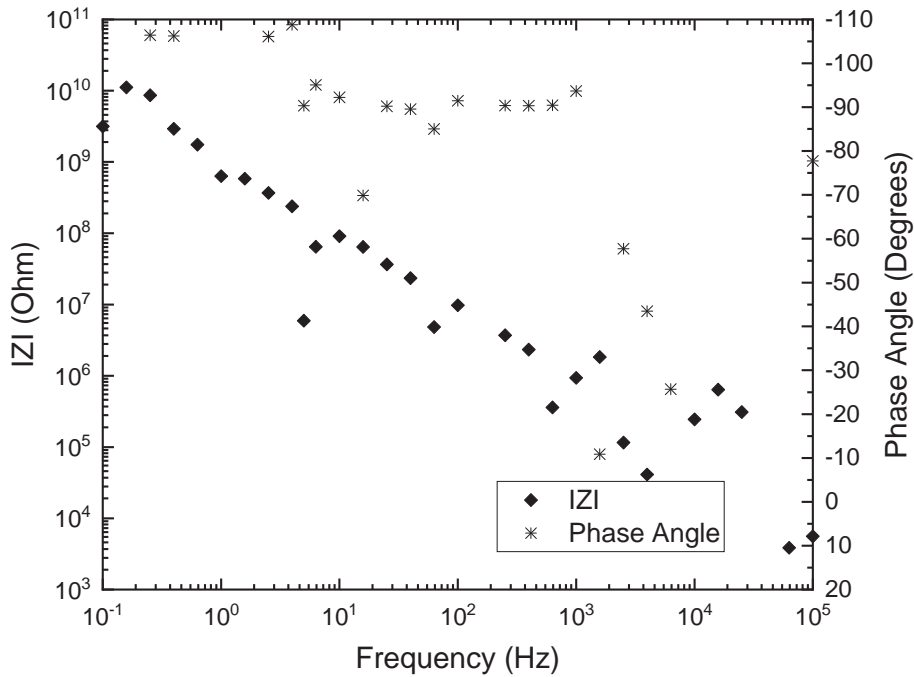


Figure 14 Pipe segment #17 EIS results at the 10:30 position.

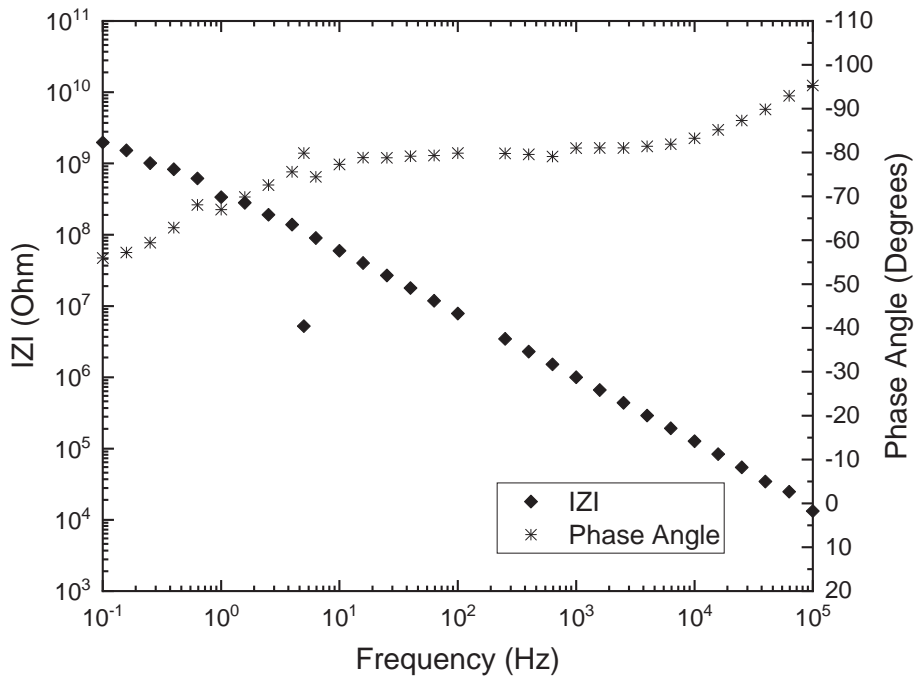


Figure 15 Pipe segment #19 EIS results at the 1:30 position.

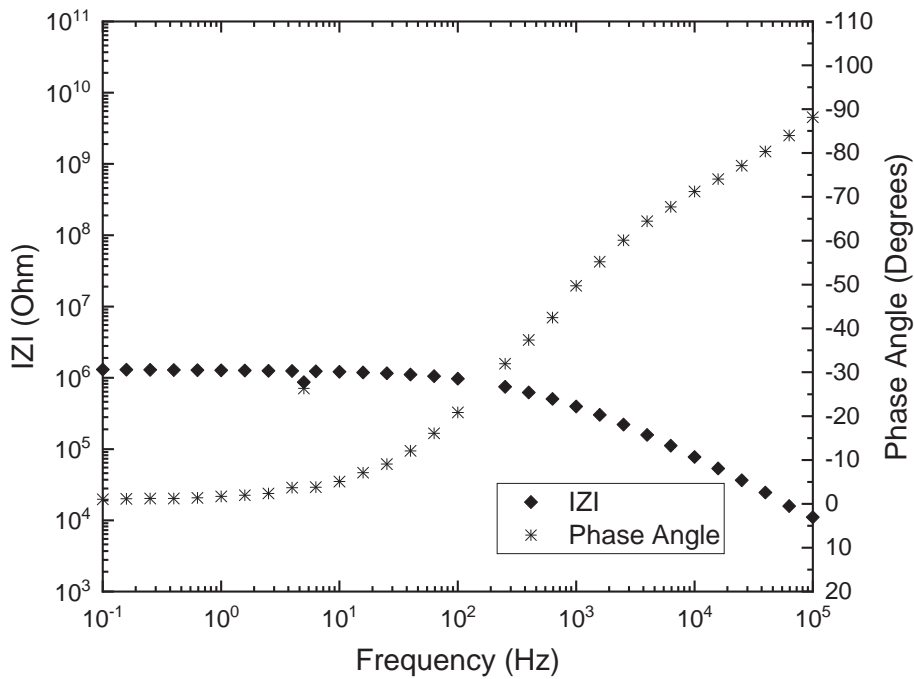


Figure 16 Pipe segment #19 EIS results at the 10:30 position

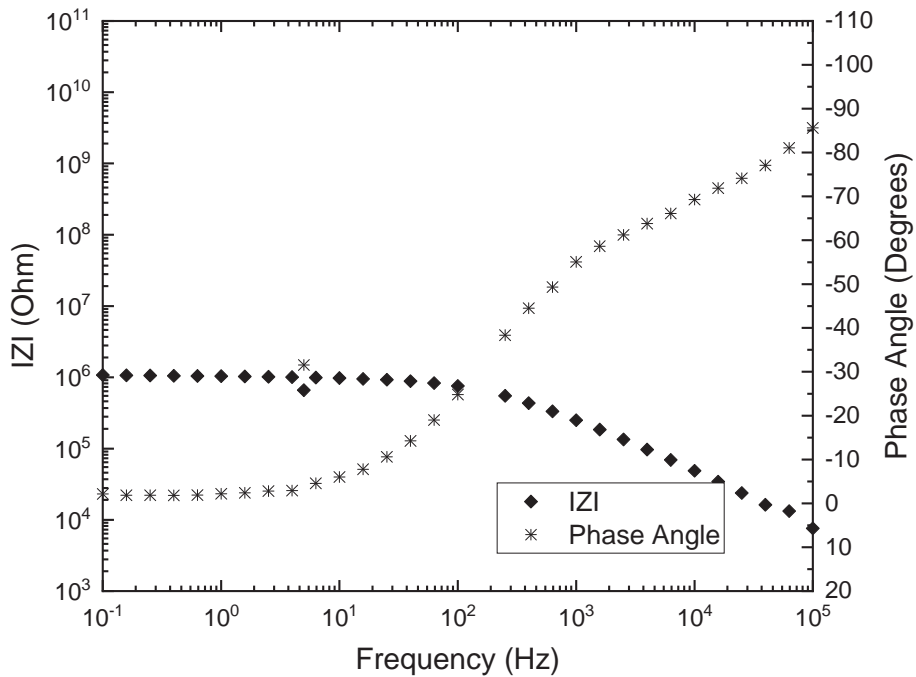


Figure 17 Pipe segment #19 EIS results at the 10:30 position, second test

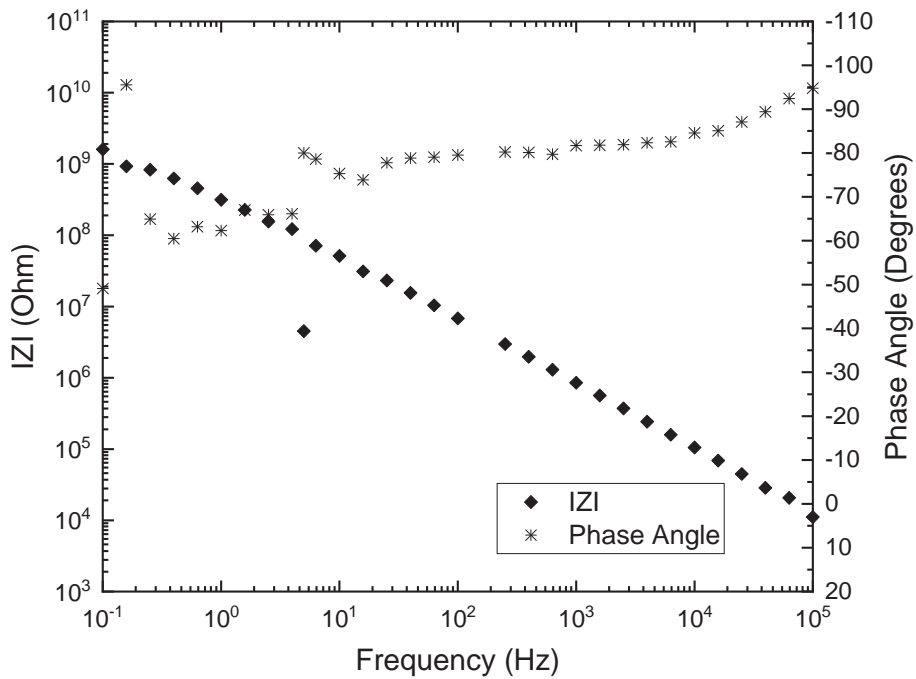


Figure 18 Pipe segment #21 EIS results at the 10:30 position

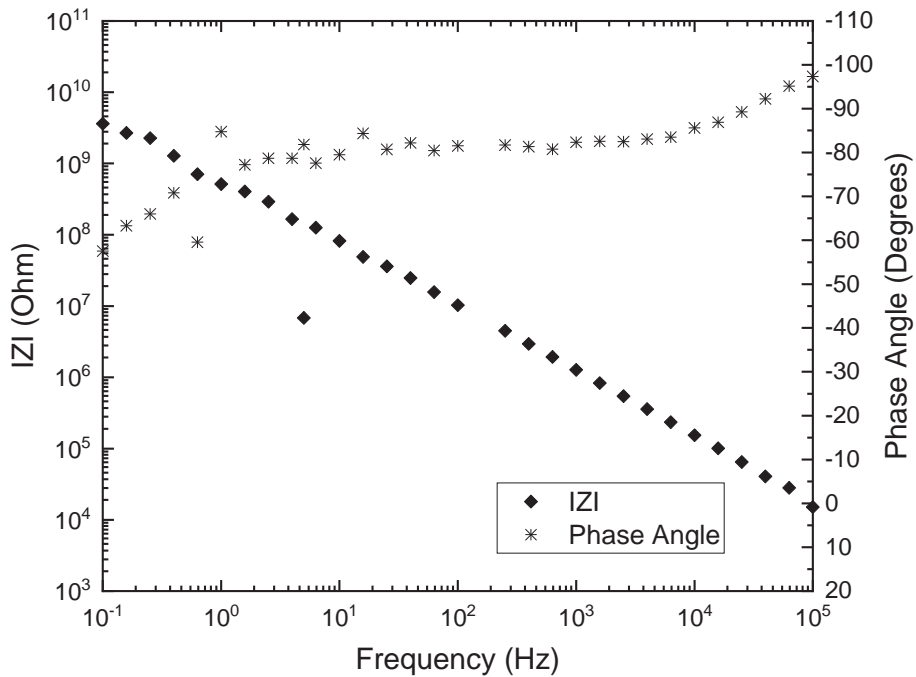


Figure 19 Pipe segment #23 EIS results at the 1:30 position

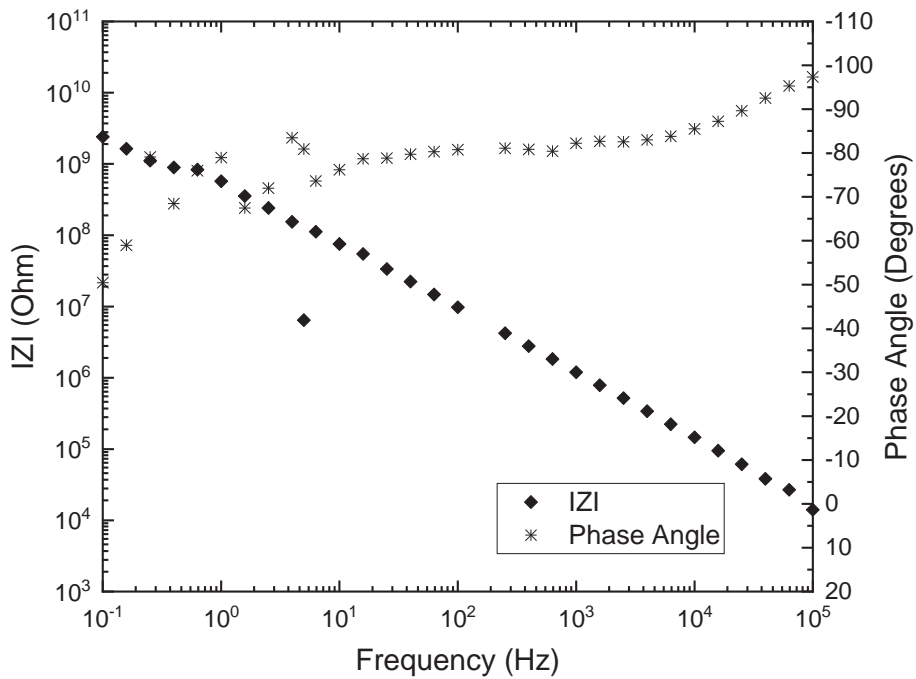


Figure 20 Pipe segment #25 EIS results at the 10:30 position

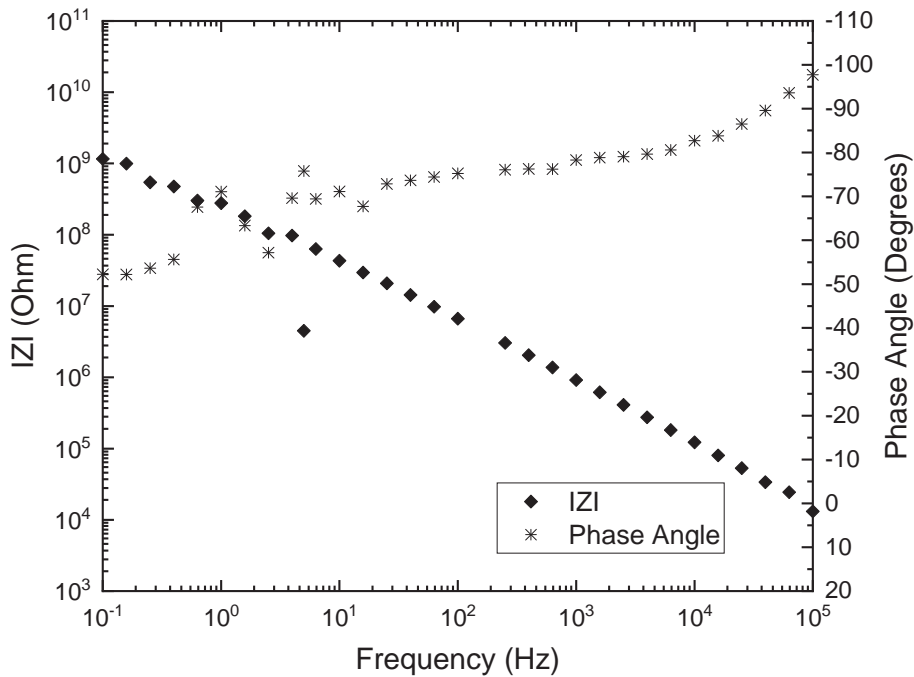


Figure 21 Pipe segment #27 EIS results at the 1:30 position

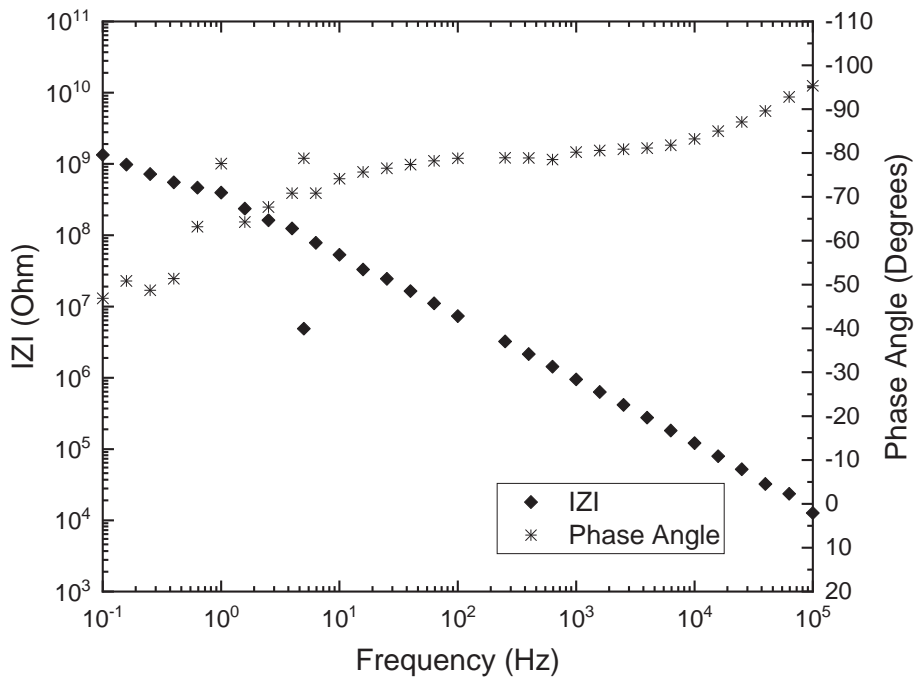


Figure 22 Pipe segment #29 EIS results at the 10:30 position

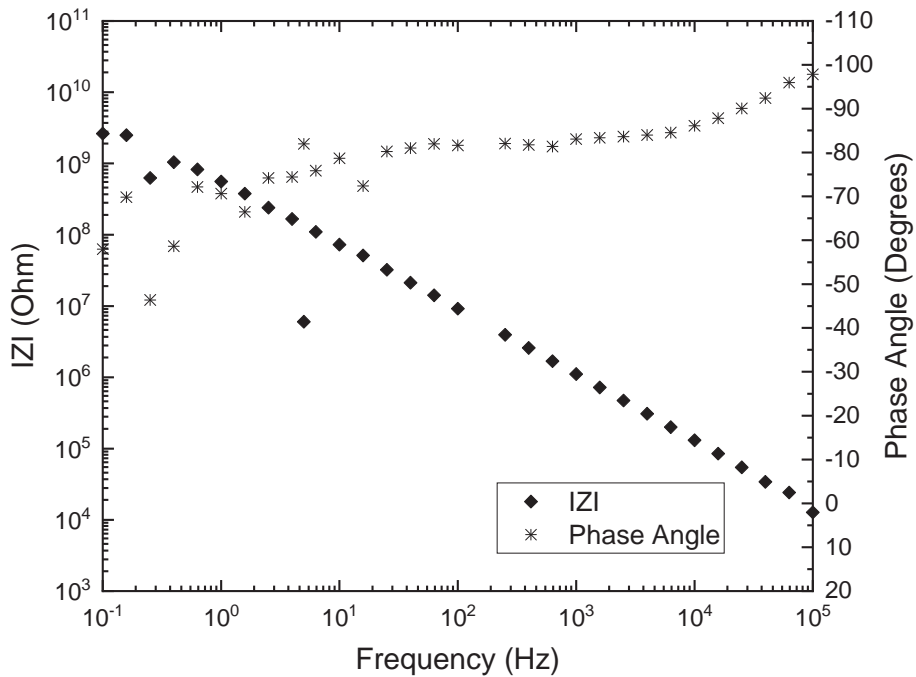


Figure 23 Pipe segment #31 EIS results at the 10:30 position

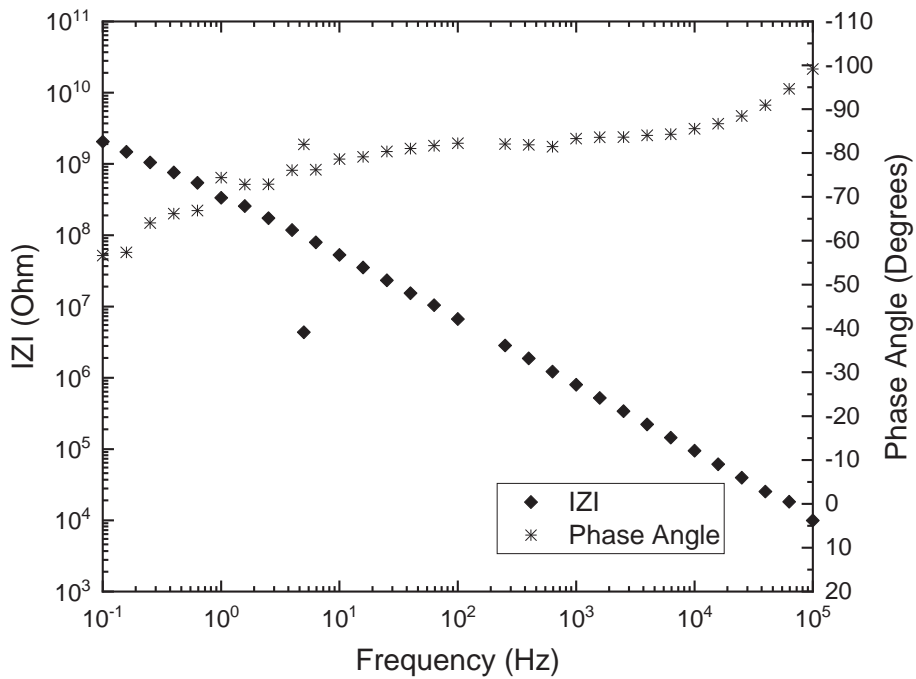


Figure 24 Pipe segment #33 EIS results at the 10:30 position

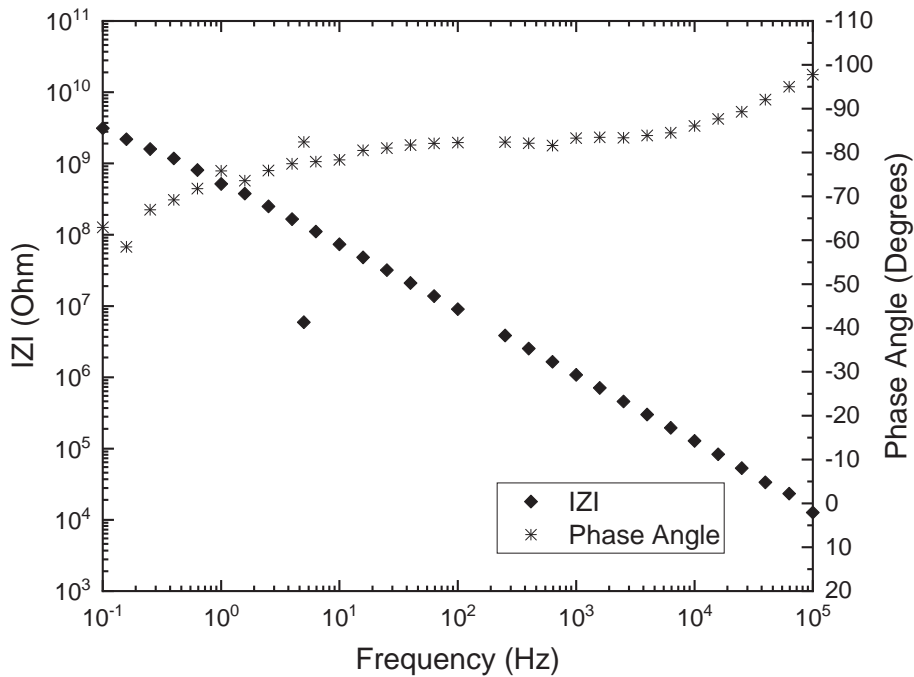


Figure 25 Pipe segment #35 EIS results at the 10:30 position

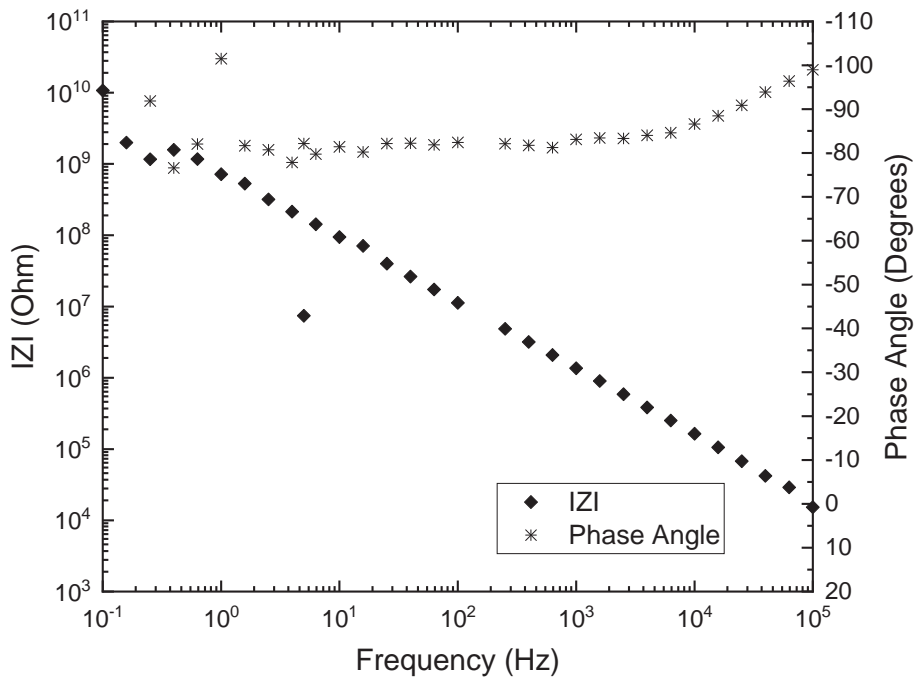


Figure 26 Pipe segment #37 EIS results at the 1:30 position

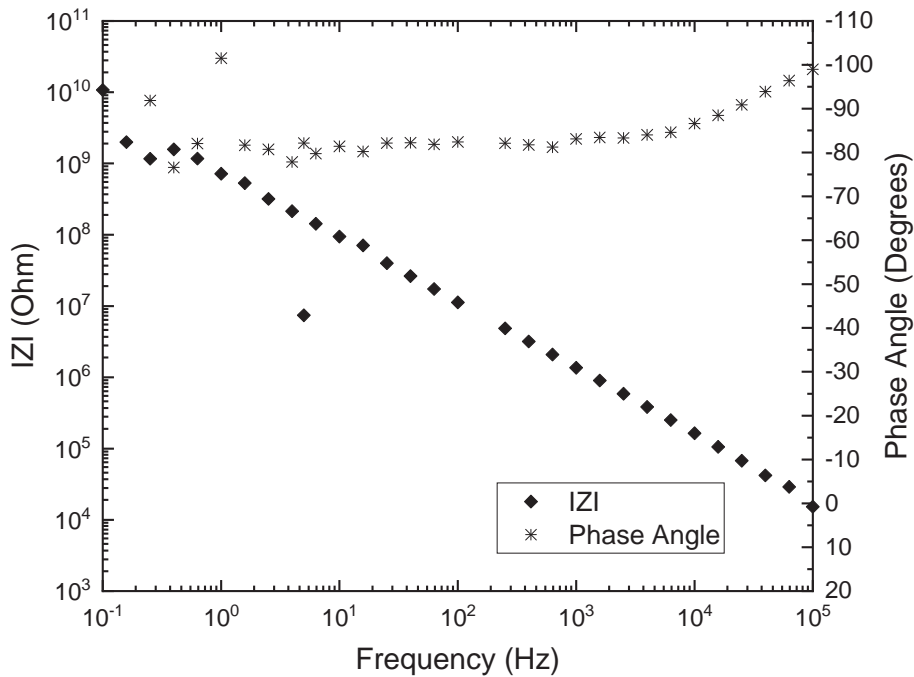


Figure 27 Pipe segment #39 EIS results at the 1:30 position

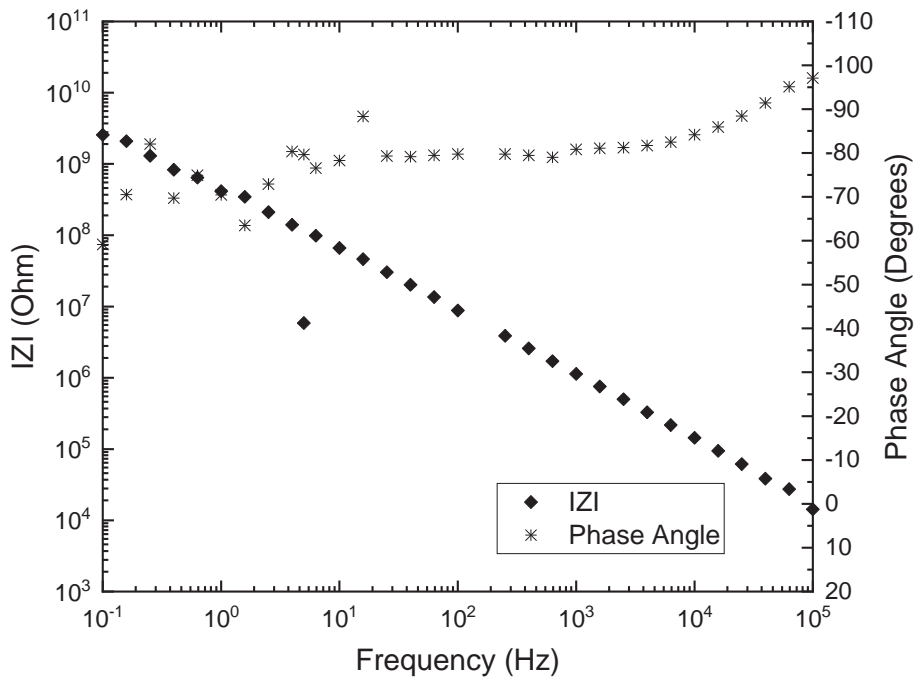


Figure 28 Pipe segment #41 EIS results at the 10:30 position

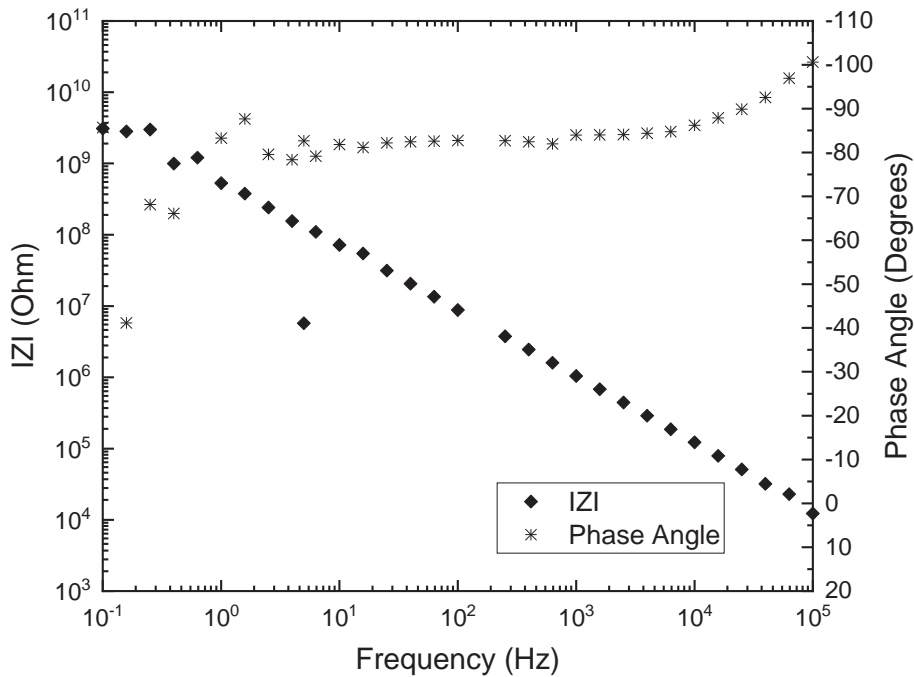


Figure 29 Pipe segment #43 EIS results at the 10:30 position

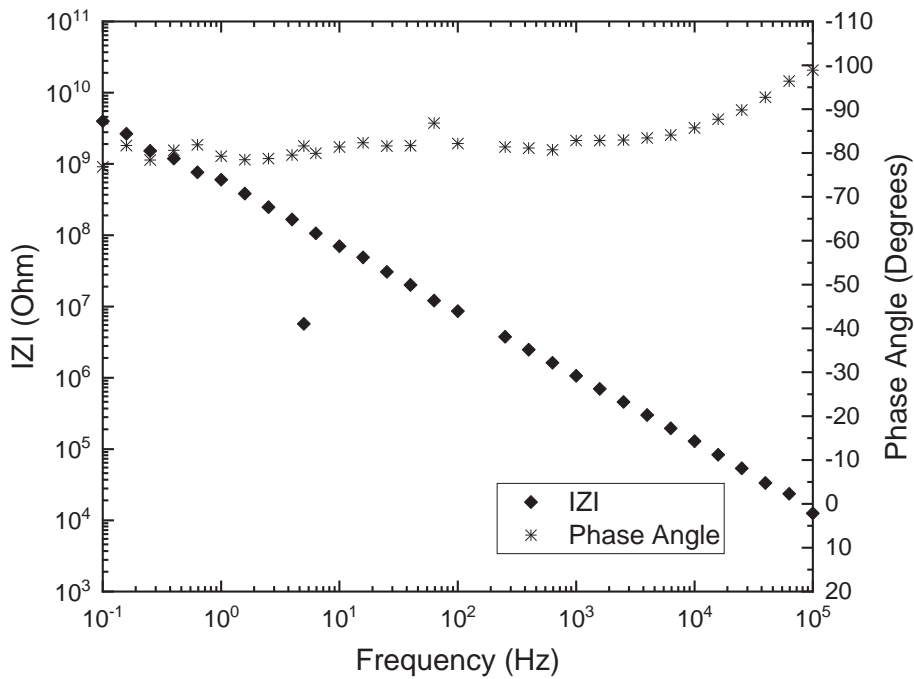


Figure 30 Pipe segment #45 EIS results at the 10:30 position

